letnik/volume **53** - št./no. **12/07** - str./pp. **805-920**
Ljubljana, dec./Dec. 2007, zvezek/issue **511**

STROJNIŠKI VESTNIK

JOURNAL OF MECHANICAL ENGINEERING

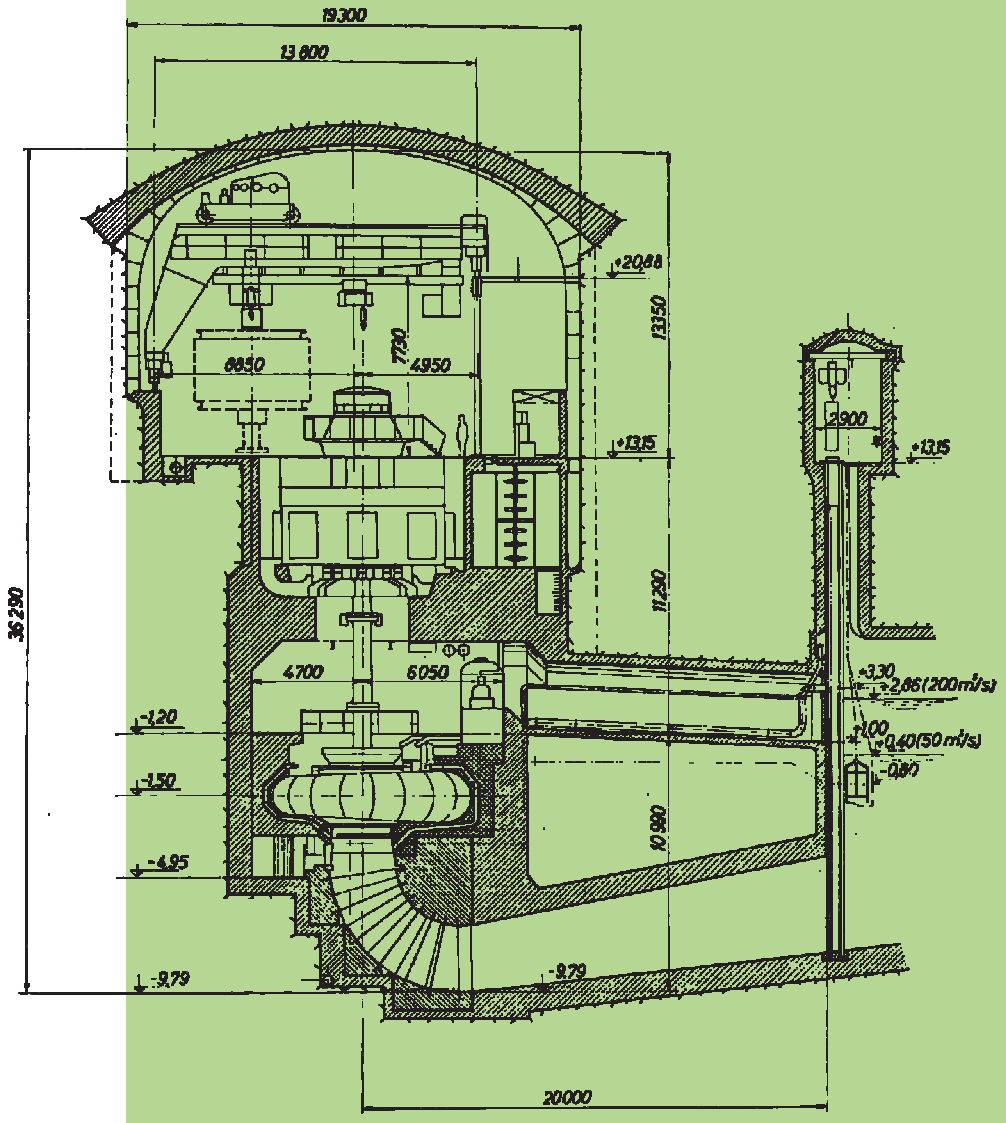

cena 3,34 EUR

9 770039 248001

ISSN 0039-2480

Vsebina - Contents

Strojniški vestnik - Journal of Mechanical Engineering
letnik - volume 53, (2007), številka - number 12
Ljubljana, december - December 2007
ISSN 0039-2480

Izhaja mesečno - Published monthly

Razprave

Papers

Osebne vesti

Personal Events

Strojniški vestnik - Journal of Mechanical Engineering 53(2007)12, 806-818
UDK - UDC 531/534
Izvirni znanstveni članek - Original scientific paper (1.01)

Analitično spremljanje razvoja elastoplastičnega stanja med upogibom nosilcev pravokotnega prereza

Analytical Tracing of the Evolution of the Elasto-Plastic State during the Bending of Beams with a Rectangular Cross-Section

Miroslav Halilovič - Boris Štok
(Fakulteta za strojništvo, Ljubljana)

Prispevek obravnava elastoplastično analizo upogibnice nosilcev pravokotnega prereza, ki so obremenjeni z določenimi vrstami obremenitev, pri čemer material ni utrjevalen. Z upoštevanjem teorije majhnih pomikov in majhnih deformacij so izpeljane analitične rešitve, s katerimi lahko analiziramo elastoplastični problem upogiba nosilcev v celoti analitično. To omogoča spremljanje razvoja elastoplastičnega odziva s širjenjem plastičnega območja po trdnini s povečevanjem obremenitve, t.j. tako širjenje vzdolž osi nosilca kot širjenje po globini prereza, od nastanka plastičnih deformacij do porušitve.

(Ključne besede: nosilci, elastoplastične analize, analitične funkcije, porušitve)

The deflection analysis of beams with rectangular cross-sections is considered under specific loading conditions and assuming elasto-plastic behaviour with no hardening. Within the framework of the small-strain and small-displacement approach, analytical solutions are derived that enable the elasto-plastic analyses of beams to be performed in a closed analytical form. As a consequence, clear tracing of the evolution of the elasto-plastic response with a propagation of the plastic zone through the solid body, i.e., its spreading along the beam's longitudinal axis as well as its penetration through the cross-section, is enabled as loads increase, from the appearance of a first plastic yielding in the structure until its collapse.

(Keywords: beams, elastioplastic analysis, analytic functions, beam collapse)

0 UVOD

Upogib nosilcev, ki se pogosto pojavlja v tehnični praksi, je bil že mnogokrat obravnavan tudi z zahtevnejšimi postopki, še posebej v primeru elastičnih problemov ([4], [7], [10] in [11]). Elastoplastične analize nosilcev, pri katerih predpostavimo nastanek plastičnih členkov, z uporabo katerih izračunamo mejne obremenitve, ki povzročijo porušitev konstrukcije, spadajo v področje teorije mejnih stanj ([2] in [5]). Ker vodilne enačbe elastoplastičnega problema upogiba nosilcev v splošnem niso rešljive analitično, v literaturi srečamo predvsem numerične in eksperimentalne rezultate ([1], [6], [8] in [9]). Analitična rešitev je navedena kvečjemu za nespremenljivo porazdelitev notranjega momenta, medtem ko je za kvadratično porazdelitev prikazan le izračun posameznega primera [3]. Ob

0 INTRODUCTION

The bending of beams, which is frequently addressed in technical practice, has been adequately and thoroughly analysed, considering even more rigorous approaches, especially for elastic problems ([4], [7], [10] and [11]). The elasto-plastic analyses of beams, which with the assumed formation of plastic hinges limit the fully plastic loads, are evaluated. Those causing a structure to collapse are treated within a framework of the limit-analysis theory ([2] and [5]). Since, in general, the governing equation of the elasto-plastic beam-bending problem is not to be solved analytically; it is numerical solutions and experimental results that are met in the literature ([1], [6], [8] and [9]). An analytical solution is described, at most, for a constant bending-moment distribution, while for a quadratic bending moment the distribution is derived only for a

predpostavki elastoplastičnega materiala brez utrjevanja smo se v prispevku osredotočili na raziskavo elastoplastičnega upogiba nosilcev pravokotnega prereza. Posamezne rešitve, izpeljane ob predpostavki, da je porazdelitev notranjega momenta največ kvadratična, v celoti omogoča analitično spremljati razvoj elastoplastičnega stanja v konstrukciji ob monotonem in sorazmernem povečevanju obremenitev.

1 VODILNE ENAČBE PROBLEMA

Naj bo raven nosilec prečnega prereza A (sl. 1) izpostavljen elastoplastičnemu upogibu v ravnini (x,z), kjer je x vzdolžna os nosilca, medtem ko sta y in z glavni osi prereza. Medtem ko upoštevamo, da je obnašanje snovi v elastičnem področju skladno s Hookovim zakonom, posebnih zahtev za nepovračljivo obnašanje trenutno ne postavimo. Upoštevamo še Bernoulli-Navierjevo hipotezo o ravnosti prereza in njegovi pravokotnosti na nevtralno os. V skladu z naravo obravnavanega problema je napetostno stanje $\sigma_{ij}(x,y,z)$ popisano tako, da so naslednje rezultante enake nič:

particular problem [3]. By assuming an elasto-plastic material with no hardening, we concentrate in this paper on an investigation of the elasto-plastic bending of beams with a rectangular cross-sectional area. The particular solutions derived under the assumption of, at most, a quadratic bending moment distribution enable the fully analytical tracing of the evolution of the elasto-plastic state in structural components using the monotonic and proportional application of loads to a structure.

1 GOVERNING EQUATIONS

Let us consider a straight beam with a cross-sectional area A, (Fig. 1), subject to elasto-plastic bending in the (x,z) plane, where x is the longitudinal axis of the beam, and y and z are the principal axes of the cross-section. While the material behaviour is assumed to obey Hooke's law in the elastic region, no restrictions on the nature of the irreversible inelastic response are imposed on the moment. Also, the Bernoulli-Navier assumptions on the cross-section's planarity and perpendicularity to the neutral axis are respected. The established stress state $\sigma_{ij}(x,y,z)$ is characterized, in accordance with the nature of the considered problem, by the following resultants being zero:

$$\int_A \sigma_{xy}\mathrm{d}A = T_y(x) = 0 \ , \ \int_A \left(\sigma_{xz}y - \sigma_{xy}z\right)\mathrm{d}A = M_x(x) = 0 \ , \ \int_A \sigma_{xx}y\mathrm{d}A = -M_z(x) = 0 \qquad (1).$$

Predpostavljeno je tudi, da so zunanje sile v skladu z:

Furthermore, it is assumed, that the external loads are in accordance with:

$$\int_A \sigma_{xx}\mathrm{d}A = N(x) = 0 \qquad (2),$$

medtem ko sta preostali rezultanti:

while the remaining two resultants:

$$\int_A \sigma_{xx}z\mathrm{d}A = M_y(x) \ , \ \int_A \sigma_{xz}\mathrm{d}A = T_z(x) = \frac{\mathrm{d}M_y(x)}{\mathrm{d}x} \qquad (3)$$

v splošnem od nič različni. Z upoštevanjem ničelnih napetostnih komponent ($\sigma_{yy}(x,y,z)= \sigma_{zz}(x,y,z)= \sigma_{yz}(x,y,z)=0$) in Bernoulli-Navierjeve hipoteze sledi linearna porazdelitev osnih deformacij ε_{xx} po višini prereza, kar v primeru elastičnega odziva (sl. 1a) vodi tudi do linearne porazdelitve napetosti $\sigma_{xx}(x,y,z)$. Če uvedemo poenostavljen zapis $\sigma_{xx}=\sigma$ in $M_y=M$, lahko to zvezo glede na prvo od enačb (3) zapišemo kot:

are non-zero, in general. By considering the zero stress components, $\sigma_{yy}(x,y,z)=\sigma_{zz}(x,y,z)= \sigma_{yz}(x,y,z)=0$, the Bernoulli-Navier assumptions lead to a linear distribution of the axial strain ε_{xx} across the cross-sectional height, and consequently, in the case of an elastic response (Fig. 1a), to a linear stress $\sigma_{xx}(x,y,z)$ distribution, too. By introducing simplified notations, $\sigma_{xx}=\sigma$ and $M_y=M$, this relationship can be written, in accordance with first of Equations (3), as:

$$\sigma(x,z) = \frac{M(x)}{I}z \qquad (4),$$

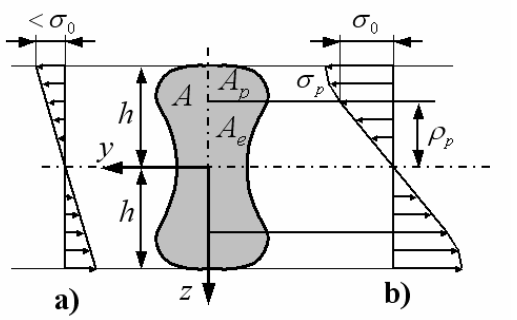

Sl. 1. *Porazdelitev napetosti pri problemu upogiba nosilcev: a) elastična, b) elastoplastična*
Fig. 1. *Stress distribution in a beam-bending problem. a) elastic, b) elasto-plastic*

kjer je I vztrajnostni moment prereza glede na glavno os y. Slika 1b prikazuje napetostno stanje, ko upogibne napetosti presežejo mejo tečenja σ_0. V primeru elastoplastičnega odziva je napetostno stanje odvisno od narave trenutnega odziva:

where I is the area moment of inertia with respect to the principal axis y. Fig. 1b describes the stress state when the bending stress exceeds the yield stress σ_0. In the case of an elastic-plastic response, the respective stress distribution is governed by the nature of the actual response:

$$\sigma(x,z) = \operatorname{sign}\left(M(x)\right)\begin{cases} \dfrac{z}{\rho_\mathrm{p}(x)}\sigma_0 & \ldots \ |z| \le \rho_\mathrm{p}(x) \\ \operatorname{sign}(z)\,\sigma_\mathrm{p}\left(\varepsilon_\mathrm{p}(x,z)\right) & \ldots \ |z| > \rho_\mathrm{p}(x) \end{cases} \tag{5}.$$

Pri tem je primerjalna plastična deformacija ε_p vzeta kot absolutna vrednost vzdolžne plastične deformacije $\varepsilon_{xx}=\varepsilon$, medtem ko $\sigma_\mathrm{p}(\varepsilon_\mathrm{p})$ označuje zvezo med napetostmi in plastičnimi deformacijami, ki jo določa enoosni natezni preizkus. Parameter $\rho_\mathrm{p}(x)$ popisuje stopnjo plastične deformacije določenega prereza in označuje ločnico med elastičnim in plastičnim območjem prereza. Ta parameter je povezan z upogibnim momentom z enačbo (3), pri čemer je upoštevana porazdelitev napetosti (5):

Here, the equivalent plastic strain ε_p is taken as the absolute value of the axial plastic strain $\varepsilon_{xx}=\varepsilon$, while $\sigma_\mathrm{p}(\varepsilon_\mathrm{p})$ denotes the stress-plastic strain relationship, as determined from a uniaxial tensile test. The parameter $\rho_\mathrm{p}(x)$ describes the degree of plastic loading of the particular section and shows the boundary between the elastic and plastic regions of the section. This parameter is related to the bending moment with Equation (3), considering the stress distribution (5):

$$\int_{A_\mathrm{p}} \operatorname{sign}(z)\,\sigma_\mathrm{p}\left(\varepsilon_\mathrm{p}(x,z)\right) z\,\mathrm{d}A + \int_{A_\mathrm{e}} \frac{z^2}{\rho_\mathrm{p}(x)}\sigma_0\,\mathrm{d}A = \left|M(x)\right| \tag{6}.$$

Najprej definirajmo elastični in plastični mejni moment $M_\mathrm{e}(x)$ in $M_\mathrm{p}(x)$. Elastični mejni moment $M_\mathrm{e}(x)$ je notranji upogibni moment, ki še vedno povzroča samo elastične deformacije v prerezu pri vzdolžni koordinati x in ga izračunamo z limitiranjem enačbe (6), upoštevajoč $A_\mathrm{e}\to A$, $A_\mathrm{p}\to 0$ in $\rho_\mathrm{p}(x)\to h$. Plastični mejni moment je notranji upogibni moment, pri katerem postane prerez v celoti plastično deformiran in ga izračunamo z limitiranjem enačbe (6), upoštevajoč $A_\mathrm{e}\to 0$, $A_\mathrm{p}\to A$ in $\rho_\mathrm{p}(x)\to 0$. Naj poudarimo, da velja enačba (6) za dani notranji upogibni moment $|M(x)|$ le, če je prerez delno plastično deformiran, tj.

Let us first define the elastic and plastic limit moments, $M_\mathrm{e}(x)$ and $M_\mathrm{p}(x)$. The elastic limit moment $M_\mathrm{e}(x)$ is the bending moment, which still causes only an elastic deformation in the cross-section at a longitudinal position x, and can be computed using the limit of Equation (6), i.e., $A_\mathrm{e}\to A$, $A_\mathrm{p}\to 0$ and $\rho_\mathrm{p}(x)\to h$. The plastic limit moment $M_\mathrm{p}(x)$ is the bending moment where the cross-section is fully plastically deformed, and can be computed using the limit of Equation (6), i.e., $A_\mathrm{e}\to 0$, $A_\mathrm{p}\to A$ and $\rho_\mathrm{p}(x)\to 0$. Let us emphasize that for a given bending moment $|M(x)|$ Equation (6) is valid only when the cross-section is partially plastically deformed, i.e., $0<M_\mathrm{e}(x)\le|M(x)|\le M_\mathrm{p}(x)$. With regard to the limit elastic

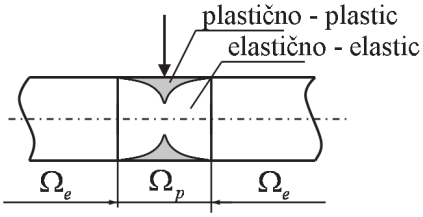

Sl. 2. *Razdelitev na elastična in elastoplastična polja vzdolž nosilca*
Fig. 2. *Elastic and elastic-plastic domain decomposition along the beam*

$0<M_e(x)\leq|M(x)|\leq M_p(x)$. Glede na velikost elastičnega mejnega momenta $M_e(x)$ lahko nosilec razdelimo na polja tako, da Ω_e zajema prereze z elastičnim odzivom, Ω_p pa prereze, na katerih je elastični mejni moment presežen (sl. 2).

Zveza med ukrivljenostjo nevtralne osi, ki je podana z $R(x)$, in njenim povesom $w(x)=w(x,z=0)$ v z smeri je enaka:

$$\varepsilon(x,z)=\frac{z}{R(x)}\approx -z\frac{\mathrm{d}^2 w}{\mathrm{d}x^2} \tag{7}.$$

Posledica Bernoulli-Navierjeve hipoteze o ravnosti prereza je, da na tistem prerezu, kjer se pojavijo tako elastične kakor plastične deformacije, porazdelitev deformacij sledi Hookovemu zakonu, ki velja v elastičnem delu prereza:

$$\varepsilon(x,z)=\varepsilon_e(x,z)=\frac{\sigma_e(x,z)}{E} \tag{8}.$$

Z upoštevanjem enačb (7) in (8) sledi:

$$-z\frac{\mathrm{d}^2 w}{\mathrm{d}x^2}=\frac{\sigma_e(x,z)}{E} \tag{9}.$$

Če sedaj uporabimo enačbi (4) in (5), dobimo diferencialno enačbo za oba možna primera, tako za elastični odziv kakor za odziv, ko so se v prerezu A že pojavile tudi plastične deformacije:

$$\frac{\mathrm{d}^2 w}{\mathrm{d}x^2}=\begin{cases}-\dfrac{M(x)}{E\,I} & \ldots\ x\in\Omega_e\\[2ex] \operatorname{sign}\left(-M(x)\right)\dfrac{\sigma_0}{E\,\rho_p(x)} & \ldots\ x\in\Omega_p\end{cases} \tag{10}.$$

Da se izognemo težavam, ki nedvomno nastanejo pri reševanju diferencialne enačbe (10) v primeru elastoplastičnega odziva in poljubnega prereza A, se v nadaljevanju osredotočimo na nosilce pravokotnega prereza, definiranega s širino b in višino $2h$, obe konstanti vzdolž osi x ($A=2bh$, $I=2/3bh^3$). Snovne lastnosti vzamemo

moment $M_e(x)$, the whole beam can be decomposed into domains along the beam, where Ω_e consists of cross-sections with a pure elastic response, while Ω_p consists of all the cross-sections where the elastic limit moment is exceeded (Fig. 2).

The relationship between the curvature of the neutral axis, given by the respective radius $R(x)$ and its deflection $w(x)=w(x,z=0)$, in the z direction is:

The Bernoulli-Navier assumptions about the cross-section's planarity have the consequence that at a particular cross-section where both the elastic and plastic strains are present, the strain distribution of the cross-section is followed by Hooke's law, which is valid in the elastic part of the cross-section, therefore:

Considering Equations (7) and (8) it follows that:

Using Equations (4) and (5) the differential equation governing the two possible cases, i.e., that of the pure elastic response and that of the evolved plastic strains in the cross-section A, can be deduced:

In order to escape from a stack of difficulties, which arise when solving the differential equation (10) in the case of an elasto-plastic response and an arbitrary cross-sectional area A, we will limit ourselves in what follows to a consideration of beams with a rectangular cross-section, defined by a width b and a height $2h$, constant along the x axis ($A=2bh$, $I=2/3bh^3$). The material properties are likewise

kot nespremenljive in izotropne ($\sigma_p(\varepsilon_p)=\sigma_0$). Globina plastičnega območja je določena z velikostjo upogibnega momenta $M(x)$ in s pripadajočo stopnjo preseganja elastičnega mejnega momenta M_e ($|M(x)|>M_e$):

assumed to be constant and isotropic, assuming no plastic hardening ($\sigma_p(\varepsilon_p)=\sigma_0$). The depth of the plastic zone is determined with the magnitude of the bending moment $M(x)$ and the degree by which the limit elastic moment M_e is exceeded ($|M(x)|>M_e$):

$$\rho_p(x) = h\sqrt{3\left(1-\frac{|M(x)|}{bh^2\sigma_0}\right)} \tag{11}.$$

Upoštevajoč $\rho_p=h$ in $\rho_p=0$ dobimo iz zgornje enačbe mejne vrednosti upogibnega momenta $M_e = 2bh^2\sigma_0/3$ in $M_p = bh^2\sigma_0$. Torej so z $|M(x)|=M_e$ vzpostavljeni pogoji za začetek plastičnih deformacij, medtem ko se pri plastičnem mejnem momentu $|M(x)|=M_p$ plastična cona razširi čez celoten prerez.

By considering $\rho_p=h$ and $\rho_p=0$, the limit values $M_e = 2bh^2\sigma_0/3$ and $M_p = bh^2\sigma_0$ of the bending moment are obtained from this equation. Thus, with $|M(x)|=M_e$ the conditions for the initiation of plastic deformation are established, whereas the fulfilment of $|M(x)|=M_p$, the latter being termed the fully plastic moment, causes the plastic zone to spread over the whole of the cross-section.

Vodilno enačbo upogibnega problema (10), definirano na območju Ω, ($\Omega=\Omega_e\cap\Omega_p$, $\Omega_e\cup\Omega_p=0$), lahko končno preoblikujemo v:

The governing equation (10) of the bending problem, which is defined over a domain Ω, ($\Omega=\Omega_e\cap\Omega_p$, $\Omega_e\cup\Omega_p=0$), is finally transformed to:

$$\frac{d^2w}{dx^2} = \begin{cases} -\dfrac{3M(x)}{2Ebh^3} & \ldots\ x\in\Omega_e \\ \dfrac{K}{\sqrt{M_p-|M(x)|}} & \ldots\ x\in\Omega_p \end{cases} \tag{12},$$

kjer je K definiran kot:

where the constant K is defined as:

$$K = \operatorname{sign}\left(-M(x)\right)\sqrt{\frac{b\sigma_0^3}{3E^2}} \tag{13}.$$

2 ANALITIČNA REŠITEV

Medtem ko je analitična rešitev razmeroma preprosta v primeru elastičnega odziva ($x\in\Omega_e$), pa to ne velja za elastoplastični primer ($x\in\Omega_p$). Toda za najpogostejše primere obremenitve, pri katerih je porazdelitev notranjega upogibnega momenta $M(x)$ dana v polinomski obliki $M(x)=P_n(x)$, lahko analitično rešitev izpeljemo. Pri obremenitvi nosilca s zunanjimi točkovnimi silami in momenti ter zvezno porazdeljeno obtežbo je odvisnost momenta $M(x)$ največ polinom drugega reda $M(x)=P_2(x)=m_2x^2+m_1x+m_0$. Ta zveza gotovo zadovoljivo pokriva večino dejanskih obremenilnih primerov.

V primeru elastičnega odziva ($x\in\Omega_e$) se torej lahko rešitev $w(x)$ eksplicitno zapiše v obliki:

2 ANALYTICAL SOLUTION

While a closed-form explicit solution is relatively trivial in the case of the elastic response ($x\in\Omega_e$), this is not true for the elasto-plastic case ($x\in\Omega_p$). However, for the most common loading cases that result in bending-moment distributions $M(x)$ with a polynomial form, $M(x)=P_n(x)$, such analytical solutions can be readily deduced. Namely, the application of concentrated loads, moments and uniformly distributed loads on a beam structure results in moment functions $M(x)$ of, at most, a second-order polynomial $M(x)=P_2(x)=m_2x^2+m_1x+m_0$. This functional relationship allows for a satisfactory analysis of the majority of real loading cases.

In fact the corresponding solution $w(x)$ in the case of an elastic response ($x\in\Omega_e$) results explicitly in the form of:

$$w(x) = -\frac{x^2}{8Ebh^3}\left(m_2x^2+2m_1x+6m_0\right)+C_1x+C_2 \quad , \quad x\in\Omega_e \tag{14},$$

medtem ko je v primeru elasto-plastičnega odziva ($x\in\Omega_p$) rešitev $w(x)$ izpeljana za vsako stopnjo n=0,1,2 predpostavljenega polinoma $M(x)=P_n(x)$ posebej. Eksplicitno izpeljane rešitve so torej:

while in the case of an elasto-plastic response ($x\in\Omega_p$) the respective particular solutions $w_p(x)$ are deduced separately for each of the possible degrees n=0, 1 and 2 of the assumed polynomial function $M(x)=P_n(x)$. The explicit results of these deductions are as follows:

n=0:

n=0:

$$w(x)=\frac{K}{2\sqrt{M_p-|m_0|}}x^2+C_1x+C_2 \quad , \quad x\in\Omega_p \tag{15}$$

n=1:

n=1:

$$w(x)=\frac{4K}{3m_1^2}\sqrt{\left(M_p-|M(x)|\right)^3}+C_1x+C_2 \quad , \quad x\in\Omega_p \tag{16}$$

n=2:

n=2:

$$w(x)=\begin{cases}\dfrac{K}{2\sqrt{|m_2|^3}}\left[T(x)\,\arcsin\dfrac{T(x)}{|D|}+\sqrt{D^2-T^2(x)}\right]+C_1x+C_2 & ;\ \operatorname{sign}\left(M(x)\right)m_2>0\\ \dfrac{K}{2\sqrt{|m_2|^3}}\left[T(x)\,\operatorname{arsh}\dfrac{T(x)}{|D|}-\sqrt{D^2+T^2(x)}\right]+C_1x+C_2 & ;\ \operatorname{sign}\left(M(x)\right)m_2<0\end{cases} \tag{17}$$

, $x\in\Omega_p$.

V zgornji enačbi je $T(x)=\mathrm{d}M(x)/\mathrm{d}x=2m_2x+m_1$ notranja prečna sila, D pa konstanta, izračunana iz koeficientov polinoma drugega reda kot

From the above, $T(x)=\mathrm{d}M(x)/\mathrm{d}x=2m_2x+m_1$ is the shear force and D is a constant obtained from the second-order polynomial coefficients as

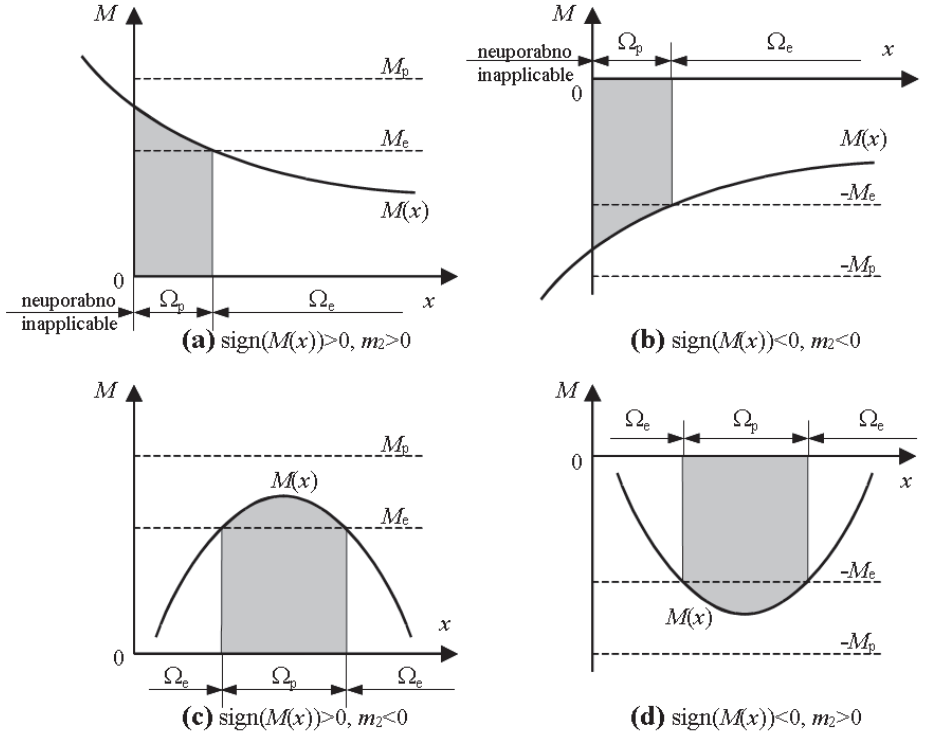

Sl. 3. *Mogoče kvadratične porazdelitve momenta, ki povzročijo plastično tečenje*
Fig. 3. *Possible parabolic moment distributions causing plastic yielding*

$D^2 = B^2 - 4AC$, pri čemer je ta polinom definiran z enačbo $f(x)=M_p-|M(x)|=Ax^2+Bx+C$.

Pravilna izbira rešitve za upogibnico $w(x)$ v primeru kvadratične porazdelitve momenta $M(x)$ je odvisna od oblike uvedene odvisnosti $f(x)$ v elastoplastičnem območju Ω_p. Oblika odvisnosti, ki jo prikazuje slika 3, predstavlja dve fizikalno različni možnosti, kar posledično vodi k dvojnosti rešitve za $w(x)$. Matematično vzeto sta ti dve možnosti za dano porazdelitev momenta $M(x)$ enolično definirani z zmnožkom vodilnega koeficienta m_2 in predznaka momenta $M(x)$. Iz prikazanih grafov za vse mogoče porazdelitve $M(x)$ izhaja, da sta porazdelitvi (a) in (b), ki ju lahko popišemo tudi s $\text{sign}(M(x))\cdot m_2>0$, enakovredni glede na potek odvisnosti $f(x)$, predstavljeno z ukrivljenostjo $d^2w/dx^2<0$. Podobna enakovrednost, opredeljena z ukrivljenostjo $d^2w/dx^2>0$, velja tudi za porazdelitvi (c) in (d), ki pa ju lahko popišemo s $\text{sign}(M(x))\cdot m_2<0$.

Skratka, analitično lahko izračunamo upogibnico nosilcev pravokotnega prereza z uporabo enačb (14) in (17), pri čemer uporabimo enačbo (13) za K.

3 SPLOŠNI OPIS POSTOPKA REŠEVANJA

Ko določimo porazdelitev notranjega upogibnega momenta $M(x)$ za celotni nosilec, ki je za statično določene probleme odvisna samo od zunanjih sil in ne od razvoja plastičnega stanja, območje konstrukcije Ω razdelimo na $N_{ED}+N_{PD}$ polj glede na trenutno mehansko stanje: N_{ED} elastičnih polj $\Omega_e^{(i)}$, $(i=1,...,N_{ED})$ in N_{PD} elastoplastičnih polj $\Omega_p^{(j)}$, $(j=1,...,N_{PD})$. Število polj, na katero razdelimo konstrukcijo, je odvisno od števila različnih predpisov odvisnosti porazdelitve momenta $M(x)$. Takšna razdelitev, ki v celoti pokriva reševanje elastičnega odziva, zahteva dodatne razdelitve, ko se v kateremkoli polju pojavijo plastične deformacije. Takšna razdelitev na koncu prinese N_{PD} polj $\Omega_p^{(j)}$, kjer absolutna vrednost upogibnega momenta $M(x)$ preseže elastični mejni moment M_e, ter N_{ED} polj $\Omega_e^{(i)}$, kjer elastični mejni moment ni presežen. V vsakem od tako dobljenih polj je upogibnica $w(x)$ popisana z eno od enačb (14) do (17), kar privede do problema

$D^2 = B^2 - 4AC$, the considered polynomial being defined by the relation $f(x)=M_p-|M(x)|=Ax^2+Bx+C$.

Regarding the correct selection of the deflection line solution $w(x)$ in the case of a parabolic moment distribution $M(x)$, attention is to be paid to the established functional behaviour of the function $f(x)$ in the elasto-plastic domain Ω_p. This behaviour is characterized, as shown in Fig. 3, by two physically different situations which appear alternatively, and lead, as a consequence, to the duality of the solution $w(x)$. Mathematically, the moment distribution $M(x)$ given these situations is uniquely defined by the product of the leading polynomial coefficient m_2 and the sign of the moment $M(x)$. From the displayed graphs of all possible moment distributions $M(x)$ it follows that the distributions (a) and (b), which are otherwise characterized by the sign of $(M(x))\cdot m_2>0$ are equivalent with respect to the functional behaviour of the function $f(x)$, represented by the curvature $d^2w/dx^2<0$. Similar equivalence, yielding the curvature $d^2w/dx^2>0$, can be attributed to the distributions (c) and (d) that are characterized by the sign of $(M(x))\cdot m_2<0$.

To summarize, the explicit deflection curve for beams with a rectangular cross-section can be calculated with Equations (14) to (17), using Equation (13) for the constant K.

3 GENERAL DESCRIPTION OF THE SOLVING PROCEDURE

After the determination of the bending-moment distribution $M(x)$ over the whole beam, which is for statically determinate problems dependent only on the external loads and not on the plastic state evolution, the structure domain Ω should be partitioned in accordance with the actual mechanical state into $N_D=N_{ED}+N_{PD}$ sub-domains: N_{ED} elastic sub-domains $\Omega_e^{(i)}$, $(i=1,...,N_{ED})$ and N_{PD} elasto-plastic sub-domains $\Omega_p^{(j)}$, $(j=1,...,N_{PD})$. The number of sub-domains that the structure is divided into is first dictated by the number of different functions defining the moment distribution $M(x)$. This partitioning, which completely covers the solution of the problem under the presumed elastic response, needs, however, a further subdivision if in any of these sub-domains the plastic yielding occurs. The latter subdivision finally yields N_{PD} sub-domains $\Omega_p^{(j)}$, i.e., regions where the absolute value of the bending moment $M(x)$ exceeds the elastic limit moment M_e, and N_{ED} sub-domains $\Omega_e^{(i)}$, where the elastic limit moment is not exceeded. In each of the thus obtained sub-domains the deflection $w(x)$ is governed by a corresponding

iskanja vrednosti pripadajočih neznanih integracijskih konstant $\{C_1,C_2\}_j$; (j=1,...,N_D), saj je preostanek odvisnosti $w(x)$ eksplicitno znan. Sistem enačb, ki ga je treba rešiti, če želimo izračunati skupno $2\cdot N_D$ neznanih konstant, je sestavljen z upoštevanjem robnih pogojev in pogojev skladnega prehoda. Naj na tem mestu poudarimo, da je za statično določene konstrukcije sistem vedno linearen in razmeroma majhen, saj je število polj razmeroma majhno celo za zahtevne konstrukcije. Pri statično nedoločenih konstrukcijah pa se pojavijo dodatne neznanke, toda celotni sistem enačb se da v splošnem prevesti na majhen sistem nelinearnih enačb, ki ga je pa treba rešiti numerično. Opisana metoda je zelo učinkovita in preprosta za uporabo, kar bo prikazano v računskem primeru.

4 RAČUNSKI PRIMER

V nadaljevanju bo obravnavan mehanski odziv dvakrat členkasto podprtega nosilca s previsnim poljem, ki je obremenjen s točkovno silo F ($F\geq 0$) na prostem koncu in z zvezno obtežbo q ($q\geq 0$) med podporama (sl. 4). Naj parameter λ ($0<\lambda\leq 1$) pomeni obremenitveni parameter, ki določa stopnjo vnesene obremenitve glede na mejno obremenitev ($\lambda=1$), pri kateri se pojavi izguba funkcionalnosti konstrukcije, ki preide v mehanizem. Nadalje naj λ_e pomeni stopnjo obremenitve, ki ustreza tisti mejni elastični obremenitvi, pri kateri se plastične deformacije še niso pojavile. Za obremenjevanje, katerega posledica je elastični odziv ($\lambda\leq\lambda_e$), je značilna sorazmernost, torej je:

function given by (14) to (17), which results in the problem of finding the respective values of a set of unknown integration constants $\{C_1,C_2\}_j$; (j=1,...,N_D), because the rest of the function $w(x)$ is explicitly known. The system of equations needed to solve the unknown constants, their number being $2\cdot N_D$ in total, is obtained upon the implementation of the corresponding boundary and continuity conditions. Here, let us emphasize that for an arbitrary statically determinate structure this system is always linear and rather small, as the number of sub-domains is relatively low, even in the case of complex structures. For statically indeterminate structures additional unknowns appear, but the whole system of equations can be generally reduced to a small system of nonlinear equations that should be solved numerically. The described method is highly efficient and simple to use, which will be demonstrated through a numerical example.

4 NUMERICAL EXAMPLE

The mechanical response of a simply supported overhanging beam that is subject to a concentrated force F ($F\geq 0$) at its free end and to a uniformly distributed load q ($q\geq 0$) between the supports (Fig. 4), will be considered in the following. Let the parameter λ ($0<\lambda 1$) be the role of the loading parameter that defines the level of the applied loading measured with respect to the limit loading ($\lambda=1$), by which the loss of the structural functionality with the transition to a mechanism occurs. Furthermore, let λ_e denote the loading level corresponding to the elastic limit loading, which is still characterized by the absence of plastic strain in the structure. The application of the loads that result in a linear elastic response ($\lambda\leq\lambda_e$) is characterised by proportionality, therefore:

$$M^{\lambda}(x)=\frac{\lambda}{\lambda_e}M^{e}(x)=\lambda M^{p}(x) \qquad (18),$$

kjer $M^{e}(x)$ in $M^{p}(x)$ označujeta odvisnost upogibnega momenta pri stopnji obremenitve $\lambda=\lambda_e$ in $\lambda=1$, medtem ko je $M^{\lambda}(x)$, ki je shematično prikazan na sliki 4, porazdelitev momenta glede na stopnjo obremenitve λ.

Pri razvoju plastičnih deformacij je poleg obremenitvenega parametra λ pomembno tudi razmerje obeh obremenitev. To razmerje označimo s koeficientom ψ:

where $M^{e}(x)$ and $M^{p}(x)$ denote the functional dependencies of the bending moment at the load levels $\lambda=\lambda_e$ and $\lambda=1$, respectively, and $M^{\lambda}(x)$, shown schematically in Fig. 4, is the respective moment dependence corresponding to the load level λ.

Of importance for the evolution of the plastic strains there is, along with the increase of the loading parameter λ, the ratio established between the two loads. Let us denote the considered load ratio with the coefficient ψ:

$$\psi=\frac{F}{qL_1} \qquad (19).$$

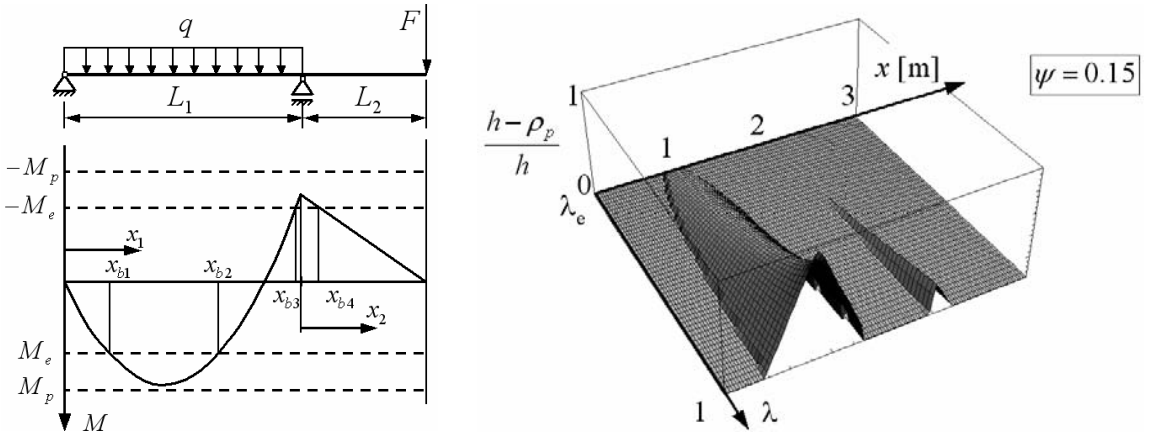

Sl. 4. *Računski primer ter širjenje plastičnega območja s povečevanjem stopnje obremenitve* λ ($\lambda_e<\lambda\leq1$)
Fig. 4. *Numerical example and plastic-zone propagation with increasing load level* λ ($\lambda_e<\lambda\leq1$)

Ker pri predpostavljenem sorazmernem obremenjevanju razmerje med obremenitvama q in F ostaja nespremenjeno, oznaki obremenitve zaradi celovitosti informacije razširimo z indeksom ψ, torej $q\rightarrow q_\psi$ in $F\rightarrow F_\psi$. Obremenjevanje ($d\lambda>0$) je torej podano z:

Since by assumed proportional loading the ratio between the loads q and F remains fixed for any load level λ, the load notations may be enlarged in order to complete the information by adding the index ψ, i.e., $q\rightarrow q_\psi$ and $F\rightarrow F_\psi$. The application of the loads ($d\lambda>0$) is thus characterised by:

$$F_\psi = \lambda F_\psi^{\mathrm{p}} \ \wedge \ q_\psi = \lambda q_\psi^{\mathrm{p}} \quad ; \quad 0<\lambda\leq 1 \tag{20},$$

kjer q_ψ^{p} in F_ψ^{p} označujeta velikost obremenitev, ki povzročijo porušitev konstrukcije, kar se dejansko zgodi s pojavom plastičnega členka. Odvisnost upogibnega momenta $M(x)$ ($0\leq x=x_1\leq L_1 \ \wedge \ 0\leq x=x_2\leq L_2$) je izražena z brezrazsežnima koordinatama $\xi(\xi L_1=x_1)$ in $\eta(\eta L_2=x_2)$, kjer je $0\leq\xi,\eta\leq1$,

where q_ψ^{p} and F_ψ^{p} denote the magnitudes of the loads causing the collapse of the structure, which actually happens during the occurrence of a plastic hinge. The bending-moment function $M(x)$ ($0\leq x=x_1\leq L_1 \ \wedge \ 0\leq x=x_2\leq L_2$) is expressed in terms of the non-dimensional coordinates $\xi(\xi L_1=x_1)$ and $\eta(\eta L_2=x_2)$, where obviously $0\leq\xi,\eta\leq1$,

$$\begin{aligned} M_1(\xi) &= F_\psi L_2\left[\frac{m}{2\psi}(1-\xi)-1\right]\xi = q_\psi L_1^2\left[\frac{1}{2}(1-\xi)-\frac{\psi}{m}\right]\xi \\ M_2(\eta) &= F_\psi L_2(\eta-1) = q_\psi L_1^2\frac{\psi}{m}(\eta-1) \qquad ; \quad m=\frac{L_1}{L_2} \end{aligned} \tag{21}.$$

Glede na razvoj elastoplastičnega stanja se v odvisnosti od obremenilnega razmerja ψ pojavi več mogočih primerov. Če prevladuje obremenitev q, tj. $0\leq\psi\leq\psi_1=\left(2-\sqrt{15/2}\right)m$, se plastifikacija nosilca pojavi med podporama, če pa prevladuje sila F, tj. $\psi_3=\left(7-2\sqrt{15}\right)m/6\leq\psi<\infty$, se nosilec plastificira pod desno podporo, v obeh primerih ne glede na stopnjo obremenitve ($\lambda_e<\lambda\leq1$). Značilnost primerov, kjer je obremenilno razmerje $\psi_1<\psi<\psi_3$, je obstoj dveh plastičnih področij pri velikosti momenta ob porušitvi. V teh primerih, razen za obremenilno razmerje

In relation to the load ratio ψ, several possible cases can occur ψ, regarding the elasto-plastic state evolution. While the prevailing of the load q, i.e., $0\leq\psi\leq\psi_1=\left(2-\sqrt{15/2}\right)m$ results in the plastification of the beam between the supports, the prevailing of the load F, i.e., $\psi_3=\left(7-2\sqrt{15}\right)m/6\leq\psi<\infty$, leads to the beam plastification at the right support, both regardless of the load level ($\lambda_e<\lambda\leq1$). The load cases corresponding to the load ratio $\psi_1<\psi<\psi_3$ are characterized at the moment of collapse by the existence of two separate plastic regions. Typical for the elasto-plastic evolution in the latter cases, except for $\psi=\psi_2=\left(3/2-\sqrt{2}\right)m$,

$\psi = \psi_2 = \left(3/2 - \sqrt{2}\right)m$, pri katerem nastaneta dva plastična členka hkrati, je za razvoj elasto-plastičnega stanja značilno, da se najprej pojavi eno plastično območje ($\lambda_e<\lambda\leq\lambda^*<1$), šele nato pa tudi drugo ($\lambda^*<\lambda\leq 1$).

Oglejmo si primer razvoja elasto-plastičnega stanja za primer, ko je m=2 in ψ=0,15. Ker je $\psi_1<\psi<\psi_2$, se plastične deformacije najprej pojavijo med podporama pri stopnji obremenitve λ_e in šele nato se pojavijo plastične deformacije pri stopnji obremenitve λ^* pri desni podpori. Rešitev problema, ki naj vsebuje tudi izračun upogibnice konstrukcije $w(x)$, je dobljena z upoštevanjem pripadajočih splošnih rešitev (14) do (17) glede na izkazan mehanski odziv pri danem obremenilnem razmerju ψ in pri vsiljeni stopnji obremenitve λ, pri čemer so izpolnjeni robni pogoji in pogoji skladnega prehoda na mejah med elastičnimi in elastoplastičnimi polji. Če si ogledamo odvisnost elasto-plastičnega dela rešitve za $\lambda_e<\lambda\leq\lambda^*$, opazimo, da rešitev sestavljajo štiri različne funkcije, ki popisujejo obnašanje v treh elastičnih in enem elastoplastičnem polju. Upoštevaje naravo snovnega odziva v teh poljih, je enačba (14) kot delna rešitev uporabljena trikrat, enačba (17) pa enkrat. Toda povečevanje obremenitve, izpolnjujoč odvisnost $\lambda^*<\lambda\leq 1$, je povezano s plastifikacijo novega polja, kar privede do šestih različnih odvisnosti za popis končne rešitve, pri čemer je v treh poljih obnašanje elastično, v treh pa elastoplastično, kar je jasno razvidno iz porazdelitve momentov, prikazane na sliki 4. Tu je znova glede na prikazano porazdelitev momenta enačba (14) uporabljena trikrat, enačba (16) enkrat in (17) dvakrat. Da bi določili rešitev upogibnice $w(x)$ v celoti, preostane še izračun sistema 8 (ali 12) linearnih enačb z 8 (ali 12) neznanimi konstantami C_i. Z rešitvijo sistema, ki je dobljen z upoštevanjem robnih pogojev in pogojev skladnega prehoda, na koncu dobimo eksplicitni izraz za upogibnico $w(x)$.

Širjenje plastičnega območja vzdolž nosilca enolično določa enačba $M^{\lambda}(x)=M_e$, ko se vsiljene obremenitve povečujejo ($d\lambda>0 \wedge 0<\lambda\leq 1$), medtem ko je širjenje plastičnega območja v globino nosilca dano z enačbo (11). Ker je sorazmernost notranjih veličin ohranjena med celotnim postopkom obremenjevanja za katerokoli obremenilno razmerje ψ, je velikost stopnje

i.e., the load ratio, which leads to the appearance of two plastic hinges at the same time, is that the first plastic region is created ($\lambda_e<\lambda\leq\lambda^*<1$), and only afterwards ($\lambda^*<\lambda\leq 1$) is it followed by the appearance of the second plastic region.

Let us now present the elasto-plastic state evolution for the case where m=2 and ψ=0.15. Because $\psi_1<\psi<\psi_2$, the plastic strains first occur between the supports at load level λ_e and then at load level λ^* the plastic strains also occur at the right support. The solution of the problem, when the deflection of the structure $w(x)$ is to be evaluated as well, is obtained by considering the respective general solutions (14) to (17), according to the proven deformation response behaviour at a given load ratio ψ and load level λ applied and fulfilling the associated boundary conditions and continuity conditions at the interfaces between the elastic and the elasto-plastic sub-domains. Observing the functional dependence of the elasto-plastic part of the solution for $\lambda_e<\lambda\leq\lambda^*$, we find that it consists of four distinct functions that describe the respective response behaviour in three elastic sub-domains and one elasto-plastic sub-domain. Considering the evidenced nature of the material response in these sub-domains, Equation (14) is applied as the corresponding particular solution three times, and Equation (17) once. But a further increase in the loads, fulfilling the relation $\lambda^*<\lambda\leq 1$, is accompanied by the plastification of new sub-domains, which demands six distinct functions for the corresponding solution description, three covering the elastic response and three covering the elasto-plastic response in the respective sub-domains, which is clearly seen from the moment distribution in Fig. 4. Again with regard to the shown bending-moment distribution, Equation (14) is applied three times, while Equation (16) is used once and (17) twice. There remains, in order to determine the solution of the deflection line functions $w(x)$ entirely, a derivation of a corresponding system of 8 (or 12) linear equations with 8 (or 12) constants C_i as unknowns. By solving this system, which is obtained by the imposition of the corresponding boundary and continuity conditions, an explicit expression for the solution $w(x)$ is finally determined.

The propagation of the plastic domain along the beam structure is uniquely defined by the equation $M^{\lambda}(x)=M_e$ as the applied loads are increased ($d\lambda>0 \wedge 0<\lambda\leq 1$), while the penetration of the plastic region inside the beam is given by Equation (11). Also, as the proportionality of the internal forces is preserved through the whole loading, the magnitude of the elastic limit load level

obremenitve, ki ustreza mejni elastični obremenitvi, vedno enaka λ_e=2/3. V nadaljevanju prikazani rezultati so dobljeni z upoštevanjem naslednjih geometrijskih in snovnih podatkov: dolžini nosilca L_1=2m in L_2=1m, širina prereza b=20mm ter njegova polovična višina h=20mm, modul elastičnosti E=210 GPa in meja tečenja σ_0=300MPa. Za dano geometrijsko obliko nosilca je na sliki 4 prikazan razvoj plastičnih deformacij, ko se stopnja obremenitve zveča in je v koraku $\lambda_e<\lambda\leq 1$. S te slike, ki predstavlja širino in globino plastičnih območij, lahko opazimo, da se je plastifikacija najprej pojavila med podporama in šele nato ob desni podpori. Ker je razvoj plastičnih deformacij sorazmeren obremenitvi, se edini plastični členek prav tako pojavi med podporama.

Vpliv upoštevanja snovne nelinearnosti v mehanskem odzivu vsekakor velja ovrednotiti kvantitativno, s čimer ocenimo smiselnost uporabe elastoplastičnih enačb (14) do (17) v primerjavi z izključno uporabo enačbe (14), pri katerih je neelastični vpliv zanemarjen. Ker so statične veličine, kakor so napetostne rezultante in reakcijske sile, neodvisne od narave odziva snovi v primeru statično določenega problema, analizo omejimo samo na izračun deformacijskih veličin, kot so poves $w(x)$, relativni zasuki $\varphi_\varepsilon(x)$ v okolici x ter mesto največjega pomika x_w med podporama. Kot merilo odstopanja od linearnega odziva, označenega z indeksom "e", uporabimo naslednje veličine: $r_w(x)$ za odstopanje pomikov ter $r_\varphi(x)$ za odstopanje relativnih zasukov okrog točke (v ε-okolici x), kjer se pojavi plastični členek. Opazovane veličine so definirane z:

$$r_w(x)=\left(\frac{w(x)}{w^e(x)}-1\right)\cdot 100\%\,,\quad r_\varphi(x)=\left(\frac{\varphi(x+\Delta)-\varphi(x-\Delta)}{\varphi^e(x+\Delta)-\varphi^e(x-\Delta)}-1\right)\cdot 100\% \qquad (22).$$

V obravnavanem primeru je smiselno opazovati naslednje veličine: $r_w(x_C)$ na prostem koncu, $r_w(x_M)$ in $r_\varphi(x_M)$ pa na mestu največjega notranjega upogibnega momenta med podporama, pri čemer je Δ=10mm. Opazovane veličine so predstavljene v preglednici 1.

Vrednosti veličin v preglednici kažejo, da se pri sorazmernem večanju obremenitve od $\lambda=\lambda_e$ do $\lambda\to 1$ vpliv nelinearnosti povečuje, pri čemer je tabeliranje narejeno za boljši prikaz ob uporabi enakomernega obremenilnega koraka ($\Delta\lambda$=konst.). Konec koncev je to tudi

is always, irrespective of the load ratio ψ, equal to λ_e=2/3. The results were calculated using the following geometrical and material data: lengths of the beam L_1=2m and L_2=1m, cross-sectional width b=20mm and half-height h=20mm, the modulus of elasticity E=210 GPa and the yield stress σ_0=300MPa. For this particular geometry of the structure there is, plotted in Fig. 4, a plastic strain evolution, as the load level is increased within the interval $\lambda_e<\lambda\leq 1$. From this figure, which represents the depth and the width of the plastic zone, it can be seen that the first plastic yielding occurs between the supports, but after that it appears also at the right support. Since the plastic strain evolution is proportional to the loading, the only plastic hinge occurs between the supports.

The impact of considering the material non-linearity in the mechanical response is certainly appropriate for being analysed quantitatively, thus estimating the reasonableness of using the elasto-plastic Equations (14) to (17) in comparison to Equation (14), where the inelasticity of the response is neglected. With the static quantities, i.e., the stress resultants and support reaction forces, independent of the nature of the material response in a statically determinate problem, such an estimation analysis reduces to an evaluation of the deformation quantities, such as the displacement $w(x)$, the relative rotation $\varphi_\varepsilon(x)$ in the ε-neighbourhood of x and the location of the maximum displacement x_w between the supports. As a measure for the deviation from the linear response, denoted by a suffix "e", the following quantities can be used: $r_w(x)$ for the displacement deviations and $r_\varphi(x)$ for the relative rotation deviations around the point (in the neighbourhood of x), where the plastic hinge occurs. The inspected quantities' definitions are as follows:

It is reasonable in the investigated example to observe the following quantities: $r_w(x_C)$ at the free end, $r_w(x_M)$ and $r_\varphi(x_M)$ at the position of the maximum bending moment between the supports, taking Δ=10mm. The observed quantities are presented in Table 1.

The tabulated quantities show that the proportional increase of the considered loading from $\lambda=\lambda_e$ to $\lambda\to 1$, the tabulation being made for greater evidence on the basis of an equidistant load-step incrementation ($\Delta\lambda$=const.), leads to the growing influence of the non-linearity. As a matter of fact, this

Preglednica 1. *Odstopanje elastoplastičnega od elastičnega odziva*
Table 1. *Deviations of elastic-plastic from the linear elastic response*

λ_i	$r_\varphi(x_M)$ [%]	$r_w(x_M)$ [%]	$r_w(x_C)$ [%]
$8/12 = \lambda_e$	0,0	0,0	0,0
9/12	2,6	0,9	3,7
10/12	13,1	5,7	22,3
11/12	45,4	20,4	79,0
$1 - 1 \cdot 10^{-9}$	13972,5	582,8	2027,9

pričakovano. S širjenjem plastičnega območja in s posledičnim slabljenjem elastične odpornosti konstrukcije je odstopanje od elastične rešitve vedno izrazitejše s približevanjem $\lambda \rightarrow 1$. V bližini singularne točke, kjer je dosežena končna vrednost $\lambda=1$, vse opazovane veličine izkazujejo naglo povečanje, pri čemer se asimptotično približujejo neskončnosti. Pri $\lambda=1$ je najbolj obremenjen prerez v celoti plastificiran in konstrukcija, v tem primeru statično določena, se spremeni v mehanizem s pojavom plastičnega členka. Ko se to zgodi, je izvirna namembnost in nosilnost konstrukcije izgubljena, kar je enako porušitvi.

5 SKLEP

V prispevku je predstavljena zelo preprosta in učinkovita metoda za obravnavanje elastoplastičnega obnašanja ravnih nosilcev. Postopek temelji na eksplicitnih odvisnostih upogibnice za delno plastificirana polja nosilca pravokotnega prereza, obremenjenega z značilnimi obremenitvami, vključujoč točkovne sile in momente ter zvezno porazdeljeno obtežbo. Eksplicitne oblike odvisnosti upogibnic, prikazane z enačbami (14) do (17), so bile uspešno izpeljane analitično na osnovi klasične teorije upogiba nosilcev, kar pomeni trden matematični okvir za elastoplastično analizo tovrstnih črtnih konstrukcij.

Z uporabo eksplicitno izpeljanih rešitev postane postopek reševanja elastoplastičnih problemov upogiba nosilcev zelo preprost, ne glede na to, da snov izkazuje nelinearno obnašanje. Ker je končna rešitev dobljena z razrešitvijo razmeroma majhnega sistema enačb, je tak postopek tudi učinkovit. Predstavljena metoda je torej uporabna za spremljanje razvoja plastičnega deformiranja med sorazmernim obremenjevanjem nosilcev.

is to be expected. Namely, with the intensification of the plastic propagation and consecutive weakening of the structural elastic resistance the departure from linearity becomes more and more apparent as the loads approach $\lambda \rightarrow 1$. Near the singularity point, where the ultimate load level $\lambda=1$ is reached, all the observed quantities exhibit a rapid increase, with their values asymptotically approaching infinity. At $\lambda=1$ the most stressed cross-section becomes fully plastified, and the structure, the problem being a statically determinate one, transforms into a mechanism due to the occurrence of a plastic hinge. When this happen, the originally designed functionality and load-carrying capacity of the structure are lost, which is equivalent to a collapse.

5 CONCLUSIONS

In the paper a very simple and efficient method for the elasto-plastic behaviour of straight beams is presented. The approach is based on the explicit deflection line functions for partially plastic domains of a beam with a rectangular cross-section under characteristic loading cases, including the application of concentrated forces and moments as well as the application of uniformly distributed loads. Explicit forms of the deflection lines, listed in Equations (14) to (17), were successfully analytically derived, following the classical beam-bending formulation, thus forming a firm mathematical framework for the elastic-plastic analyses of the considered kind of beam structures.

By taking the derived explicit solutions into account the procedure needed to solve an elasto-plastic bending-beam problem becomes very simple, irrespective of the exhibited non-linear material behaviour. Since the solution is obtained by solving a relatively small system of equations, this procedure is also efficient. The presented method can be used to trace the plastic-yielding evolution during the proportional loading of beams.

6 LITERATURA
6 REFERENCES

[1] Goodier J.N., Hodge P.G. (1985) Elasticity and plasticity. *John Wiley & Sons Inc.*, New York.
[2] Kaliszky S. (1989) Plasticity, theory and engineering applications. *Akadémiai Kiadó*, Budapest.
[3] Prager, W., Hodge, P.G. (1951) Theory of perfectly plastic solids. *Dover Publications Inc.*, New York.
[4] Reissner, E. (1973) On one-dimensional, large-displacement, finite-strain beam theory. *Stud. Appl. Math*. 52, 87-95.
[5] Mendelson, A. (1968) Plasticity: theory and application. *MacMillan Company*, New York.
[6] Saje, M., Planinc, I., Turk, G., Vratanar, B. (1997) A kinematically exact finite element formulation of planar elastic-plastic frames. *Comput. Methods Appl. Mech. Eng.* 144 (1/2), 125-151.
[7] Saje, M., Srpčič, S. (1985) Large deformations of in-plane beam. *Int. J. Solids Struct.* 21 (12), 1181-1195.
[8] Smith J.O., Sidebottom O.M. (1965) Inelastic behavior of load-carrying members. *John Wiley & Sons Inc*., New York.
[9] Štok B., Kosel F. (1985) On determination of tool geometry by elasto-plastic bending of beams under pure bending condition (in slovene). In: *Proceeding of 4th Yugoslav Symposium on Plasticity*, Tuheljske toplice.
[10] Vratanar, B., Saje, M. (1999) A consistent equilibrium in a cross-section of an elastic-plastic beam. *Int. J. Solids Struct.* 36 (2), 311-337.
[11] Życzkowski M. (1981) Combined loadings in the theory of plasticity. *PWN-Polish Scientific Publishers*, Warsaw.

Naslov avtorjev: Miroslav Halilovič
prof. dr. Boris Štok
Univerza v Ljubljani
Fakulteta za strojništvo
Aškerčeva 6
1000 Ljubljana
boris.stok@fs.uni-lj.si

Authors' Address: Miroslav Halilovič
Prof. Dr. Boris Štok
University of Ljubljana
Faculty of Mechanical Eng.
Aškerčeva 6
SI-1000 Ljubljana, Slovenia
boris.stok@fs.uni-lj.si

Prejeto: 20.7.2007
Received:

Sprejeto: 28.9.2007
Accepted:

Odprto za diskusijo: 1 leto
Open for discussion: 1 year

Strojniški vestnik - Journal of Mechanical Engineering 53(2007)12, 819-833
UDK - UDC 678.017
Izvirni znanstveni članek - Original sceintific paper (1.01)

Analitični model določevanja mehanskih lastnosti biopolimernih kompozitov - mikromehanski postopek

A Model for Predicting the Mechanical Properties of Wood-Plastic Composites - A Micro-Mechanical Approach

Aleš Hančič[1] - Franc Kosel[2] - A. R. Campos[3] - A. M. Cunha[4] - Gašper Gantar[1]
([1]TECOS Razvojni center orodjarstva Slovenije, Celje; [2]Fakulteta za strojništvo, Ljubljana; [3]PIEP - Innovation in Polymer Engineering, Portugal; [4]University of Minho, Portugal)

V zadnjem desetletju prejšnjega stoletja se je pričel razvoj novih kompozitov, sestavljenih iz naravnih vlaken in cenejših polimerov, kakor sta npr. HDPE in PP. Zaradi relativno kratkega časa prisotnosti na trgu in naključnih lastnosti vlaken do sedaj še ni bilo poskusov analitičnega določevanja mehanskih lastnosti omenjenih kompozitov. V tem prispevku je uporabljen mikromehanični postopek, imenovan posplošena metoda celic (PMC - GMC) za popis lastnosti injekcijsko brizganih biopolimernih kompozitov, sestavljenih iz polipropilena (PP) ali polistirena (PS) ter lesnih ali celuloznih vlaken. Glavni problem pri analitičnim postopku je, da naravna vlakna nimajo enotne dolžine, prereza ali oblike, zato jih je težko popisati z običajnimi matematičnimi modeli, tako da so v prispevku uporabljene povprečne vrednosti geometrijskih lastnosti vlaken. Kompoziti so bili najprej pregledani z optičnim in elektronskim mikroskopom z namenom določiti lastnosti in razporeditev vlaken. Ti podatki so bili nato uporabljeni pri ugotavljanju elastičnega in plastičnega odziva kompozita ter njegovih porušnih vrednosti, ki so bile izračunane po Tsai-Hillovi porušni hipotezi. Rezultati so bili nato primerjani z eksperimentalnimi podatki, tako da je bilo mogoče oceniti praktično uporabnost te metode. Časovno odvisne mehanske lastnosti materiala tu niso bile upoštevane zaradi zapletenosti in naključnih lastnosti vlaken.

(Ključne besede: biopolimerni kompoziti, posplošena metoda celic, naravna vlakna, mehanske lastnosti)

The development of a new composite that is made up of natural fibres and low-price polymers, such as HDPE or PP, began in the 1990s. Because this material is relatively new to the market and due to the random characteristics of the fibres, no attempts have been made to analytically define the mechanical properties of this material. In this paper a micro-mechanical approach, called the generalised method of cells (GMCs), is introduced to describe the properties of injection-moulded wood-plastic composites made up of polypropylene (PP) or polystyrene (PS) and wood or cellulose short fibres. The main problem with an analytical approach is that the natural fibres are not uniform in shape and size, which makes them hard to fit into standard mathematical models. In this paper the average values of the fibre sizes were used. The materials were first scanned with optical and electron microscopes to determine the fibre properties and their scatter. These values were then used to determine the elastic and plastic response of the composite together with the maximum strength and elongation of the composite, where the Tsai-Hill failure-criterion was used. The results were then compared to the experimental data in order to evaluate the practical usefulness of this method. The time-dependent mechanical behaviour of the composite was not considered due to the complex and random properties of the fibre.

(Keywords: wood-plastic composites, generalised method of cells (GMC), natural fibres, mechanical properties)

0 UVOD

V zadnjem desetletju prejšnjega stoletja se je pričel razvoj novih kompozitov, v katerih so bile združene dobre lastnosti tako lesa kakor tudi

0 INTRODUCTION

The development of a new composite began in the 1990s. This composite combined the good properties of wood and polymer [1]. It became

polimerov [1]. Izkazalo se je, če čistemu polimeru, na primer polietilenu (PE), dodamo lesna vlakna, se njegove mehanske lastnosti znatno izboljšajo. Povečata se mu elastični modul *E* in natezna trdnost, obdrži pa tudi nekatere dobre lastnosti lesa, ob tem pa je kompozit razmeroma dobro odporen proti vremenskim pojavom.

Ker so naravna vlakna naključno oblikovana v razmeroma zapletene geometrijske oblike, je njihov popis mnogo težavnejši v primerjavi z drugimi kratkimi, npr. steklenimi ali ogljikovimi vlakni, ki so ravna in imajo nespremenljiv prerez. Pri le-teh, namreč lahko, če poznamo splošno usmeritev vlaken ter lastnosti posameznega vlakna, dokaj natančno določimo elasto-plastične lastnosti kompozita [2]. Vendar je pri naravnih vlaknih to problem, saj je nemogoče določiti lastnosti posameznega lesnega ali celuloznega vlakna, vlakna so mnogo prekratka, da bi na njih opravili natezni preizkus. Povrh tega se njihove lastnosti ob toplotnem postopku kompozita spremenijo, saj je za učinkovito brizganje mešanico treba segreti na okrog 190 °C. Vlakna po postopku tudi niso ravna, ampak zvita, kar še dodatno otežuje njihov popis.

Metoda celic in njena posodobljena različica, tj. posplošena metoda celic (PMC), ki ju je v 90. letih razvil Jacob Abudi [3], je analitični mikromehanski model za določevanje elastičnih in plastičnih lastnosti vlaknatih kompozitov. Temelji na predpostavki, da so vlakna periodično urejena, med njimi pa je osnovni material. Periodična narava kompozita omogoči, da ga razdelimo na med seboj enake gradnike ali celice, nato pa obravnavamo le posamezno celico. Lastnosti posamezne celice so tako veljavne za celotni kompozit. Tako lahko popišemo kompozite z dolgimi vlakni (dvojna periodičnost celic), kratkimi vlakni (trojna periodičnost), laminate ter tudi porozne materiale [4]. V nadaljevanju prispevka so predstavljeni teoretični model PMC, eksperimentalno delo ter primerjava med eksperimentalnimi in teoretičnimi, s PMC pridobljenimi podatki.

1 OPIS POSPLOŠENE METODE CELIC

Ker opisujemo prekinjani kompozit s kratkimi vlakni, je treba uporabiti metodo celic s trojno periodičnostjo. Tu so vlakna periodično urejena v osnovi v identične kvadre, kar prikazuje

evident that if wood particles are added to a polymer matrix such as polyethylene (PE) the mechanical properties of the new composite are significantly improved. The Young's modulus *E* and the tensile strength are increased and, additionally, the composite is also weather resistant.

Natural fibres have a much more complex and random geometry than other short fibre fillers, such as glass or carbon fibres, which are straight and have a constant cross-section. With these types of fibres, knowing the general orientation and properties of an individual fibre, means that the elasto-plastic properties of the composite can be determined with a high degree of accuracy [2]. On the other hand, it is nearly impossible to determine the properties of an individual wood or cellulose fibre because it is much too short for tensile tests. Furthermore, their properties are changed after thermally processing the composite due to heating to at least 190°C, which is required for an effective injection. In addition, the fibres are not straight after the processing; they are curled, which makes their description even more difficult

The method of cells and its modernised version, the generalised method of cells (GMCs), were developed in the 1990s by Jacob Abudi [3]. They represent an analytical micro-mechanical model for determining the elastic and plastic properties of the composites. It is based on the assumption that the fibres are arranged in a periodic array and the space between them is occupied by the matrix material. The periodic nature of the composite makes it possible to divide it into equal building blocks or cells, and then to study only an individual cell. The properties of the one cell are then representative of the whole composite. Thus, composites with long fibres (double periodicity) or short fibres (triple periodicity), laminates and porous materials can be described [4]. In the remainder of the paper a theoretical model of GMCs is presented, as well theoretical work and a comparison between the experimental and theoretical results based on the GMCs.

1 DESCRIPTION OF THE GENERALISED METHOD OF CELLS

Since a discontinuous composite with short fibres is being described, the method of cells with a triple periodic array has to be used. Here, the fibres are periodically arranged in identical rectangular

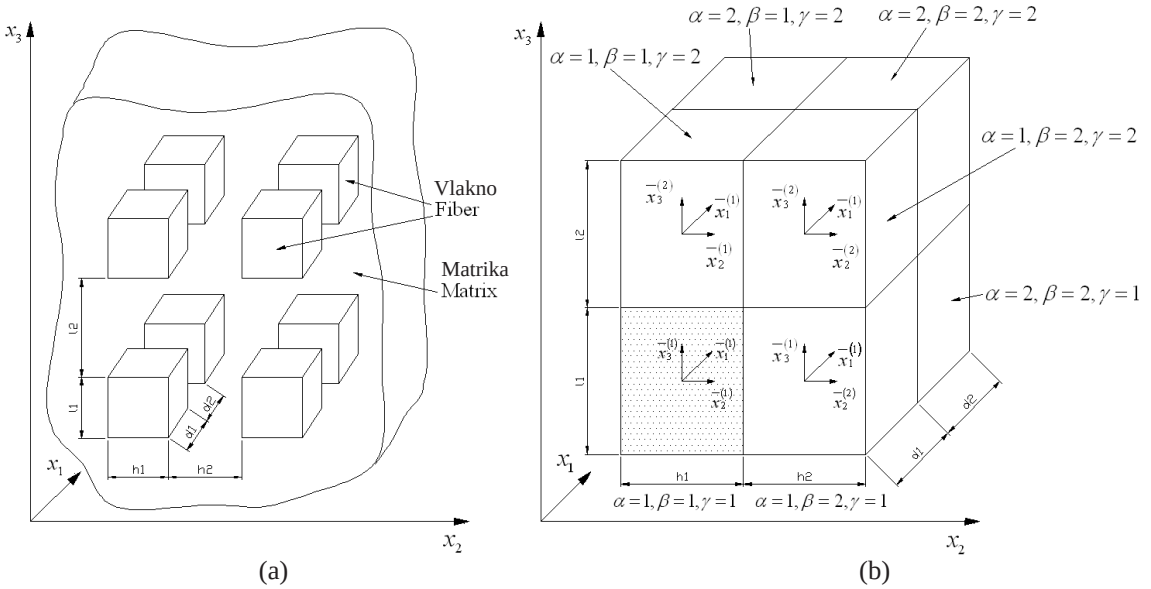

Sl. 1. *(a) Kompozit z vključki vlaken, urejenimi v trojno periodično razporeditev, (b) predstavitvena celica z osmimi podcelicami α, β, γ = 1,2*

Fig. 1. (a) Composite with fibre inclusions, arranged in a triply periodic array, (b) Representative cell with eight subcells α, β, γ = 1,2

slika 1a. Kvader $d_1h_1l_1$ označuje vlakno in skupaj s parametri d_2, h_2 in l_2, ki označujejo razmik med vlakni, predstavljajo eno celico, kakor jo prikazuje slika 1b. Izmere te celice so d_1+d_2, h_1+h_2 in l_1+l_2 v ustreznih smereh x_1, x_2 in x_3. Celica je razdeljena v osem podcelic za $\alpha, \beta, \gamma = 1,2$, v središču katerih so lokalni koordinatni sistemi $\left(\bar{x}_1^{(\alpha)}, \bar{x}_2^{(\beta)}, \bar{x}_3^{(\gamma)}\right)$, katerih smeri so vzporedne z glavnimi sorednicami. Glede na sliko 1b lahko pomik v katerikoli točki znotraj podcelice $\alpha\beta\gamma$ prikažemo z enačbo (1) po teoriji prvega reda:

parallelepipeds, as shown in *Fig. 1a*. The parallelepiped $d_1h_1l_1$ represents the fibre, and together with the parameters d_2, h_2 and l_2, which denote the spacing between the fibres, it represents a single cell, as shown in *Fig 1b*. The dimensions of this cell are d_1+d_2, h_1+h_2 and l_1+l_2 in the corresponding directions x_1, x_2 and x_3. The cell is divided into eight subcells, where $\alpha, \beta, \gamma = 1,2$. In the centre of each subcell a local system of coordinates $\left(\bar{x}_1^{(\alpha)}, \bar{x}_2^{(\beta)}, \bar{x}_3^{(\gamma)}\right)$ is introduced, which is oriented in parallel with the main coordinate system. Referring to *Fig. 1b,* the displacement at any point within the subcell $\alpha\beta\gamma$ can be expressed in the framework of the first-order theory by equation (1) [3]:

$$u_i^{(\alpha\beta\gamma)} = w_i^{(\alpha\beta\gamma)} + \bar{x}_2^{(\alpha)} \phi_i^{(\alpha\beta\gamma)} + \bar{x}_2^{(\beta)} \chi_i^{(\alpha\beta\gamma)} + \bar{x}_3^{(\gamma)} \psi_i^{(\alpha\beta\gamma)}, \quad i = 1,2,3 \tag{1},$$

kjer je $w_i^{(\alpha\beta\gamma)}$ premik središča podcelice in $\phi_i^{(\alpha\beta\gamma)}, \chi_i^{(\alpha\beta\gamma)}$ in $\psi_i^{(\alpha\beta\gamma)}$ so mikrospremenljivke, ki ponazarjajo premo odvisnost pomika $u_i^{(\alpha\beta\gamma)}$ glede na lokalne koordinate $\bar{x}_1^{(\alpha)}, \bar{x}_2^{(\beta)}, \bar{x}_3^{(\gamma)}$. Komponente deformacijskega tenzorja so:

where $w_i^{(\alpha\beta\gamma)}$ is the displacement of the centre of the subcell and $\phi_i^{(\alpha\beta\gamma)}, \chi_i^{(\alpha\beta\gamma)}$ and $\psi_i^{(\alpha\beta\gamma)}$ are micro-variables that characterise the linear dependence of the displacement $u_i^{(\alpha\beta\gamma)}$, referring to the local coordinates $\bar{x}_1^{(\alpha)}, \bar{x}_2^{(\beta)}, \bar{x}_3^{(\gamma)}$. The components of the small strain tensor are:

$$\varepsilon_{ij}^{(\alpha\beta\gamma)} = \frac{1}{2}\left(\partial_i u_j^{(\alpha\beta\gamma)} + \partial_j u_i^{(\alpha\beta\gamma)}\right), \quad i, j = 1,2,3 \tag{2},$$

kjer so parcialni odvodi ∂_i in ∂_j podani po pravilu: $\partial_1 = \partial / \partial \bar{x}_1^{(\alpha)}, \partial_2 = \partial / \partial \bar{x}_2^{(\beta)}$ *in* $\partial_3 = \partial / \partial \bar{x}_3^{(\gamma)}$. Za oba materiala, tako osnovo kakor vlakna, določimo

Where the partial derivations ∂_i and ∂_j are $\partial_1 = \partial / \partial \bar{x}_1^{(\alpha)}, \partial_2 = \partial / \partial \bar{x}_2^{(\beta)}$ *and* $\partial_3 = \partial / \partial \bar{x}_3^{(\gamma)}$. Both materials, the matrix and the fibres, are treated as

popolnoma elastične lastnosti. Povprečno napetost v celotnem kompozitu σ_{ij} lahko zapišemo v obliki:

perfectly elastic. The average stress in the whole composite σ_{ij} is given by:

$$\bar{\sigma}_{ij} = \frac{1}{V}\sum_{\alpha=1}^{2}\sum_{\beta=1}^{2}\sum_{\gamma=1}^{2} v_{\alpha\beta\gamma}\,\bar{\sigma}_{ij}^{(\alpha\beta\gamma)} \tag{3},$$

kjer so $V=(d_1+d_2)(h_1+h_2)(l_1+l_2)$, $v_{\alpha\beta\gamma}=d_\alpha h_\beta l_\gamma$ in $\bar{\sigma}_{ij}^{(\alpha\beta\gamma)}$ povprečna napetost v podcelici. Podobno velja tudi za povprečno deformacijo ε_{ij}:

where $V=(d_1+d_2)(h_1+h_2)(l_1+l_2)$, $v_{\alpha\beta\gamma}=d_\alpha h_\beta l_\gamma$ and $\bar{\sigma}_{ij}^{(\alpha\beta\gamma)}$ is the average stress in the subcell. It is similar to the average strain in the composite ε_{ij}:

$$\bar{\varepsilon}_{ij} = \frac{1}{V}\sum_{\alpha=1}^{2}\sum_{\beta=1}^{2}\sum_{\gamma=1}^{2} v_{\alpha\beta\gamma}\,\bar{\varepsilon}_{ij}^{(\alpha\beta\gamma)} \tag{4}.$$

Pri prečno izotropnem materialu, kjer je x_1 smer anizotropije, so napetosti in deformacije povezane takole:

For transversely isotropic material, where x_1 is the anisotropy direction, the stresses are related to strains in the following form:

$$\left\{\sigma^{(\alpha\beta\gamma)}\right\}=\left\{C^{(\alpha\beta\gamma)}\right\}\left(\left\{\varepsilon^{(\alpha\beta\gamma)}\right\}-\left\{\varepsilon^{I(\alpha\beta\gamma)}\right\}\right)-\{\Gamma\}\Delta T \tag{5},$$

kjer sta stolpec komponent tenzorja napetosti in deformacij:

where the columns of stress and strain tensor components:

$$\begin{gathered}\left\{\sigma^{(\alpha\beta\gamma)}\right\}=\left\{\sigma_{11}^{(\alpha\beta\gamma)},\sigma_{22}^{(\alpha\beta\gamma)},\sigma_{33}^{(\alpha\beta\gamma)},\sigma_{12}^{(\alpha\beta\gamma)},\sigma_{13}^{(\alpha\beta\gamma)},\sigma_{23}^{(\alpha\beta\gamma)}\right\}\\ \left\{\varepsilon^{(\alpha\beta\gamma)}\right\}=\left\{\varepsilon_{11}^{(\alpha\beta\gamma)},\varepsilon_{22}^{(\alpha\beta\gamma)},\varepsilon_{33}^{(\alpha\beta\gamma)},\varepsilon_{12}^{(\alpha\beta\gamma)},\varepsilon_{13}^{(\alpha\beta\gamma)},\varepsilon_{23}^{(\alpha\beta\gamma)}\right\}\\ \{\sigma\}=\mathbf{C}\{\varepsilon\}\end{gathered} \tag{6}$$

$$\mathbf{C}^{(\alpha\beta\gamma)}=\begin{pmatrix} c_{11}^{(\alpha\beta\gamma)} & c_{12}^{(\alpha\beta\gamma)} & c_{12}^{(\alpha\beta\gamma)} & 0 & 0 & 0\\ c_{12}^{(\alpha\beta\gamma)} & c_{22}^{(\alpha\beta\gamma)} & c_{23}^{(\alpha\beta\gamma)} & 0 & 0 & 0\\ c_{12}^{(\alpha\beta\gamma)} & c_{23}^{(\alpha\beta\gamma)} & c_{33}^{(\alpha\beta\gamma)} & 0 & 0 & 0\\ 0 & 0 & 0 & c_{44}^{(\alpha\beta\gamma)} & 0 & 0\\ 0 & 0 & 0 & 0 & c_{44}^{(\alpha\beta\gamma)} & 0\\ 0 & 0 & 0 & 0 & 0 & c_{66}^{(\alpha\beta\gamma)} \end{pmatrix} \tag{7}$$

$\left\{\varepsilon^{(\alpha\beta\gamma)}\right\}$ pomeni deformacijski stolpec v plastičnem področju. Lastnosti elastičnosti za transverzno izotropni material v podcelici $\alpha\beta\gamma$ so predstavljene v enačbi (7) [5]. Za oba materiala, osnovo in vlakna, določimo popolnoma elastične lastnosti, tako da predpostavimo $\left\{\varepsilon^{(\alpha\beta\gamma)}\right\}=0$, čeprav bomo v nadaljevanju določevali lastnosti kompozita tudi v plastičnem področju. To dosežemo s t.i. prirastkovnim popisom, pri katerem krivuljo σ–ε v plastičnem področju ponazorimo z nizom premic [6]. ΔT v enačbi (5) označuje spremembo temperature. Ker v naslednjih izračunih predpostavimo, da je ta nespremenljiva, se ta del enačbe nadalje zanemari.

$\left\{\varepsilon^{(\alpha\beta\gamma)}\right\}$ denotes the strain column in a plastic area. The elastic compliance inverse for the transversely isotropic material in the subcell $\alpha\beta\gamma$ is presented in equation (7) [5]. Because both materials, the matrix and the fibres, are treated as perfectly elastic, it can be assumed that $\left\{\varepsilon^{(\alpha\beta\gamma)}\right\}=0$. Nevertheless, the plastic properties of the composite will also be described in what follows. This is achieved with an incremental presentation, where the curve σ–ε in the plastic area is described by a series of linear lines. ΔT in Equation (5) denotes the temperature difference. Since it is assumed that the difference vanishes, it can be omitted in subsequent calculations.

Premiki in napetosti na mejah podcelic morajo biti enaki, tako da se vzpostavi mikroravnotežje. Primer takega ravnotežja med prvima dvema podcelicama $\alpha=1,2$ je prikazan v enačbi (8):

Displacements and stresses have to be continuous at the subcells' $\alpha=1,2$ interfaces, where a micro-equilibrium is established. An example of such an equilibrium between the first two subcells is presented in Equation (8):

$$u_i^{(1\beta\gamma)}\Big|_{\bar{x}_1^{(1)}=\frac{d_1}{2}} = u_i^{(2\beta\gamma)}\Big|_{\bar{x}_1^{(2)}=-\frac{d_2}{2}}$$
$$\sigma_{1i}^{(1\beta\gamma)}\Big|_{\bar{x}_1^{(1)}=\pm\frac{d_1}{2}} = \sigma_{1i}^{(2\beta\gamma)}\Big|_{\bar{x}_1^{(2)}=\mp\frac{d_2}{2}} \quad (8).$$

Podobno naredimo na vseh mejah med podcelicami β, $\gamma = 1,2$. Na podlagi teh izrazov izločimo mikrospremenljivke $\phi_i^{(\alpha\beta\gamma)}$, $\chi_i^{(\alpha\beta\gamma)}$ in $\psi_i^{(\alpha\beta\gamma)}$ in izpeljemo niz enačb, ki ponazarjajo celostno obnašanje kompozita s kratkimi vlakni [4]. To naredimo z izrazi, ki povežejo mikrodeformacije v podcelicah z makrodeformacijami v kompozitu skozi ustrezni tenzor $\vec{A}$ [4]. Povezava med povprečnim raztezkom in napetostjo v vsaki podcelici ter celotnim raztezkom in napetostjo je sedaj:

A similar process is used on all the borders between the subcells β, $\gamma = 1,2$. By doing this the micro-variables $\phi_i^{(\alpha\beta\gamma)}$, $\chi_i^{(\alpha\beta\gamma)}$ and $\psi_i^{(\alpha\beta\gamma)}$ can be eliminated and a series of equations that represent the overall behaviour of the short-fibre composite can be obtained [4]. This is achieved by establishing the relationships that connect the micro-strains in the subcells to the macro-strains in the composite by an appropriate tensor $\vec{A}$ [4]. The average stress and strain in each subcell and can now be expressed by the total strain in the following way:

$$\bar{\varepsilon}^{(\alpha\beta\gamma)} = \vec{A}^{(\alpha\beta\gamma)}\bar{\varepsilon} \text{ in/and } \bar{\sigma}^{(\alpha\beta\gamma)} = \vec{C}^{(\alpha\beta\gamma)}\vec{A}^{(\alpha\beta\gamma)}\bar{\varepsilon} \quad (9).$$

Tenzor $\vec{A}$ je sestavljen iz naslednjih komponent:

Tensor $\vec{A}$ consists of the following components:

$$\vec{A} = \begin{pmatrix} \vec{A}_M \\ \vec{A}_G \end{pmatrix}^{-1} \begin{pmatrix} 0 \\ \vec{J} \end{pmatrix} \quad (10),$$

kjer pomenijo: $\vec{A}_M$ elastične lastnosti materialov v podcelicah, $\vec{A}_G$ geometrijske izmere celice in $\vec{J}$ povprečne raztezke celotnega kompozita. Na koncu lahko vpeljemo dejanski elastični tenzor kompozita $\vec{B}$:

where $\vec{A}_M$ represents the elastic properties of the subcell materials, $\vec{A}_G$ is the geometrical dimensions of the cell and $\vec{J}$ is the average strain of the whole composite. Now the effective elastic tensor $\vec{B}$ of the composite can be established:

$$\bar{\sigma} = \vec{B}\bar{\varepsilon} \quad (11),$$

kjer je $\vec{B}$ podan z naslednjo enačbo:

where $\vec{B}$ is:

$$\vec{B} = \frac{1}{V}\sum_{\alpha=1}^{2}\sum_{\beta=1}^{2}\sum_{\gamma=1}^{2} v_{\alpha\beta\gamma}\vec{C}^{(\alpha\beta\gamma)}\vec{A}^{(\alpha\beta\gamma)} \quad (12).$$

Za ponazoritev odpovedi materiala je uporabljena Tsai-Hillova porušna hipoteza. Med obremenjevanjem materiala se za vsak vnaprej določen prirastek raztezka preveri, ali je v določeni podcelici prišlo do porušitve. V tem primeru Tsai-Hillova hipoteza prevzame obliko enačbe (13):

For the composite failure the Tsai-Hill failure criterion is used. While loading the material with force, every increment of strain defined in advance is checked for failure in any of the subcells. In this case the Tsai-Hill criterion assumes the form of Equation (13):

$$\begin{aligned}&\left(G^{(\alpha\beta\gamma)}+H^{(\alpha\beta\gamma)}\right)\left(\sigma_{11}^{(\alpha\beta\gamma)}\right)^2+\left(F^{(\alpha\beta\gamma)}+H^{(\alpha\beta\gamma)}\right)\left(\sigma_{22}^{(\alpha\beta\gamma)}\right)^2+\left(F^{(\alpha\beta\gamma)}+G^{(\alpha\beta\gamma)}\right)\left(\sigma_{33}^{(\alpha\beta\gamma)}\right)^2-2H^{(\alpha\beta\gamma)}\sigma_{11}^{(\alpha\beta\gamma)}\sigma_{22}^{(\alpha\beta\gamma)}-\\&-2G^{(\alpha\beta\gamma)}\sigma_{11}^{(\alpha\beta\gamma)}\sigma_{33}^{(\alpha\beta\gamma)}-2F^{(\alpha\beta\gamma)}\sigma_{22}^{(\alpha\beta\gamma)}\sigma_{23}^{(\alpha\beta\gamma)}+2L^{(\alpha\beta\gamma)}\left(\sigma_{23}^{(\alpha\beta\gamma)}\right)^2+2M^{(\alpha\beta\gamma)}\left(\sigma_{13}^{(\alpha\beta\gamma)}\right)^2+2N^{(\alpha\beta\gamma)}\left(\sigma_{12}^{(\alpha\beta\gamma)}\right)^2=1\end{aligned} \quad (13)$$

$G^{(\alpha\beta\gamma)}, H^{(\alpha\beta\gamma)}, F^{(\alpha\beta\gamma)}, L^{(\alpha\beta\gamma)}, M^{(\alpha\beta\gamma)}$ in $N^{(\alpha\beta\gamma)}$ so porušne trdnosti materiala v podcelici $\alpha\beta\gamma$. Zaradi velikega števila linearnih enačb je treba rešitev poiskati z računalnikom.

$G^{(\alpha\beta\gamma)}, H^{(\alpha\beta\gamma)}, F^{(\alpha\beta\gamma)}, L^{(\alpha\beta\gamma)}, M^{(\alpha\beta\gamma)}$ and $N^{(\alpha\beta\gamma)}$ are the failure strengths of the material in the subcell $\alpha\beta\gamma$. Because of the large number of linear equations involved, the solution has to be found by using a computer.

2 EKSPERIMENTALNO DELO

2.1 Brizganje

Da bi raziskali vpliv količine naravnih vlaken, je bilo treba pripraviti več mešanic iz različnih osnovnih polimerov in z različnimi deleži vlaken. Za osnovo smo uporabili PP K948 ter PS Empera 524N. Naravna vlakna so bila sestavljena iz surove celuloze ali mehkega borovega lesa. Njihova vhodna dolžina se je spreminjala od 0,035 do 0,7 mm, razmerje med dolžino in premerom vlakna a_r pa je bilo pred postopkom med 3 in 30. Vendar pa so se med sestavljanjem zrn in med brizganjem v polžu vlakna lomila, tako da je bila končna največja dolžina 0,18 mm in a_r okoli 7 mm. Ker je bilo treba zrna PS za potrebe brizganja pripraviti na višji temperaturi kakor za PP, to je na 205 °C namesto 180 °C, se je to poznalo na mehanskih lastnostih vlaken, saj je bil elastični modul za več ko polovico manjši. Sestava mešanic in parametri brizganja so podani v preglednicah 1 in 2.

Vsak kompozit je bil najprej sušen 4 ure pri temperaturi 100 °C in nato izbrizgan v običajni preizkušanec za natezni preizkus po standardu ISO 527-2.

2 EXPERIMENTAL WORK

2.1 Injection moulding

In order to research the influence of the quantity of natural fibres, several mixtures from various matrix polymers and with different fractions of fibres were prepared. PP K948 and PS Empera 524N were used as the base materials. The natural fibres were made of cellulose or pine soft wood. Their input lengths varied from 0.035 to 0.7 mm and the aspect ratio of the length and the diameter of a fibre a_r was between 3 and 30 before processing. But during the compounding of the granulate and during the injection moulding, the fibres broke down. Therefore, the maximum output length was 0.18 mm and the value of a_r was around 7. The composite that used PS as a matrix needed to be prepared for injection at a higher temperature than for PP, i.e., at 190°C instead of 180°C. This had a clear influence on the fibres' mechanical properties and the Young's modulus was less than half the size of the fibres mixed with PP. The injection-moulding parameters and the composition of mixtures are shown in Tables 1 and 2.

Each mixture was dried for 4 hours at 100°C and then injected into a standard dog-bone shape specimen for tensile testing according to the standard ISO 527-2.

Preglednica 1. *Parametri brizganja*
Table 1. *Injection-moulding parameters*

	PP	PS
Temperatura grelnika [°C] Heater temperature [°C]	180	190
Temperatura orodja [°C] Mould temperature [°C]	30	30
Dodatni tlak [MPa] Packaging pressure [MPa]	500	544
Hitrost brizganja [mm/s] Injection speed [mm/s]	30	17
Čas hlajenja [s] Cooling time [s]	20	35

Preglednica 2. *Sestava testiranih kompozitov [7]*
Table 2. *Composition of tested composites [7]*

Osnova Matrix	Masni delež vlaken Fibre mass ratio [%]	Volumski delež vlaken Fibre volume ratio [%]	Povprečna dolžina vlaken Average fibre length [mm]	a_R
PP*	50	0,73	0,1	3
PP*	60	0,79	0,1	3
PP*	40	0,63	0,1	3
PP	50	0,73	0,1	3
PP	60	0,79	0,1	3
PS	40	0,63	0,035	3,5
PS	50	0,73	0,035	3,5
PS	30	0,55	0,14	5
PS	20	0,41	0,14	5
PS	20	0,41	0,18	6,5

*Kompozitu so bila dodana mehka lesna vlakna namesto celuloznih
* Instead of cellulose, soft-wood fibres were added*

2.2 Natezni preizkus ter določevanje mehanskih in geometrijskih lastnosti vlaken

Material smo enoosno obremenjevali v smeri x_1 ter merili trenutno vzdolžno dejansko napetost v kompozitu $\sigma_{ef} = \bar{\sigma}_{11}$ in vzdolžni dejanski raztezek $\varepsilon_{ef} = \bar{\varepsilon}_{11}$. Natezni preizkus je bil opravljen pri hitrosti raztezanja 3 mm/min. Vzdolžni modul elastičnosti E_A smo izračunali iz strmine krivulje $\varepsilon_{ef} - \sigma_{ef}$ po standardu za polimerne materiale ISO 527-1.

Za izračun po PMC je treba poznati natančne podatke o vhodnih materialih, kar se v primeru naravnih vlaken izkaže za velik problem, saj je težko dobiti že tako navaden podatek kakor je gostota. Navedena gostota izdelovalca velja samo za vlakna, ki jih dobimo ob dostavi, vendar pa je na mikroravni okoli njih veliko praznega prostora, ki se seveda ob mešanju s polimerom zapolni. Zato je bilo treba meriti gostoto in prostornino kompozita. Ob poznavanju gostote osnove lahko potem s sklepnim računom izračunamo gostoto posameznega vlakna ter od tu po enačbi (14) prostorninski delež vlaken, ki ga potrebujemo za izračun po PMC:

$$v_f = \frac{V_f}{V_f + V_m} = \frac{\frac{m_f}{1-m_f} \cdot \frac{\rho_m}{\rho_{com}}}{1 + \frac{m_f}{1-m_f} \cdot \frac{\rho_m}{\rho_{com}}} \quad (14),$$

V_f in m_f pomenita prostornino in maso vlaken, V_m označuje prostornino osnovnega materiala, medtem ko ρ_m in ρ_{com} pomenita gostoto osnove in gostoto kompozita. Poleg prostorninskega deleža je treba

2.2 Tensile testing and the definition of mechanical and geometrical fibre properties

The material was uniaxially loaded with stress in the x_1 direction and then the axial effective stress $\sigma_{ef} = \bar{\sigma}_{11}$ and the effective strain $\varepsilon_{ef} = \bar{\varepsilon}_{11}$ in the composite were measured. Tensile testing was then performed at a strain speed of 3 mm/min. The axial Young's modulus E_A was calculated from the inclination of the $\varepsilon_{ef} - \sigma_{ef}$ curve according to the standard for polymer materials ISO 527-1.

To apply the GMCs, precise data about the input materials have to be known, which can be a problem with natural fibres. Even data as trivial as the density is hard to obtain. The density specified by the manufacturer only applies to received fibres in bulk packaging; it does not take into account the micro-voids of space around the fibres, which are then of course filled with matrix. Consequently, the density and the volume of the composite needed to be measured. From this data the density of an individual fibre can be derived. The expression for the fibre-volume ratio is then:

where V_f and m_f are the volume and the mass of the fibres, V_m denotes the matrix volume and ρ_m and ρ_{com} denote the matrix and the composite density. In addition, the volume-fraction aspect ratio between the length and

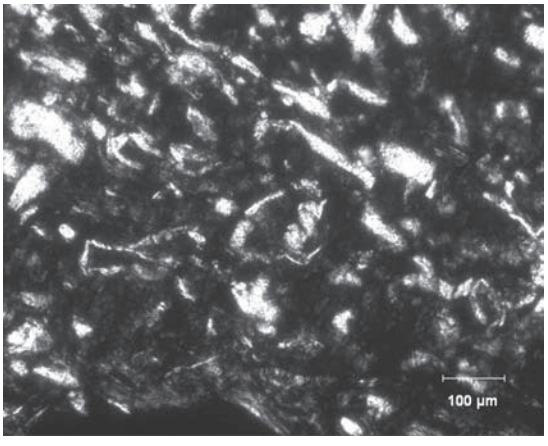

Sl. 2. *Prikaz PS s 30 % celuloznih vlaken, povečava 200X, optični mikroskop*
Fig. 2. *PS with 30 % of cellulose fibres, magnification 200X, optical microscope*

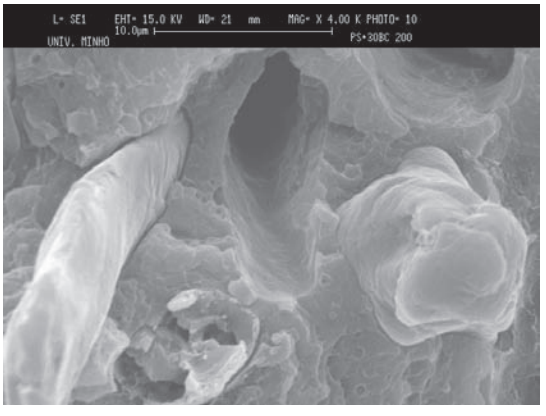

Sl. 3. *PS + 30 % celuloznih vlaken, posneto z elektronskim mikroskopom, povečava 4000X*
Fig 3. *PS with 30 % of cellulose fibres, scanned with an electron microscope, magnification 4000X.*

za izračun poznati tudi dolžino vlaken in razmerje med dolžino in premerom vlaken. Ker se vlakna zaradi trenja ob vrtenju polža lomijo, smo njihovo dolžino ugotavljali z optičnim in elektronskim mikroskopom. Povečave z optičnim mikroskopom so bile 40X in 200X (sl. 2), z elektronskim pa 500X, 1250X, 2500X ter 4000X (sl. 3). PMC ne uporablja razsežnih enot, zato se mora dolžina vlaken izraziti z razmerjem $a_r = l_f / d_f$ med dolžino vlakna l_f in premerom d_f.

3 IZRAČUN PO PMC IN PRIMERJAVA S PREIZKUSOM

V tem poglavju so opisane elasto-plastične lastnosti kompozita, izračunane z GMC ter primerjane z eksperimentalnimi podatki. Primerjava bo pokazala, ali lahko metoda celic dovolj natančno simulira dejanski potek obremenitve biopolimernih kompozitov. Za preračun po PMC smo si pomagali s programsko kodo MAC/GMC 4.0, razvito v NAS-inem raziskovalnem centru Glenn (Glenn Research Center) in v vesoljskem inštitutu Ohaja (Ohio Aerospace Institute), ki uporabnika razbremeni reševanja velikega števila linearnih enačb, ki nastanejo ob analizi kompozita. Na sliki 4 je prikazana primerjava med potekom dejanskega in teoretično izračunanega nateznega preizkusa, dobljenega s PMC.

Najtežje je bilo določiti mehanske lastnosti celuloznih vlaken, saj ti podatki za posamezna vlakna ne obstajajo, prekratka so, da bi z njimi opravili npr. natezni preizkus za posamezno vlakno, kar lahko storimo pri daljših vlaknih ([8] in [9]). Kot izhodiščne vrednosti so bile uporabljene mehanske lastnosti mehkega borovega lesa ([10] in [11]), iz katerih je prečiščena surova celuloza. Vendar pa ne smemo pozabiti, da je bila naša celuloza še toplotno obdelana, kar se je še posebej poznalo pri kompozitu na podlagi PS, saj je tu prišlo do opaznih razlik med preizkusom in izračunom, ki je vedno podal večje vrednosti. Iz tega lahko sklepamo, da je bila toplotna obremenitev vlaken tako visoka, da so se spremenile mehanske lastnosti. Po zmanjšanju elastičnega modula s 6.000 MPa na 2.300 MPa je prišlo do zadovoljivega ujemanja med teoretičnimi izračuni in izmerjenimi podatki pri vseh različnih dolžinah in prostorninskih deležih, zato lahko upravičeno sklepamo, da je to dejanski elastični modul.

Obnašanje vhodnih materialov v plastičnem področju smo simulirali s klasičnim

the diameter of an individual fibre needs to be known. Since fibres break down due to the friction induced by the rotation of the screw, their length needs to be assessed with an optical and an electron microscope. The magnifications for the optical microscope were 40X and 200X (Fig. 2), and with the electron microscope, 500X, 1250X, 2500X and 4000X (Fig. 3). The GMCs does not use dimensioned units, which is why the fibre length is expressed by a ratio $a_r = l_f / d_f$ between the fibre length l_f and its diameter d_f.

3 CALCULATION ACCORDING TO THE GMCS AND A COMPARISON WITH THE EXPERIMENT

In this section the elasto-plastic properties of composites are calculated with the GMCs and then compared to the experimental data. The comparison will show if the GMCs can simulate, accurately enough, the loading process of wood-plastic composites. For the calculation according to the GMCs, the program code MAC/GMC 4.0 developed by the NASA I Glenn Research Center and the Ohio Aerospace Institute was used. This code can relieve the user of having to solve multiple linear equations, which result from analysing the composite. In Fig. 4 the comparison between the real and the simulated (obtained by the GMCs) tensile test is presented.

The hardest part was determining the mechanical properties of cellulose fibres, due to non-existent data for the individual fibres because they are too short to perform a single filament test that can be performed with longer fibres ([8] and [9]). The reference values were the mechanical properties of pine soft-wood ([10] and [11]), from which the cellulose was refined. But one must not forget that in the observed case the cellulose was also heat treated, which had a significant impact, especially on the fibres mixed with the PS. Here, the initial testing revealed a substantial difference between the simulation and the real tests. The results of the simulation were always higher, so the Young's modulus had to be reduced from 6,000 to 2,300 MPa. After doing this, the alignment of the curves was satisfactory for all the fibre length and volume fractions, so it can be concluded with reasonable confidence that this is a realistic Young's modulus.

The behaviour of the input materials in the plastic area was simulated by the classical

Preglednica 3. *Vstopni parametri testiranih materialov*
Table 3. *Input parameters of tested materials*

	E_A [MPa]	E_T [MPa]	G [MPa]	ν	σ_{el} [MPa]	$G=R_m$ [MPa]	F [MPa]	H [MPa]	L [MPa]	M [MPa]	N [MPa]
PP	1.245	1.245	496	0,33	5,1	20,6	20,6	20,6	6,9	7,0	7,0
PS	1.252	1.252	500	0,33	17,6	22	22	22	7,0	7,2	7,2
Cel./les (PP)	6.000	300	600	0,3	9	55	12	12	15	15	15
Cel. (PS)	2.300	250	500	0,3	18	35	8	10	5,4	10	10

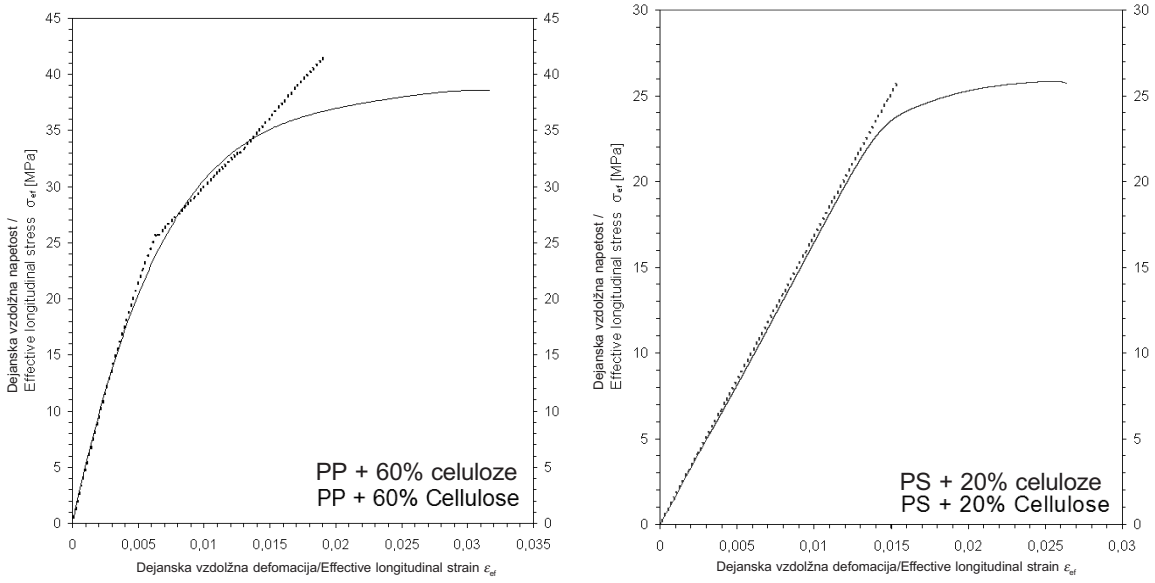

Sl. 4. *Rezultati nateznega preizkusa: ----- PMC, —— preizkus*
Fig. 4. *Results of tensile test: ----- GMCs, —— experiment*

prirastkovnim plastičnim modelom [6], v katerem krivuljo, ko napetost preseže mejo elastičnosti pa do porušitve, ponazorimo z nizom premic, kar močno poenostavi računanje, saj lahko na vsaki premici posebej računamo z običajno, linearno teorijo. V preglednici 3 so predstavljeni vstopni podatki za celulozna in lesna vlakna ter PP in PS. V obeh primerih krivulja, dobljena z PMC, zelo dobro sledi eksperimentalni krivulji (sl. 4), razlikujeta se le v točki porušitve, saj v resnici material še nekaj časa teče. To lahko pripišemo matematičnemu modelu PMC, ki določa, da je med osnovo in vlakni popolna vez in da do porušitve lahko pride samo znotraj določene podcelice $\alpha\beta\gamma$ glede na Tsai-Hillov kriterij po enačbi (13), ne pa tudi na meji med dvema materialoma. Na sliki 3 se lepo vidi praznina, ki ostane za izpuljenim vlaknom, kar pomeni da ni popustilo vlakno, ampak vez med vlaknom in osnovo. Primerjava

incremental plasticity model [6], where the curve from the yield stress to the breakage is represented by a series of linear lines. This simplifies the calculation, since the linear theory can now be used. In Table 3, the input data for cellulose and wood fibres, PP and PS, are presented. In both cases the curve obtained by the GMCs matches the experimental curve (Fig. 4) very well. The only difference is at the breaking point, where in reality the strain of the composite is much bigger. This can be attributed to the mathematical model of the GMCs, which anticipates perfect bonding between the matrix and the fibres. The failure can, in this fashion, occur only within a certain subcell $\alpha\beta\gamma$, according to the Tsai-Hill failure criterion, as described in Equation (13), and not at the interface of the two materials. In Fig. 3, the void that remains after the fibre has been pulled out is clearly shown. This means that the fibre did not break. Instead,

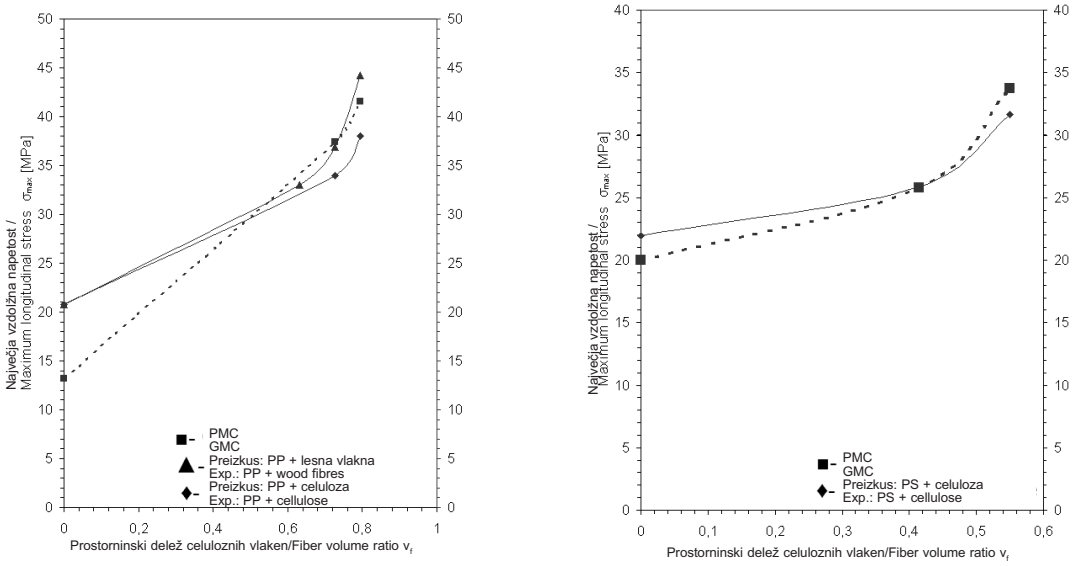

(a) (b)

Sl. 5. *Prikaz poteka natezne trdnosti v odvisnosti od prostorninskega deleža celuloznih vlaken za PP (a) in PS (b), ----- PMC, —— preizkus*

Fig. 5. *Presentation of tensile strength in relation to the fibre-volume ratio for PP (a) and PS (b), ----- GMCs, —— experiment*

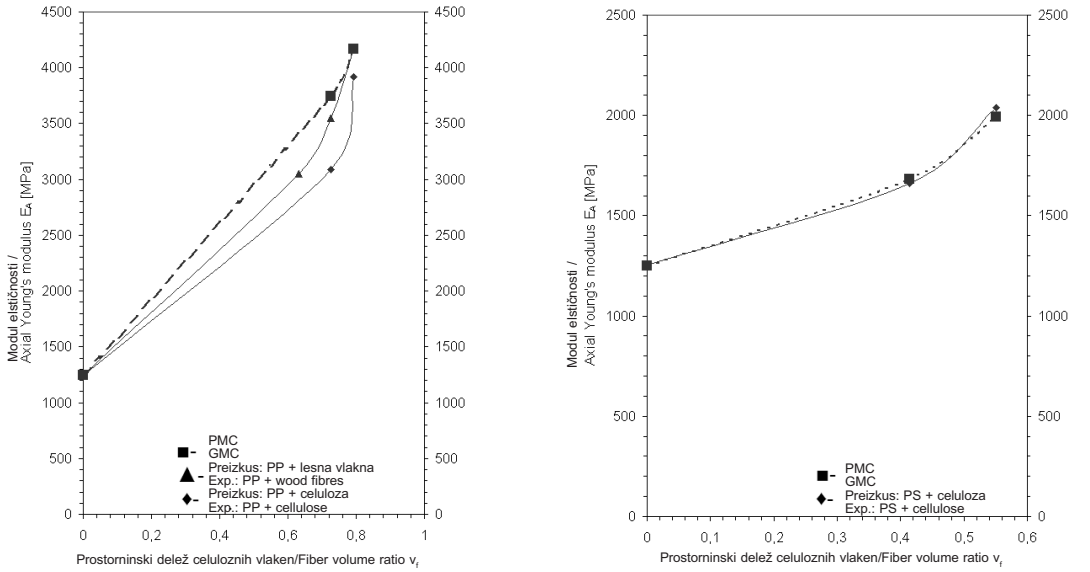

(a) (b)

Sl. 6. *Prikaz velikosti modula elastičnosti v odvisnosti od prostorninskega deleža celuloznih vlaken za PP (a) in PS (b), ----- PMC, —— preizkus*

Fig. 6. *Presentation of axial Young's modulus in relation to the fibre-volume ratio of PP (a) and PS (b), ----- GMCs, —— experiment*

rezultatov pri drugih kompozitih nas pripelje do enakih sklepov. Za potrditev uporabnosti modela PMC je bilo predvsem treba preveriti njeno odstopanje glede na preizkus pri različnih

the bond between the matrix and the fibre failed to carry the stresses any longer. When the results for the other mixtures are compared, the same conclusion can be drawn. To confirm the applicability of the

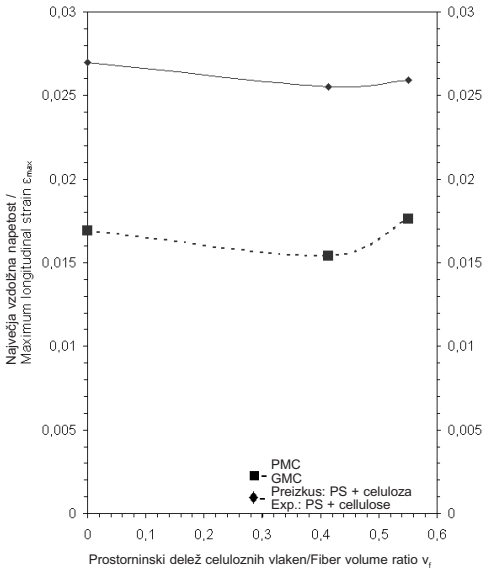

Sl. 7. *Največji raztezek ob porušitvi v odvisnosti od prostorninskega deleža celuloznih vlaken za PS (----- PMC, —— preizkus)*

Fig. 7. *Maximum strain at failure in relation to the fibre-volume ratio of PS (----- GMCs, —— experiment)*

prostorninskih deležih ter dolžinah vlaken. Na slikah 5 do 7 je prikazano spreminjanje bistvenih mehanskih lastnosti v odvisnosti od prostorninskega deleža celuloznih vlaken v kompozitu.

Iz grafov (sl. 5) je razvidno, da povečevanju deleža vlaken PMC sledijo eksperimentalno pridobljeni rezultati, saj sta si oba poteka krivulj zelo podobna, razlikujeta pa se v nekaterih končnih vrednostih, pri natezni trdnosti je največji odstopek okoli 15 %. Do večjih razlik lahko pride le pri čistem polimeru brez vlaken, simuliranje katerega pa ni namen metode celic. Še do večjega ujemanja pride pri merjenju vzdolžnega modula elastičnosti, kjer se krivulji skoraj prekrivata (sl. 6). Iz tega in grafov na sliki 4 lahko sklepamo, da PMC zelo dobro simulira obnašanje biopolimernih kompozitov v elastičnem področju, medtem ko v plastičnem področju, predvsem ko se material bliža porušitvi, daje manj natančne rezultate. To se še potrdi v primerjanju dejanskega in izračunanega največjega raztezka (sl. 7). Tu se zopet potrdi ugotovitev, da so usmerjenosti krivulj različnih mešanic podobne, vendar pride med PMC in preizkusom do prevelikih razlik v absolutnih vrednostih (do 37 %). Do teh razlik pride, ker PMC določa popolno vez med vlaknom in osnovo, medtem ko v resnici pride do popustitve vezi med površinama, kar zmanjša strižne sile v materialu,

GMCs, its deviation from the experiment at various fibre-volume ratios and fibre lengths had to be tested. The charts in Fig. 5 to 7 represent the changing of the main mechanical properties in reference to the volume ratio of cellulose fibres in the composite.

From Fig. 5 it is evident that by increasing the fibre data the trends of both curves are very similar. The difference exists only in the end values, where the ultimate stress can differ by up to 15%. Greater errors appear only for a pure polymer without fibres, but these conditions are not meant for the GMCs to simulate. Even greater matching appears when the axial Young's modulus is measured, where the curves are almost interlacing (Fig. 6). From this and from the charts in Fig. 4 it can be inferred that the GMCs simulates the behaviour of the wood-plastic composites very well in the elastic area, while in the plastic area, especially near the failure, the results are less accurate. This is also confirmed when comparing the simulated and the real ultimate strain (Fig. 7). Here, the tendencies of the curves of different compounds are similar, but there are great differences between the GMCs and the experiment in terms of the absolute values (up to 37 %). These differences occur because the GMCs anticipates perfect bonding between the fibre and the matrix, while in reality failure occurs at the interface of two surfaces. This reduces the shear forces in the material, which enables further deformation of the composite. Apart

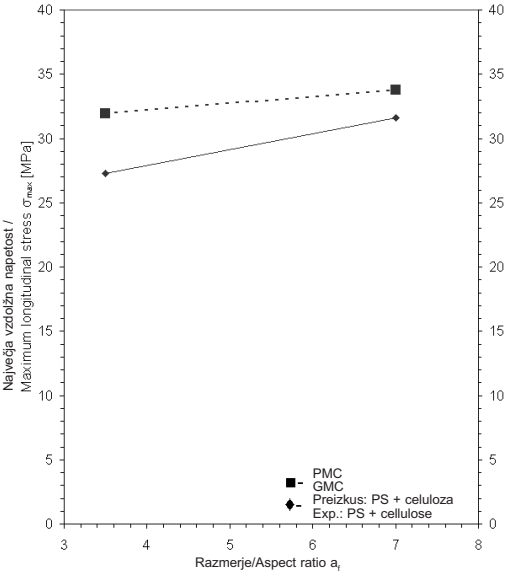

Sl. 8. *Vpliv dolžine vlakna na porušno trdnost kompozita (----- PMC, —— preizkus)*
Fig. 8. *Influence of fibre length on tensile strength of the composite (----- GMCs, —— experiment)*

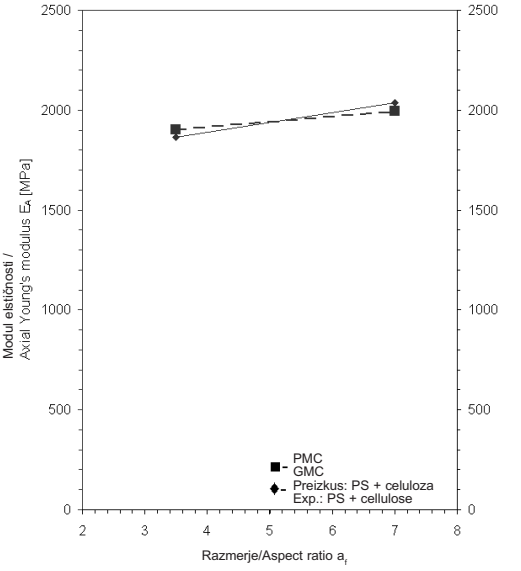

Sl. 9. *Vpliv dolžine vlakna na modul elastičnosti kompozita za PS (----- PMC, —— preizkus)*
Fig. 9. *Influence of fibre length on axial Young's modulus (----- GMCs, —— experiment)*

to omogoči, da se kompozit še naprej deformira. Poleg prostorninskega deleža vlaken v kompozitu ima na njegove mehanske lastnost velik vpliv tudi dolžina vlaken oz. razmerje med dolžino in premerom a_r. Tudi tu se jasno pokaže učinkovitost PMC, saj lepo napove izboljšanje mehanskih lastnosti z daljšanjem vlaken (sl. 8 in 9).

4 SKLEP IN RAZPRAVA

Prispevek je osredotočen na analizo zmožnosti posplošene metode celic določiti elasto-plastični odziv biopolimernih kompozitov. Analizirali smo kompozite z osnovo iz PP ali PS, dodali pa smo jim celulozna ali lesna vlakna različnih dolžin. Izkazalo se je, da po pridobitvi ustreznih vrednosti za lastnosti vlaken (njihovo neposredno merjenje je nemogoče), lahko PMC zelo dobro napove obnašanje kompozita. Izračunane vrednosti vzdolžnega modula elastičnosti (enoosna obremenitev) ter natezne trdnosti so bile v področju merjenja, to je pri masnem deležu vlaken med 20 % in 60 %, zelo blizu dejanskim. Večje razlike pa so se pojavile pri primerjanju raztezkov, saj je v resnici prišlo pri vseh mešanicah do bistveno večjih raztezkov, kot jih je pokazal izračun. To lahko pripišemo že prej omenjeni popolni vezavi med vlaknom in osnovo, ki jo predvideva pri svojem računanju PMC.

from the fibre-volume ratio, the length, i.e., the fibre aspect ratio between the length and the diameter a_r, also has a great impact on the mechanical properties. The effectiveness of GMCs is demonstrated here because it clearly predicts the improvement in mechanical properties with the lengthening of the fibres (Figs. 8 and 9).

4 CONCLUSION AND DISCUSSION

This paper focuses on an analysis of the applicability of the generalised method of cells to predict the elasto-plastical response of wood-plastic composites. Composites with PP and PS matrixes and cellulose or wood fibre inclusions of various lengths were analysed. It was shown that after obtaining appropriate values for the fibre properties (their direct measurement is impossible), the GMCs can predict with great accuracy the trends of composite behaviour. The calculated values of the axial Young's modulus (unidirectional load) and the tensile strength were, in the measured range, very close to real values (for fibre volume ratios from 20 to 60%). Greater differences occurred when measuring the strain. In reality failure occurred at much larger strains than presented in the simulation. This can be attributed to the perfect bonding between the matrix and the fibre that is anticipated by the GMCs.

Ob vsem tem se postavlja vprašanje, ali lahko v praksi uporabimo PMC za napoved mehanskega odziva biopolimernih materialov. Primerjava rezultatov preizkusov in izračuna pokaže, da lahko, vendar z omejitvami. Problemi se pojavijo predvsem pri nepoznavanju lastnosti celuloznih vlaken, saj ti izgubijo del svoje trdnosti pri toplotnem obremenjevanju med postopkom, zaradi vrtenja polža v valju brizgalnega stroja pa se vlakna tudi skrajšajo. Daljša so vstopna vlakna, večje je zmanjšanje dolžine. Da bi se izognili vsakokratnemu mikroskopiranju izbrizganega materiala, lahko najdemo približno skrajšanje vlaken v nekaterih virih [12]. PMC tudi ne upošteva naključne usmerjenosti ter predvsem zvitosti ter neenakomernega prereza vlaken, kar tudi zmanjšuje njeno učinkovitost pri napovedovanju odziva biopolimernih kompozitov. V nadaljnjih testiranjih bi bilo treba tudi upoštevati nepopolno vez med osnovo in vlakni, kakor je to naredil Bednarcyk [13] za kovinska vlakna ter vpliv dodatkov za izboljšanje vezi med osnovo in vlakni [1]. Vzpostaviti bi bilo treba tudi nabor podatkov z mehanskimi lastnostmi različnih vrst naravnih vlaken, saj povprečni uporabnik v industriji zelo težko pridobi ustrezne vhodne podatke. Prav tako v prispevku niso bile upoštevane časovno odvisne mehanske lastnosti materiala zaradi zapletenosti in naključnih lastnosti vlaken, kar pa bo predmet prihodnjih raziskav. Razvoj PMC tudi še ni končan, prav tako pa se biopolimerni kompoziti šele uveljavljajo, tako da lahko v prihodnosti pričakujemo dodatke k PMC, ki bodo upoštevali specifične lastnosti naravnih vlaken.

Zahvala

Na koncu bi se prvi avtor rad zahvalil IPC-ju – Inštitutu za polimere in kompozite z Oddelka za polimerno inženirstvo Univerze v Minhu, Portugalska in inštitutu PIEP (Innovation in Polymer Engineering), prav tako s Portugalske, ki sta omogočila izvedbo preizkusov, ter Javni agenciji za raziskovalno dejavnost RS, ki je s financiranjem bilateralnega projekta "Optimizacija postopka in sredstev za neobičajno večsnovno brizganje" ("Process and Tool Optimization for Nonconventional Multimaterial Moulding") omogočila izvedbo projekta. Avtor se želi zahvaliti tudi Vesoljskemu inštitutu iz Ohaja (Ohio Aerospace Institute), ki je priskrbel programsko kodo MAC/GMC.

All this raises the question of whether the GMCs can be used to predict the mechanical response of wood-plastic composites. The comparison of the experimental and calculated results shows that the answer is yes, but with limitations. Problems arise because the properties of the cellulose fibres are not known. They lose a part of their strength while they are heat treated during the processing. A reduction in the length also occurs due to the screw rotation in the cylinder of the injection-moulding machine. The longer the input fibres are, the greater the reduction is. To avoid repetitive microscopy of the injected materials, an approximate fibre-length reduction can be found in some papers [12]. The GMCs does not take into account the random fibre orientation and especially their curved shapes and non-uniform cross-section, which also reduces its capability to predict the response of wood-plastic composites. In further testing the imperfect bonding between the fibre and the matrix should be taken into account, as was done by Bednarcyk [13] for metal fibres. The impact of coupling additives should also be taken into account here [1]. A database with the mechanical properties of different natural fibres should also be established, because presently an average industrial user obtains the correct input data with great difficulty. Also, in the paper, the time-dependent mechanical behaviour of the composite was not yet considered due to complex and random properties of the fibre, and this will be the subject of our future research. Moreover, the development of the GMCs is not yet finished, and wood-plastic composites have just only begun to take their place among other composites. This means that in the future, improvements of the GMCs can be expected, which will take into account the specific properties of the natural fibres.

Acknowledgements

The first author would like to thank the IPC, the Institute for Polymers and Composites, Department of Polymer Engineering, University of Minho, Portugal and the PIEP, the Innovation in Polymer Engineering, also in Portugal, for help with the experiments. The author would also like to thank the Slovenian Research Agency for financing the bilateral project "Process and Tool Optimization for Nonconventional Multimaterial Moulding" and the Ohio Aerospace Institute for providing the MAC/GMC code.

5 LITERATURA
5 REFERENCES

[1] A. Hančič, A. Glojek (2006) Injection moulding of wood-plastic composites, *RPD 2006 Conference Rapid Product Development*, Marinha Grande, Portugal, pp. 1-2

[2] F. J. W. Van Hattum, C. A. Bernardo (1999) A model to predict the strength of short fiber composites, Department of Polymer Engineering University of Minho, Guimaraes, Portugal, *Polymer Composites*, (1999), Vol. 20, No. 4, pp. 524-532

[3] J. Abudi (1991) Mechanic of composite materials - a unified micromechanical approach, Faculty of Engineering, Tel-Aviv University, Ramat-Aviv, Israel, *Elsevier* ISBN 0-444-88452-1, pp. 76-82

[4] D. H. Pahr, S. M. Arnold (2001) The applicability of generalised method of cells for analyzing discontinuously reinforced composites, Institute of Lightweight Structures and Aerospace Engineering, Viena University, Austria, Life Prediction Branch, NASA Glenn Research Center, Cleveland, USA, *Elsevier* Composites: Part B 33 (2002), pp. 166-168

[5] M. W. Hyer (1998) Stress analysis of fiber-reinfoced composite materials, *WCB McGraw-Hill*, ISBN 0-07-016700-1, pp. 40-50

[6] B. A. Bednarcyk, S. M. Arnold (2002) MAC/GMC 4.0 users manual – keywords manual, Ohio Aerospace Institute, Ohio, *NASA/TM*—2002-212077/VOL2, pp. 21-25

[7] A. Glojek (2005) Poročilo o rezultatih raziskovalnega projekta v okviru EUREKE v letu 2005, Projekt EUREKA E! 2819 Factory Ecoplast, *TECOS*, Celje, pp. 23

[8] M. C. Paiva, I. Ammar, A. R. Campos, R. B. Cheikh, A. M. Cunha (2006) Alfa fibres: Mechanical, morphological and interfacial characterization, *Department of Polymer Engineering University of Minho*, Guimares, Portugal, pp. 2-3

[9] J. M. Whitney, I. M. Daniel, R. B. Pipes (1984) Experimental mechanics of fiber reinforced composite materials, Revised Edition, *The Society for Experimental Mechanics*, Connecticut ISBN 0-13-295196-7, pp. 151-153

[10] D. W. Green, J. E. Winandy, D. E. Kretschmann, Mechanical properties of wood, New Orleans, LA. Madison, *WI: Forest Products Society*, pp. 6-8

[11] M. Rujnić-Sokele, M. Šercer, B. Bujanić (2004) Influence of recycling on mechanical properties of wood-thermoplastic composite, *Polimeri (Časopis za plastiku i gumu)* (2004), Vol. 25 No. 1-2, pp. 13

[12] N. M. Stark, R. E. Rowlands (2002) Effects of wood fiber characteristic on mechanical properties of wood/polypropylene composites, U.S. Department of Agriculture Forest Service Forest Products Laboratory, Madison, *Wood and Fiber Science* (2003) Vol. 35, pp. 168-172

[13] B. A. Bednarcyk, S. M. Arnold (2000) Transverse tensile and creep modeling of continuously reinforced titanium composites with local debonding, Ohio Aerospace Institute, Ohio, *International Journal of Solids and Structures* 39 (2002), pp. 1987-2010

Naslovi avtorjev:
Aleš Hančič
dr. Gašper Gantar
TECOS
Razvojni center orodjarstva Slovenije
Kidričeva 25
3000 Celje
ales.hancic@tecos.si

prof. dr. Franc Kosel
Univerza v Ljubljani
Fakulteta za strojništvo
Aškerčeva 6
1000 Ljubljana

A. R. Campos
PIEP - Innovation in Polymer
Engineering
Portugal

A. M. Cunha
University of Minho
Department of Polymer Engineering
IPC-Institute for Polymers and Composites
Portugal

Authors' Addresses:
Aleš Hančič
Dr. Gašper Gantar
TECOS
Slovenian Tool and Die Development Centre
Kidričeva 25
SI-3000 Celje, Slovenia
ales.hancic@tecos.si

Prof. Dr. Franc Kosel
University of Ljubljana
Faculty of Mechanical Engineering
Aškerčeva 6
SI-1000 Ljubljana, Slovenia

A. R. Campos
PIEP - Innovation in Polymer
Engineering
Portugal

A. M. Cunha
University of Minho
Department of Polymer Engineering
IPC-Institute for Polymers and Composites
Portugal

Prejeto: 15.6.2007
Received:
Sprejeto: 28.9.2007
Accepted:
Odprto za diskusijo: 1 leto
Open for discussion: 1 year

Strojniški vestnik - Journal of Mechanical Engineering 53(2007)12, 834-843
UDK - UDC 620.172.21:678.7
Izvirni znanstveni članek - Original scientific paper (1.01)

Predvidevanje nelinearnega lezenja izdelkov

Prediction of the Nonlinear Creep Deformation of Plastic Products

Jan Spoormaker[1] - Ihor Skrypnyk[2] - Anton Heidweiller[3]
([1]Spoormaker Consultancy, The Netherlands; [2]Goodyear Corporate Research, USA; [3]Delft University of Technology, The Netherlands)

Prispevek na primeru nelinearnega lezenja materiala vstopnika zraka prikazuje sodobne zmožnosti analiz z MKE, zapletenih 3D viskoelastičnih deformacij izdelkov iz plastike. Predstavljena je pomembnost tovrstnih zmožnosti za konstruiranje zapletenih komponent iz plastike.

Model nelinearne viskoelastičnosti je vključen kot podprogram v tržne programske rešitve, ker le-te še ne dajejo tovrstne uporabe. V prispevku so podane posebnosti modela in njegova numerična izvedba v tržnem programskem paketu MSC.MARC.

(Ključne besede: nelinearno lezenje, sprostitve napetosti, analize končnih elementov, polimerni izdelki)

Based on an example of the non-linear creep deformations of an air inlet, this paper demonstrates modern capabilities in the FEA modeling of complex 3D visco-elastic deformations in relation to the design of plastic products. The importance of such capabilities for designing complex plastic components is discussed.

Because commercial FEA packages do not yet render these capabilities "off the shelf", the non-linear visco-elasticity model is incorporated through a user subroutine. The specifics of the constitutive model and its numerical implemen-tation are outlined for the case of implementation in the commercial FEA package MSC.MARC.

(Keywords: non-linear creep, stress relaxation, FEA modeling, plastic product design)

0 INTRODUCTION

The everyday design practice for plastic components relies on relatively simple but effective tools. Just a decade ago these tools would typically include linear elastic finite-element analysis (FEA). In the case when a long-term prediction was required, these FEA calculations would make use of the isochronous curves. Due to the technical limitations of computer hardware even linear visco-elastic FEA calculations were not usually possible.

It is well known, however, that most engineering plastics feature pronounced non-linear visco-elastic behaviour. Accounting for such long-term behaviour is important for designing sustainable, reliable plastic products.

The advances in computer hardware and FEA techniques over the years brought the capabilities of visco-elasticity modelling within the reach of designers of plastic products. The main obstacle that remains here, however, is the lack of well-established models for the time-dependent non-linear behaviour that would be readily available in commercial FEA software.

This paper considers a relatively simple example of the product design of a plastic air inlet (Fig. 1). One of the main design constraints in this case is related to the long-term creep of the product. Based on this design case the capabilities and the importance of non-linear visco-elastic FEA modelling for plastic design are demonstrated.

The prediction of the creep behaviour of the air inlet was a demonstration project for a company that designs and manufactures plastic products for the automotive industry. The upper beam of the air inlet is loaded with 60 N for a period of 10 hours.

The latter task itself consists of two challenges: experimental measurement of the time-dependent behaviour of plastic material and a FEA

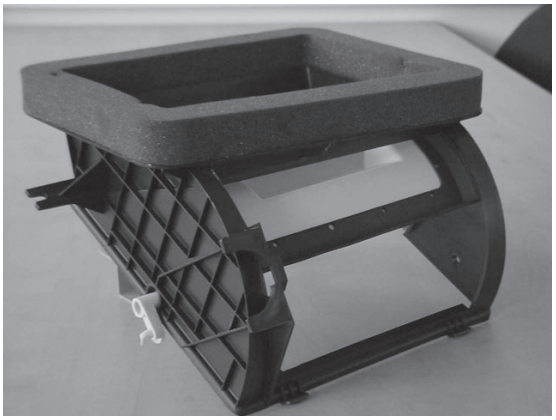

Fig. 1. P*hotograph of the air inlet*

simulation using a non-linear visco-elastic constitutive model.

In order to answer these types of questions, it is necessary to be capable of predicting non-linear visco-elastic deformations of complex three-dimensional solids.

The creep behaviour of the applied plastic, PP with talc, had been measured in an inaccurate way and resulted then in a discrepancy between the predicted behaviour and the behaviour determined in the experimental verification. After accurately measuring the creep behaviour the discrepancy between the prediction and the experimental verification was sufficiently small to demonstrate the possibilities of predicting non-linear creep deformation.

1 NON-LINEAR VISCO-ELASTICITY MODEL OF THE RLAXATION TYPE

The traditional constitutive model for visco-elasticity (Leaderman (1943), Schapery (1969)) is a creep-type dependency, where strains are given as functions of stress, time and, possibly, temperature. This convention comes from the comparative ease and cost efficiency of creep experiments (vs. their relaxation counterpart).

It is necessary to mention, however, that the commercial FEA software packages are displacement based, meaning that a constitutive dependence should be provided in the form of stresses as functions of strains, time and temperature (MARC, Vol. D (1998)). In an incremental form the dependence will look as follows:

$$\Delta\bar{\sigma} = \mathbf{D}\Delta\bar{\varepsilon} + \mathbf{G}\left(\theta_i, \Delta t, \ldots\right) \qquad (1).$$

This means that a creep-type dependency should be inverted at each increment of the solution process. The inversion of the non-linear tensorial equation will easily lead to non-convergence (Skrypnyk, Spoormaker & Smit (2000)), making the task of implementing the creep-type models into the FEA very complicated.

It is much easier (Skrypnyk & Spoormaker (2000)) to handle the implementation of the relaxation-type models, which originate from the Maxwell relaxation model (Fig. 2).

These models have a structure similar to (1), and thus do not require inversion. Earlier authors proposed a generalization to the Schapery model of the relaxation type:

$$\sigma(t) = E_0 g_0(\varepsilon) + \sum_i g_{1i}(\varepsilon) \int_0^t \exp[-\lambda_i(\zeta_i - \zeta_i')] \frac{\partial[g_{2i}(\varepsilon)]}{\partial\xi} d\xi$$
$$\zeta_i(\xi) = \int_0^\xi \frac{d\xi}{a_i(\varepsilon)}; \quad \zeta_i'(t) = \int_0^t \frac{dt}{a_i(\varepsilon)} \qquad (2).$$

Here $\zeta(t)$ and $\zeta(\xi)$ denote strain-reduced functions.

Although the functions in Equation (2) might be chosen from among the wide range of function types (polynomial, exponential, etc.), the following forms seem to be preferable for a description of the experimental data for many plastics:

$$E_0 \cdot g_0(\varepsilon) = \left[E\varepsilon + D_0\varepsilon^{\alpha_0}\right] \qquad (3)$$

$$g_{1i}[\varepsilon] = \exp[\beta_i \varepsilon] \qquad (4)$$

$$g_{2i}[\varepsilon] = D_{1i}\varepsilon^{\alpha_i} \qquad (5)$$

$$a_i[\varepsilon] = \exp[\gamma_i \varepsilon] \qquad (6).$$

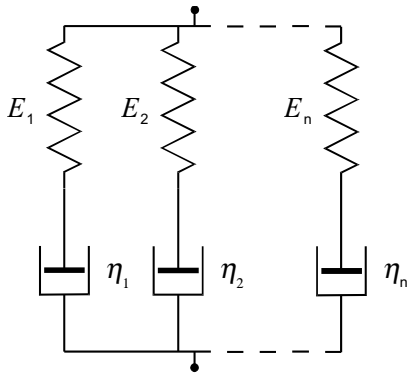

Fig. 2. *Dashpot-spring schematics for the generalized Maxwell model*

2 MODEL CALIBRATION

The relaxation-type models, like Equation (2), usually require material characterization based on relaxation tests, which is more complex and expensive than creep experiments. This is because Equation (2) seamlessly downgrades to an analytical approximation of a relaxation curve:

$$\sigma[\varepsilon_k, t] = E_0 g_0[\varepsilon_k] + \\ + \sum_i \exp(-\lambda_i t / a_i[\varepsilon_k]) g_{i1}[\varepsilon_k] g_{i2}[\varepsilon_k] \quad (7),$$

when the strain history is kept constant: $\varepsilon(t) = \text{const}$. In order to overcome the impediment of relaxation testing, a special calibration procedure has been developed (Skrypnyk & Spoormaker (2000)) that makes it possible to estimate the parameters in Equation (2) based on creep tests.

The procedure is based on the minimization of the relative deviation between the experimental data (creep-recovery tests) and the corresponding model prediction. This relative deviation can be considered as a functional that depends on the material functions (3) to (6). In other words, it may be determined as a function of the model parameters $I\{D_i, \alpha_i, \beta_i, \gamma_i\}$ and, therefore, the parameter identification procedure involves the problem of multi-variables function minimization.

In order to accomplish this, however, the simulations of creep-recovery tests are necessary. Unlike with the creep-type model, it cannot be accomplished in analytic form, but must be carried out numerically.

Since the numerical scheme for calculations of an arbitrary loading history of visco-elastic materials using hereditary integrals, the so-called Henriksen procedure (1984), is already well established and features a high rate of calculations, it can be used within the parameter-identification procedure (for multiple evaluations).

The above procedure itself will be described in the next paragraph, concerning the model implementation into the FEM program. Here, let us simply assume that $\varepsilon[\sigma_k, t; \{D_i, \alpha_i, \beta_i, \gamma_i\}]$ are the results of calculations of the creep-relaxation curve for the $\{D_i, \alpha_i, \beta_i, \gamma_i\}$ set of model parameters and the stress level σ_k. The correspondent test data would be denoted as $\varepsilon[\sigma_k, t]$. Then, the functional of the total error can be written as follows:

$$I\{D_i, \alpha_i, \beta_i, \gamma_i\} = \\ = \frac{1}{N\tau_{end}} \sum_{k=1}^{N} \int_0^{\tau_{end}} \left| \frac{\hat{\varepsilon}[\sigma_k, t] - \varepsilon[\sigma_k, t; \{D_i, \alpha_i, \beta_i, \gamma_i\}]}{\hat{\varepsilon}[\sigma_k, t]} \right| d\tau \quad (8)$$

N is the number of loading levels $\sigma\sigma_k$.

The minimization algorithm developed is based on Powell's method, described in Numerical Recipes (1989) for multi-variables' function minimization. For the evaluation of the integral in (8) the Romberg integration procedure described in Numerical Recipes (1989) is deployed. This procedure usually implies an equal distribution of the integration points t over the integration period $[0, t_{end}]$ with a continuously increasing number of integration points, until the preset accuracy of the integration is reached. However, when the normal time scale is used, this integration procedure puts 90% of the integration points within the last time decade. Thus, the minimization procedure would produce a resulting set that describes the material behaviour very accurately only for the last time decade, but may be far from reality for most of the other decades. In order to overcome this obstacle, the integration was performed over the logarithmic time scale:

$$\tau = \log(t);\ \tau_{end} = \log(t_{end}) \quad (9).$$

In this case, the Romberg procedure distributes the integration points equally over all time decades.
The choice of fixed λ_i -parameters (inverted relaxation times) gives additional advantages for the mini-mization procedure developed:

1. It makes the procedure unconditionally stable (the program runs, until a minimum is found).
2. It decreases the number of parameters (to be estimated) and as a result makes the procedure faster.
3. If the $\{\lambda_i = 10^{-i}\}$ set is chosen, it covers the entire creep-recovery period and yields a fair approximation for each time decade.

Another point that significantly influences the efficiency of the minimization process is a proper choice of the "starting point" for minimization. This was accomplished in three steps. Firstly, available creep data were approximated by the following relations:

$$\hat{\varepsilon}[\sigma_k, t] = A_{[0,k]} + \sum_{i=1}^{n} A_{[i,k]} \left(1 - \exp\left(-t/10^i\right)\right)$$
$$A_{[i,k]} = B_i \left(\sigma_k\right)^{\eta_i} \qquad (10).$$

A combination of the principle of locally separated variables and the Prony series form for time functions provides a good approximation for an arbitrary creep-data set.

Next, the representation (10) is used to find a variation of stresses in time for constant strain levels (which were chosen from the range [0, $0.3\varepsilon_{\max}$], where $\varepsilon_{\max}$ – is the maximum creep strain measured in the test):

$$B_0 (\sigma(t))^{\eta_0} + \sum_{i=1}^{n} B_i (\sigma(t))^{\eta_i} \left(1 - \exp\left(-t/10^i\right)\right) = \text{const.} \qquad (11).$$

The non-linear Equation (11) was solved for different time moments t using Brent's method, Numerical Recipes (1989).

The last stage consisted of an approximation of the obtained relaxation dependencies $\sigma(t)$ by a generalized representation similar to (7):

$$\sigma[\varepsilon_k, t] = C_{[0,k]} + \sum_i C_{[i,k]} \exp(-t/10^i)$$
$$C_{[i,k]} = D_i \left(\varepsilon_k\right)^{\alpha_i} \qquad (12).$$

The obtained parameter set $\{D_i, \alpha_i\}$ was chosen as the initial for the minimization procedure. The starting va-lues for the parameters $\{\beta_i, \gamma_i\}$ were set to zero. The above procedure makes it possible to start the minimization from 20–60% of the total deviation for an arbitrary set of experimental data. Creep tests on plastics cannot be reproduced to within 3 to 5 % and the errors in the FEA simulation are usually of the order of 5 to 10%. There is, therefore, no reason to strive for a fit better than 3 to 5% of total deviation between the data and the model prediction.

3 IMPLEMENTATION OF THE RELAXATION MODEL INTO FEA MSC.MARC

3.1 Extension of the model to the 3-D formulation

Below, the 3-D representation of the developed model is briefly presented. The assumptions are as follows:

- the strains are small enough to accept a conventional definition of stress and strain tensors;
- the behaviour of the visco-elastic material is, to a certain extent, similar to the elastic behaviour;
- the material is compressible and originally isotropic;
- the deviatoric and hydrostatic part of the deformation process are completely uncoupled;
- the rate of viscous flow is proportional to the deviatoric part of the deformation.

As a result, the following 3-D representation is proposed:

$$\bar{\sigma} = \mathbf{M}[\nu_0]\tilde{g}_0[\hat{\varepsilon}]\bar{\varepsilon} + \mathbf{M}[\nu_1]\sum_{i=1}^{n} g_{1i}[\hat{\varepsilon}] \int_0^t \exp\left[-\lambda_i(\zeta - \zeta')\right] \frac{\partial\left[\tilde{g}_{2i}[\hat{\varepsilon}]\bar{\varepsilon}\right]}{\partial\xi} d\xi \qquad (13)$$

$$\zeta(t) = \int_0^t \frac{dt}{a\left[\varepsilon(t)\right]} \qquad (14).$$

Here, the functions in Equation (13) are modified in such a way that for the case of uniaxial loading:

$$g_0[\varepsilon] = \tilde{g}_0[\hat{\varepsilon}]\bar{\varepsilon}$$
$$g_{1i}[\varepsilon] = \tilde{g}_{1i}[\hat{\varepsilon}]\bar{\varepsilon} \qquad (15).$$
$$g_{2i}[\varepsilon] = \tilde{g}_{2i}[\hat{\varepsilon}]\bar{\varepsilon}$$

The following vector and matrix notations are used above:

$$\bar{\sigma} = \left\{ \sigma_{xx} \quad \sigma_{yy} \quad \sigma_{zz} \quad \tau_{xy} \quad \tau_{yz} \quad \tau_{zx} \right\}^T \qquad (16)$$

$$\bar{\varepsilon} = \left\{ \varepsilon_{xx} \quad \varepsilon_{yy} \quad \varepsilon_{zz} \quad \gamma_{xy} \quad \gamma_{yz} \quad \gamma_{zx} \right\}^T \qquad (17)$$

$$\mathbf{M}[\nu] = \begin{cases} \dfrac{2(1-\nu)}{1-2\nu}, & \text{if } i = j \text{ and } i, j \le 3 \\ \dfrac{2\nu}{1-2\nu}, & \text{if } i \ne j \text{ and } i, j \le 3 \\ 2, & \text{if } i = j \text{ and } i, j > 3 \\ 0, & \text{if } i \ne j \text{ and } i, j > 3 \end{cases} \qquad (18).$$

3.2 Main elements of the numerical algorithm for model implementation into the FEA code

The MSC.MARC package was chosen for the implementation of the relaxation model (13)-(14), because of its open structure (which enables easy access to the variables, like stresses, strains, time increment, etc. via user subroutines), and extensive features to handle the geometrically and physically non-linear problems. The constitutive relations in MSC.MARC can be modelled using the capabilities of the user subroutine HYPELA2. As mentioned above, the model should be presented in incremental form as follows:

$$\Delta\bar{\sigma} = \mathbf{D}\Delta\bar{\varepsilon} + \mathbf{G}\left(\theta_i, \Delta t, \ldots\right) \qquad (19).$$

Here, **D** – is Jacobian $\mathbf{D} = \partial\sigma_{ij} / \partial\varepsilon_{ij}$; **G** denotes the vector of stress increment due to the variation of the internal parameters θ_i.

Therefore, the relation (13) has to be rewritten in an incremental form. For sufficiently regular functions $g_{2i}(\varepsilon)$, such that $\partial^2\left[\tilde{g}_{2i}(\varepsilon)\bar{\varepsilon}\right]/\partial t^2 << 1$, the hereditary integral with the exponential kernel functions:

$$\theta_i(t) = \int_0^t \exp\left(-\lambda_i(\xi - t)\right)\frac{\partial\left[g(\hat{\varepsilon})\bar{\varepsilon}\right]}{\partial\xi}d\xi \qquad (20)$$

can be calculated recurrently, following the Henriksen scheme (Henriksen (1984)):

$$\theta_i(t) = \exp(-\lambda_i\Delta t)\theta_i(t-\Delta t) - \Delta\left[g_i(\varepsilon)\bar{\varepsilon}\right]\Gamma_i(\Delta t) \qquad (21),$$

where:

$$\Gamma_i(\Delta t) = \frac{1-\exp(-\lambda_i\Delta t)}{\lambda_i\Delta t} \qquad (22).$$

To write the constitutive Equation (13) in the incremental form (19), the total differential of the right-hand side of Equation (13) has to be derived. Zhang (1995) published similar derivations for the Schapery model (Schapery (1969)). As a result, a quite cumbersome expression with low convergence was obtained. At the same time, certain assumptions can considerably simplify the resulting relations with only a small loss of accuracy (Lai (1995)). If we assume that the effective strain is constant within the time increment:

$$\frac{\partial\varepsilon}{\partial\bar{\varepsilon}} = 0 \qquad (23)$$

the stress increment can be represented as follows:

$$\begin{aligned}\Delta\bar{\sigma} = {} & \mathbf{M}[\nu_0]\tilde{g}_0(\hat{\varepsilon})\Delta\bar{\varepsilon} + \\ & + \mathbf{M}[\nu_1]\sum_{i=1}^{n}[g_{1i}(\hat{\varepsilon})\left(\exp(-\lambda_i\Delta t)-1\right)\theta_i(t-\Delta t) + \\ & + \Delta\left[\tilde{g}_{2i}(\hat{\varepsilon})\Delta\bar{\varepsilon}\right]\Gamma_i(\Delta t)]\end{aligned} \qquad (24)$$

and expressions for the Jacobian **D** and the vector **G** can be derived:

$$\mathbf{D} = \mathbf{M}[\nu_0]\tilde{g}_0(\hat{\varepsilon}) + \mathbf{M}[\nu_1]\sum_{i=1}^{n}\tilde{g}_{2i}(\hat{\varepsilon})\Gamma_i(\Delta t)$$

$$\mathbf{G} = \mathbf{M}[\nu_1]\sum_{i=1}^{n} g_{1i}(\hat{\varepsilon})\left(\exp(-\lambda_i\Delta t)-1\right)\theta_i(t-\Delta t) \qquad (25).$$

If necessary, the reduced time increment can be estimated as follows:

$$\Delta\zeta = \frac{\Delta t}{a\left(\varepsilon(t-\Delta t)\right)} \qquad (26).$$

The above presented numerical scheme (24) to (26) is recurrent. To estimate the stress field at the end of the current time increment, only the data for the strain field ε and the internal parameters θ_i from the previous step are needed. Depending on whether the effective strain in relations (24) to (26) is estimated for the beginning or for the end of an increment, the numerical scheme is explicit or implicit.

The STATE VAR option is used to store an array of θ_i data. In this case the FEA code handles the θ_i array itself, which enables restarting and adaptive meshing technology to be used together with the non-linear visco-elasticity material model.

4 EXPERIMENTAL STUDIES

The experimental part of the study consisted of:

- measuring the creep of the air-inlet material: polypropylene (PP) with 40% talc;
- designing a test fixture and measuring the deflection of the middle part of the upper beam of the air inlet.

4.1 Results from the creep experiments

Two sets of creep experiments were performed. The first set was carried out on "dog-bone" specimens (5 cm in length), deploying a large tensile-test set-up. The MTS extensometer (Fig. 3) has a range of 10% and this is a rather high range for the lowest strain levels tested.

The creep data obtained from the first test set was fitted to model (2) to (6) using the

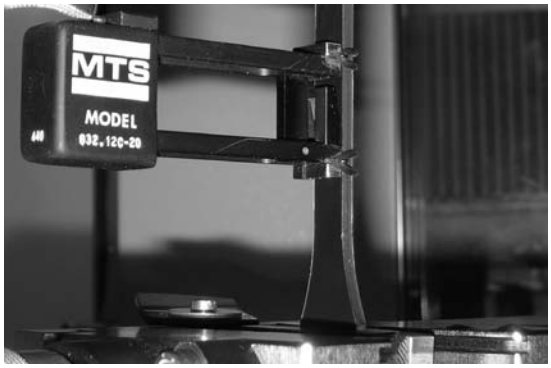

Fig. 3. *Creep/recovery measurements set-up with "dog-bone" specimen and MTS extensometer*

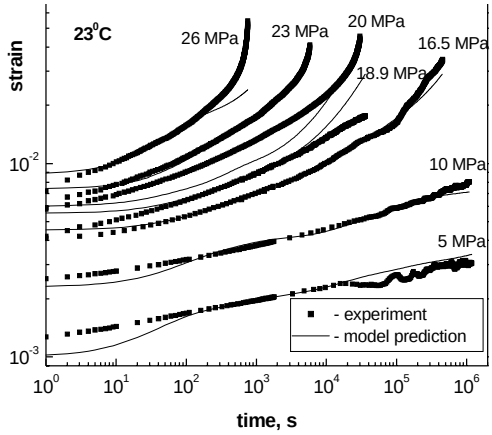

Fig. 4. *Creep-test data and model predictions for PP with 40% talc*

calibration procedure described above (see paragraph 3).

The test results and the model predictions are depicted in Fig. 4. The agreement between the experimental and modeling results for this test set was rather poor. It seemed that the reason for such a disagreement is erroneous test data obtained for the stress level of 20 MPa and, possibly, some errors in the testing methodology at the initial stages of creep.

This initial conclusion, however, turned out to be not correct. One should keep in mind that the calibration procedures like the one described in paragraph 3 are based on the optimization of the total error (Equation (8)), i.e., the deviation between the data and the prediction at all times and load levels. If the test data are rather irregular, the obtained prediction results might not necessarily deviate in the areas where the data are erroneous, but where the data are correct. The latter happens because the model parameters (3) to (6) are estimated for all sets of test data and, therefore, influence the modeling results at all levels. As it proved to be in this case, the test data were unreliable at low stress levels, not at 20 MPa. This becomes obvious when plotting (Fig. 5) the creep moduli for the three lowest stress levels (5, 10 and 16.5 MPa). If we assume that at this stress range the material behaves as linear visco-elastic, the creep moduli should be almost the same. The creep moduli for 16.5MPa are neither similar to those for 5MPa and 10MPa nor are they completely different.

Nevertheless, the initial experimental study (Fig. 4) made it possible to obtain approximate model parameters for the model (2) to (6). Using this set of parameters an initial FEA simulation of the air inlet was performed. The FEA mesh and the applied boundary conditions are depicted in Fig. 14. A sketch of the typical results is given in Fig. 6.

From the FEA results it became clear that the air inlet does not experience stress levels higher

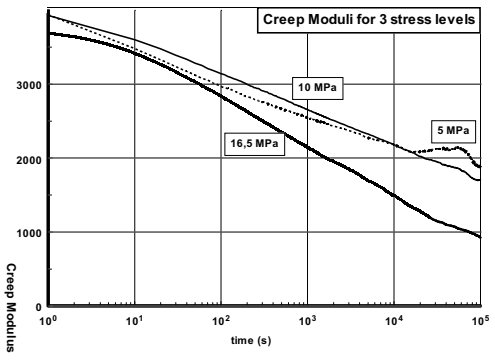

Fig. 5. *Creep moduli for PP with 40% talc for three loading levels*

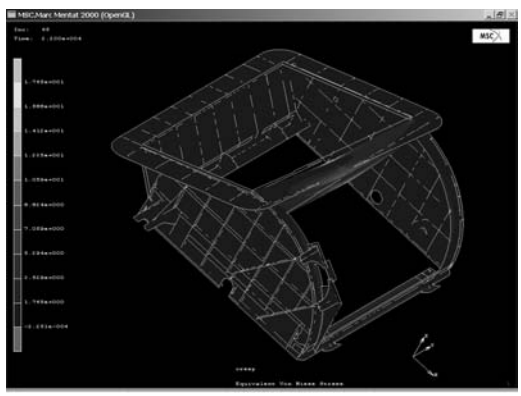

Fig. 6. *Distribution of Von Misses stresses of the air inlet loaded at the middle of the upper beam*

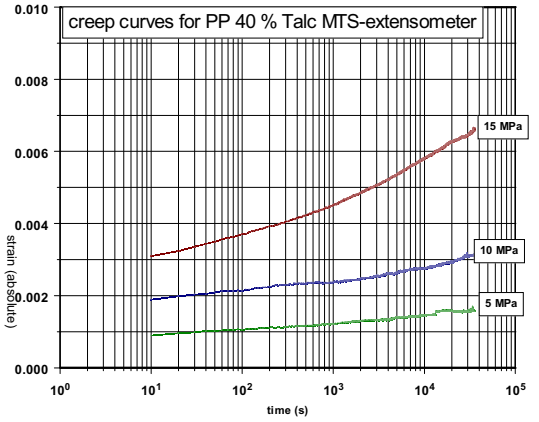

Fig. 7. *Creep-test data for PP with 40% talc for the loading levels of up to 15 MPa, measured using long specimens*

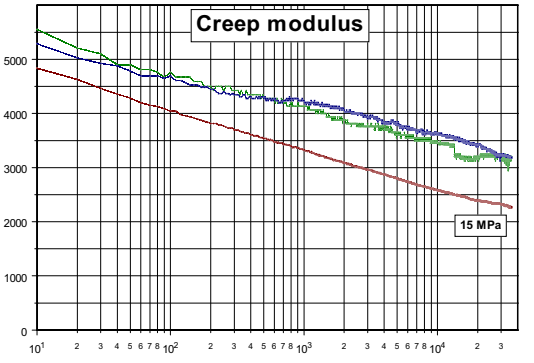

Fig. 8. *Creep moduli recalculated from Figure 7*

than 15 MPa. At the same time, an initial set of creep tests were performed for the levels up to 26 MPa and the data for lower stress levels (which are of interest) appeared to be unreliable.

Therefore, the creep experiments were performed again for the three lowest levels (5MPa, 10MPa and 15MPa) using relatively large specimens. The resulting creep curves are shown in Fig. 7 and the creep moduli are given in Fig. 8. The latter plot proves that the material remains in the area of linear visco-elasticity for the stress levels of 5MPa and 10MPa, but becomes non-linear visco-elastic above that range of loading.

The creep-test results from the second test were deployed to calibrate the model (2) to (6) using the procedure described in paragraph 3.

The results of the model calibration are given in Fig. 9. The resulting set of model parameters for the model (2) to (6) are given in Table 1.

Because of the small number of creep curves (as well as the shortened time of the creep tests),

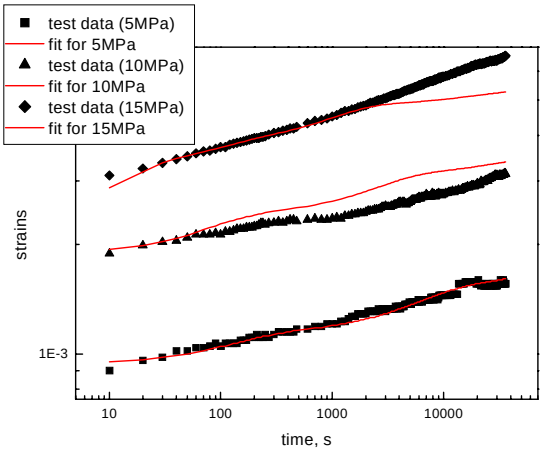

Fig. 9. *Creep-test data and model predictions for PP with 40% talc for the loading ranges of up to 15 MPa*

Table 1. *Set of model parameters for PP with 40% talc (at 23°C)*

Term, i	E				
0	$0.27095427 \cdot 10^4$				
	D_i	α_i	β_i	γ_i	λ_i
1	$0.31352655 \cdot 10^3$	0.88982058	2.5333602	$-0.66960937 \cdot 10^2$	10^{-2}
2	$0.38198521 \cdot 10^2$	0.86928058	$0.76228033 \cdot 10^3$	$-0.15235806 \cdot 10^4$	10^{-3}
3	$0.26457767 \cdot 10^3$	0.78604436	$-0.51668278 \cdot 10^2$	$-0.57895746 \cdot 10^3$	10^{-4}
4	$0.68070737 \cdot 10^4$	1.3374238	$-0.27413947 \cdot 10^3$	$-0.330784 \cdot 10^3$	10^{-5}

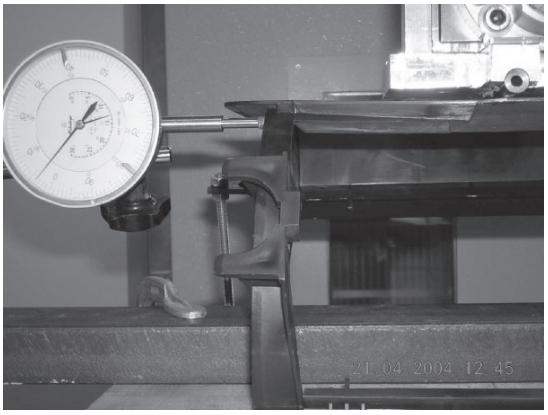

Fig. 10. *Experimental setup with the air inlet*

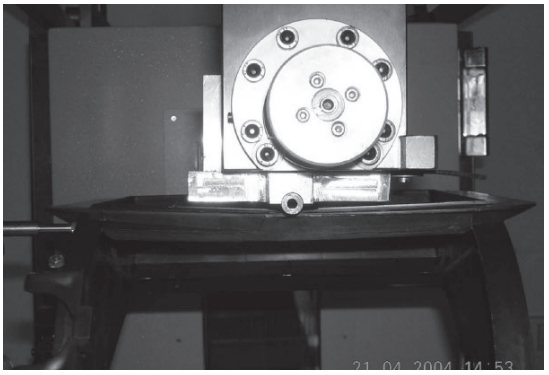

Fig. 11. *Close-up photo of loaded upper beam of the air inlet*

the fitting results do deviate from experimental data, especially for longer testing times. The integral deviation between the fitting results and the test data, however, is only 6.6%, which can be considered satisfactory for engineering applications. Further improvement of the fitting results was considered to be an overfitting, since in the process of achieving it some parameters of the model got too high values, which we consider as "non-physical" and such that would disturb the numerical robustness of the model.

4.2 Measuring the creep deflection of the air inlet

The air inlet was fixed to a testing setup, as depicted in Fig. 10. A special fixture was developed in order to position the upper plane in the horizontal plane, as depicted. The upper beam was loaded in the middle of the upper beam with a constant load of 60N for 10 hours (Fig. 11). The upper beam in the middle is not completely flat. Therefore, a cylinder was used to exert the load and allow some twisting of this beam.

The vertical deflection of the beam at the point of loading was recorded (to be compared with the FEA predictions).

4.3 FEA verification of the developed approach

The accuracy of the created approach to the prediction of the long-term behavior of the air inlet was verified using MSC.MARC 2000. In order to achieve a high accuracy for the FEA prediction the complete air inlet was meshed with shell elements (13,000 elements with 7 layers), see Fig. 14. The out-of-core solver procedure was applied (for this MSC.MARC option ELSTO was deployed). The accuracy requested for the FEA calculation was 5%. A higher accuracy would significantly increase the calculation time, but was considered not necessary, since the model has been fitted with only a 6.6% accuracy.

The results of the FEA predictions for the middle of the upper beam were compared to the experimental data (Fig.12). The deviation between the test data and the prediction was less than 5.5% for the entire modeling period. This should be considered as satisfactory, since the accuracy of the constitutive model was around 6.6% and the accuracy of the FEA analysis was 5%.

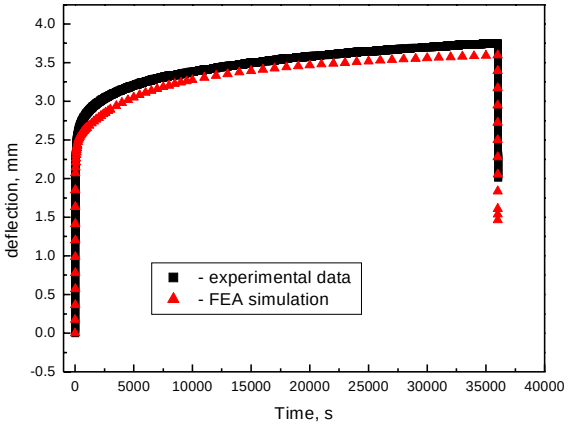

Fig. 12. *Long-term deformation of the upper beam of the inlet at the middle. Comparison of experimental results vs. FEA prediction.*

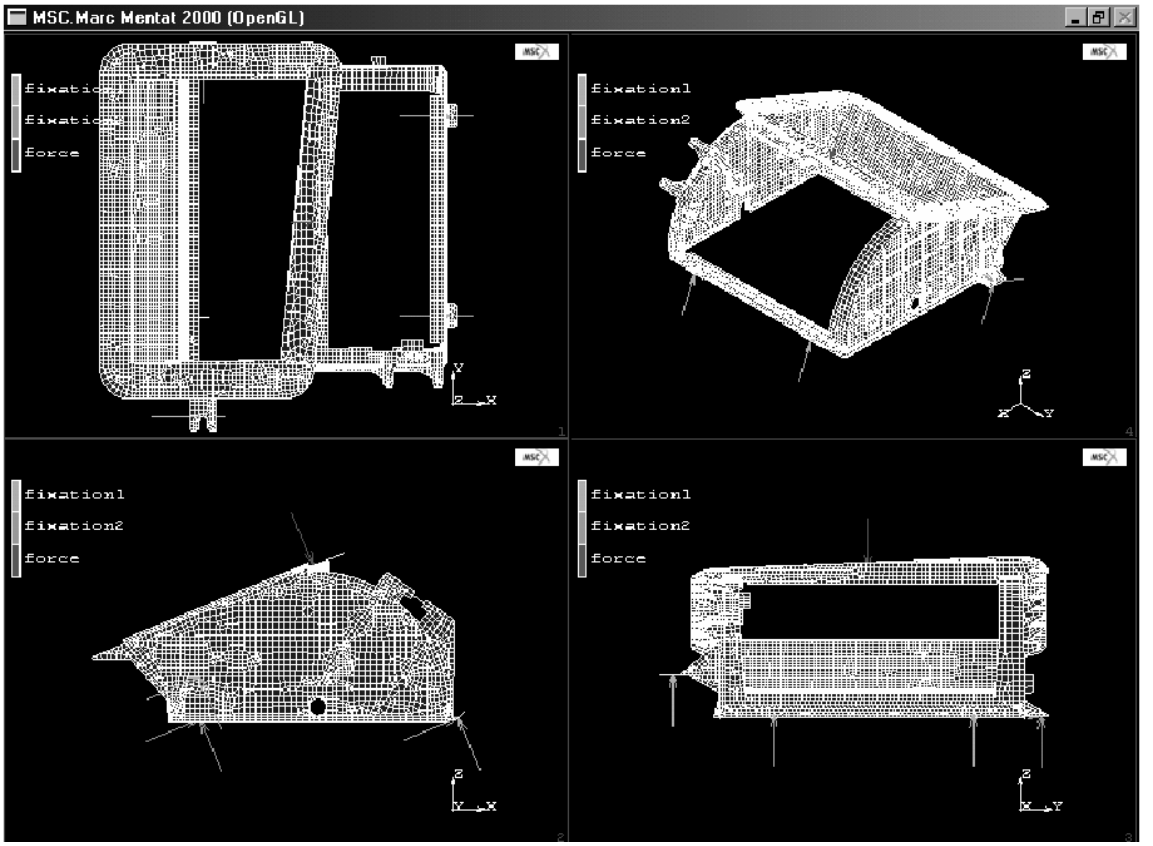

Fig. 13. *Finite-element model*

5 CONCLUSIONS

1. The presented example of a design problem related to a long-term constraint demonstrated that the long-term deformation of complex 3-D plastic products can be successfully predicted by using commercially available FEA software and modern constitutive models for non-linear visco-elasticity.
2. For successful FEA modeling it is critical to have reliable experimental data for a range of parameters (stresses, strains, time period and temperature), in which the designed product is supposed to operate. For non-linear plastic materials (which are rather typical) at least two iterations between the tests and the FEA simulations are usually required to reach an accurate predictive capability.

6 NOMENCLATURE

α_i, β_i, γ_i, D_i	coefficient in material functions $g_i(\varepsilon)$
ε	strain (one-dimensional formulation)
$\varepsilon_{cr}[\sigma_k, t]$	experimental creep data for stress level σ_k at t
$\bar{\varepsilon}$	pseudo-vector notation for strain tensor
ε_{ij}	elements of the strain tensor
$\zeta(t)$	reduced time
λ_i	coefficients in exponential decay series, which relates to relaxation times
η	viscosity in the Maxwell model
ν	Poisson's ratio
ξ	dummy variable in the hereditary integral $\xi < t$
σ, $\sigma(t)$	stress and stress history (scalar notation)
$\bar{\sigma}$	pseudo-vector notation for stress tensor
$\sigma[\varepsilon_k, t]$	experimental relaxation data at ε_k strain level
θ_i.	internal parameters
$A_{[i,k]}$	matrix with constants in the fitting procedure
$B_{[i,k]}$	matrix with constants in the fitting procedure

$C_{[i,k]}$	matrix with constants in the fitting procedure		hereditary integral
		$g(\varepsilon)$	non-linear functions in Schapery models
$\boldsymbol{D}$	stiffness matrix		
E_0	Young's modulus	G	vector of stress increments
$F_i(t)$	time-dependent part of relaxation function, kernel functions of	I	functional of total error
		t	time

7 REFERENCES

[1] Henriksen, M. (1984) Nonlinear visco-elastic stress analysis - a finite element approach, *Computers & Structures*, 18, pp.133-139.

[2] Lai, J. (1995) *Non-linear time-dependent deformation behavior of high density polyethylene*, Ph.D. thesis, *TU Delft*, 157 p.

[3] Leaderman, H. (1943) Elastic and creep properties of filamentous materials and other high polymers, *Textile Foundation*, Washington D. C.

[4] MARC, Volume D: User subroutines and special routines, Rev. K.7, (1998), MARC Analysis Research Corp.

[5] Schapery, R. A. (1969) On the characterization of non-linear visco-elastic materials, *Journal Polymer Eng. Science*, 9, pp. 295-310.

[6] Skrypnyk I.D., Spoormaker J.L., Smit W. (2000) Implementation of constitutive model in FEA for nonlinear behaviour of plastics // Time dependent and nonlinear effect in polymers and composites, *ASTM STP* 1357, – P. 83-97.

[7] Skrypnyk, I.D. and J.L. Spoormaker (2000) Relaxation model for FEM analysis of plastic product behaviour, *ANTEC-proceedings*, Vol. XLVI, pp. 1504-1508.

[8] Zhang, L**.,** (1995) Time-dependent behaviour of polymers and unidirectional polymeric composites Ph.D. thesis, *TU Delft*, 172 p.

Authors' Addresses:

Prof. Jan Spoormaker
Delft University of Technology
Landbergstraat 15
2628 CE Delft, The Netherlands
info@spoormaker-consultancy.com

Dr. Ihor Skrypnyk
Mechanics of Materials and Surface Physics
Goodyear Corporate Research
Akron, 44309 OH, USA
ihor.skrypnyk@goodyear.com

Mag. Anton Hiedweiller
Delft University of Technology
Landbergstraat 15
2628 CE Delft, The Netherlands
a.j.heidweiller@tudelft.nl

Prejeto: 2.5.2007
Received:

Sprejeto: 27.6.2007
Accepted:

Odprto za diskusijo: 1 leto
Open for discussion: 1 year

Strojniški vestnik - Journal of Mechanical Engineering 53(2007)12, 844-857
UDK - UDC 658.51
Pregledni znanstveni članek - Review scientific paper (1.02)

Razvoj naprednih metod za vodenje proizvodnih postopkov

The Development of Advanced Methods for Scheduling Production Processes

Tadej Tasič - Borut Buchmeister - Bojan Ačko
(Fakulteta za strojništvo, Univerza v Mariboru)

Načrtovanje rokov in zmogljivosti spada v področje vodenja proizvodnje. Termininiranje pomeni razporejanje omejenih virov opravilom v določenem časovnem obdobju. Torej gre za postopek odločanja s ciljem optimizacije enega ali več meril. Splošno obsega grobo (dolgoročno), srednjeročno in podrobno (kratkoročno) načrtovanje. Zadnjemu dajemo zaradi neposredne povezave z opravilno učinkovitostjo največji pomen. V prispevku so predstavljeni razviti postopki terminiranja: prednostna pravila, omejeno iskanje v snopu in hevristično preiskovanje glede na omejitve. Vse je podkrepljeno s prikazom na primerih.

(Ključne besede: načrtovanje proizvodnih postopkov, deterministično razvrščanje, termininiranje, prednostna pravila)

The planning of dates and capacities belongs to the area of production management. Scheduling represents the allocation of scarce sources to tasks in a definite period of time. So it is about a process of deciding, with the goal of optimization, about one or more criteria. In general it includes rough (long-term), medium-term and detailed (short-term) planning. The last of these has the greatest importance because of a direct connection with operational effectiveness. Some developed scheduling procedures are presented in the paper, i.e., the priority (dispatching) rules, the filtered-beam search, and the constraint-guided heuristic search. All this is substantiated with described examples.

(Keywords: production process planning, deterministic sequencing, scheduling, priority rules)

0 UVOD

"Termininiranje pomeni načrtovanje postopkov dela z dodeljevanjem virov dela opravilom in določitvijo njihovih začetnih časov. Različne komponente problemov termininiranja so opravila, omejitve, viri in optimizacijska merila. Opravila morajo biti programirana tako, da zadovoljijo določene zahteve. Seveda pa v praksi navadno upoštevamo več meril." [1].

V zadnjih desetletjih se je dosti naredilo na teoretičnih raziskavah s področja determinističnega razvrščanja. Število in raznolikost različnih modelov sta presenetljivi. Ko rešujemo probleme razvrščanja, menimo, da je število delovnih mest in strojev končno – določeno. Tako število delovnih nalogov označimo z n, število strojev pa z m. Običajno dodamo indeks (števec), in sicer j dodelimo delovnim mestom, i pa strojem.

0 INTRODUCTION

"Scheduling is to forecast the processing of work by assigning resources to tasks and fixing their start times. The different components of a scheduling problem are the tasks, the potential constraints, the resources and the objective function. The tasks must be programmed to optimise a specific objective. Often it will be more realistic in practice to consider several criteria." [1].

In the past few decades a considerable amount of theoretical research has been done in the field of deterministic scheduling. The number and variety of different models is astounding. In all the scheduling problems considered, the number of jobs and the number of machines are assumed to be finite. The number of jobs is denoted by n and the number of machines by m. Usually, the subscript j refers to a job and the subscript i to a machine.

Optimizacijska merila lahko razdelimo na dva tipa: na povezana s časom dokončanja naloge in povezana s stroški. V načrtovanju rokov in zmogljivosti uporabljamo za reševanje problemov različne metode, ki se razlikujejo glede na zapletenost problema. Za preproste primere uporabljamo hevristična prednostna pravila (npr. pravilo najkrajšega časa obdelave, pravilo najzgodnejšega dobavnega roka, pravilo najzgodnejšega prihoda itn.). Kadar imamo na voljo več strojev, je nujna razširitev z dodatnim pravilom dodelitve nalog strojem. V primeru enakih strojev običajno uporabljamo pravilo prvega razpoložljivega stroja, ta dodeli naročilo prvemu stroju, ki je na voljo. Če stroji niso enaki, se najbolj uporablja pravilo najhitrejšega stroja, ki dodeli naročilo najhitrejšemu med razpoložljivimi stroji.

Za načrtovanje projektov uporabljamo Ganttove diagrame ali gantograme. Pogosta metoda za pomoč pri izvajanju med seboj logično povezanih dejavnosti z namenom, da bi dosegli vnaprej postavljen cilj, je tudi tako imenovano mrežno načrtovanje (mrežni diagrami).

Za bolj zapletene probleme v sodobni proizvodnji pa moramo posegati po matematično-analitičnih metodah reševanja problemov. Preprost primer je Johnsonov algoritem [2], prikazan na sliki 1, kjer so:

J – nalog, ki izpolnjuje zahteve,
p – skupni čas opravila,
C_{max} – skupni čas izvedbe vseh nalogov,
prmu – vrstni red izvajanja nalogov.

Druga možnost je uporaba računalniških simulacij, ki dinamično prikazujejo potek nekega postopka in omogočajo ob spremembah

Optimization criteria can be divided into two types: criteria that are connected with the time of the completion of a job, and criteria connected with costs. When planning dates and capacities, we usually use different methods for solving problems. They differ in terms of the complexity of a problem (in simple cases we use heuristic dispatching rules – for example the rule of the shortest processing time, the earliest due date rule, the first-come first-served rule, etc.). When we can use several machines, an additional rule is a necessary solution for the allocation of tasks to the machines. In the case when machines are identical we normally use the rule of the first available machine, which assigns an order to the first available machine. If the machines are not identical, the rule of the fastest machine is the most appropriate, and this assigns an order to the fastest among the available machines.

When planning projects we help ourselves with Gantt diagrams or Gantt charts. A frequent method for help, using performance of activities that are mutually connected with the intention of reaching a goal that is set in advance, is also network modelling (network diagrams).

For more complicated problems in modern production we have to implement mathematical-analytical methods for solving problems. A simple example is Johnson's algorithm, which is shown in Figure 1 [2], where:

J – a set of jobs, that satisfies a condition,
p – processing time,
C_{max} – completion time of all jobs,
prmu – indicates that the operations occur on the machines in the same order.

The second possibility is the use of computer simulations that dynamically show the course of a

/***T** je niz nalog, ki jih moramo razporediti*/		/***T** is the set of jobs to schedule*/
Naj bo / Let:	$\boldsymbol{U} = \left\{ J_i \in T \,\middle\vert\, p_{i,1} < p_{i,2} \right\};$	
Naj bo / Let:	$\boldsymbol{V} = \left\{ J_i \in T \,\middle\vert\, p_{i,1} \geq p_{i,2} \right\};$	
Razporedi **U** naraščajoče po vrednostih $p_{i,1}$;		Sort U by increasing values of $p_{i,1}$;
Razporedi **V** padajoče po vrednostih $p_{i,2}$;		Sort V by decreasing values of $p_{i,2}$;
	$\boldsymbol{S} = \boldsymbol{U} \,//\, \boldsymbol{V};$	
	$C^*_{\max} = C_{\max}(S);$	
Izpiši / Print:	$S,\ C^*_{\max};$	

Sl. 1. *Johnsonov algoritem za F2|prmu|C_{maks} problem*
Fig. 1. *Johnson's algorithm for the F2|prmu|C_{max} problem*

parametrov in razmer pri delu vnaprejšnje določevanje stanj načrtovanega postopka. Eno prvih preglednic terminiranja zasledimo v Conway, Maxwell in Miller [3]. V znanstveni literaturi zasledimo mnogo raziskav s teh področij, nekatere novejše prispevke so objavili avtorji: Lawler idr. [4], Brah in Wheeler [5], Polajnar idr. [6], Brucker [7], Buchmeister idr. [8], Gomes in Meile [9], Blažewicz idr. [10], Garcia-Sabater [11], Nyman in Levitt [12], Leung [13], Palmer [14], Koo in Jang [15].

1 NAČIN OZNAČEVANJA PROBLEMOV TERMINIRANJA ($\alpha \mid \beta \mid \gamma$)

Vsak problem terminiranja opišemo s trojčkom $\alpha \mid \beta \mid \gamma$. Polje α opisuje stroje in vsebuje en zapis. Polje β podaja podrobnosti o lastnostih postopkov in omejitvah. Lahko je prazno, z enim ali več zapisi. Polje γvsebuje cilj optimizacije (funkcijo, katero minimiziramo) in ima običajno en zapis [16].

Mogoči zapisi v polju α:

1 – en stroj,
$\boldsymbol{P}_m$ – m enakih vzporednih strojev,
$\boldsymbol{Q}_m$ – m različnih vzporednih strojev,
$\boldsymbol{F}_m$ – m v vrsto postavljenih strojev,
$\boldsymbol{J}_m$ – m različnih strojev (vsak nalog ima svoje zaporedje opravil) itn.

Nekaj mogočih zapisov v polju β:

$\boldsymbol{r}_j$ – čas prihoda naloga (sprostitev),
$\boldsymbol{s}_{jk}$ – od zaporedja nalogov odvisni pripravljalni in končni časi,
prec – omejitev glede predhodno izvedenih opravil (strogo zaporedje),
prmu – omejitev glede enakega vrstnega reda nalogov po strojih (ni prehitevanja),
block – zastoji v sistemu (npr. zaradi polnih zalogovnikov),
brkdwn – izpadi (nedelovanje) strojev itn.

Nekaj mogočih zapisov v polju γ:

$\boldsymbol{C}_{max}$ – skupni časi izvedbe vseh nalogov,
$\boldsymbol{L}_{max}$ – največje odstopanje roka dobave
$\sum \boldsymbol{w}_j \boldsymbol{T}_j$ – skupna utežena kasnitev nalogov itn.

2 PREDNOSTNA PRAVILA

S prednostnim pravilom priredimo vsakemu nalogu, ki je v čakalni vrsti pred določenim delovnim mestom, prednostno število (skalarno vrednost). To število potem določa položaj naloga v čakalni vrsti v primerjavi z drugimi čakajočimi

process, and make possible a forecast of the planning-process conditions when it comes to changes of parameters out of the conditions of the work. One of the first studies about scheduling was published by Conway, Maxwell and Miller [3]. In the scientific literature we can find many researches, some of the newest in this area are in the publications of Lawler et al. [4], Brah and Wheeler [5], Polajnar et al. [6], Brucker [7], Buchmeister et al. [8], Gomes and Meile [9], Blažewicz et al. [10], Garcia-Sabater [11], Nyman and Levitt [12], Leung [13], Palmer [14], Koo and Jang [15].

1 THE NOTATION OF SCHEDULING PROBLEMS ($\alpha \mid \beta \mid \gamma$)

A scheduling problem is described by a triplet, $\alpha \mid \beta \mid \gamma$. The α field describes the machine environment and contains a single entry. The β field provides details of the processing characteristics and constraints. This field may contain no entries, a single entry, or multiple entries. The γ field contains the objective to be optimized and usually contains a single entry.

Possible entries in the α field:

1 – single machine,
$\boldsymbol{P}_m$ – m identical parallel machines,
$\boldsymbol{Q}_\mathrm{m}$ – m different parallel machines,
$\boldsymbol{F}_m$ – flow shop with m machines,
$\boldsymbol{J}_m$ – job shop with m machines (each job has a unique routing), etc.

Some possible entries in the β field:

$\boldsymbol{r}_j$ – release date,
$\boldsymbol{s}_{jk}$ – sequence-dependent setup times,
prec – precedence constraints,
block – blocking (full buffers between operations),
brkdwn – breakdowns of machines, etc.

Some possible entries in the γ field:

$\boldsymbol{C}_{max}$ – makespan (completion time of all jobs),
$\boldsymbol{L}_{max}$ – maximum lateness,
$\sum \boldsymbol{w}_j \boldsymbol{T}_j$ – total weighted tardiness.

2 THE PRIORITY RULES

With a priority rule we can arrange a priority value (a scalar value) to each job (an order) that is in the waiting queue in front of a defined working place (a machine). This value then defines the position of a job in the waiting queue in comparison

nalogi. Nalog z največjo prednostjo se prvi izvede. Po dogovoru je to največje oziroma najmanjše prednostno število ([6], [17] in [18]).

Prednostna pravila so lahko statična ali dinamična, lokalna ali celotna, temeljna ali sestavljena in druga. Uporaba sestavljenih, seštevno ali množilno vezanih pravil omogoča sočasno kompromisno izpolnjevanje več proizvodnih ciljev. Raziskave pa kažejo, da stopnja učinkovitosti pri posameznih ciljih ni večja kakor pri uporabi temeljnih prednostnih pravil [6].

Prednostna pravila se delijo na:
- pravila, ki vključujejo čase opravil,
- pravila, ki vključujejo dobavni rok,
- pravila, ki ne vključujejo ne časov opravil, ne dobavnih rokov in na
- kombinirana pravila.

2.1 Primeri prednostnih pravil

SPT:

$$\min \sum_{j \in O_i} p_{ij} \tag{1}$$

kjer so: i – števec nalogov,
j – števec opravil,
O – zaporedje vseh opravil naloga,
p – skupni čas opravil.

Prednost ima nalog z najmanjšim skupnim časom vseh opravil(najmanjši obseg dela).

EDD:

$$\min d_i \tag{2}$$

kjer je: d – dobavni rok naloga.

Prednost ima nalog z najzgodnejšim dobavnim rokom.

LRPT:

$$\max \sum_{j \in P_i} p_{ij} \tag{3}$$

kjer je: P – zaporedje preostalih opravil naloga.

Prednost ima nalog z največjim skupnim časom preostalih opravil.

LS:

$$\min\left(d_i - t - \sum_{j \in P_i} p_{ij} \right) \tag{4}$$

kjer je: t – trenutni čas.

Prednost ima nalog z najmanjšo časovno rezervo med dobavnim rokom in trenutnim

to other waiting jobs. After an agreement this is the largest, or the smallest, priority value ([6], [17] and [18]).

A priority rule can be static or dynamic, local or global, basic or complex, etc. The use of complex, additive or multiplicative tied rules makes it possible that more of the production goals are simultaneously improved. Research shows us that the degree of effectiveness in single goals is not higher than the one, which is achieved with basic priority rules [6].

The priority rules are divided into:
- rules that include operation times,
- rules that include the due date,
- rules that include neither operation times nor due dates,
- complex (composite) rules.

2.1 Examples of priority rules

SPT (Shortest Processing Time):

$$\min \sum_{j \in O_i} p_{ij} \tag{1}$$

where: i – index of jobs (counter),
j – index of operations (counter),
O – sequence of all operations of jobs,
p – processing time.

The job with the shortest processing times of all operations (the smallest extent of work) has the priority.

EDD (Earliest Due Date):

$$\min d_i \tag{2}$$

where: d – due date.

The job with the earliest due date has the priority.

LRPT (Longest Remaining Processing Time):

$$\max \sum_{j \in P_i} p_{ij} \tag{3}$$

where: P – sequence of remaining operations of a job.

The job with the longest remaining processing time has the priority.

LS (Least Slack):

$$\min\left(d_i - t - \sum_{j \in P_i} p_{ij} \right) \tag{4}$$

where: t – actual (current) time.

The job with the least slack between due date and actual date, considering the processing time of

datumom z upoštevanjem skupnega časa preostalih opravil. Pri nalogih z enakim dobavnim rokom deluje kot LRPT; pri nalogih z enakim skupnim časom preostalih opravil pa kot EDD.

LSS:

$$\min\left(d_i - r_i \; - \sum_{j\in 0_i} p_{ij}\right) \tag{5}$$

kjer je: r – čas prihoda naloga.

Prednost ima nalog z najmanjšo časovno zalogo (zračnostjo), pri čemer se upoštevajo dobavni rok, čas prihoda naloga in skupni čas vseh opravil. Izračunana vrednost se s časom ne spreminja.

WSPT:

$$\min \sum_{j\in O_i} w_{ij} \cdot p_{ij} \tag{6}$$

kjer je: w – utež naloga.

Prednost ima nalog z najmanjšim uteženim skupnim časom vseh opravil.

ATC:

Pravilo ATC je sestavljeno prednostno pravilo, ki kombinira pravilo WSPT (najmanjši uteženi čas obdelave) in pravilo LS (najmanjša zračnost). S pravilom ATC razvrstimo vsakič po en nalog. Ko je stroj prost, izračunamo vrednost funkcije $I_j(t)$ za vse čakajoče naloge. Nalog z največjo vrednostjo izberemo za obdelavo na stroju. Vrednost funkcije $I_j(t)$ za čakajoče naloge se s časom spreminja.

$$I_j(t) = \frac{w_j}{p_j} \cdot e^{-\frac{\max\left(d_j - p_j - t, 0\right)}{k \cdot \bar{p}}} \tag{7}$$

kjer sta: k – izkustveno določen parameter pogleda naprej,

$\bar{p}$ – povprečni čas obdelave preostalih delovnih nalogov.

Če je k zelo velik, se pravilo ATC zoži v pravilo WSPT, če pa je zelo majhen, pa v pravilo LS, če ni zakasnelih delovnih nalogov, oziroma v pravilo WSPT za zakasnele naloge.

2.2 Uporaba zahtevnega prednostnega pravila

Podrobneje obravnavamo pravilo stroškov kasnitve z upoštevanimi pripravljalno-zaključnimi časi (ATCS). Pravilo je narejeno za problem $1|s_{jk}|\sum w_j T_j$. Cilj je minimizirati vsoto uteženih kasnitev, s tem da so pripravljalni in končni časi odvisni od zaporedja delovnih nalogov. Posledično

the remaining operations, has the priority. When all the jobs have the same due date it works as LRPT; when jobs have the same processing time of remaining operations it works as EDD.

LSS (Least Static Slack):

where: r – arrival time of a job.

The job with the least slack, where the due date, the arrival time of the job and the processing time of all the operations should be considered, has the priority. The calculated value does not change with time.

WSPT (Weighted Shortest Processing Time):

where: w – weight of a job.

The job with the shortest weighted processing time for all the operations has the priority.

ATC (Apparent Tardiness Cost):

The ATC rule is a complex priority rule that combines the WSPT rule (Weighted Shortest Processing Time) and the LS rule (Least Slack). The ATC rule always selects one job at a time. Every time a machine becomes free, we calculate the value of the function $I_j(t)$ for all the waiting jobs. The job with the highest function value is chosen for processing on the machine. The value of the function $I_j(t)$ for all the waiting jobs is time dependent.

where: k – empirically defined parameter (look ahead),

$\bar{p}$ – mean processing time of the remaining jobs.

If k is very large, the ATC rule narrows into the WSPT rule, and if it is very small it narrows into the LS rule, if there are no overdue jobs it narrows into the WSPT rule for the overdue jobs.

2.2 Application of a complex priority rule

We observe the rule of tardiness costs with considered setup times (ATCS). The apparent tardiness cost with setups (ATCS) rule is designed for the $1|s_{jk}|\sum w_j T_j$ problem. The objective is to minimize the sum of the weighted tardinesses, but now the jobs are subject to sequence-dependent setup

je prednost vsakega delovnega naloga *j* odvisna od delovnega naloga, ki je bil pravkar končan na stroju. Pravilo ACTS je kombinirano; WSPT + LS + LSS na podlagi ene vrednosti (skalar). Izračun vrednosti delovnega naloga *j* v času *t*, ko je bil delovni nalog *l* končan na stroju, prikazuje naslednja enačba:

times. This implies that the priority of any job *j* depends on the job just completed on the machine just freed. The ACTS rule combines the WSPT rule, the LS rule, and the LSS rule in a single ranking index. The rule calculates the index of job *j* at time *t* when job *l* has completed its processing on the machine:

$$I_j(t,l) = \frac{w_j}{p_j} \cdot e^{-\frac{\max(d_j - p_j - t, 0)}{k_1 \cdot \bar{p}}} \cdot e^{-\frac{s_{lj}}{k_2 \cdot \bar{s}}} \quad (8),$$

kjer so: $\bar{s}$ – povprečna vrednost pripravljalnih in končnih časov preostalih delovnih nalogov, ki čakajo na razvrščanje,
k_1 – parameter, odvisen od dobavnih rokov,
k_2 – parameter, odvisen od pripravljalnih in končnih časov.

Parametra k_1 in k_2 sta funkciji treh faktorjev:
- faktorja ozkosti dobavnih rokov:

where: $\bar{s}$ – the mean of the setup times of the remaining jobs,
k_1 – the due-date-related scaling parameter,
k_2 – the setup-time-related scaling parameter.

The parameters k_1 and k_2 are functions of three factors:
- the due-date tightness factor:

$$\tau = 1 - \frac{\bar{d}}{\hat{C}_{max}} \quad (9),$$

- faktorja razpona dobavnih rokov:

- the due-date range factor:

$$R = \frac{d_{max} - d_{min}}{\hat{C}_{max}} \quad (10),$$

- faktorja obsega pripravljalnih in končnih časov:

- the setup-time severity factor:

$$\eta = \frac{\bar{s}}{\bar{p}} \quad (11).$$

Tudi skupni čas izvedbe nalogov na enem stroju je odvisen od razvrstitve zaradi pripravljalnih in končnih časov. Preprosto ocenitev proizvodnega časa vseh *n* nalogov na enem stroju prikazuje naslednja enačba:

Even with a single machine the makespan is now schedule dependent because of the setup times. A simple estimate for the makespan on a single machine is the following:

$$\hat{C}_{\max} = \sum_{j=1}^{n} p_j + n \cdot \bar{s} \quad (12).$$

Ta ocenitev bo najverjetneje precenila skupni proizvodni čas zaradi tega, ker bo končno razvrščanje izkoristilo pripravljalne in končne čase, da bodo nižji od povprečnih. Definiciji τ in R morata upoštevati omenjeno ocenitev skupnega proizvodnega časa. Poizkusne študije pravila ATCS predlagajo izbor parametrov k_1 in k_2 takole:

This estimate will most likely overestimate the makespan because the final schedule will take advantage of the setup times, which are lower than average. The definitions of τ and R have to be modified by replacing the makespan with its estimate. An experimental study of the ATCS rule has suggested the selection of parameters k_1 and k_2:

$$k_1 = 4{,}5 + R, \; R < 0{,}5$$
$$k_1 = 6 - 2 \cdot R, \; R \geq 0{,}5 \quad (13)$$
$$k_2 = \frac{\tau}{2\sqrt{\eta}} \quad (14).$$

2.2.1 Primer razvrščanja s pravilom ATCS

Za primer vzemimo $1|s_{jk}|\sum w_j T_j$ za štiri delovne naloge, katerih normativni časi, roki dobave in uteži so prikazani v preglednici 1.

2.2.1 Example of scheduling with the ACTS rule

Consider an instance of $1|s_{jk}|\sum w_j T_j$ with the four jobs in Table 1 (the processing times, due dates and weights are presented).

Preglednica 1. *Štirje delovni nalogi (osnovni podatki)*
Table 1. *Four jobs (basic data)*

Nalog Job	1	2	3	4
p_j	13	9	13	10
d_j	12	37	21	22
w_j	2	4	2	5

Preglednica 2. *Pripravljalni in končni časi prvega naloga v zaporedju*
Table 2. *Setup times for the first job in the sequence*

Nalog Job	1	2	3	4
s_{0j}	1	1	3	4

Preglednica 3. *Od zaporedja odvisni pripravljalni in končni časi*
Table 3. *The sequence-dependent setup times*

Nalog Job	1	2	3	4
s_{1j}	-	4	1	3
s_{2j}	0	-	1	0
s_{3j}	1	2	-	3
s_{4j}	4	3	1	-

Pripravljalni in končni časi s_{0j} za prvi delovni nalog v zaporedju so predstavljeni v preglednici 2.

Od zaporedja odvisni pripravljalni in končni časi nalogov, ki sledijo prvemu, so prikazani v tretji preglednici.

Za uporabo pravila ATCS moramo določiti povprečni normativni čas $\bar{p}$ in povprečni pripravljalni in zaključni čas $\bar{s}$. Povprečni normativni čas je 11,25, povprečni pripravljalni in končni čas pa 2. Ocena izdelovalnega časa je podana z enačbo:

The setup times s_{0j} of the first job in the sequence are presented in Table 2.

The sequence-dependent setup times of the jobs following the first job are shown in Table 3.

To use the ATCS rule the mean processing time $\bar{p}$ and the mean setup time $\bar{s}$ have to be determined. The mean processing time is 11.25 and the mean setup time is 2. The estimate for the makespan is in the following equation:

$$\hat{C}_{max} = \sum_{j=1}^{n} p_j + n \cdot \bar{s} = 45 + 4 \cdot 2 = 53 \qquad (15),$$

kjer so:
- faktor razpona dobavnih rokov $R = 25/53 \approx 0{,}47$,
- faktor ozkosti dobavnih rokov $\tau = 1 - 23/53 \approx 0{,}57$,
- faktor obsega pripravljalno-zaključnih časov pa je $\eta = 2/11{,}25 \approx 0{,}18$.

Z uporabo enačb (13) in (14) določimo parameter $k_1 = 5$ in parameter $k_2 = 0{,}7$ (zaokroženo). Da določimo, kateri delovni nalog bo prvi, moramo izračunati $l_j(0, 0)$ za vse $j = 1, \ldots, 4$.

where:
- the due-date range factor $R = 25/53 \approx 0.47$,
- the due-date tightness coefficient $\tau = 1 - 23/53 \approx 0.57$,
- the setup-time severity coefficient is $\eta = 2/11.25 \approx 0.18$.

Using the Equations (13) and (14), the parameter k_1 is 5 and the parameter k_2 is 0.7 (rounded). To determine which job goes first, $l_j(0, 0)$ has to be calculated for $j = 1, \ldots, 4$.

$$l_1(0,0) = \frac{2}{13} \cdot e^{-\frac{\max(12-13,0)}{56,25}} \cdot e^{-\frac{1}{1,4}} \approx 0,15 \cdot 1 \cdot 0,51 \approx 0,075$$

$$l_2(0,0) = \frac{4}{9} \cdot e^{-\frac{\max(37-9,0)}{56,25}} \cdot e^{-\frac{1}{1,4}} \approx 0,44 \cdot 0,61 \cdot 0,51 \approx 0,137$$

$$l_3(0,0) = \frac{2}{13} \cdot e^{-\frac{\max(21-13,0)}{56,25}} \cdot e^{-\frac{3}{1,4}} \approx 0,15 \cdot 0,87 \cdot 0,103 = 0,013$$

$$l_4(0,0) = \frac{5}{10} \cdot e^{-\frac{\max(22-10,0)}{56,25}} \cdot e^{-\frac{4}{1,4}} \approx 0,50 \cdot 0,81 \cdot 0,057 \approx 0,023$$

Iz zgornjih enačb je razvidno, da ima delovni nalog 2 največjo prednost. Ker je njegov pripravljalni in končni čas 1, je njegov čas dokončanja 10 (1 do 9). V drugem ponavljanju morajo biti izračunani $l_1(10, 2)$, $l_3(10, 2)$ in $l_4(10, 2)$. Da poenostavimo izračun, lahko vrednosti $k_1 \cdot \bar{p}$ in $k_2 \cdot \bar{s}$ pustimo enake (vmes je nalog 2 že izločen). Z nadaljnjo uporabo pravila ATCS je končni rezultat zaporedje nalogov (2,4,3,1) in vsota uteženih kasnitev enaka 98. Preračun vseh možnosti kaže, da je to zaporedje optimalno. Opazimo lahko, da je vselej izbran delovni nalog z najmanjšim pripravljalnim in končnim časom glede na predhodni nalog.

3 OMEJENO ISKANJE V SNOPU

Ta metoda temelji na zamisli "razvejaj in omeji". Preštevne metode "razvejaj in omeji" so trenutno najbolj razširjene za iskanje optimalnih rešitev za probleme "NP-hard" pri razvrščanju. Glavna pomanjkljivost teh metod je v tem, da po navadi porabijo ogromno časa, saj je lahko število obravnavanih vozlišč zelo veliko.

Za primer vzemimo stroj z n čakajočimi delovnimi nalogi. Predpostavimo, da so bili za vsako vozlišče na ravni k izbrani delovni nalogi za prvih k leg. Na ravni 0 je eno vozlišče z n vejami do n vozlišč na ravni 1. Vsako vozlišče na ravni 1 je razvejano v n-1 vozlišč na ravni 2, kar pomeni skupno n·(n-1) vozlišč na ravni 2. Na ravni k je n!/(n-k)! vozlišč. Na najnižji ravni, to je na n, je število vozlišč n!. Metoda "razvejaj in omeji" skuša izločiti vozlišča z določanjem spodnje meje doseganja cilja (ciljne funkcije) za vse delne razvrstitve, ki rastejo iz danega vozlišča. V primeru, da je spodnja meja višja od vrednosti ciljne funkcije za že znano razvrstitev, je moč vozlišče izločiti in se njegov "potomec" ne upošteva. Če dosežemo predhodno dokaj dobro razvrstitev nalogov z uporabo določene hevristične metode, preden se odločimo za uporabo metode "razvejaj in omeji", je mogoče tako izločiti mnogo vozlišč. Kljub postopku izločanja pa ponavadi ostane vseeno preveč vozlišč za preračun. Prednost "razvejaj in omeji" je v tem, da smo po preračunu po vseh vozliščih prepričani, da je rešitev optimalna.

From the calculation we can see that job 2 has the highest priority. Because its setup time is 1, its completion time is 10 (1 to 9). At the second iteration, $l_1(10, 2)$, $l_3(10, 2)$ and $l_4(10, 2)$ have to be calculated. To simplify the computations the values of $k_1 \cdot \bar{p}$ and $k_2 \cdot \bar{s}$ can be kept the same (job 2 has been already completed). Continuing the application of the ATCS rule results in the sequence (2,4,3,1) with the sum of the weighted tardinesses equal to 98. Complete enumeration shows that this sequence is optimal. Note that this sequence always selects, whenever the machine is freed, one of the jobs with the smallest setup time.

3 THE FILTERED-BEAM SEARCH

This method is based on the ideas of branch and bound. Enumerative branch-and-bound methods are currently the most widely used methods for obtaining optimal solutions to "NP-hard" scheduling problems. The main disadvantage of branch and bound is that it is usually extremely time consuming, because the number of nodes one must consider is very large.

Consider, for example, a single machine problem with n jobs. Assume that for each node at level k, jobs have been selected for the first k positions. There is a single node at level 0, with n branches emanating from it to n nodes at level 1. Each node at level 1 branches out into n-1 nodes at level 2, resulting in a total of n·(n-1) nodes at level 2. At level k, there are n!/(n-k)! nodes. At the bottom level, level n, there are n! nodes. The branch-and-bound method attempts to eliminate a node by determining a lower bound on the objective for all the partial schedules that sprout out of that node. If the lower bound is higher than the value of the objective under a known schedule, then the node may be eliminated and its offspring disregarded. If one could obtain a reasonably good schedule through some clever heuristic before going through the branch-and-bound procedure, then it might be possible to eliminate many nodes. Even after these eliminations there are usually still too many nodes to be evaluated. The main advantage of branch and bound is that, after evaluating all the nodes, the final solution is known with certainty to be optimal.

Omejeno iskanje v snopu pomeni prilagoditev metode "razvejaj in omeji", saj ne upoštevamo vseh vozlišč po ravneh. Za razvejanje se upoštevajo samo najbolj obetavna vozlišča na ravni k, preostala na tem ravni trajno zbrišemo. Število vozlišč, ki jih obdržimo, pomeni širino snopa izbora. Ključna sestavina metode je način vrednotenja obetavnosti posameznih vozlišč. Če izločanju posvetimo malo časa, je metoda hitra, lahko pa nas stane dobrega rezultata, saj lahko izločimo obetavna vozlišča. Na drugi strani pa preveč previdno izločanje vozlišč pomeni veliko časovno potratnost postopka. V ta namen se uporablja filter. Za vsa vozlišča na ravni k naredimo grobo napoved. Na njenih predvidevanjih izberemo vozlišča za nadaljnji preračun, preostala pa zbrišemo. Število izbranih vozlišč za preračun označuje širino filtra. Na podlagi preračuna izbranih vozlišč izluščimo skupino vozlišč (toliko kolikor znaša širina snopa, nikakor pa ne več ko širina filtra), iz katerih bomo izvedli nadaljnje razvejanje.

3.1 Primer

Za primer vzemimo $1\|\sum w_jT_j$, torej z enakim merilom kakor v prejšnjem primeru (preglednica 4).

Ker je število delovnih nalogov majhno, naredimo samo en tip napovedi za vozlišča na katerikoli ravni. Uporabili nismo nobenega sistema filtriranja. Za širino snopa izberemo 2, kar pomeni, da na vsaki ravni obdržimo dve vozlišči. Napoved na vozlišču naredimo z razvrščanjem delovnih nalogov s pravilom ATC (ni razlikovanja pripravljalnih in končnih časov). S faktorjem razpona dobavnih rokov R = 11/37 in s faktorjem ozkosti dobavnih rokov $\tau \approx 32/37$ (glej enačbi (9) in (10)), izberemo vrednost parametra pogleda naprej k = 5.

The filtered-beam search is an adaptation of branch and bound in which not all nodes at any given level are evaluated. Only the most promising nodes at level k are selected as nodes to branch from. The remaining nodes at that level are discarded permanently. The number of nodes retained is called the beam width of the search. The evaluation process that determines which nodes are the promising ones is a crucial component of this method. Evaluating each node carefully, to obtain an estimate for the potential of its offspring, is time consuming. There is a trade-off here: a crude prediction is quick but may lead to good solutions being discarded, whereas a more thorough evaluation may be prohibitively time consuming. Here is where the filter comes in. For all the nodes generated at level k, a crude prediction is made. Based on the outcome of these crude predictions, a number of nodes are selected for a thorough evaluation, and the remaining nodes are discarded permanently. The number of nodes selected for a thorough evaluation is referred to as the filter width. Based on the outcome of a careful evaluation of all the nodes that pass the filter, a subset of these nodes (the number being equal to the beam width, which, therefore, cannot be greater than the filter width) is selected, from which further branches will be generated.

3.1 Example

Consider the instance of $1\|\sum w_jT_j$, therefore with the same objective as in the previous example (Table 4).

Because the number of jobs is rather small, only one type of prediction is made for the nodes at any particular level. No filtering mechanism is used. The beam width is chosen to be 2, which implies that at each level only two nodes are retained. The prediction at a node is made by scheduling the unscheduled jobs according to the ATC rule. With the due-date range factor R = 11/37 and the due-date tightness factor $\tau \approx 32/37$ (Equations (9) and (10)), the look-ahead parameter k is chosen to be 5.

Preglednica 4. *Podatki za štiri naloge*
Table 4. *Data for four jobs*

Nalog Job	1	2	3	4
p_j	10	10	13	4
d_j	4	2	1	12
w_j	14	12	1	12

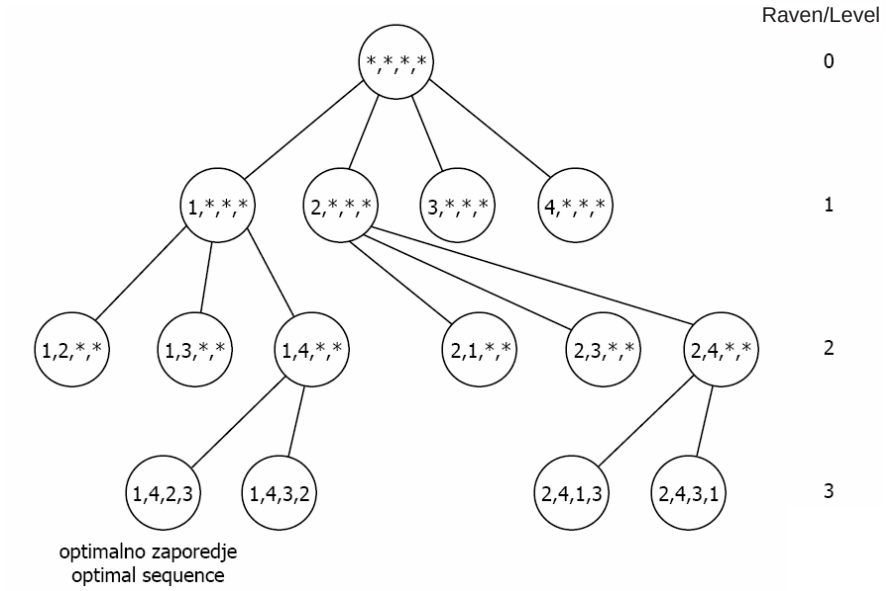

Sl. 2. *Omejeno iskanje v snopu za* $1\|\sum w_j T_j$
Fig. 2. Beam search applied to $1\|\sum w_j T_j$

Oblikujemo drevo "razvejaj in omeji", s predpostavko, da je zaporedje razvito, z začetkom v trenutku $t = 0$. Tako so na j-ti ravni drevesa delovni nalogi dani v j-to lego. Na 1. ravni drevesa imamo štiri vozlišča: (1,*,*,*), (2,*,*,*), (3,*,*,*) in (4,*,*,*), kar prikazuje slika 2. Z uporabo pravila ATC za preostale tri delovne naloge na vsakem od štirih vozlišč izražajo naslednja štiri zaporedja: (1,4,2,3), (2,4,1,3), (3,4,1,2) in (4,1,3,2) z vrednostmi ciljne funkcije 408, 436, 814 in 440. Ker je širina snopa 2, obdržimo le prvi dve vozlišči.

Vsako izmed teh dveh vozlišč se razveja v nadaljnja tri vozlišča na ravni 2. Vozlišče (1,*,*,*) se razveja v (1,2,*,*), (1,3,*,*) in (1,4,*,*), vozlišče (2,*,*,*) pa v (2,1,*,*), (2,3,*,*) in (2,4,*,*). Z uporabo pravila ATC za preostala delovna naloga v vsakem od šestih vozlišč na drugi ravni dobimo boljše rezultate v vozliščih (1,4,*,*) in (2,4,*,*), ki ju v nadaljevanju obdržimo, ostala štiri pa opustimo.

Dve vozlišči na ravni 2 se razvejata v štiri vozlišča na ravni 3 (zadnja stopnja), (1,4,3,2), (1,4,2,3), (2,4,1,3) in (2,4,3,1). Od teh štirih zaporedij je najboljše zaporedje (1,4,2,3) s skupno uteženo kasnitvijo 408. To zaporedje je optimalno.

4 HEVRISTIČNO PREISKOVANJE GLEDE NA OMEJITVE

V mnogih dejanskih primerih ni pravega cilja. Zahtevamo le izvedljivo razvrstitev, ki

A branch-and-bound tree is constructed with the assumption that the sequence is developed, starting from $t = 0$. So, at the j-th level of the tree the jobs are put into the j-th position. At level 1 of the tree there are four nodes: (1,*,*,*), (2,*,*,*), (3,*,*,*) and (4,*,*,*), see Figure 2. Using the ATC rule for the remaining jobs at each one of four nodes results in four sequences: (1,4,2,3), (2,4,1,3), (3,4,1,2) and (4,1,2,3) with objective values of 408, 436, 814 and 440. Because the beam width is 2, only the first two nodes are retained.

Each of these two nodes leads to three nodes at level 2. Node (1, *, *, *) leads to nodes (1,2,*,*), (1,3,*,*) and (1,4,*,*), and node (2,*,*,*) leads to nodes (2,1,*,*), (2,3,*,*) and (2,4,*,*). Applying the ATC rule to the remaining two jobs in each one of the six nodes at level 2 results in nodes (1,4,*,*) and (2,4,*,*) being retained and the remaining four being discarded.

Two nodes at level 2 lead to four nodes at level 3 (the last level), (1,4,3,2), (1,4,2,3), (2,4,1,3) and (2,4,3,1). Of these four sequences, sequence (1,4,2,3) is the best with a total weighted tardiness equal to 408. This sequence is optimal.

4 THE CONSTRAINT-GUIDED HEURISTIC SEARCH

In many real-world situations there is not really an objective. Rather, it is only required to

izpolnjuje določene omejitve in pravila. Postopek za razvrščanje v teh primerih je omenjen v literaturi [19] kot *preiskovanje glede na omejitve*. Ta postopek je bil zelo priljubljen med znanstveniki na področju računalništva in med strokovnjaki za umetno inteligenco [20].

Preiskovanje glede na omejitve lahko najbolje opišemo kar s primerom. Zamislimo si določeno število ne nujno enakih vzporednih strojev. Delovni nalog mora biti izveden na samo enem izmed strojev; za vsak delovni nalog je izbor mogočih strojev M_j, med katerimi lahko izbiramo. Delovni nalog j zahteva postopek $p_j = 1, j = 1, \ldots, n$ in ima čas prihoda (lansiranja) r_j ter dobavni rok d_j. Cilj je najti izvedljivo razvrstitev, v kateri so vsi delovni nalogi obdelani v okviru njihovih časovnih okvirov. V tem primeru ima optimalna razvrstitev ciljno funkcijo z vrednostjo 0 (popolna izvedljivost).

Preiskovanje glede na omejitve se lahko izvaja na podlagi naslednjih pravil: vselej razvrstimo en delovni nalog. Ko je delovni nalog razvrščen, je dodeljen določenemu stroju, ki je v tem času prost; izbrana pravila določajo, kdaj je določen delovni nalog dan v obdelavo na nekem stroju. Delovni nalogi so lahko razporejeni glede na kritičnost ali prilagodljivost; tisti z najmanjšo prilagodljivostjo je najbolj kritičen in se izvaja prvi. Poznamo več postopkov merjenja prilagodljivosti nalogov (po časovni zračnosti, po številu mogočih strojev itn.). Tudi stroje izbiramo po določenih pravilih (npr. po prilagodljivosti, merjenje po številu nalogov, ki jih stroj lahko obdela; najprej izbiramo tiste z najmanjšo prilagodljivostjo) [21].

Pomembno načelo preiskovanja glede na omejitve je tako imenovana razširitev omejitev. Dodelitev določenega delovnega naloga k danemu časovnemu koraku na stroju ima vpliv na dodeljevanje preostalih delovnih nalogov na tem stroju in na drugih strojih. Ti vplivi lahko kažejo na kršitev omejitev in povzročijo, da ostane del preiskovanega prostora neupoštevan.

4.1 Primer

Za primer vzemimo $P3|r_j, p_j = 1, M_j|\sum U_j$. $U_j = 1$, če nalog kasni, drugače je $U_j = 0$. Imamo tri stroje in devet delovnih nalogov. Časi obdelave, časi prihoda nalogov in dobavni roki so predstavljeni v preglednici 5. Neskončni čas (∞) pomeni, da naloga na danem stroju ni mogoče

generate a feasible schedule that satisfies various constraints and rules. One approach for generating schedules in these situations is referred to in the literature [19] as the constraint-guided search. This approach has been very popular among computer scientists and artificial intelligence experts [20].

The constraint-guided search may be described best with an example. Consider a number of not necessarily identical machines in parallel. A job has to be processed only on the one of the machines; for each job there may be a feasible set of machines M_j to choose from. Job j requires a processing $p_j = 1, j = 1, \ldots, n$ and has a release date r_j and the due date d_j. The goal is to find a feasible schedule in which all the jobs are processed within their respective time windows. In this case the optimal schedule has an objective of value 0 (perfect feasibility).

The constraint-guided search may operate according to the following rules. Jobs are scheduled one at a time. When a job is scheduled, it is assigned to a specific time slot on a specific machine, which is still free. During each iteration an unassigned job is selected according to a set of job rules that have been arranged in some priority. The job rules specify whether the particular job actually can be processed on a given machine. The jobs can be ordered according to their criticality or flexibility; the job with the least flexibility is the most critical and has the highest priority. The flexibility of a job can be measured in several ways (flexibility in time – slack time, flexibility with regard to the number of appropriate machines, etc.). The machines can also be ordered in such a way that the machine with the least flexibility has the highest priority (the flexibility of a machine, measured by the number of jobs that can be processed on the machine) [21].

An important concept in constraint-guided search is constraint propagation. The assignment of a particular job to a given time slot on a given machine has implications with regard to the assignment of other jobs on the given machine and on other machines. These implications may point to the violation of hard constraints and may indicate that the associated part of the search space can be disregarded.

4.1 Example

Consider the problem $P3|r_j, p_j = 1, M_j|\sum U_j$. $U_j = 1$, if $C_j > d_j$, otherwise $U_j = 0$. We have three machines and nine jobs. The processing times, release dates, and due dates of the job are presented in Table 5. If the processing time of a job on a machine is infinity (∞), then the job cannot be processed on that

Preglednica 5. *Podatki za devet delovnih nalogov*
Table 5. *Data for nine jobs*

Nalog Job	1	2	3	4	5	6	7	8	9
p_{1j}	∞	1	1	∞	1	∞	∞	1	1
p_{2j}	1	1	∞	1	1	1	∞	1	1
p_{3j}	1	1	∞	1	1	∞	1	∞	1
r_j	1	1	0	0	0	0	1	1	2
d_j	3	2	1	2	1	1	3	3	3

Preglednica 6. *Faktor prilagodljivosti devetih delovnih nalogov*
Table 6. *Flexibility factor of nine jobs*

Nalog Job	1	2	3	4	5	6	7	8	9
Φ_j	4	3	1	4	3	1	2	4	3

Preglednica 7. *Faktor prilagodljivosti časovnega koraka nalogov*
Table 7. *Flexibility factor of a job timeslot*

Stroj Machine	1	1	1	2	2	2	3	3	3
časovni korak timeslot	(1,1)	(1,2)	(1,3)	(2,1)	(2,2)	(2,3)	(3,1)	(3,2)	(3,3)
$\Phi_{(i,l)}$	2	2	2	3	4	3	2	4	3

Preglednica 8. *Dodelitev nalogov časovnim korakom*
Table 8. *Assignment of jobs to timeslots*

Stroj Machine	1	1	1	2	2	2	3	3	3
časovni korak timeslot	(1,1)	(1,2)	(1,3)	(2,1)	(2,2)	(2,3)	(3,1)	(3,2)	(3,3)
$\Phi_{(i,l)}$	2	2	2	3	4	3	2	4	3

obdelati. Cilj je najti izvedljivo razvrstitev, kjer bodo vsi nalogi pravočasno končani ($\sum U_j = 0$).

Imamo devet korakov, po tri na vsakem stroju. Vsak nalog ima svoj časovni okvir, kar pomeni omejitve. Za vsak delovni nalog lahko izračunamo faktor prilagodljivosti Φ_j. V našem primeru je izračunan kot število časovnih korakov, katerim je lahko delovni nalog dodeljen na različnih strojih. Predstavljen je v preglednici 6.

Namesto prilagodljivosti stroja definiramo prilagodljivost časovnega koraka na stroju, katero predstavlja število delovnih nalogov, ki so lahko obdelani v danem koraku. Faktor prilagodljivosti $\Phi_{(i,l)}$ koraka (*i, l*) predstavimo v spodnji preglednici. Korak (*i, l*) je *l*-ti korak na *i*-tem stroju.

Zaporedje nalogov po povečani prilagodljivosti je: 3, 6, 7, 2, 5, 9, 1, 8, 4. Prednosti časovnih korakov dajejo (možen) vrstni red (1,3), (3,1), (1,1), (1,2), (2,1), (2,3), (3,3), (3,2), (2,2).

machine. The goal is to find a feasible schedule with all the jobs completed on time ($\sum U_j = 0$).

There are nine timeslots and three on each machine. Each job has its own time window, which represents a set of constraints. For each job a flexibility factor Φ_j can be calculated. In this example: Φ_j is the number of timeslots to which a job may be assigned on the various machines. The flexibility factor Φ_j of job *j* is presented in Table 6.

Instead of the flexibility of a machine, the flexibility of a timeslot on a machine is determined. It is defined as the number of jobs that can be processed during the timeslot. The flexibility factor $\Phi_{(i,l)}$ of the job timeslot *(i, l)* is presented in Table 7.

The sequence of jobs in increasing flexibility results in: 3, 6, 7, 2, 5, 9, 1, 8, 4. The priorities of the timeslots may result in the sequence (1,3), (3,1), (1,1), (1,2), (2,1), (2,3), (3,3), (3,2), (2,2).

Delovni nalog 3 je izbran najprej. V koraku (1,3) ga ni mogočo obdelati (prepozno), zato preverjamo naprej. V (3,1) tudi ne gre (3. stroj), tako je dodeljen koraku (1,1). Delovni nalog 6 je ob upoštevanju omejitev dodeljen koraku (2,1). Končni rezultati so prikazani v preglednici 8. Vsem omejitvam je zadoščeno.

Ko je neki delovni nalog razvrščen, se lahko faktor prilagodljivosti preostalim delovnim nalogom in časovnim korakom spremeni. Zato je mogoče uporabiti nove prednosti glede na nove faktorje prilagodljivosti. V podanem primeru tega nismo uporabili.

Preiskovanje glede na omejitve ne da vedno izvedljive rešitve že po prvem koraku. Lahko se zgodi, da pri zadnjem delovnem nalogu ni mogoča nobena izvedljiva dodelitev. V tem primeru se mora metoda nasloniti na kasnejši postopek, ki lahko najde izvedljivo rešitev z izmenjavami parov nalogov.

5 SKLEP

Problemi terminiranja spadajo na področje optimizacije. Ko se posvetimo takšnemu problemu, moramo vedno iskati njegovo zahtevnost, ker le-ta določa naravo algoritma, katerega naj bi uporabili pri reševanju. Za zahtevna razvrščanja v praksi po navadi narava problema zahteva neko svojo rešitev, zato lahko ustvarimo postopke, ki so kombinacija več predstavljenih načinov in tehnik v tem prispevku. Novejši postopki pridružujejo še simulacijsko tehniko. Ker potrebne računske zmogljivosti rastejo vsaj eksponentno z velikostjo problema terminiranja, smo prisiljeni v podoptimalno reševanje, kar pomeni: v "sprejemljivo kratkem" času dobiti "dovolj dobro" rešitev (blizu optimalni). V svetu je bilo v zadnjem desetletju razvitih (v industriji in v znanosti) na stotine sistemov za terminiranje, a nerešeni splošni problemi ostajajo. Prispevek poudarja možnosti za uporabo naprednih metod terminiranja.

Sistemi terminiranja bodo v prihodnosti temeljili na: simulaciji, umetni inteligenci, grafičnih predstavitvah, poenostavljanju, lastni organizaciji, mehkih podatkih in mehki logiki.

Job 3 is selected first. It is checked to determine whether it is allowed to be processed in the timeslot (1, 3). It is not (too late). The next timeslot is tried (3,1) – not on the 3rd machine, and so on, until a timeslot is found during which it is allowed to be processed. Job 3 is then assigned to slot (1, 1). Job 6 is considered in the same manner and assigned to slot (2, 1). Continuing in this manner results in the following assignment – see Table 8. All the constraints are fulfilled.

After a job has been assigned, the flexibility factors of the remaining jobs to be assigned and the remaining timeslots available may change. It would have been possible to reorder the remaining jobs, as well as the remaining timeslots, based on the new flexibility factors. In the example above this was not done.

The constraint-guided search does not always yield a feasible solution after the first pass. It may happen that when the last job has to be assigned, no feasible assignment is possible. In this case, the method has to rely on a post-processing procedure, which, through pairwise interchanges, attempts to construct a feasible solution.

5 CONCLUSION

Scheduling problems belong to the field of optimisation. When we focus on such a problem, we must always determine its complexity, which defines the nature of the algorithm that is applicable for finding a solution. For many hard-scheduling problems with specific solutions one may design procedures that combine elements of several presented techniques in the paper. Newer approaches also associate a simulation technique. Because of the at least exponential growth of the computational capabilities with the size of a scheduling problem, we are forced to use the sub-optimal solving: in an acceptable short time we must get a sufficient (near-optimal) solution. Over the past decade, hundreds of scheduling systems have been developed in industry and academia, but there are still unsolved general problems. In the paper the application of advanced scheduling methods is emphasized.

In the future scheduling systems will be based on the following: simulation, artificial intelligence, graphical presentation, simplifications, self-organisation, fuzzy data and fuzzy logic.

6 LITERATURA
6 REFERENCES

[1] Carlier, J. and P. Chretiénne (1988) Problèmes d'ordonnancement: modelisation / complexité / algorithmes. *Masson*, Paris.

[2] Johnson, S. M. (1954) Optimal two and three stage production schedules with set-up time included, *Naval Research Logistics Quarterly*, Vol. 1, pp. 61-68.
[3] Conway, R. W., W. L. Maxwell and L. W. Miller (1967) Theory of scheduling. *Addison-Wesley*, Reading.
[4] Lawler, E. L., A. H. G. Rinnooy Kan and B. Lageweg (1975) Minimizing total costs in one-machine scheduling, *Operations Research*, Vol. 23, pp. 908-927.
[5] Brah, S. A. and G. E. Wheeler (1998) Comparison of scheduling rules in a flow shop with multiple processors: A simulation, *Simulation*, Vol. 71, No. 5, pp. 302-311.
[6] Polajnar, A., B. Buchmeister, M. Leber, K. Pandža, B. Kalpič, T. Rojs, N. Vujica-Herzog, I. Palčič, T. Fulder and P. Meža (2004) Menedžment proizvodnih sistemov (sodobni pristopi). *Fakulteta za strojništvo*, Maribor.
[7] Brucker, P. (1998) Scheduling algorithms. *Springer-Verlag*, Berlin.
[8] Buchmeister, B., Z. Kremljak, K. Pandža, A. Polajnar (2004) Simulation study on the performance analysis of various sequencing rules, *International Journal of Simulation Modelling (Int J Simul Model)*, Vol. 3, No. 2-3, pp. 80-89.
[9] Gomes, P. J. and L. C. Meile (2002) Leveraging the potential of process technology through workflow scheduling, *International Journal of Service Industry Management*, Vol. 13, No. 1, pp. 7-28.
[10] Blažewicz, J., K. H. Ecker, E. Pesch, G. Schmidt and J. Weglarz (2001) Scheduling computer and manufacturing processes, *Springer-Verlag*, Berlin.
[11] Garcia-Sabater, J. P. (2001) The problem of JIT dynamic scheduling. A model and a parametric procedure. *Proceedings of the ORP3 conference*, Paris, September 2001.
[12] Nyman, D. and J. Levitt (2001) Maintenance planning, scheduling and coordination. *Industrial Press*, New York.
[13] Leung, J. Y.-T. (2004) Handbook of scheduling: algorithms, models and performance analysis. *Chapman & Hall/CRC*, Boca Raton.
[14] Palmer, D. (2006) Maintenance planning and scheduling handbook. *McGraw-Hill*, New York.
[15] Koo, P.-H. and J. Jang (2002) Vehicle travel time models for AGV systems under various dispatching rules, *International Journal of Flexible Manufacturing Systems*, Vol. 14, pp. 249-261.
[16] T'kindt, V. and J.-C. Billaut (2002) Multicriteria scheduling. *Springer-Verlag*, Berlin.
[17] Glaser, H., W. Geiger and V. Rohde (1991) Produktionsplannung und –steuerung. *Gabler Verlag*, Wiesbaden.
[18] Ljubič, T. (2006) Operativni management proizvodnje. *Založba Moderna organizacija*, Kranj.
[19] Pinedo, M. L. (2005) Planning and scheduling in manufacturing and services, *Springer Science+Business Media*, New York.
[20] Kremljak, Z., A. Polajnar and B. Buchmeister (2005) A heuristic model for the development of production capabilities, *Journal of Mechanical Engineering*, Vol. 51, No. 11, pp. 674-691.
[21] Penker, A., M. C. Barbu and M. Gronalt (2007) Bottleneck analysis in MDF-production by means of discrete event simulation, *International Journal of Simulation Modelling (Int J Simul Model)*, Vol. 6, No. 1, pp. 49-57, doi:10.2507/IJSIMM06(1)5.084.

Naslov avtorjev: Tadej Tasič
prof. dr. Borut Buchmeister
prof. dr. Bojan Ačko
Univerza v Mariboru
Fakulteta za strojništvo
Smetanova ulica 17
2000 Maribor
tadej.tasic@uni-mb.si
borut.buchmeister@uni-mb.si
bojan.acko@uni-mb.si

Authors' Address: Tadej Tasič
Prof. Dr. Borut Buchmeister
Prof. Dr. Bojan Ačko
University of Maribor
Faculty of Mechanical Eng.
Smetanova ulica 17
2000 Maribor, Slovenia
tadej.tasic@uni-mb.si
borut.buchmeister@uni-mb.si
bojan.acko@uni-mb.si

Prejeto: 19.7.2007
Received:
Sprejeto: 28.9.2007
Accepted:
Odprto za diskusijo: 1 leto
Open for discussion: 1 year

Strojniški vestnik - Journal of Mechanical Engineering 53(2007)12, 858-873
UDK - UDC 681.5
Pregledni znanstveni članek - Review scientific paper (1.02)

Računalniški in strojni vid v robotizirani montaži

Computer and Machine Vision in Robot-based Assembly

Niko Herakovič
(Fakulteta za strojništvo, Ljubljana)

Ob vse zahtevnejšem svetovnem trgu ponujajo robotizirani montažni sistemi dobre rešitve za racionalizacijo in večjo prilagodljivost montažnih postopkov. V modernem postopku montaže obstaja močno izražena potreba po naprednem robotiziranem prijemanju sestavnih delov in po zmožnostih izvajanja montažnih posegov v nestrukturiranih okoljih z naključno urejenimi objekti. Robotski montažni sistemi z računalniškim vidom, ki so bili pomembna tema raziskav v preteklih štirih desetletjih, so dandanes dozoreli do te mere, da so primerni za uspešno uporabo v naprednih nalogah robotizirane montaže. V tem prispevku je podan pregled raziskovalnega dela na področjih avtomatiziranih montažnih sistemov s strojnim vidom.

(Ključne besede: robotizirana montaža, strojni vid, robotski vid, razpoznavanje objektov)

Against the background of an increasingly demanding world market, robotic assembly systems offer good prospects for the rationalisation and flexibilisation of assembly processes. In modern assembly there is a strong need for advanced robot grasping and for the capability to perform assembly operations in non-structured environments with randomly positioned objects. Vision-based robotic assembly systems, which has been the topic of continuous research interest for almost four decades, have now matured to the point where they can be effectively applied to advanced robot-based assembly tasks. This paper gives an overview of the research work related to the field of automated vision systems for assembly.

(Keywords: robotiuc assembly, machine vision, robot vision, object recognition)

0 UVOD

Industrijska montaža je del proizvodnega postopka (sl. 1) in jo je mogoče definirati kot urejeno zaporedje fizičnih nalog ravnanja, v katerih so ločeni oz. nepovezani deli ali komponente približani drug drugemu in spojeni ali sestavljeni v specifično celoto.

Montaža je opravilo proizvodnega postopka, ki je odločilen dejavnik konkurenčnosti industrije nasploh. Na prvi pogled je presenetljivo, da se tako pomemben izdelovalni postopek, ki lahko doseže do 30% izdelovalnih stroškov končnega izdelka [1], še vedno izvaja pretežno ročno. V primerih, ko je zahtevana visoka stopnja kakovosti izdelkov, pomeni ročna montaža izredno velik delež stroška v izdelovalnem postopku, ker morajo biti v tem primeru vključeni delavci z dragocenimi izkušnjami in posebnimi znanji. Ročna montaža zahteva tudi

0 INTRODUCTION

Industrial assembly is a part of the production process (see Fig. 1) and can be defined as an ordered sequence of physical handling tasks in which discrete parts and components are brought together and joined or mated to form a specified configuration.

Assembly is a production-process operation that is a crucial factor in the competitiveness of industry in general. It is surprising that such an important manufacturing process, which can represent up to 30% of the manufacturing costs of an end product [1], is still mainly performed by hand. However, manual assembly becomes expensive, if high levels of quality are to be achieved, because the procedure involves highly skilled human workers. Also, a great deal of verification and inspection is needed to compensate

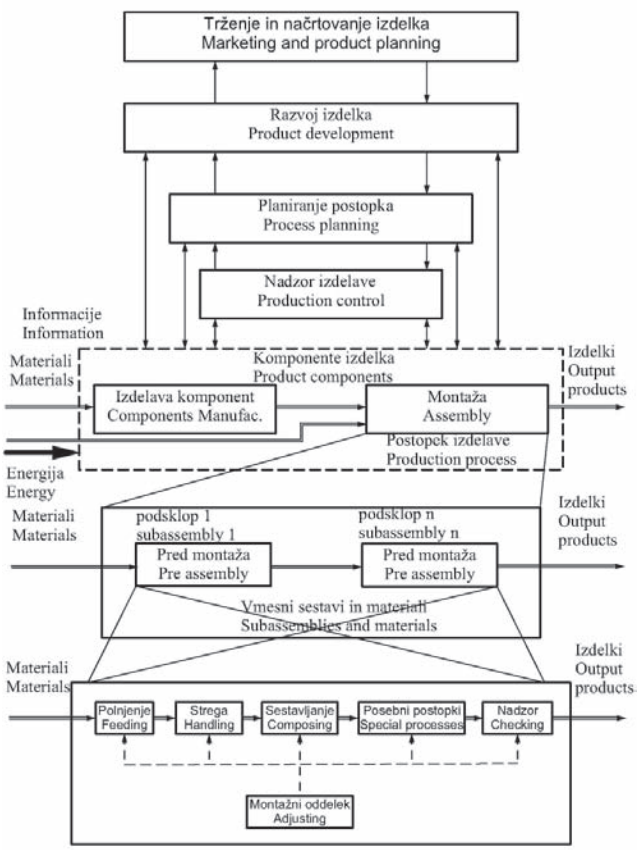

Sl. 1. *Montaža kot del proizvodnega postopka [2]*
Fig. 1. *Assembly as part of the production process [2]*

večjo stopnjo nadzora za nadomestilo mogočih človeških pomanjkljivosti oz. napak. Ročna montaža je pogosto tudi težka, utrudljiva in časovno potratna.

Zaradi teh razlogov je podjetjem, katerih montaža temelji v glavnem na ročnih montažnih postopkih, pogosto težko slediti zahtevam trga. Te težave so izrazite še posebej v primerih, kadar zahteva trg izdelke, ki morajo izpolniti velike zahteve glede kakovosti, cene in dobavnega roka. Ključna beseda pri doseganju teh ciljev je nenehno izboljševanje izdelka in proizvodnje. Montaža je pogosto najšibkejši člen v celotnem proizvodnem postopku, predvsem zato, ker ta dejavnost zavzema bistveni del celotnih proizvodnih stroškov in izdelovalnega časa, kar je prikazano na sliki 1a in b. Glavni razlogi za to so povečana cena dela in različnost izdelkov ter zmanjšanje količine posameznih izdelkov.

Ob upoštevanju vseh teh dejstev in ob nenehnem nižanju cen robotov in montažnih sistemov na ključ in še posebej ob upoštevanju nenehnega izboljševanja zmožnosti in

for potential human insufficiencies. What is more, manual assembly is often difficult, tedious and time consuming.

For this reason it is often difficult for companies to follow market demands, when their assembly is mainly based on the manual assembly processes. This becomes even more true, as the market requires products that satisfy high expectations in the areas of quality, price and delivery time. The key word in achieving this goal is the continuous refinement of product and production. Assembly is often the weakest point in the whole production process, because this activity takes up a substantial part of the total production costs and the throughput time (Fig. 2). The main reasons for this fact are the increasing labour costs, the variety of products, and a reduction in the quantity of products.

Taking into consideration all these facts, together with the constant price reductions for robots and overall turnkey systems in assembly and especially with the continually improving

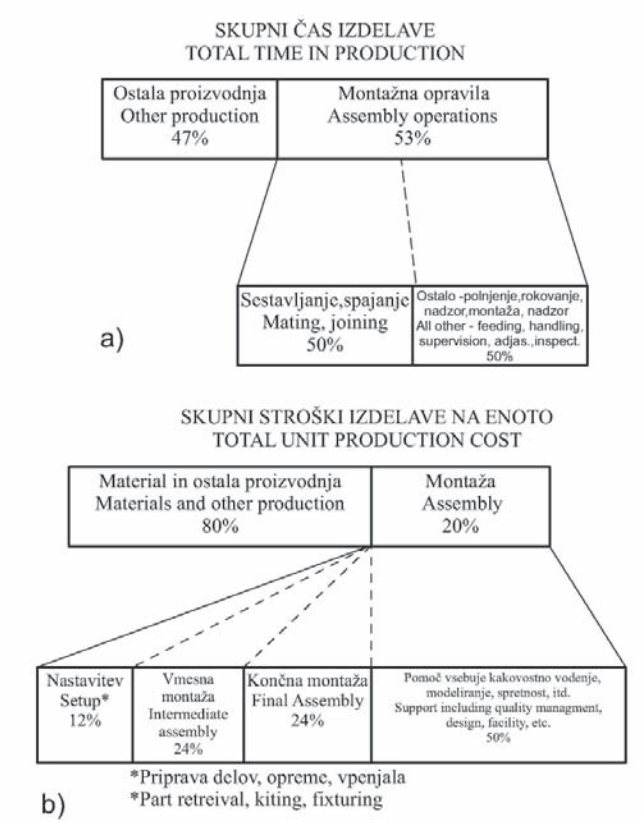

Sl. 2. *Tipična povprečna razčlemba a) proizvodnega časa in b) stroškov izdelave industrijskega izdelka [5]*
Fig. 2. *Typical average breakdown of a) the production time and b) the production costs of industrial products [5]*

učinkovitosti robotov in strojnega vida, so razumljivi razlogi za znatno povečanje področja robotizirane montaže v svetu v zadnjih nekaj letih ([3] in [4]). Robotizirana montaža pa ni obetajoča le v velikoserijski proizvodnji, ampak je primerna mnogokrat tudi v srednje in maloserijski proizvodnji ([1] in [2]).

Montaža, kot del proizvodnih sistemov, obsega ravnanje s sestavnimi deli in podsklopi, ki so bili v glavnem izdelani ob različnih časih in po možnosti celo na različnih krajih [5]. Montažna naloga tako izhaja iz zahtev po sestavljanju različnih delov, podsklopov in snovi, kakršna so maziva in adhezivi, v končne sestave večje zahtevnosti ob določenih količinah in znotraj določenih časovnih okvirov.

Tipična montažna celica, katere natančna razporeditev se lahko spreminja, je običajno sestavljena iz računalniško krmiljenih naprav (roboti, prijemala itn.), komponent in vpenjalnih pripomočkov, ki lahko opravijo ali podprejo opravljanje ene ali več naslednjih nalog [6]:

performance of robots and machine-vision systems, it is possible to understand the reasons for the considerable growth in the area of robot-based assembly in the world in the past few years ([3] and [4]). Robotic assembly also offers good prospects for small and medium-sized batch production ([1] and [2]).

Assembly, as a part of production systems, involves the handling of parts and subassemblies, which have mostly been manufactured at different times and possibly even in separate locations [5]. Assembly tasks thus result from the requirement to join certain individual parts, sub-assemblies and substances such as lubricants and adhesives into final assemblies of higher complexity in a given quantity and within a given time period.

A typical assembly cell, the exact configuration of which may vary, will be made up of computer-controlled devices (robots, grippers, etc.), components, and fixtures that can functionally accomplish or support one or all of the following tasks [6]:

- prijemanje organiziranih/naključno razmeščenih ciljnih delov s traku ali zaboja,
- ravnanje in nameščanje/sestavljanje delov,
- razpoznavanje delov in predmetov pred, med montažo in po montaži,
- preverjanje kakovosti in nadzor,
- načrtovanje in nadzor prožil in prijemal za izvajanje fizične montaže.

Industrijski roboti lahko dandanes izvajajo montažne in strežne naloge z velikimi hitrostmi in natančnostjo. Kljub temu imajo roboti v primerjavi s človekom slabše zmožnosti čutnega zaznavanja in zato potrebujejo napredne čutne zmožnosti za izvajanje zahtevnejših nalog v nestrukturiranem okolju ([7] in [8]). V postopku montaže se od računalniškega vida v glavnem zahteva pridobivanje podatkov za uporabljene robotske sisteme, da bi lahko le-ti zanesljivo prijemali predmete in izvajali montažne naloge. Uporaba sistema vida pri montaži večinoma vključuje različne izzive, še posebej na področju pridobivanja podatkov, spremembe koordinat, nespremenljivega razpoznavanja predmetov s sistemi vida, kakor tudi za razpored in vključitev sistema vida v robotsko okolje.

1 RAČUNALNIŠKI IN STROJNI VID

Strojni vid pomeni zaznavanje podatkov vida in njihovo razlago z uporabo računalnika in pomeni zaradi tega vsestransko robotsko zaznavalo. Obstajajo naraščajoče zahteve po zahtevnejših in hitrejših zmožnostih obdelovanja slik za uspešnejše uvajanje sistemov vida v napredne industrijske uporabe, npr. napredna avtomatizacija montaže.

Strojni oz. robotski vid je uporaba računalniškega vida v industriji in proizvodnji, v glavnem v robotskih uporabah. Medtem ko je računalniški vid v glavnem osredotočen na strojno obdelovanje slike, zahteva strojni vid še dodatno opremo, predvsem digitalne vhodno/izhodne naprave in računalniško omrežje za krmiljenje druge proizvodne opreme in pripomočkov, npr. robotskih rok [9]. Specifične prednosti sistemov strojnega vida vključujejo natančnost, doslednost, stroškovno učinkovitost in prilagodljivost.

Izhajajoč iz prvotnega namena je računalniški vid del raziskovalne panoge, imenovane umetna inteligenca. Mnoge metode, npr. nevronske mreže in strojno učenje, ki so bile razvite

- the grasping of an organized/randomly positioned target part from a belt or a bin,
- the manipulation and placement/assembly of parts,
- the recognition of parts and objects before, during and after assembly,
- the quality control and inspection,
- the planning and control of the actuators and grippers that carry out the physical assembly.

Industrial robots can nowadays perform assembly and material handling jobs with very high speed and impressively high precision. However, compared to human operators, robots are hampered by their lack of sensory perception and their need for advanced sensorial capabilities in order to carry out more sophisticated tasks in a non-structured environment ([7] and [8]). In assembly processes, computer vision is often required to provide data to the applied robot systems in order to allow the reliable grasping of objects and the performing of assembly tasks. Using a vision system for the assembly often involves several challenges, especially in the areas of data acquisition, coordinate transformation, invariant object recognition with vision systems as well as for the configuration and integration of vision systems into the robot environment.

1 COMPUTER AND MACHINE VISION

Machine vision is concerned with the sensing of vision data and its interpretation by a computer and thus serves as a versatile robotic sensor. There is a growing demand requiring more complex and faster image-processing capabilities in order to allow the implementation of vision systems into sophisticated industrial applications, like advanced assembly automation.

Machine or robot vision is the application of computer vision to industry and manufacturing, mainly in robots. As computer vision is mainly focused on machine-based image processing, machine vision most often also requires digital input/output devices and computer networks to control other manufacturing equipment, such as robotic arms [9]. The specific advantages of machine-vision systems include precision, consistency, cost effectiveness and flexibility.

Because of its primary mission, computer vision is a part of a research discipline called artificial intelligence. Many methods, like neural networks and machine learning, developed in the

na področju umetne inteligence, so uporabljene v računalniškem vidu. Računalniški vid je povezan tudi z drugimi raziskovalnimi panogami, npr. z nevropsihologijo, psihofiziko, fiziko, računalniško grafiko, digitalnim obdelovanjem signalov itn. [10].

Vsekakor je bilo na tem področju opravljenega veliko raziskovalnega dela. V mnogih primerih s področja montažnih postopkov, še posebej pri pobiranju delov iz zabojev, mora robot zaznavati 3-D prostor v svojem delovnem okolju, da lahko deluje učinkovito. Pridobivanje 3-D podatkov in opisovanje 3-D prostora je zahtevna naloga in še vedno ostaja predmet osnovnih raziskav. Nekatere raziskave ([11] do [13]) obravnavajo umetne sisteme vida, ki temeljijo na nevronski morfologiji biološkega človeškega sistema vida s ciljem razviti računalniške nevronske sestave in umetne sisteme vida z uporabo nevronskih vzorcev, matematičnih modelov in računskih zgradb.

Osnovne sestavine računalniškega sistema vida so prikazane na sliki 3. Pojav oz. videz 3-D slike je odvisen v glavnem od osvetlitve, lege in usmeritve zaznavala vida.

V sistemu strojnega vida je vključenih veliko različnih komponent. Sam načrt sistema je odvisen v glavnem od različnih dejavnikov, kakor so okolje, namen uporabe in pa seveda razpoložljiva denarna sredstva. Kljub temu imajo vsi sistemi strojnega vida mnoge skupne komponente. Tipični sistem strojnega vida za naloge sestavljanja oz. montaže sestoji iz več naslednjih deležev ([9], [14] do [16]):

- ena ali več digitalnih ali analognih kamer (črno-bele ali barvne) s primerno optiko za zbiranje slik;
- vmesnik kamere za digitalizacijo slik (VDS - FG);
- procesor (pogosto OR ali vgrajen procesor, npr. DSP) – ko so procesorji in VDS vgrajeni v samo

field of artificial intelligence, are used in computer vision. Computer vision is also linked with other research disciplines like neurophysiology, psychophysics, physics, computer graphics, digital signal processing etc. [10].

Nevertheless, there are many research activities in this direction. In many cases in the area of assembly processes, especially in bin picking, a robot must perceive its 3-D environment to be effective. Jet recovering 3-D information and describing it still remains the subject of fundamental research. Some research works ([11] to [13]) deal with artificial vision systems based on the neural morphology of the biological human vision system, aiming to design computational neural structures and artificial vision systems following neural paradigms, mathematical models and computational architectures (Neuro-Vision Systems).

The basic components of a computer-vision system are presented in Fig. 3. The appearance of the 3-D scene depends mostly on the illumination, the position and the direction of the vision sensor.

In a machine-vision system, a variety of components are included. The system's layout mainly depends on factors like the environment, the application and the budget. Nevertheless, there are several common ingredients to all vision systems. A typical machine-vision system for assembly tasks consists of several of the following components ([9], [14] to [16]):

- One or more digital or analog cameras (black-and-white or colour) with suitable optics for acquiring images,
- A camera interface for digitizing images (frame grabber),
- A processor (often a PC or embedded processor, such as a DSP) – when processors and frame

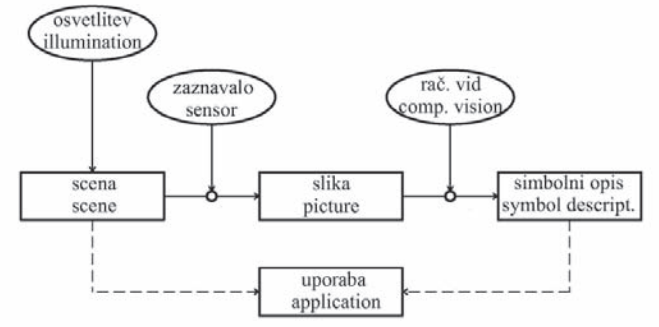

Sl. 3. *Sestava tipičnega računalniškega sistema vida [10]*
Fig. 3. *Structure of a typical computer-vision system [10]*

kamero, se takšna kamera imenuje »pametna kamera«;
- vhodno/izhodna strojna oprema oz. komunikacijske povezave;
- optika – leče za izostritev želenega vidnega polja na zaznavalo za zbiranje slike;
- vir svetlobe (svetleče diode, fluorescentne ali halogenske luči itd.);
- programska oprema za obdelavo slik in iskanje ustreznih značilnosti;
- zaznavalo za sinhroniziranje za iskanje delov, da bi bilo mogoče sprožiti snemanje slike in obdelavo podatkov;
- prožila za sortiranje oz. izmet prepoznanih delov.

Najpogosteje uporabljena zaznavala vida v robotizirano podprti montaži so dandanes črno-bele (ali barvne, za nekatere uporabe) kamere CCD. 2-D stroji vid sestoji iz običajnih kamer CCD za zaznavo slik, v okviru robota pa je izvedena obdelava in prinesene odločitve, kako je treba ravnati s sestavnimi deli za montažo. Takšni sistemi so primerni za ravnanje z deli, ki ležijo plosko na prenosnem traku ali v zaboju z ločevalnimi ponjavami.

Za tiste dele, ki ležijo neurejeno drug čez drugega ali pa zdrsnejo ob stran, ko se deli zataknejo oz. ko so deli razporejeni naključno v prenosnem zaboju, mora strojni vid znati oceniti globino. Za oceno globine so najpogosteje uporabljeni stereosistemi strojnega vida. Za takšne uporabe je nujno treba uporabiti 3-D strojni vid, da bi dobili 3-D obseg slike in usmeritev v 3-D prostoru. Takšno 3-D informacijo lahko zagotovijo različna laserska zaznavala v sodelovanju z 2-D kamerami, zaznavali s strukturirano svetlobo in stereokamere, skupaj z različnimi algoritmi ([17] do [19]). Vendar kljub temu, da ti sistemi dobro delujejo, lahko posredujejo stereosistemi strojnega vida nenatančno oceno globine, posebej še v primerih ko opazovana slika ne vsebuje izrazitih struktur oz. tekstur ali v primerih s prešibko osvetlitvijo opazovane scene. V glavnem pa so stereosistemi vida omejeni z osnovno razdaljo med dvema kamerama, katerih ocena globine je tembolj nenatančna, kolikor večja je razdalja med njima.

Različne raziskave obravnavajo problem ocene globine z uporabo enookih vidnih značilnic, kakor so spremembe teksture in gradientov, razostritev, barva itn. Z upoštevanjem učnega algoritma naključnega polja po Markovu za zajemanje oz. razpoznavanje nekaterih teh enookih značilnic in z njihovim vključevanjem v sistem

grabbers are integrated into the camera itself, such cameras are called “smart cameras”,
- Input/Output hardware or communication links,
- Optics - lenses to focus the desired field of view onto the image sensor,
- Light source (LED, fluorescent or halogen lamps etc.),
- A program to process the images and detect the relevant features,
- A synchronizing sensor for part detection to trigger image acquisition and processing,
- Actuators to sort or reject the processed parts.

The most commonly used vision sensors in robot-based assembly are nowadays black-and-white (or colour for some applications) CCD (charge-coupled device) cameras. 2D-vision systems consist of standard industrial CCD cameras used to take images that are processed by the robot to make decisions on how parts should be handled. Such systems are appropriate for parts, which are laying flat on a belt or in a bin with separator sheets.

For parts that can stack upon each other or that can shift from side to side as the parts stack up or when parts are oriented randomly in a bin, a depth estimation for a vision system is necessary. Stereo vision systems are normally used for depth estimation. For such applications 3-D vision systems have to be applied to get a range image and the orientation of a part in 3D-space. Different laser sensors in conjunction with 2-D cameras, sensors with structured light and stereo cameras, together with different algorithms, can provide 3-D information ([17] to [19]). Even though these systems work well, stereo vision systems can provide inaccurate depth estimations, especially in cases with textureless regions of images or in situations with insufficient illumination of the scene. Most of all, stereo vision is fundamentally limited by the baseline distance between the two cameras, which tends to provide inaccurate depth estimations, as the distances considered get larger.

Different research approaches address the depth-estimation problem by using monocular visual cues, such as texture variations and gradients, defocus, colour, etc. By applying a Markov Random Field learning algorithm to capture some of these monocular cues and by incorporating them into a stereo vision system, a significantly better accuracy

stereovida oz. kombiniranjem s stereovidom, je dosežena bistveno boljša natančnost in ocena globine kot z uporabo le enookih ali stereoznačilnic posamično ([20] in [21]).

Nekateri drugi prispevki obravnavajo 3-D vid in oceno lege predmeta v okolju robotizirane montaže. Postopek, ki ga obravnava L. P. Ray [22] na oceni trirazsežne lege in usmeritve predmetov s pomočjo ene ali več enookih slik s predpogojem, da so identitete predmetov znane in da so na voljo trirazsežni geometrijski modeli. Glavna pomanjkljivost teh rešitev je dejstvo, da ni mogoče doseči delovanja v dejanskem času, ki je potrebno v mnogih montažnih opravilih. Rešitev tega problema je predlagal Winkler [23]. V tej raziskavi je prikazana rešitev tega problema z uporabo strategije skupin značilnosti za oceno lege 3-D predmetov v dejanskem času iz 2-D pogleda na predmet. Predlagana metoda temelji na nevronskih mrežah in sistematičnem učenju Kohonenove samoorganizacijske skupine značilnosti predmeta in s tem izpolnjuje natančnostne zahteve ocene lege predmeta v več ko 90% vseh preučenih primerov.

Z namenom doseči ekonomsko upravičen in prilagodljivi avtomatski montažni sistem z robotom SCARA, ki bo deloval v naključnem, neurejenem okolju, so bile izvedene nekatere raziskave, ki predlagajo uporabo preprostih 2-D kamer CCD v povezavi z dodatnimi zaznavali sile in vgrajenimi prestrojljivimi logično mehkimi krmilniki [24]. Eksperimentalni rezultati potrjujejo zadovoljivo raven delovanja krmiljenega robota za izvedbo preizkusnih montažnih nalog.

Prispevek Sharsteina in Szelinskega [25] podaja zelo dober pregled sistemov s stereovidom in algoritmov, ki so jih razvili in predlagali različni raziskovalci v preteklih desetletjih. V svojih raziskovalnih delih avtorji predstavljajo taksonomijo strnjenih dvosistemskih stereometod, primerjajo znane stereometode in predstavljajo preizkuse, ki vrednotijo delovanje in učinek mnogih različic.

V robotizirani montaži imajo zaznavala vida drugačno vlogo kakor npr. pri premičnih robotih, pri katerih je njihova glavna naloga raziskovanje oz. odkrivanje okolja. Robotizirana montažna celica predstavlja razmeroma dobro organizirano okolje in je prej del vgrajenega proizvodnega postopka kakor pa izolirana enota. To dejstvo olajšuje nekatere bistvene zahteve za učinkovito robotizirano montažo. Posebej prihaja to do izraza pri uporabah, kjer se je treba izogibati dragim in

in the depth estimation is obtained than is possible by using either monocular or stereo cues on their own ([20] and [21]).

Some other papers treat monocular 3-D vision and the object-pose estimation in a robot assembly environment. The approach described by L. P. Ray [22] is based on the estimation of the three-dimensional position and orientation of objects from one or more monocular images with the prerequisite that the identities of the objects are known and that the three dimensional geometrical models are available. The main weakness of these solutions is the fact that they fail to achieve the real-time performance necessary in many assembly applications. A solution to this problem is proposed by [23]. In this research approach a feature-map strategy for the real-time 3-D object pose estimation from individual 2-D perspective views is presented. Based on a neural network and the systematic training of Kohonen's self-organizing feature map, the method satisfies the accuracy requirements of the object-pose estimation in more than 90% of all the considered cases.

With the intention of achieving an economic and flexible automatic assembly system working with a SCARA-robot, operating in a random environment, some research activities present the use of simple 2-D CCD cameras in conjunction with additional force sensors and embedded fuzzy sliding-mode controllers [24]. The experimental results prove that the robotic motion-control performance is good enough to execute the investigated assembly tasks.

The paper of Sharstein and Szelinski [25] offers a very good overview of stereo-vision systems and algorithms, developed by different researchers over the past few decades. In their work the authors present the taxonomy of dense, two-frame stereo methods, compare existing stereo methods and present experiments evaluating the performance of many different variants.

In robotic assembly, vision sensors have a different role than, for example, in mobile robots, where the tasks usually involve exploration of the environment. A robotic assembly cell represents a relatively well-ordered environment and is part of an integrated manufacturing process, rather than operating in isolation. This facilitates the fulfilment of some of the major requirements for effective robot assembly. This is especially helpful for applications where expensive and complex

zapletenim sistemom strojnega vida. Uporaba teh sistemov v robotiziranih montažnih sistemih je lahko poenostavljena v primerih, ko so izdelki in komponente oblikovani za robotizirano montažo in v primerih, ko prihajajo izdelki v sistem z razmeroma natančno definirano lego in usmeritvijo [26].

Rahlo nesimetričen vijačni del (sl. 4) v ročnem dodajanju in vstavljanju (montaži) ne bi pomenil večjih težav, medtem ko bi bil potreben v avtomatizirani stregi in montaži za isti del drag sistem strojnega vida, da bi lahko prepoznal usmeritev izdelka. Dejansko je mogoče reči, da je ena od mogočih koristi uvajanja avtomatizacije v montažo izdelka prisila v ponovno vrednotenje in spremembo oblike oz. konstrukcije izdelka, kar ima lahko za posledico ne samo preprostejšega prepoznavanja izdelka, ampak tudi druge stroškovne prihranke ali izboljšave kakovosti (npr. Poka-Yoke oblikovanje).

Glavna vloga zaznaval vida v robotizirani montažni celici je primerjava stvarnosti s pričakovanji in ovrednotenje odstopanj. Pravzaprav to pomeni zaznavanje prisotnosti oz. odsotnosti pravilnih delov in merjenje za zagotovitev toleranc in položajnih napak pri iskanju komponent med posameznimi fazami montaže.

Po eni strani so že dandanes uspešno izvedene mnoge industrijske uporabe z računalniškim vidom in roboti, posebej v robotiziranih montažnih celicah. Vendar imajo v teh uporabah izdelki oz. predmeti preprosto (2D) obliko in/ali so organizirani na strukturiran način. Po drugi strani pa še vedno ostaja problem pobiranja iz zaboja, pri katerem imajo predmeti 3-D obliko in so v zabojih naključno organizirani. Kljub mnogim raziskavam, ki so in še potekajo na tem področju ter ponujajo posebne rešitve in izboljšave za premagovanje problema pobiranja ([19], [27] do [29]), ostaja ta najstarejši izziv v robotiki še vedno nerešen.

machine-vision systems should be avoided. The application of vision systems in robot-based assembly systems can be simplified, when products and components are designed for a robot-based assembly, and if parts are fed to the system with a relatively accurate position and orientation [26].

A slightly asymmetrical screwed part (see Fig. 4) would not present significant problems in manual handling and insertion, whereas for automatic handling, an expensive vision system would be needed to recognize its orientation. In fact, it can be said that one of the possible benefits of introducing automation in the assembly of a product is that it forces a reconsideration of its design, which might not only facilitate the recognition of the part, but might also be used to implement other cost-saving or quality-related improvements (e.g., the Poka-Yoke design).

The major role of vision sensors in a robot assembly cell is to compare reality with expectations and to evaluate the discrepancies. Essentially, this means detecting the presence or absence of correct parts and measuring to allow for the detection of component tolerances and positioning errors during the relevant stages of assembly.

On one hand, many industrial assembly applications are successfully being handled nowadays using computer vision and robots, especially in robot-based assembly cells. However, for these applications objects have a simple (2D) shape and/or are organized in a structured manner. On the other hand, a general so-called "bin picking", where the objects have a 3-D shape and are randomly organized in a box, still remains a problem. Despite much research that offers special solutions and improvements in overcoming the bin-picking problem ([19], [27] do [29]), the oldest challenge in robotics still remains unsolved.

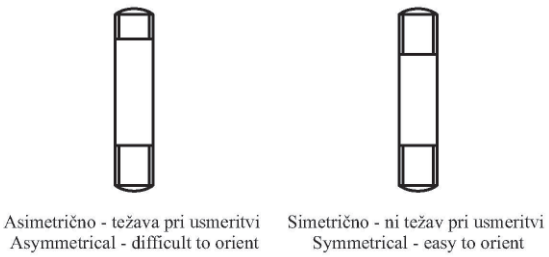

Sl. 4. *Sprememba konstrukcije za poenostavitev avtomatskega dodajanja in usmeritve [26]*
Fig. 4. *Design change to simplify automatic feeding and orientation [26]*

2 PREPOZNAVANJE PREDMETOV

V robotizirani montaži teži prepoznavni sistem strojnega vida k posnemanju človekovega čutila vida in mora biti zmožen zaznavati in prepoznavati montažne dele tako dobro, kakor to počnejo ljudje. Trirazsežno prepoznavanje predmetov zahteva 3-D predstavo predmeta, razpoznavo predmeta iz njegove slike, oceno njegovega lege in usmeritve ter zapis različnih večkratnih pogledov na predmet za avtomatsko ustvarjanje oz. izgradnjo modela. Pomembne stopnje v oblikovanju in razvoju sistema prepoznavanja so prikazane na sliki 5.

Tipičen postopek pri reševanju nalog prepoznavanja predmeta z uporabo običajne obdelave slike in metod računalniškega vida običajno obsega pet korakov ([27], [30] do [33]):

- Iskanje oz. predobdelava – je obdelava signalov na nizki stopnji, ki izlušči informacijo iz slike in jo predstavi v neki obliki preprostih simbolov ([34] do [38]).
- Razvrščanje oz. segmentiranje – temelji na preprostih simbolih nizke stopnje. Preproste značilnosti predmeta so združene v višjo stopnjo značilnosti, ki podajo več informacij za izbiro in preverjanje ujemanja v naslednjih korakih ([39] do [41]).
- Indeksiranje oz. izvleček značilnosti – izbiranje iz stabilnih značilnosti predmeta oz. modela iz knjižnice modelov in iskanje načina hitre primerjave nabora značilnosti z izbranim modelom, da se izognemo iskanju skozi vse modele. Kritična komponenta pri tem je stabilen, reprezentativen sistem izločitve značilnosti predmeta, ki mora biti razvit v fazi izločitve značilnosti, da bi omogočil izločitev ključnih značilnosti za specifično problemsko

2 OBJECT RECOGNITION

In robot assembly, a vision-recognition system aims to mimic the human sense of vision and must be capable of perceiving and detecting assembly parts as well as the humans can. Three-dimensional object recognition entails a representation of a 3-D object, an identification of the object from its image, an estimation of its position and orientation, and the registration of multiple views of the object for automatic model construction. The important stages in the design and development of a recognition system are presented in Fig 5.

A typical approach for handling the object-recognition tasks using traditional image processing and computer-vision methods usually consists of five steps ([27], [30] to [33]):

- Detection or pre-processing – is the low-level signal processing that extracts the information from the scene and represents it as some form of primitive symbols ([34] do [38]).
- Grouping or segmentation – is based on the low-level symbols, the primitive features are grouped into higher-order features, which give more information for the selection and matching in the next steps ([39] do [41]).
- Indexing or feature extraction – selecting from the stable object features the most likely model from a library of models (model base) and finding a way of quickly comparing a set of features with a model, avoiding a search through all the models. As a critical component, a stable, representative feature-extraction system should be developed to extract the key features for a specific problem domain in the feature-

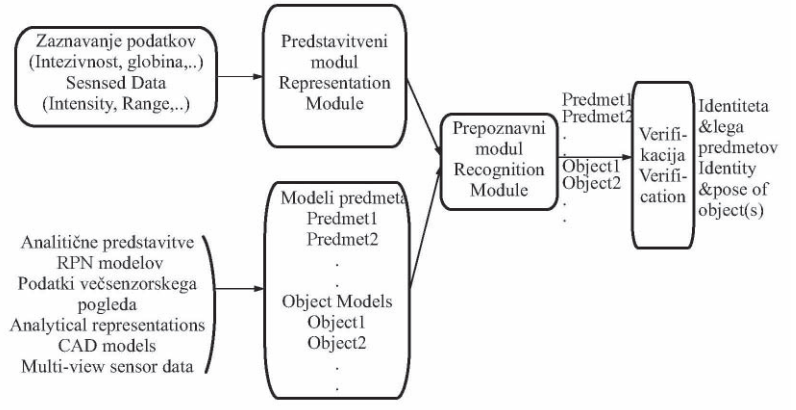

Sl. 5. *Ključne komponente sistema za 3-D prepoznavanje objektov [30]*
Fig. 5. *Key components of a 3-D object recognition system [30]*

področje. Rezultat izločanja značilnosti je običajno značilnostni vektor [27]. Za predstavitev predmeta je običajno uporabljena ena od naslednjih dveh metod:
  - o postopek, ki temelji na pojavu – uporabljena je informacija o pojavu predmeta ([31] in [40]),
  - o metoda, ki temelji na modelu – uporabljena je informacija o geometričnih značilnostih, tipu in prostorskih povezavah ([34] in [39]).
- Ujemanje oz. klasifikacija – iskanje najboljšega ujemanja med značilnostmi slike oz. predmeta in značilnostmi modela in rešitev problema lokaliziranja predmeta. V tej fazi uporabi sitem razvrščanja identificirane ključne značilnosti predmeta za razlikovanje skupin predmetov, ki so predmet zanimanja. Algoritmi oz. metode za te faze so na splošno odvisni od področja opazovanja, še posebej v primerih, ko je uporabljena klasična obdelava slike in tehnike računalniškega vida. Različni primeri za učenje, npr. nevronske mreže ali postopki z genetskim programiranjem, so običajno uporabljeni v fazi ujemanja oz. klasifikacije [27].
- Preizkušanje – potrditev ocenjenega prepoznavanja in lokalizacija objekta ([27] in [36]).

V pomoč nalogam prepoznavanja in lokalizacije predmeta so na voljo opisi vsakega predmeta, ki ga je treba prepoznati in jih lahko računalnik uporabi. Opisi predmeta lahko temeljijo na pojavu predmeta ali na modelu ali pa so kombinacija obeh postopkov.

Glede na razsežnost prostorskega opisa predmeta, obstajajo različni tipi prepoznavanja problema [42]:
- prepoznavanje 2-D predmeta iz posamezne 2-D slike,
- prepoznavanje 3-D predmeta iz posamezne 2-D slike,
- prepoznavanje 3-D predmeta iz posamezne 3-D slike (globinski podatki),
- prepoznavanje 2-D ali 3-D predmeta iz več 2-D slik istega objekta, posnetih iz različnih točk pogleda.

V preteklih desetletjih je bil dosežen velik napredek na področju raziskav prepoznavanja 2-D predmetov iz posameznih 2-D slik in prepoznavanja 3-D predmetov iz globinskih podatkov. Precejšen napredek je bil dosežen tudi pri prepoznavanju 2-D in 3-D predmetov z uporabo kombinacije več 2-D slik istega predmeta, kar zagotavlja npr. stereo ali dvooki (binokularni) vid. Kljub nekaterim dobrim raziskovalnim rezultatom ostaja področje prepoznavanja predmetov

extraction stage. The result of feature extraction is normally a feature vector [27]. There is usually one of two methods of representation applied:
  - o appearance-based approach – information about the appearance of the object is used ([31] in [40]),
  - o model-based methods – information about geometrical features, type and spatial relations of the object is used ([34] and [39]),
- Matching or classification – finding the best fitting between the scene features and the model features and solving the localization problem. In this stage, a classifier system uses extracted key features to distinguish the classes of the objects of interest. The algorithms or methods for these stages are generally domain dependent, particularly when using traditional image processing and computer-vision techniques. Learning paradigms such as neural networks or genetic programming approaches have usually been applied to the matching or classification stage [27],
- Verification – verifying the estimated identity and location of an object ([27] and [36]).

To facilitate the task of identification and localization, a description of each object to be recognized is available to the computer and can be used. These descriptions can either be model-based or appearance-based, or a combination of both.

Based on the dimensionality of their spatial description, various types of object-recognition problems can be stated [42]:
- recognition of a 2-D object from a single 2-D image,
- recognition of a 3-D object from a single 2-D image,
- recognition of a 3-D object from a single 3-D image (a range map),
- recognition of a 2-D or 3-D object from multiple 2-D images taken from different viewpoints, etc.

In recent decades much progress has been made in the research of recognizing 2-D objects in single 2-D images and in recognizing 3-D objects in range maps. Considerable progress has also been made in the recognition of 2-D or 3-D objects using multiple 2-D images, as in binocular or stereo vision. However, today object recognition remains

še vedno v veliki meri nerešen problem in zato še vedno zelo dejavno področje raziskovanja.

Podatki sestavnih delov za montažo so običajno pridobljeni s kamero CCD, ki zagotavlja podatke o intenziteti predmeta, ali pa z laserskim snemanjem, ki zagotavlja globinske podatke. Iz teh podatkov je treba najprej izluščiti značilnosti predmeta za njegovo prepoznavo, ki vsebuje preverjanje ujemanja značilnosti slike s pomočjo globinskih ali intenzitetnih podatkov s predhodno znano predstavo predmeta, ki izhaja iz znanega modela predmeta.

Nekatere značilnosti, npr. ukrivljenosti, so neodvisne od točke pogleda na predmet. Po pregledu posameznih znakov ukrivljenosti predmeta z uporabo različnih postopkov, je mogoče definirati lokalna površinska področja, ki spadajo v skupino osem osnovnih prvobitnih tipov: vrh, jama, greben, dolina, sedlast greben, sedlasta dolina, najmanjša nagnjenost in ravnina. Za določitev oz. prepoznavanje teh ukrivljenosti predmeta so bili predlagani različni algoritmi ([43] do [45]). Težava, ki se pojavi pri teh postopkih je dejstvo, da so ugotovljene oz. prepoznane ukrivljenosti predmeta močno odvisne od izbranih izhodišč in zaporedja povezav med robovi. Nekateri drugi postopki [46] zato predlagajo dinamično programiranje in bolj prilagodljivo oceno ukrivljenosti, da bi se izognili prej omenjenim problemom. V tem primeru so robovi urejeni kot vozlišča grafa in medsebojno povezani skozi grafe.

Druge skupne značilnosti, ki so izluščene iz predmeta, so robovi, ploščata področja itn. Zaznavanje roba je zelo pomemben korak v nižji stopnji obravnave slike in je uporabno pri meritvah razdalje od prepreke. V [38] je predlagan nov postopek, ki obljublja mnogo hitrejše zmožnosti zaznavanja robov, kakor to omogočajo predhodno znani detektorji robov.

Veliko različnih postopkov in metod je bilo razvitih ali pa so bili obravnavani na področju zaznavanja in prepoznavanja predmeta v preteklih desetletjih. Dokaj temeljit pregled opravljenega predhodnega raziskovalnega dela po avtorjih je obravnavan v [30] in [42]. Avtorji obravnavajo probleme prepoznavanja, metodologije in algoritme kot npr. zahtevnost oblike predmeta, velikost podatkovne baze modela predmeta, učenje, individualne in generične kategorije predmetov, upogljivost predmetov, zasenčenje in odvisnost od točke pogleda na predmet, predstavitve predmeta in prepoznavne strategije (zaznavala za zbiranje slik, modeli, strategije ujemanja) in prepoznavanje 3-D predmeta poljubnih oblik.

largely unsolved and is still a very active field of research.

The data about assembly parts is usually obtained with a CCD camera, giving intensity data or by laser line scanning, which gives a range or depth map. From this data, features have to be extracted for object recognition, which involves the matching of image features from either range or intensity data, against a previous internal representation of the object (a model).

Certain features like curvatures are independent of the view point for the object. After inspection of the respective signs of an object's curvature using different approaches, it is possible to define the local surface area as being one of eight fundamental primitive types: peak, pit, ridge, valley, saddle ridge, saddle valley, minimal and flat. Different algorithms have been proposed to extract the curvatures from an object ([43] to [45]). The difficulty of these approaches is that extracted curvatures are very dependent on the selected starting points and the order of the edge linking. Some other approaches [46] propose dynamic programming and relaxation to avoid such problems. In this case the edges are organized as nodes of a graph and linked to each other through graphs.

Other common features that are extracted from objects are edges, planar regions, etc. Edge detection is a very important step in low-level image processing and can be used in a measurement of a distance from the obstacle. In [38] a new approach is proposed, which promises much faster edge-detection capabilities than previously known edge detectors can provide.

Many different approaches and methods have been developed or tackled in the field of object detection and recognition by different researchers in recent years. A detailed survey of previous work has been treated by [30] and [42]. The authors discuss the recognition problems, methodologies and algorithms like object-shape complexity, the size of the object model database, learning, individual and generic object categories, the non-rigidity of objects, occlusion and viewpoint-dependency, object representations and recognition strategies (image sensors, models, matching strategies) and 3-D free-form object recognition.

Pomembno področje raziskovanja prepoznavanja predmetov predstavljajo učno/ prilagodljivi algoritmi. Ena izmed glavnih prednosti sistema učenja je zmožnost učenja oz. izluščenja uporabnih značilnosti iz podatkov za urjenje oz. učenje in uporaba teh značilnosti v okviru testnih podatkov. Nekateri avtorji [37] uporabljajo verjetno približno pravilni model za svoje strategije učenja. Avtorji v teh raziskavah izmerijo uspeh relativno glede na porazdelitev opazovanih predmetov brez privzema porazdelitve. Drugi avtorji [36] modelirajo pojav predmeta z uporabo več različnih pogledov na predmet, vključno s stopnjo učenja in utrjevanja znanja, v kateri se sistem uči izluščiti značilke modela s slik za učenje sistema in s pomočjo tega prepozna predmet. Model uporablja verjetnostne porazdelitve za karakterizacijo pomena, lege, meritve različnih diskretnih značilnosti pojava predmeta in tudi opisuje topološke povezave med značilnostmi predmeta. Postopek ujemanja značilnosti, ki kombinira lastnosti tako iterativne vrste kakor tudi ujemanja grafov, uporablja informacijo nedoločnosti značilnosti, ki jo zapiše model in tako usmerja ujemanje med modelom in sliko.

V zadnjih 25 letih, od leta 1980, so nevronski in genetski primeri za učenje (nevronske mreže, genetski vzorci in genetsko programiranje) pritegnili pozornost kot zelo obetajoče metode za reševanje avtomatskega prepoznavanja tarče oz. predmeta in zaznavanje problema. Predvsem ponujajo nevronski in genetski sistemi potencialno močne zmožnosti za učenje ter prilagoditve in so zato zelo primerni za avtomatsko prepoznavanje predmetov v dejanskem času ([23] in [47]).

Vendar na splošno velja, da trenutno razpoložljivi sistemi računalniškega vida še vedno niso tako prilagodljivi in splošni kakor biološki sistemi. Uspešni tržni sistemi računalniškega vida so običajno prilagojeni in oblikovani za reševanje dobro definiranih in/ali specifičnih nalog. Za reševanje problemov zaznavanja kombinirajo računalniški sistemi vida pogosto raznovrstne običajne strategije ali uporabljajo celo strategije, ki so bile razvite individualno za posebne uporabe ([48] do [50]).

V proizvodnem postopku robotizirane montaže se zelo pogosto pojavlja potreba po prijemanju in upravljanju zahtevnih predmetov. Večina sistemov robotskega vida terja celotno poznavanje tako oblike kakor lege sestavnih delov. Zaradi dejstva, da so sistemi strojnega vida običajno

A very important field of research in object recognition is represented by the area of learning/ adaptive algorithms. One of the major advantages of a learning system is the ability to learn/extract the useful features from the training data set and to apply these features to the test data. Some authors [37] use a PAC (Probably Approximately Correct) model for their learning strategies. In this research the authors quantify success relative to the distribution of the observed objects, without making assumptions on the distribution. In [36] authors model the appearance of an object using multiple views, including a training stage in which the system learns to extract the models' characteristics from training images and recognizes objects with it. The model uses probability distributions to characterize the significance, position, intrinsic measurements of various discrete features of appearance and also describes topological relations among the features. A matching procedure, combining qualities of both iterative alignment and graph matching, uses feature-uncertainty information recorded by the model to guide the search for a match between the model and the image.

In recent 25 years, since the late 1980s, neural and genetic learning paradigms (neural networks, genetic paradigms and genetic programming) have attracted attention as very promising methods for solving automatic target recognition and detection problems. In particular, neural and genetic systems offer potentially powerful learning and adaptive abilities and are very suitable for automatic object recognition in real time ([23] and [47]).

In general, the currently available computer-vision systems for object recognition are still not as adaptive and universal as biological systems. Successful commercial systems for computer vision are usually designed to solve well-defined and/or specific tasks. For solving tasks computer-vision systems often combine multiple standard strategies or even apply strategies that have been developed individually for a specific application ([48] to [50]).

In robot-based-assembly production processes, there is very often a need for the grasping and manipulating of complex objects. Most robot-vision systems require a complete knowledge of both the shape and the position of the assembly parts. Due to the fact that vision systems are often

posebej prilagojeni individualnim 2-D oblikam in načinom dodajanja sestavnih delov v montažni sistem, zahteva sprememba sestavnega dela običajno tudi časovno potratno prilagoditev celotnega sistema. To je lahko stroškovni problem predvsem pri majhnih serijah. Glede na predhodno omenjene poglede, obstaja v praksi potreba po učinkovitih robotih z naprednimi zmogljivostmi strojnega vida, ki bi omogočali prepoznavanje zahtevnih in naključno organiziranih oz. pozicioniranih sestavnih delih, ki ležijo na prenosnem traku ali pa v zaboju in o katerih je znanega zelo malo ali pa ni znanih celo nič podatkov o legi in geometrijski obliki delov. Predvsem zaradi problemov »senčenja« oz. prekrivanja robov še vedno ni rešen t.i. problem pobiranja naključno izbranih 3-D sestavnih delov iz zaboja.

Mnogi raziskovalci se ubadajo s tem temeljnim problemom, ki pomeni eno od preostalih preprek za širše uvajanje sistemov strojnega vida v robotizirano montažo. V iskanju primerne rešitve so uporabljene predhodno opisane metodologije in algoritmi za zaznavanje in prepoznavanje predmetov. V nekaterih raziskavah ([51] in [52]) so bili uporabljeni skupinski podatki o predmetu za rekonstrukcijo predmeta z uporabo nadkvadričnih predstavitev in dekompozicijskih dreves. Temelječ na laserskih bralnikih za zaznavanje 3-D predmeta so bili uporabljeni postopki, ki temeljijo na modelu objekta v kombinaciji s RPN modelom ([19] in [53]) ali značilnostmi harmoničnih oblik ([27] in [28]), ki so nespremenljivi glede na premik, merilo in 3-D zavrtitev. V nekaj raziskavah je bil uporabljen tudi sistem stereovida skupaj z naborom dveh nevronskih mrež (ki sta nato primerjani med seboj), in sicer mreža polmerske osnovne funkcije in prema mreža [54]. Iz tega je predlagan algoritem za razčlenjevanje delno zakritih predmetov v zaboju in lokalizacijo vrhnjih predmetov. Eksperimentalni rezultati so pokazali, da bi lahko bil predlagani algoritem primeren za mnoge uporabe pobiranja sestavnih delov iz zabojev, če je osvetljevanju predmetov namenjena posebna pozornost.

Rezultati zgoraj omenjenih raziskav na področju pobiranja sestavnih delov iz zabojev so zelo obetajoči, vendar so raziskave še vedno bolj ali manj v raziskovalni fazi. Kljub temu, da prijemanje še vedno ni optimalno in za nekatere predmete celo neizvedljivo, kažejo vsi prispevki izboljšano natančnost in učinkovitost pri pobiranju sestavnih delov iz zabojev in pri sortiranju.

specifically adapted to the individual 2D-shapes and the individual way the parts are fed to the system, a change of the produced parts usually requires a time-consuming adaptation of the overall system. This could represent a cost problem, especially for small series. With respect to the above-mentioned aspects, there is a need for efficient robots with advanced machine-vision capabilities that allow the recognition of complex, and randomly organized parts, lying on a conveyor belt or in a bin, with little or no prior knowledge about the pose and the geometry of the parts. In particular, the so-called bin-picking problem - the picking of randomly organized 3-D parts in a bin - has not yet been solved in general, primarily due to severe occlusion problems.

Many researchers are dealing with this basic problem, which represents one of the remaining obstacles to the widespread introduction of vision systems to robot-based assembly. In searching for appropriate solutions, the above-mentioned methodologies and algorithms for object detection and recognition are applied. In ([51] and [52]) range maps have been applied for the reconstruction of objects using super quadric representations and decomposition trees. Based on laser scanners for 3-D object detection a model-based approach in combination with CAD models ([19] and [53]) or Harmonic Shape Context features ([27] and [28]), which are invariant to translation, scale and 3-D rotation, have been applied. Also, some research has been done on applying stereo vision together with a set of two neural networks (which are then compared with each other), i.e., the Radial Basis Function nets and the Simple Feedforward nets [54]. An algorithm for the segmentation of partially occluded bin objects and the location of the topmost object is proposed. The experimental results have shown that the proposed algorithm might be appropriate for many bin-picking applications if special attention is paid to the lighting situation.

The results of the above-mentioned research in bin picking are very promising, but the research is still more or less in the research stage. Even though grasping is not optimal, and for some objects not feasible, all contributions show an improved accuracy and efficiency in bin picking and sorting.

3 SKLEPI

Uporaba računalniškega in strojnega vida v robotiziranem montažnem postopku pomeni hkrati velik potencial in izzive tako za raziskave kakor tudi za industrijske uporabe, kar je razvidno iz mnogih raziskav, povzetih v tem prispevku. Z lahkoto je mogoče zaznati, da bodo naslednje generacije montažne tehnologije vključevale vsestranske sisteme strojnega vida z visoko stopnjo prilagodljivosti in robustnosti.

Prispevek podaja kratek pregled najnovejših raziskovalnih naporov na področju strojnega vida in montažnih postopkov. Obravnavani so različni postopki in tematika, ki zadeva montažo, robotizirano montažo, strojni vid prepoznavanje predmetov, vključno s t.i. pobiranjem sestavnih delov iz zabojev.

3 CONCLUSION

The application of computer- and machine-vision in robot assembly processes provides immense potential and challenges at the same time. This is true for both research and industrial applications, as can be seen by the recent developments summarised in this paper. It can easily be perceived that the next generation of assembly technology will include versatile machine-vision systems with a high level of versatility and robustness.

The paper provides a brief overview of the most recent research efforts in the area of machine vision in assembly processes. Various approaches and issues relating to assembly, robot assembly, machine vision and object recognition including the bin-picking problem are addressed.

4 LITERATURA
4 REFERENCES

[1] Rowland J. J., Lee M. H. (1995) Intelligent assembly systems, *World Scientific*, ISBN 981022494X

[2] Rampersad H. K. (1994) Integrated and simultaneous design for robotic assembly, *John Wiley & Sons*, England, ISBN 0 471 95018 1

[3] Handelsman, M. (2006) Vision, tactile sensing simplify many tasks, www.industrialcontroldesignline.com

[4] www.pro-portal.com/poslovna_sfera.htm

[5] Nof S. Y., Wilhelm W. E., Warnecke H-J. (1997) Industrial assembly, *Chapman & Hall*, ISBN 0 412 55770 3

[6] Cecil J., Powell D., Vasquez D. (2007) Assembly and manipulation of micro devices – A state of the art survey, *Robotics and Computer Integrated Manufacturing* 23 (2007) 580-588, www.elsevier.com

[7] King F.G., Puskorius G.V., Yuan F., Meier R.C., Jeyabalan V., Feldkamp, L.A. (1988) Vision guided robots for automated assembly, *IEEE, International Conference on Robotics and Automation*, Proceedings, Volume 3, 1988, p. 1611 – 1616

[8] Peńa-Cabrera M., Lopez-Juarez I, Rios-Cabrera R., Corona-Castuera J. (2005) Machine vision approach for robotic assembly, *Assembly Automation*, 25/3 (2005), 204-216

[9] Davies E.R., (2005) Machine vision: Theory. *Algorithms Practicalities*, 2005, Elsevier/Morgan Kaufman Publishers, ISBN 0-12-206093-8

[10] Solina F. (2006) Računalniški vid nekdaj in danes, *ROSUS 2006 Maribor*, Proceedings, 3-12 (in Slovene)

[11] Gupta M.M., Knopf G. (1993) Neuro-vision systems: A tutorial, a selected reprint, Volume IEEE, Neural networks Council Sponsor, *IEEE Press*, New York

[12] Hou Z.-G., Song K.-Y., Gupta M., Tan M. (2007) Neural units with higher-order synaptic operations for robotic image processing applications, Springer, *Soft Computing*, 2007, Vol. 11, Nr. 3, pp. 221-228

[13] Shapiro L.G., Stockman G.C. (2001) Computer vision, *Prentice Hall.*

[14] Griot M., Machine vision, www.mellesgriot.com/products/machinevision/

[15] Batchelor B.G. (2006) Natural and artificial vision, *Cardiff University*, http://bruce.cs.cf.ac.uk/index

[16] Batchelor B.G., Whelan P.F. (2002) Intelligent vision systems for industry, e-book, http://bruce.cs.cf.ac.uk/index

[17] Baba M., Narita D., Ohtani K. (2004) A new method of measuring the 3-D shape and surface reflectance of an object using a laser rangefinder, *IMTC 2004, Instrumentation and Measurement Technology Conference*, Corno, Italy, 2004.

[18] Thorsley M., Okouneva G., Karpynczyk J. (2004) Stereo vision algorithm for robotic assembly operations, *First Canadian Conference on Computer and Robot Vision* (CRV 2004).
[19] Schraft R.D., Ledermann T. (2003) Intelligent picking of chaotically stored objects, *Assembly Automati*, Vol.23, Nr. 1, 2003, pp. 38-42
[20] Saxena A, Schulte J., Ng A.Y., (2007) Depth estimation using monocular and stereo cues, *20th International Joint Conference on Artificial Intelligence* (IJCAI), 2007
[21] Saxena A, Chung S.H., Ng A.Y., (2007) 3-D depth reconstruction from a single still image, *International Journal of Computer Vision* (IJCV), Aug. 2007
[22] Ray L.P. (1990) Monocular 3D vision for a robot assembly, *International Conference on Systems Engineering*, IEEE, 1990
[23] Winkler S., Wunsch P., Hirzinger G. (1997) A feature map approach to real-time 3-D object pose estimation from single 2-D perspective views, *19. DAGM Symposium*, Proceedings, 1997
[24] Huang S.-J., Tsai J.-P. (2005) Robotic automatic assembly system for random operating condition, *International Journal of Advanced Manufacturing Technology* 27 (2005), 334-344
[25] Scharstein D., Szelinski R. (2002) A taxonomy and evaluation of dense two-frame stereo correspondence algorithms, *International Journal of Computer Vision* 47(1/2/3) 2002, 7-42
[26] Boothroyd G. (2005) Assembly automation and product design, *CRC Press*, 2005
[27] Kirkegaard J. (2005) Pose estimation of randomly organized stator housings using structured light and harmonic shape context, Master Thesis, *Aalborg University*, Denmark
[28] Kirkegaard J., Moeslund T.B. (2006) Bin-picking based on harmonic shape contexts and graph-based matching, *The 18th International Conference on Patern Recognition* (ICPR'06), 2006 IEEE
[29] Hema C.R., Paulraj M.P., Nagarajan R., Sazali Y. (2007) Segmentation and location computation of bin objects, *International Journal of Advanced Robotic Systems*, Vol. 4, No. 1 (2007), pp. 57-62
[30] Jain A.K., Dora C. (2000) 3D object recognition: Representation, *Statistics and Computing*, 10 (2000), 167-182
[31] Pope A. (1994) Learning object recognition models from images, Ph.D. research Proposal, *University of British Columbia.*
[32] Faugeras O. (1993) Three-dimensional computer vision – a geometric viewpoint, *The MIT Press*, 1993, ISBN 0-262-06158-9
[33] Yli-Jaaski A., Ade F. (1996) Grouping symmetrical structures for object segmentation and description, *Computer Vision and Image Understanding*, 63(3) 1996, 399-417
[34] Motai Y., Kosaka A. (2004) Concatenate feature extraction for robust 3D elliptic object localization, *Symposium on Applied Computing*, ACM 2004, Cyprus
[35] Pope A.R., Lowe D.G. (2000) Probabilistic models of appearance for 3-D object recognition, *International Journal of Computer Vision*, 40(2) 2000, 142-167
[36] Pope A.R., Lowe D.G. (1996) Learning appearance models for object recognition, *Proceedings of International Workshop on Object Representation for Computer Vision*, Springer, Berlin, 1996, pp. 201-219
[37] Roth D., Yang M.-H., Ahuja N. (2002) Learning to recognize objects, *Neural Computation* 14/2002, 1071-1103
[38] Vujović I., Petrović I., Kezić D. (2007) Wavelet-based edge detection for robot vision applications, *Proceedings of 16th International Workshop on Robotics in Alpe-Adria-Danube Region – RAAD 2007*, Ljubljana
[39] Lowe D.G. (1987) Three-dimensional object recognition from single two-dimensional images, *Artificial Intelligence*, 31,3(1987), pp. 355-395
[40] Balslev I., Eriksen R.D. (2002) From belt picking to bin picking, *Proceedings of SPIE – The International Society for Optical Engineering*
[41] Guichard F., Tarel J.P. (1999) Curve finder perceptual grouping and a Kalman like fitting, *Proceedings of the 7th IEEE International Conference on Computer Vision*
[42] Antrade-Cetto J., Kak A.C. (2000) Object recognition, Wiley Encyclopedia of Electrical Engineering, J.G. Webster ed., *John Wiley & Sons*, Sup. 1, 2000, pp. 449-470

[43] Fischler M., Bolles R. (1986) Perceptual organization and curve partitioning, *PAMI* 1986, 8(1):100-105
[44] Rosin P., West G. (1995) Nonparametric segmentation of curves into various representations, *PAMI* 1995, 17(12):1140-1153
[45] Cox I., Rehg J., Hingorani S. (1993) A bayesian multiple-hypothesis approach to edge grouping and contour segmentation, *IJCV* 1993, 11(1):5-24
[46] Alter T., Basri R. (1998) Extracting sailent curves from images: An analysis of the saliency network, *IJCV* 1998, 27(1):51-69
[47] Klobučar R., Pačnik G., Šafarič R. (2007) Uncalibrated visual servo control for 2 DOF parallel manipulator with neural network, *Proceedings of 16th International Workshop on Robotics in Alpe-Adria-Danube Region – RAAD 2007*, Ljubljana
[48] Forsyth D.A., Pnce J. (2002) Computer vision: A modern approach, *Prentice Hall*
[49] Sharma R., Srinivasa N. (1996) A framework for robot control with active vision using neural network based spatial representation, *Proceedings of the 1996 IEEE International Conference on Robotics and Automation*, Mineapolis
[50] Trucco E., Verri A. (1998) Introductory techniques for 3-D computer vision, *Prentice Hall*
[51] Boughorbel F., Zhang Y., Kang S., Chidambaram U., Abidi B., Koschan A., Abidi M. (2003) Laser ranging and video imaging for bin picking, *Assembly Automation*, Vol. 23, No. 1, 2003, pp. 53-59
[52] Goldfeder C., Allen P.K., Lackner C., Pelossof R. (2007) Grasp planning via decomposition trees, *IEEE ICRA*, Rome, 2007
[53] Kristensen S., Estable S., Kossow M., Broesel R. (2001) Bin-picking with a solid state range camera, *Robotics and Autonomous Systems* 35 (2001), 143-151
[54] Hema C.R., Paulraj M.P., Nagarajan R., Sazali Y. (2007) Segmentation and location computation of bin objects, *International Journal of Advanced Robotic Systems*, Vol 4., No. 1 (2007), pp. 57-62

Naslov avtorjev: doc. dr. Niko Herakovič
Univerza v Ljubljani
Fakulteta za strojništvo
Aškerčeva 6
1000 Ljubljana
niko.herakovic@fs.uni-lj.si

Authors' Address: Doc. Dr. Niko Herakovič
University of Ljubljana
Faculty of Mechanical Eng.
Aškerčeva 6
SI-1000 Ljubljana, Slovenia
niko.herakovic@fs.uni-lj.si

Prejeto: 6.7.2007
Received:
Sprejeto: 28.9.2007
Accepted:
Odprto za diskusijo: 1 leto
Open for discussion: 1 year

Strojniški vestnik - Journal of Mechanical Engineering 53(2007)12, 874-884
UDK - UDC 621.9.048
Strokovni članek - Speciality paper (1.04)

Alternativna strategija za izdelavo mikroorodij v masovni proizvodnji

An alternative strategy for microtooling for replication processes

Boštjan Jurišević[1] - Jožko Valentinčič[1] - Oki Blatnik[1] - Davorin Kramar[1] - Henri Orbanić[1] - C. Masclet[2] - Matthieu Museau[2] - H. Paris[2] - Mihael Junkar[1]
([1]Fakulteta za strojništvo, Ljubljana; [2]G-SCOP Laboratory, University of Grenoble, France)

Mikroproizvodnja je ena od najhitreje rastočih vej industrije z vedno večjim trgom novih izdelkov. V tem prispevku je predstavljena alternativna strategija izdelave mikroorodij, ki je bila preizkušena na primeru izdelka s področja mikrofluidnih uporab. Orodje za masovno proizvodnjo izdelkov s postopkom tlačnega brizganja ali vtiskovanja je izdelano s postopkom potopne mikro-elektroerozijske obdelave (MEDM). Posebnost predstavljene strategije je v izdelavi elektrod MEDM z vodnim curkom (VC). Orodje je bilo uporabljeno za vtiskovanje v polimerni material. Globalno gledano, poteka strategija izdelave od izdelave elektrode za postopek MEDM, s katero bo izdelano orodje za masovno proizvodnjo, pa do izdelave mikroizdelka. Posebno pozornost smo posvetili lastnostim vsakega od postopkov in izbiri obdelovalnih parametrov ter tako izbiro najboljše kombinacije obdelovalnih postopkov za izdelavo končnega izdelka. Med raziskavo je prišlo do številnih odkritij. To znanje bo pripomoglo razvoju zanesljive in stroškovno najboljše strategije izdelave mikroorodij, kar je podrobneje opisano v prispevku. Poleg tega je podan pregled drugih podobnih raziskovalnih dejavnosti na Univerzi v Ljubljani.

(Ključne besede: mikroorodja, rezanje s curkom, vodni curek, potopna elektroerozija, procesne verige)

Microproduction is one of the fastest-growing fields in industry, with new demands from the market increasing every day. This work presents an alternative microtooling strategy, which was applied to a microfluidic device case study. This original strategy for a replication process, like hot embossing or injection molding, is based on the combination of the micro-electro-discharge machining (MEDM) process and an electrode machined with water-jet technology (WJ). The final tool was tested with a hot-embossing process by making some test parts in polymers. The process is considered in its global perspective, starting with the fabrication of the tool electrode that will be used to produce the mold involved in the final cast of the microproduct. The addressed issue consists of identifying the capability of each process and then choosing the machining process parameters that will allow the best process combination to obtain the final microproduct. During this investigation several ideas emerge. They should help to identify the most advantageous characteristics of the involved processes in order to develop a reliable and cost-effective tooling strategy, which are discussed in this contribution. Additionally, an insight is given into similar research activities at the University of Ljubljana.

(Keywords: microtooling, water jet cutting, micro die sinking EDM, process chains)

0 UVOD

Svetovni trg mikrotehnologij je ocenjen na 40 milijard evrov z 20-odstotno letno rastjo [1]. Po drugi strani je samo evropski trg izdelkov, ki vsebujejo mikrokomponente, ocenjen na 550 milijard evrov letno. V drugi polovici dvajsetega stoletja je na področju mikrotehnologije

0 INTRODUCTION

The global market for microsystems technology is €40 billion, with a growth rate of 20% per year [1]. On the other hand, the European market for products containing microsystems technology is estimated to be €550 billion annually. In the late 20th century microproduction was the domain of silicon-

prevladovala izdelava mikroelektronskih izdelkov iz silicija, toda v zadnjih letih se je pojavilo veliko povpraševanje po mikro izdelkih iz različnih materialov [2]. V ta namen se intenzivno razvijajo nove tehnologije mikroobdelave.

Pomembni področji uporabe mikroizdelkov sta medicina in biotehnologija. Razvoj diagnostičnih naprav, npr. laboratorij na ploščici, omogoča zgodnje odkrivanje ter učinkovito spremljanje in zdravljenje različnih bolezni [3]. Ker so take uporabe namenjene široki uporabi po vsem svetu, je treba razviti zanesljivo in cenovno ugodno metodo proizvodnje. Kandidati so seveda izdelovalni postopki, ki se uporabljajo v masovni proizvodnji, npr. vroče vtiskovanje, tlačno brizganje ter podobni postopki. Pri tem je potrebno oblikovalske oz. konstrukterske ter izdelovalne naloge rešiti že na stopnji izdelave orodja. Značilnosti materiala orodja in težave pri izdelavi orodja z enim obdelovalnim postopkom terjajo podrobno študijo zahtev za izdelek in značilnosti, ki jih lahko dosežejo izdelovalni postopki. Inteligentna kombinacija izdelovalnih postopkov, t.i. izdelovalna veriga, je primerna za izdelavo orodij.

Veliko razmeroma zapletenih strategij je predstavljenih v literaturi ([4] in [5]), da bi zadostili potrebam mikrofluidnih sistemov. V tej raziskavi je prikazana alternativna strategija izdelave mikroorodij na primeru izdelave laboratorija na ploščici, pri čemer glavne geometrijske značilnosti predstavljajo mikrokanali. Orodje je bilo preizkušeno z vtiskovanjem v polimerni material in rezultati so predstavljeni v nadaljevanju.

V prvem poglavju je podana izbrana strategija izdelave orodja za vtiskovanje mikroizdelkov. Lastnosti obravnavanih obdelovalnih postopkov, t.j. VC in PPME so podani v prvem poglavju. Študija predlagane izdelovalne verige je podana v drugem poglavju in vodi do razprave glede celotne optimizacije postopkov, ki je podana v tretjem poglavju. Sklepi in obeti za nadaljnje izboljšanje zmožnosti obdelovalne verige so podani v zadnjem, četrtem poglavju.

1 PREDLAGANA STRATEGIJA IZDELAVE MIKROORODIJ

Ni tehnologije, ki bi zadostila rasti zahtev glede izdelave zahtevnih 3D mikrooblik in integraciji raznih oblikovnih elementov različnih

based microelectronic techniques; only in recent years has the demand for non-silicon-based microproducts arisen [2]. As a result, new microproduction processes are constantly being developed in order to meet the demands of the market.

An important area of applications for micro-devices is medicine and biotechnology in general. The development of diagnostic devices such as the lab-on-a-chip analyzer makes possible the early discovery of various diseases and effective monitoring of the therapy [3]. Since the application is intended to be applied on a large scale, worldwide, a reliable and cost-effective production method is required. Natural candidates are replication processes like hot embossing or injection molding. However, design and manufacturing issues are switched to the tooling part of the overall process. Due to the specific characteristics of the tool material and the difficulty in obtaining the finished tool with a single process, a study of the product requirements and the achievable characteristics of the related manufacturing process is required. The intelligent combination of such processes, i.e., a process chain, can be proposed as a strategy for tooling.

Various relatively complex strategies have been proposed in the literature ([4] and [5]) to satisfy the needs of microfluidic systems. In this investigation an alternative tooling strategy is presented along with an application example, i.e., a simple lab-on-a-chip part, mainly featuring micro-channels. The final tool was tested on a polymer material using the hot-embossing process, and the results are presented.

In the first section the selected strategy to manufacture the tool for the embossing of the microproducts is presented. The characteristics of the machining processes, i.e., the WJ and MEDM processes, are considered in the first section. A case study of the proposed process chain is presented in the second section, which leads to a discussion about the optimization of the whole process, given in section three. Finally, the conclusions, including possible prospects to enhance the overall process-chain capability, are given in the last, fourth section.

1 PROPOSED MICROTOOLING STRATEGY

There is still a lack of a single technology that can satisfy the constantly increasing requirements associated with the manufacture of complex 3D micro structures,

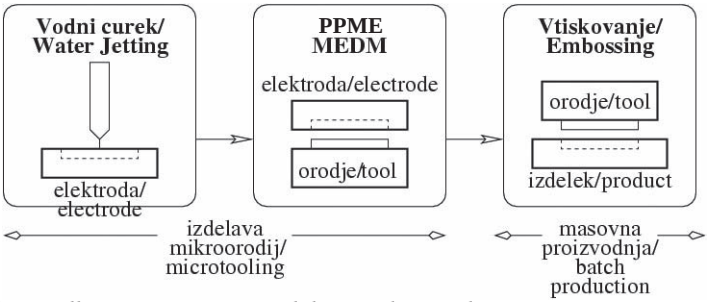

Sl. 1. *Predlagana strategija izdelave mikroorodij za masovno proizvodnjo*
Fig. 1. *Proposed microtooling strategy*

velikostnih razredov v zahetvno 3D obliko ([6] in [7]). Zato se je porodila zamisel po kombinaciji raznih mikroizdelovalnih tehnologij in tako uporabi delne prednosti vsake od njih. Ob pričakovanju masovne proizvodnje, izdelovalno verigo sestavljata izdelava orodja, ki izpolnjuje specifične zahteve za določeno orodje, in izdelovalnega postopka, ki se uporablja v masovni proizvodnji. Predstavljena strategija izdelave mikroorodij temelji na izdelavi bakrene elektrode z vodnim curkom (VC) ter izdelave končnega orodja za vtiskovanje s postopkom potopne mikroelektroerozije (PPME - MEDM), kar prikazuje slika 1.

Med predstavljeno raziskavo je bila podrobno opazovana vsaka faza predlagane strategije izdelave mikroorodij z namenom določitve prednosti in omejitev vpletenih postopkov. Oba postopka (VC in PPME), vpletena v izdelavo mikroorodja za vtiskovanje, sta podrobneje opisana v nadaljevanju.

1.1 Izdelava mikroorodij z vodnim curkom

Obdelava z VC je razmeroma nov postopek, razvit v zadnjih treh desetletjih. Pri tem postopku pride do odnašanja materiala obdelovanca zaradi erozivnega delovanja VC. Poleg obdelave z VC obstaja tudi postopek obdelave z abrazivnim vodnim curkom (AVC). Razlika med postopkoma je v dodajanju abrazivnih delcev pri slednjem, kar bistveno izboljša učinkovitost postopka s vidika odnašanja materiala obdelovanca. Kljub temu je bil v predstavljeni raziskavi uporabljen postopek obdelave z VC, ker omogoča izdelavo tanjših rezov. Učinkovitost odnašanja materiala ni pomenila pretirane ovire, ker so bile količine odnesenega materiala razmeroma majhne.

and the integration of them for features on different length scales ([6] and [7]). Thus, the idea of combining some compatible micromanufacturing process to take advantage of their specificities has emerged. Aiming at batch production with a replication process, the process chain consists of producing the replication tool, fulfilling the specific requirements for such a part, and the technology for batch production. The proposed microtooling strategy consists of machining the MEDM electrode in copper (which is obviously not an appropriate material for theembossing) with water-jet technology and then the production of the final tool in tool steel with MEDM, as shown in Figure 1.

During this investigation, we first considered each phase of the proposed microtooling strategy in order to specify the advantages and limitations of the involved technologies. Observations helped to define more precisely what can be done originally, and also to define any possible process enhancement by tuning the parameters. Both technologies (water jetting and MEDM) involved in the tooling phase are presented and described in the following.

1.1 Water-jetting technology in microtooling

Water-jetting technology is a relatively new machining process developed in the past three decades. The basic principle involved is material removal due to erosion by a high-speed water jet (WJ) when impacting on the workpiece. In addition to WJ machining, we used abrasive water jet (AWJ) machining, which is a similar process. The only difference is that abrasive particles are added to the WJ in order to substantially improve the performance of the process. However, a WJ is much more suited to micromanufacturing because the jet diameter is smaller than with AWJ machining, while the machining performance is still acceptable due to the small volume of removed material. This consequently reduces the field of potential materials that can be machined with this technique.

V zgodnjih osemdesetih letih prejšnjega stoletja je bilo napovedano, da bodo obdelovalni postopki prihodnosti zmožni obdelovati vse vrste materialov na energijsko učinkovit način [8]. Obdelava z VC in AVC je zelo prilagodljiva ter omogoča obdelavo praktično vseh znanih materialov. Poleg tega skoraj ne povzroča toplotno prizadete cone v obdelovancu.

Po drugi strani je največja pomanjkljivost postopka v doseganju velikih natančnosti obdelave. Običajna natančnost izmer znaša približno 100 μm, medtem ko je za zdaj največja mogoča približno 50 μm. V primerjavi z drugimi postopki mikroobdelave, na primer mikrofrezanje, se zdi obdelava z VC neprimerna za področje mikroobdelave. Dodatna pomanjkljivost postopka je v nadzorovanju globine prodiranje curka v material obdelovanca pri 3D obdelavi, saj je ta tehnologija namenjena predvsem obrisnemu rezanju. Kljub temu je izdelava mikroorodij z VC mogoča v primeru, ko končni izdelek vsebuje le 2D oblike, kakor je prikazano na sliki 2.

1.2 Tehnologija PPME

Pri vseh elektroerozijskih postopkih (EPO) se površina električno prevodnega obdelovanca

As already anticipated in the early 1980s, manufacturing technologies of the future will have the ability to machine a variety of different materials in an energy-efficient way [8]. Water-jetting technology, especially AWJ machining, is a very flexible process, which can be used for virtually any known material. Additionally, there is almost no heat-affected zone on the machined part, which represents a clear advantage compared to other processes, like laser material removal.

The main disadvantage of this technology is the achievable machining accuracy. Normally, the dimensional accuracy is about 100 μm, while state-of-the-art accuracy is down to 50 μm. Such poor accuracy compared to other micromachining processes, like micro-milling, could indicate that this process does not fit the requirements of microproduction. In fact, this assertion is partially wrong. We must consider the 3D aspect of the machined feature and distinguish the water-jet axis from the other axes. The drawback when machining 3D features is controlling the depth of penetration of the jet, since this technology is mostly used for cutting through the workpiece material. As a result, a WJ can be still applied when the significant features are contained in the plane perpendicular to the water jet direction. Thus, the final product has only 2D-relevant features, as illustrated in Figure 2.

1.2 MEDM technology

Electrical discharge machining (EDM) is a machining process in which the surface of a metal

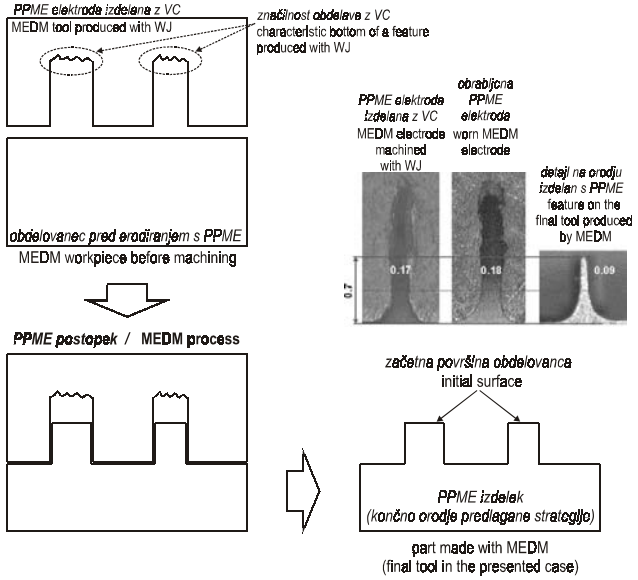

Sl. 2. *Posebnosti tehnologije VC pri izdelavi mikroorodij za PPME [9]*
Fig. 2. *MEDM tool production with WJ [9]*

Preglednica 1. *Primerjava postopkovnih parametrov EPO in PPME*
Table 1. *EDM and MEDM machining parameters*

Postopkovni parameter Machining parameter	EPO/EDM	PPME/MEDM
razelektritveni tok discharge current	do/to 200 A	do/to 3 A
trajanje razelektritve discharge duration	do/to 1000 μs	do/to 50 μs
premor med razelektritvami pulse interval	do/to 1000 μs	do/to 200 μs

oblikuje kot posledica razelektritev v reži med elektrodo in obdelovancem. Reža med elektrodo in obdelovancem se izpira z dielektrično tekočino. Postopek sestoji iz številnih naključno porazdeljenih posameznih razelektritev. Med samo razelektritvijo nastane tok plazme, ki rabi kot prevodnik med elektrodo in obdelovancem in kot vir toplote. Na mestu razelektritve nastane krater, katerega velikost je odvisna od energije razelektritve. Energijo razelektritve se nastavi s tokom in trajanjem razelektritve. Napetost razelektritve, ki tudi določa energijo razelektritve, se ne da izrecno nastaviti, ker je odvisna od reže med elektrodo in obdelovancem [10]. Stopnja odvzema materiala (MRR) je definirana s prostornino posameznega kraterja in frekvenco nastajanja kraterjev oz. energijo in frekvenco razelektritev. Slednje je določeno s trajanjem razelektritev in premorom med dvema razelektritvama. Velikost reže med elektrodo in obdelovancem je običajno med 0,01 in 0,1 mm. Stopnja odvzema na obdelovancu je približno 100-krat večja kakor na elektrodi, kar pomeni obrabo elektrode.

Razlika med EPO in PPME je v natančnosti podajalnega sistema elektrode oz. servosistema ter preostalih postopkovnih parametrov. Primerjava postopkovnih parametrov postopkov EPO in PPME je podana v preglednici 1.

Med obdelavo z PPME običajno uporabljamo paličaste elektrode. Pot elektrode je podobno kakor pri frezanju nadzorovana z računalniškim krmilnikom. Najmanjše elektrode, dostopne na trgu, imajo premer 170 μm. Manjše premere lahko izdelamo z žičnim EPO brušenjem ali jedkanjem [11].

1.3 Primer mikrofluidne uporabe

Kombinacija zgoraj predstavljenih tehnologij ni očitna. Predlagana strategija temelji na analizi komplementarnosti VC — prednost VC postopka pred AVC je v tanjšem curku, ki omogoča

workpiece is formed by discharges occurring in the gap between the tool, which serves as an electrode, and the workpiece. The gap is flushed by the third interface element, the dielectric fluid. The process consists of numerous randomly ignited mono-discharges. During a discharge, a plasma channel is formed as the current conductor and the heat generator. At the spot of the discharge a crater appears. The size of the crater depends on the discharge energy, which can be set on the machine by adjusting the discharge current and the discharge duration. The discharge voltage, which also determines the discharge energy, cannot be adjusted on the machine explicitly, since it depends on the gap width between the workpiece and the electrode [10]. The material removal rate (MRR) is determined by the crater size and the frequency of the crater generation, i.e., the discharge energy and the frequency of the discharges. The latter is influenced by the discharge duration and the pulse interval between two discharges. The gap width between the workpiece and the electrode is in the range 0.01–0.1 mm. The MRR is around 100 times higher on the workpiece than on the electrode.

The main difference between the EDM process and the MEDM is in the accuracy of the electrode feeding system, also called the servo system, and the machining parameters. The comparison is given in Table 1.

The MEDM machining is usually performed with a rod electrode, whose path is controlled by a CNC controller. The commercially available rod electrodes have diameters down to 170 μm. Smaller electrode diameters are obtained by wire EDM grinding or etching [11].

1.3 The proposed strategy

A combination of the two previously presented technologies is not an obvious method. The proposed strategy is based on an analysis of the complementarities of WJ (preferred to AWJ because of the smaller jet

izdelavo manjših oblik (kanalov, reber itn.) — in postopka PPME. Glavna prednost kombinacije dveh postopkov je delitev zahtevanih izmer v dva sklopa. Izmere v oseh *x* in *y* so določene pri obdelavi z VC in morajo biti zagotovljene s pravilno izbiro obdelovalnih parametrov postopka PPME. Tretja izmera (višina) je odvisna le od globine obdelave PPME.

2 ŠTUDIJA NA PRIMERU: MIKROFLUIDNI PRIPOMOČEK

Predlagana strategija izdelave mikroorodij in kasnejšega vtiskovanja je bila preizkušena na izdelku, prikazanem na sliki 3. Primer izdelka je bil izbran zaradi značilnih oblik, izmer in kakovosti površin, ki se pojavljajo pri mikrofluidnih izdelkih.

V prvem koraku je bila bakrena elektroda izdelana z uporabo obdelave z VC. Obdelava je potekala na sistemu za rezanje z AVC izdelovalca OMAX (tip: 2652A/20HP) priključenega na visokotlačno črpalko oz. hidravlični ojačevalnik proizvajalca Böhler (tip: Ecotron 403), ki zmore tlake vode do 410 MPa. Glede na predhodne izkušnje je bil tlak vode nastavljen na 300 MPa, podajalna hitrost na 10 mm/min, razdalja med šobo in obdelovanci na 2 mm. VC je bil oblikovan v šobi s premerom 100 mm. Čas obdelave je znesel 4,9 min. Tako izdelana elektroda za PPME je prikazana na sliki 4.

V naslednjem koraku je bilo izdelano mikroorodje za vtiskovanje s postopkom PPME na elektroerozijskem stroju tipa 200M-E izdelovalca IT Elektronika. Za izdelavo mikroorodja so bili

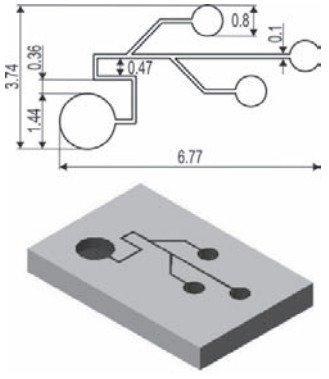

Sl. 3. *Skica in 3D model opazovanega primera s področja mikrofluidnih uporab*
Fig. 3. *Sketch and 3D model of the presented case study: a microfluidic device (lab-on-a-chip)*

diameter that allows a smaller minimum dimension of features like ribs, channels, etc.) and MEDM. The main advantage is being able to divide the dimension required into two stages. The dimensions in *x* and *y* axes are defined by the WJ process, and must be further guaranteed by MEDM through process-parameter control. The third dimension (height) only depends on the depth of the machining with the MEDM process.

2 CASE STUDY: A MICROFLUIDIC DEVICE

The proposed microtooling strategy was tested and the embossing operations were performed on the part shown in Figure 3. This case study was selected because of the typical dimensions, shapes and surface-quality requirements for microfluidic products.

In the first step the MEDM tool was machined in copper using WJ technology. This operation was executed on the OMAX-type 2652A/20HP abrasive-water-jet cutting system powered by a Böhler Ecotron 403 hydraulic intensifier capable of reaching water pressures up to 410 MPa. Based on previous experience the water pressure was set at 300 MPa, the cutting velocity was 10 mm/min and the stand-off distance between the cutting head and the workpiece was 2 mm. The high-speed water jet was generated in an orifice with a diameter of 100 μm. The machining time was 4.9 min and the resulting MEDM tool is shown on Figure 4.

In the next step of the proposed microtooling strategy the final tool for embossing was produced with MEDM on an EDM machine IT Elektronika 200M-E. The following process

Sl. 4. *Elektroda za PPME, izdelana z VC*
Fig. 4. *MEDM electrode machined with WJ technology*

uporabljeni naslednji postopkovni parametri: tok razelektritve i_e=1 A, vžigna napetost u_i=180 V, trajanje razelektritve t_e=8 μs ter premor med razelektritvami t_o=36 μs. Globina erodiranja je bila nastavljena na 700 μm. Čas erodiranja je bil približno 12 ur.

Mikroorodje za masovno proizvodnjo z vtiskovanjem, izdelano s postopkom PPME, je prikazano na sliki 5.

Med obdelavo s PPME se elektroda obrablja, kar je treba upoštevati pri načrtovanju tehnologije. Slika 6 prikazuje obrabljeno elektrodo po izdelavi mikroorodja za vtiskovanje, kjer je opaziti zaokrožene robove na elektrodi kot posledico obrabe elektrode. Najpreprostejša rešitev za zmanjšanje vpliva obrabe elektrode pri postopku PPME bi bila uporaba dveh povsem enakih elektrod, eno za grobo in drugo za fino obdelavo. Ker je praktično nemogoče izdelati dve enaki elektrodi z VC ta možnost odpade. Razlog je v za zdaj nedodelanem vpenjalnem in nastavitvenem sistemu sedanjih naprav za obdelavo z VC.

Uporaba dveh elektrod, ene za fino in druge za grobo obdelavo, torej v našem primeru ni priporočljiva zaradi problemov nastavitve in vpenjanja, ki bi povzročali večje napake, kakor jih povzroča obraba elektrode. To je očitno ena od ovir, ki omejuje določitev zaporedja obdelovalnih opravil. Tako predlagana strategija sloni na enostopenjski obdelavi PPME s skrbno izbranimi obdelovalnimi parametri, ki povzročajo najmanjšo obrabo.

V zadnji fazi predstavljene raziskave je bilo izdelano mikroorodje preizkušeno z vtiskovanjem v polimerni material. Rezultat preizkusa je prikazan na sliki 6.

parameters were applied: discharge current i_e=1 A, ignition voltage u_i=180 V, discharge duration t_e=8 μs and pulse interval t_o=36 μs. The eroding depth was set at 700 μm, consuming about 12 hours of machining time.

The resulting tool made in tool steel for the embossing process is shown in Figure 5.

During MEDM machining the electrode is subject to wear, which has to be taken into account when designing the technology. The wear results in rounding of the edges of the electrode (Figure 6). The simplest solution would be to use two equal electrodes, one for rough MEDM machining and the other for the finishing. Unfortunately, this is not an option within this strategy because it is very difficult to machine two identical electrodes with WJ technology. The main reason lies in the rather poor positioning and clamping system that is available in water-jetting technology.

The use of rough electrodes in addition to a finishing electrode is therefore not advisable because the repositioning of one relative to other would generate geometric errors that are probably worse than the errors due to the electrode wear. This is clearly the kind of obstacle that limits the choice of process sequence. Hence, the proposed strategy is based on single-step MEDM manufacturing with parameters chosen to narrow the electrode-wear effect.

In the final step the performance and the functionality of the machined tool were tested by embossing the polymer materials, as shown in Figure 6.

Sl. 5. *Orodje za masovno proizvodnjo izdelano s PPME*
Fig. 5. *Final tool produced by the MEDM process*

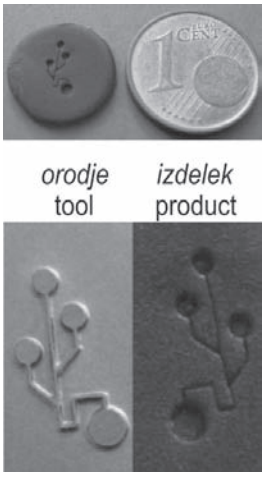

Sl. 6. *Testni primer, izdelan z vtiskovanjem v polimerni material*
Fig. 6. *Test part made of polymers by embossing*

3 RAZPRAVA

Predlagana strategija izdelave mikroorodij je bila eksperimentalno opazovana po posameznih fazah od izdelave bakrene elektrode z VC, erodiranja orodja s PPME pa vse do izdelave končnega izdelka in polimernega materiala s postopkom vtiskovanja.

Analiza obdelovalnih časov je pokazala, da je bila večina časa porabljena za erodiranje orodja do globine 700 μm, kar je trajalo približno 12 ur. Izdelava elektrode za PPME je bila bistveno hitrejša. Razmeroma veliko območje okoli sistema kanalov v kombinaciji z višino reber na orodju zahteva odvzem večje prostornine materiala, kar se kaže v daljšem obdelovalnem času. Nasprotno je čas, potreben za izdelavo bakrene elektrode z VC neprimerno krajši; za izdelavo elektrode je bilo potrebnih le 4,9 minut. Poudariti je treba, da elektroda, izdelana s postopkom VC, ki predstavlja časovno najkrajšo fazo izdelave orodja, že definira večino od pomembnih značilnosti končnega izdelka. Nadalje to pomeni, da so nekateri

3 DISCUSSION

The proposed microtooling strategy has been experimentally observed from the machining of the MEDM electrode with a WJ, through to the production of the final tool and up to the phase where test samples were made by embossing.

The machining-time analysis showed that most of the time is spent on the MEDM operation, which took approximately 12 hours to machine the final tool, on which the features are 700-μm high. Naturally, the wide area around the channel system combined with the height of the ribs on the tool is responsible for the large volume of material needing to be removed, hence the long machining time. In contrast, the machining time of the WJ electrode was much shorter. It took only 4.9 minutes to produce the electrode. Here, it is important to note that the electrode made by WJ, which is the shortest phase of the tool manufacturing, already provides some of the definitive characteristics of the final product. This means that some controls can already

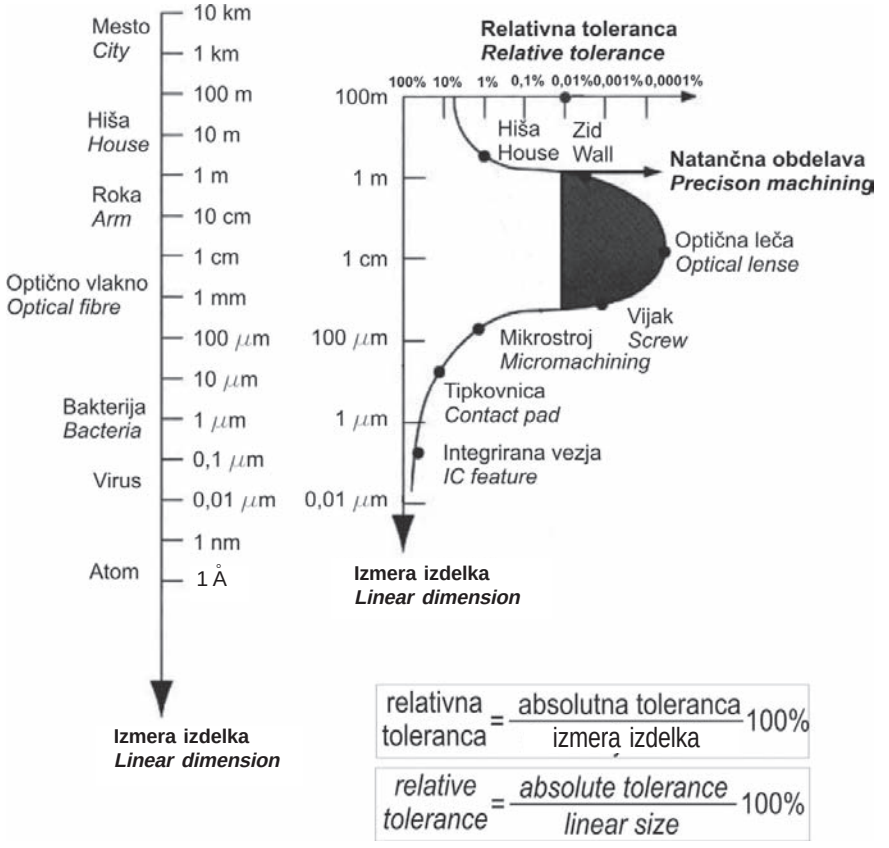

Sl. 7. *Področje natančne izdelave [12]*
Fig. 7. *Domain of precision engineering [12]*

ukrepi za zagotavljanje kakovosti lahko izvedeni že v tej fazi strategije izdelave orodja.

Kljub dejstvu, da je postopek obdelave z VC manj natančen od odrezovalnih postopkov, ki so običajno uporabljeni za izdelavo elektrod za PPME, je ta raziskava pokazala, da je z nadaljnjim razvojem lahko predlagana strategija časovno in stroškovno učinkovita alternativa znanim postopkom.

Po navadi je izraz mikroobdelava povezan z natančno obdelavo, kar ne drži popolnoma. Slednje je ponazorjeno na sliki 8, kjer se izkaže, da so relativne tolerance mikroizdelkov, ki imajo značilno izmero okoli 100 μm, primerljive s tolerancami v gradbeništvu, kjer so značilne izmere reda velikosti 10 m.

Ob upoštevanju zmogljivosti obdelave z VC z vidika natančnosti izdelave je jasno, da trenutno stanje tehnike ne omogoča izdelave orodij za masovno proizvodnjo. Kljub temu se tej tehnologiji odpira zanimivo področje mikrofluidnih sistemov, pri katerih bi hitra in poceni izdelava prototipov in s tem povezanih orodij omogočala razvijalcem teh naprav bistveno prednost. Na tem področju je bila pred kratkim začeta raziskava v sodelovanju s Kemijskim inštitutom v Ljubljani. Glavni cilj te raziskave je v opazovanju vpliva prečnega prereza mikrokanalov na kemijskem mikroreaktorju. V ta namen je bilo izdelano orodje za izdelavo mikroreaktorja. Trenutno so prvi prototipi v fazi preizkušanja. Prvi mikroreaktorji bodo izdelani z ulivanjem prozorne snovi na temelju silikona v orodje, izdelano s predlagano strategijo. V kasnejši fazi se lahko orodje uporabi za postopke kakršna sta vtiskovanje ali tlačno brizganje prozornih materialov.

4 SKLEPI

Kljub obetavnim rezultatom predstavljene raziskave je še veliko prostora za izboljšavo predlagane strategije izdelave mikroorodij. V prihodnosti bo treba odpraviti določene pomanjkljivosti, med katerimi so nekatere opisane v spodaj.

Pri izdelavi elektrod z VC lahko izdelamo še manjše detajle z uporabo manjšega premera vodnega curka. V tej raziskavi je bila uporabljena vodna šoba s premerom 100 μm, medtem ko je na trgu najmanjši razpoložljiv premer 80 μm. V laboratorijskem okolju so najmanjše razpoložljive šobe premera 10 μm in celo manj. Sama natančnost izdelave se lahko izboljša z uporabo bolj

be performed at this stage of the tooling strategy.

Despite the fact that WJ machining is less accurate than cutting processes, which are normally used to produce electrodes for MEDM, this contribution shows that with the further development of this technology, especially on the tooling side, it should represent a time- and cost-effective alternative.

Micromachining is a term that is usually amalgamated with precision machining, which is not the case. It can be clearly seen in Figure 7 that the relative tolerance of microproducts with a size of about 100 μm is similar to those in construction engineering, where the characteristic dimension is about 10 m.

Taking into consideration the achievable machining precision of WJ machining, it is clear that the current state of the art of this technology does not allow the production of tools for mass production if accuracy is the main attribute. However, the development of microfluidic systems is still an interesting field of application. The fast and cost-effective fabrication of prototypes gives the designer a powerful tool to gain significant advantages. In this respect a research study has been undertaken together with the Institute of Chemistry, in Ljubljana. The main goal of this investigation is to test the different microchannel cross-section geometries of a chemical microreactor. A microtool for the microreactor has already been produced and is currently in the testing phase. The first microreactor will be produced by filling the tool with a transparent silicon-based material, but the possibility of using other replication processes, like embossing and injection molding, are being investigated as well. Particular attention will be paid to the geometry and the impact of electrode wear.

4 CONCLUSIONS

Despite the encouraging results obtained in this investigation, there is still room for improvement with the proposed microtooling strategy. Accordingly, several issues have to be addressed, which will be further discussed.

The first stage of improvements can be made in the steps of the process chain. During the machining of the MEDM electrodes smaller features may be obtained by using smaller jet diameters. In this investigation a 100-μm orifice (nozzle) was applied, while the smallest commercially available orifices have a diameter of 80 μm and the state-of-the-art orifices reach diameters of 10 μm, or even less. Machining

izpopolnjenih poti orodja, vendar je pri obdelavi z VC največja pomanjkljivost v neustreznem vpenjalnem in nastavitvenem sistemu. Izboljšan vpenjalni in nastavitveni sistem bi omogočal izdelavo večjega števila enakih elektrod, ki bi bile uporabljene za izdelavo istega orodja (grobo in fino erodiranje).

Prva stopnja izboljšav se tiče samih obdelovalnih postopkov, vključenih v izdelovalno verigo. Za izdelavo orodja s PPME je treba bistveno več časa v primerjavi z izdelavo elektrode z VC. V veliki meri je to posledica slabih razmer pri izpiranju reže med postopkom PPME. Ponuja se možnost izdelave elektrode iz tanke pločevine, kjer se izdela želene oblike z rezanjem z VC. To bi omogočalo izpiranje reže med elektrodo in obdelovancem skozi elektrodo. Takšen postopek bi vplival tudi na nadaljnji razvoj strategije izdelave orodja, kar je druga stopnja izboljšav. Na primer, postopek PPME z elektrodo iz tanke pločevine ima lahko velik vpliv na obrabo elektrode, kar seveda vpliva tudi na določitev izdelovalne strategije.

Prihodnje raziskave na tem področju bodo vsebovale izsledke predstavljene študije. Z nadaljnjimi učnimi primeri bo mogoče odkriti področja, kjer bi predlagana strategija lahko nadomestila dosedanje obdelovalne postopke za izdelavo elektrod za mikroorodja, predvsem mikrofrezanje. To vključuje tudi izdelavo elektrod iz grafita, kar je bilo že uspešno preizkušeno.

precision may be improved by alternative tool paths as well, but the major drawback is the positioning and clamping systems, which both need further development. An advanced positioning system would make it possible to produce several identical electrodes for rough and smooth machining of the same final tool.

The machining of the final tool with MEDM takes an extremely long time compared to the WJ phase. This is partially so because of the poor flushing conditions in the gap between the electrode and the machined part. One possibility would be to make electrodes out of thin plates in which the desired features would be cut through the electrode. This would enable an additional flushing of the gap through the electrode itself. Of course, integrating such modifications into the manufacturing process will also surely bring some modifications to the tooling strategy. That is the second point of improvement. For example, MEDM with a thin-plates electrode would considerably change the electrode wear problem, and surely lead to a new strategy.

Further research in this field will incorporate the findings obtained during this investigation. Various new case studies will be tested in order to find the gaps between the proposed microtooling strategy and today's commonly used microtooling techniques, especially micromilling. This includes the fabrication of graphite electrodes, which was already tested and the first results are very promising.

Zahvala

Predstavljeno delo je bilo opravljeno v okviru evropskih mrež odličnosti: "Multi-Material Micro Manufacture: Technology and Applications (4M)" Network of Excellence, pogodba NMP2-CT-2004-500274 ter "Virtual Research Lab for a Knowledge Community in Production (VRL-KCiP)" Network of Excellence, pogodba: NMP2-CT-2004-507487, oba v okviru 6. Evropskega Okvirnega Programa. Predstavljeno delo je del bilateralnega projekta PROTEUS med Republiko Slovenijo in Republiko Francijo, pogodba: BI-FR/05-06-017.

Acknowledgement

This work is supported by the "Multi-Material Micro Manufacture: Technology and Applications (4M)" Network of Excellence, Contract Number NMP2-CT-2004-500274 and by the "Virtual Research Lab for a Knowledge Community in Production (VRL-KCiP)" Network of Excellence, Contract Number NMP2-CT-2004-507487, both within the EU's 6th Framework Program. This work was initiated within the context of a bilateral project PROTEUS between the Republic of Slovenia and the Republic of France, Contract Number BI-FR/05-06-017.

5 LITERATURA
5 REFERENCES

[1] Nexus MST Market Analysis (2002).
[2] Dimov, S. (2005) 4M Network of excellence: an instrument for integration of European research in multi-material micro manufacture, *First Multi-Material Micro Manufacture (4M) Conference*, Karlsruhe, Germany, xi-xv.

[3] Krawczyk, S. (2005) Lab-on-a-Chip microsystems for cancer diagnostics and for monitoring of cancer therapy, *First Multi-Material Micro Manufacture (4M) Conference*, Karlsruhe, Germany, 53-57.
[4] Nestler, J., Hiller, K., Gessner, T., Buergi, L., Soechtig, J., Stanley, R., Voirin, G., Bigot S., J. Gavillet, S. Getin, B. Fillon, M. Ehrat, A. Lieb, M.-C. Beckers, D. Dresse (2006) A new technology platform for fully integrated polymer based micro optical fluidic systems. *Proceedings of the 2nd International Conference on Multi-Material Micro Manufacture (4M)*, Grenoble, France.
[5] G. Bissacco, H. N. Hansen, P. T. Tang, J. Fugl (2005) Precision manufacturing methods of inserts for injection moulding of microfluidic systems, *Proc. of the ASPE Spring Topical Meeting*, Columbus, Ohio, USA, p. 57-63.
[6] Uriarte, L., Ivanov, A., Oosterling, H., Staemmler L., Tang, P.T., Allen, D. (2005) A comparison between microfabrication technologies for metal tooling, *First Multi-Material Micro Manufacture (4M) Conference*, Karlsruhe, Germany, 351-354.
[7] Herrero, A., Goenaga, I., Azcarate, S., Uriarte, L., Ivanov, A., Rees, A., Wenzel, C., Muller, C. (2006) Mechanical micro-machining using milling, wire EDM, die-sinking EDM and diamond turning, *Journal of Mechanical Engineering*, 52/7-8, 484-494.
[8] Peklenik, J. (1982) Round table: The impact of engineering materials on the development of fabrication processes, *Annals of the CIRP*, 31/2, 471-478.
[9] Jurišević, B., Orbanič, H., Valentinčič, J., Blatnik, O., Masclet, C., Paris, H., Museau, M., Junkar, M. (2006) Water jet based tooling strategies for microproduction. *Proceedings of the Workshop on Multi-Material Micro Manufacturing Focusing on Metal Processing and Metrology*, Budapest, Hungary, 27-33.
[10] Valentinčič, J., Junkar, M. (2004) On-line selection of rough machining parameters. *Journal of Material Processing Technology*, 149/1-3, 256-262.
[11] Bigot, S., Ivanov, A., Popov, K. (2004) A study of the micro EDM electrode wear, *First Multi-Material Micro Manufacture (4M) Conference*, Karlsruhe, Germany, 355-358.
[12] Madou, M.J. (2002) Fundamentals of microfabrication: The science of miniaturization, Second Edition, *CRC Press*.

Authors Addresses: Boštjan Jurišević
dr. Jožko Valentinčič
Oki Blatnik
dr. Davorin Kramar
dr. Henri Orbanić
prof. dr. Mihael Junkar
Univerza v Ljubljani
Fakulteta za strojništvo
Aškerčeva 6
1000 Ljubljana

C. Masclet
Matthieu Museau
H. Paris
Univerza v Grenoblu
Labortaorij G-SCOP
Francija

Authors Addresses: Boštjan Jurišević
Dr. Jožko Valentinčič
Oki Blatnik
Dr. Davorin Kramar
Dr. Henri Orbanić
Prof. Dr. Mihael Junkar
University of Ljubljana
Faculty of Mechanical Eng.
Aškerčeva 6
SI-1000 Ljubljana, Slovenia

C. Masclet
Matthieu Museau
H. Paris
University of Grenoble
G-SCOP Laboratory
France

Prejeto: 14.2.2007
Received:
Sprejeto: 25.4.2007
Accepted:
Odprto za diskusijo: 1 leto
Open for discussion: 1 year

Strojniški vestnik - Journal of Mechanical Engineering 53(2007)12, 885-897
UDK - UDC 621.923.7
Strokovni članek - Speciality paper (1.04)

Oblikovanje in izdelava polirne naprave ter polirni postopek z uporabo materiala Al 7075 T6

The Design and Manufacture of Burnishing Equipment and the Burnishing Process with Al 7075 T6 Material

Hüdayim Başak
(Gazi University, Turkey)

Polirni postopek je končna obdelava, ki jo lahko opišemo tudi kot postopek brez odrezkov. V pričujočem prispevku predstavimo polirno napravo, ki smo jo oblikovali in izdelali tako, da z njo lahko poliramo prizmatične elemente. Polirno napravo smo uporabili za poliranje prizmatično oblikovanih vzorcev Al 7075 T6, pri čemer smo upoštevali različne polirne parametre. Na koncu smo polirane površine opisali in razvrstili glede na njihovo hrapavost in trdoto.

(Ključne besede: poliranje, prizmatični obdelovanci, hrapavost površin, površinska trdota)

The burnishing process is a final process that can also be described as a chipless process. In this paper, burnishing equipment that is designed and manufactured for the burnishing of prismatic parts is introduced. This burnishing equipment was then used to burnish prismatically manufactured Al 7075 T6 samples using different burnishing parameters. The burnished surfaces were characterized in terms of roughness and hardness.

(Keywords: burnishing, prismatic parts, surface roughness, surface hardness)

0 UVOD

Poliranje je zelo natančna tehnika, ki se uporablja pri strojni obdelavi delovnih površin. Polirno tehniko uporabljamo že dolgo, saj z njo izboljšamo mehanske lastnosti in kakovost površine; poleg tega pa je zelo učinkovita tudi v serijski proizvodnji. Poliranje poveča tako kakovost površine kakor tudi mehansko trdnost. Zaradi naštetih razlogov je v večini primerov poliranje bolj primerno od brušenja [1].

Če v končno obdelavo vključimo polirni postopek, ta ponuja številne prednosti, na primer, povečanje trdote, večjo trajno nihajno trdnost in večjo odpornost proti obrabi. Kadar za poliranje uporabimo veliko silo, poliranje omogoči veliko odpornost proti poškodbam materiala. Razpoke zaradi utrujenosti se v materialu širijo od področij, na katerih se kopičijo dislokacije, ter točk, na katerih se je površina poškodovala. Zato so, z vidika širjenja razpok, značilnosti površine materiala zelo pomembne. Poškodbe površine oziroma razpoke

0 INTRODUCTION

Burnishing is a precise processing technique that is used in the machining of functional surfaces. The burnishing technique has been used for a long time because it can improve mechanical properties, surface quality and is very efficient in serial production. Burnishing increases the surface quality as well as the mechanical strength. For these reasons, the burnishing process is preferable to grinding for most applications [1].

When the burnishing process is used as a final treatment, there are a number of advantages, such as a hardness increase, higher fatigue strength and greater wear resistance. When burnishing is carried out with a great deal of force, the resistance to material defects also increases. Fatigue cracks in materials are propagated from regions of dislocation accumulation and defect points on the surfaces. For this reason, surface characteristics are very important from the crack-propagation point of view. These surface defects or surface cracks can be

lahko odpravimo prav s poliranjem. Ker poliranje zmanjša hrapavost površine, s tem zmanjša tudi možnost nastanka razpok [2].

Površine strojnih delov, ki jih izdelamo s stružnico ali frezalnim strojem, lahko obdelamo le do določene kakovostne stopnje. Za doseganje večje kakovosti pa moramo izdelke brusiti ali polirati. Izvedene in objavljene so bile že številne študije poliranja s stružnico ([2] in [3]), nismo pa še zasledili poročila o poliranju prizmatičnih obdelovancev.

Poliranje lahko spremeni značilnosti površine materiala. Vemo, da ta postopek zmanjša hrapavost površine ([4] do [6]) ter poveča njeno trdoto in odpornost proti obrabi ([7] do [11]). Poliranje lahko poveča tudi odpornost proti utrujenosti površine ([12] do [14]). Obstajajo tudi poročila o tem, da polirni parametri močno vplivajo na hrapavost in trdoto površine [15].

V prispevku smo med poliranjem materiala Al 7075 T6 spreminjali obdelovalne parametre – na primer število vrtljajev, hitrost poliranja in število prehodov polirne naprave – in material opisali glede na posledično hrapavost in trdoto površine. Določili smo vplive števila vrtljajev, hitrosti poliranja in števila prehodov naprave na hrapavost in trdoto površine.

1 OBLIKOVANJE IN IZDELAVA POLIRNE NAPRAVE

Polirno napravo smo oblikovali tako, da jo lahko uporabljamo za poliranje prizmatičnih obdelovancev (sl. 1). Na začetku oblikovalnega postopka smo se odločili, da bomo uporabljali napravo ne le v navpično delujoči osrednji frezalni enoti, ampak tudi tako, da bo lahko polirala prizmatične obdelovance. Da bi lahko polirali prizmatične obdelovance, smo kroglico namestili na končino naprave.

Za potrebe oblikovanja polirne naprave smo pregledali ustrezno literaturo, da bi se seznanili z načeli podobnih zasnov. Slika 1 prikazuje razstavljeno skico oblikovane in izdelane polirne naprave in s tem tudi prikaz njene sestave.

Ko poliranje izvajamo z veliko silo, se odpornost proti poškodbi materiala očitno poveča. Povečanje trdote površine in odpornosti proti obrabi ter zmanjšanje hrapavosti površine in širjenja razpok sta odvisni od polirnih parametrov, na primer, števila prehodov naprave, števila vrtljajev in hitrosti

removed by burnishing. Since the burnishing reduces the surface roughness, it also reduces the possibility of crack formation [2].

The surfaces of machine parts that are manufactured with a lathe or a milling machine can be machined up to a certain quality. If a better surface quality is required, they need to be ground or burnished. A number of burnishing studies involving a lathe were carried out and reported in the literature ([2] and [3]). However, the burnishing of prismatic parts has not been reported.

Burnishing can change the surface characteristics. The process is known to improve the surface roughness ([4] to [6]), and increase the surface hardness and wear resistance ([7] to [11]). Burnishing can also increase the fatigue resistance ([12] to [14]). It has also been reported that the burnishing parameters strongly affect the surface roughness and the hardness [15].

In this paper, Al 7075 T6 was burnished while varying the processing parameters – such as the number of revolutions, the feed rate and the number of passes – and characterized in terms of the surface roughness and hardness. The effect of the number of revolutions, the feed rate and the number of passes on the surface roughness and the hardness was determined.

1 DESIGN AND MANUFACTURE OF THE BURNISHING EQUIPMENT

The burnishing equipment was designed so that it can be used with prismatic parts (Figure 1). At the start of the design process it was decided to use the equipment not only in a vertical-processing centered milling unit but also so that it would be able to burnish prismatic parts. In order to burnish prismatic parts, a ball was placed at the end of the equipment.

For the design of the burnishing equipment, a literature review was made to check the principles of similar designs. An exploded view and installation drawing of the designed and manufactured burnishing equipment is shown in Figure 1.

When burnishing is applied under excessive force, the resistance to material defects definitely increases. The increases in the surface hardness, the wear resistance, and the reduction in the surface roughness and crack-propagation centers all depend on burnishing parameters, such as the number of passes, the number of revolutions, the applied force.

delovanja. Polirni postopek smo izvedli ob upoštevanju vseh teh parametrov.

Materiale potrebne za izdelavo polirne naprave, smo določili glede na položaj, ki ga ima posamezni del v celotni sestavi naprave. Za dele, ki so kritični z vidika trdnosti, smo izbrali C3425, za preostale dele pa SAE1050. Dele, ki so kritični z vidika trdnosti, smo pred montažo utrdili s toplotno obdelavo. Povprečna trdota ojačanih delov je bila med 55 in 65 HRc.

Ker je poliranje izvedeno s kroglico, ki je nameščena na končino naprave, je bilo treba izdelati kroglični ležaj z zelo natančnimi vrednostmi površine. V fazi oblikovanja smo zelo natančno načrtovali okrov, pri čemer smo upoštevali premo gibanje polirne palice, tako da je celotna naprava delovala brezhibno.

Sila poliranja je sorazmerna trdnosti tlačne vzmeti. Zato lahko to silo spremenimo z zamenjavo polirne vzmeti. Ker smo uporabili

The burnishing process was carried out, considering all these parameters.

Materials selection for the burnishing equipment was made after considering the positions of each part in the installed equipment. C3425 was used for the strength-critical parts and SAE1050 was used for the other parts. The strength-critical parts were hardened by heat treatments prior to installation. The mean hardness of the strengthened parts was measured to be between 55 and 65 HRc.

Since the burnishing is carried out by the ball placed at the end of the equipment, a ball bearing was manufactured with very precise surface values. At the design stage, the main body of the equipment was planned carefully by considering the linear movement of the equipment's bar and so that the whole system worked perfectly.

The burnishing force is proportional to the strength of the pressure spring. As a result, this force can be changed by changing the burnishing spring.

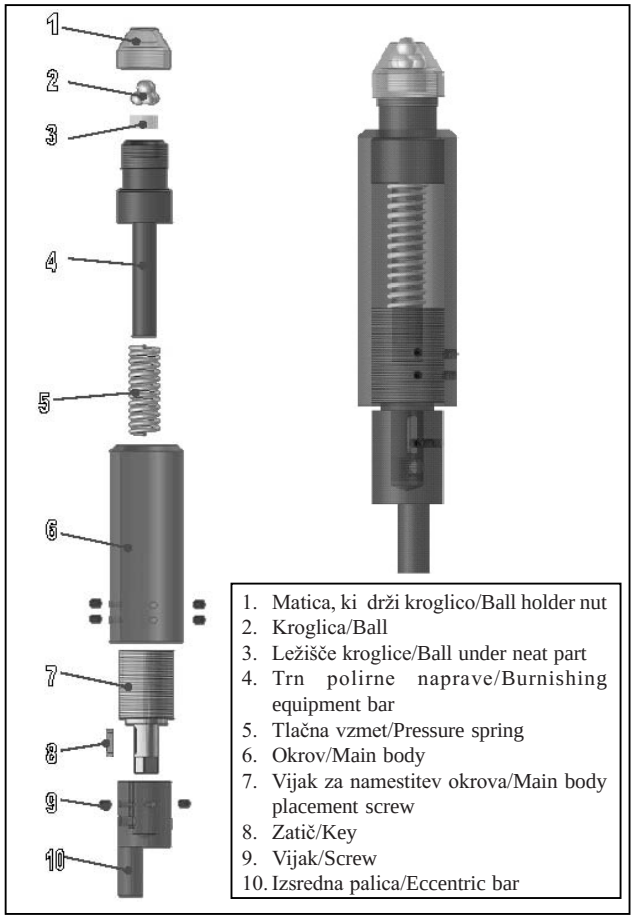

Sl.1. *Razstavljena slika in prikaz sestave oblikovane in izdelane polirne naprave*
Fig. 1. *An exploded view and installation drawing of the designed and manufactured burnishing apparatus*

vzmeti različnih trdnosti, smo to dejstvo upoštevali pri oblikovanju naprave. Zaradi izsrednega gibanja polirne palice smo napravo oblikovali tako, da vzdrži vibracije. Da bi odpravili napake, ki jih povzročajo vibracije, smo uporabili tlačno vzmet.

2 PREIZKUŠANJE NAČINOV IN POGOJEV DELOVANJA

Polirni postopek smo izvedli ob upoštevanju parametrov, ki so podani v preglednici 1. Slika 2 prikazuje fotografijo poliranja.

Poliranje smo izvedli ob upoštevanju parametrov iz preglednice 1. Pri tem smo ugotavljali

Since springs with different strengths were used, this fact was taken into account when designing the machine. Because of the eccentric movement of the equipment bar, the machine was designed to allow for the vibration. The pressure spring was used to remove the defects caused by this vibration.

2 EXPERIMENTAL METHODS AND CONDITIONS

The burnishing process was carried out using the parameters given in Table 1. A photograph of the burnishing process is shown in Figure 2.

The burnishing was carried out using the parameters given in Table 1. The effect of the number

Preglednica 1
Table 1

Material

Aluminijeva zlitina (Al 7075 T6), 80×120 mm, prizmatični obdelovanec s povprečno hrapavostjo površine 1,780µm
Aluminum alloy (Al 7075 T6) 80×120 mm prismatic part with a mean surface roughness of 1.780µm

Kemična sestava aluminijeve zlitine Al 7075 (%) [16]
The chemical composition of the Al 7075 aluminum alloy (%) [16]

Cu	*Zn*	*Mg*	*Si*	*Mn*	*Fe*	*Cr*	*Ti*	*Drugo Other*	*Al*
1,20	5,10	2,10	0,40	0,30	0,50	0,18	0,20	0,15	drugo balance
2,00	6,10	2,90	maks max	maks max	maks max	0,28	maks max		

Mehanske lastnosti aluminijeve zlitine Al 7075 [16]
Mechanical properties of Al7075 aluminum alloy [16]

Odpornost proti zlomu Fracture strength [MPa]	*Natezna trdnost Yield strength [MPa]*	*Raztegljivost Ductility [%]*	*Strižna trdnost Shear strength [MPa]*
572	503	11	331

Polirna naprava Burnishing equipment

Naprava je izdelana iz C3415 in SAE1050 ter ima kroglico s kakovostjo površine 0,15-µm.
The equipment is manufactured from C3415, SAE1050 and with a ball that has a 0.15-µm surface quality.

Polirni parametri Burnishing parameters

Hitrost poliranja [mm/rev], število vrtljajev [vrt/min], število prehodov naprave [n], tlačna sila [kN], premer kroglice [mm]
Feed rate [mm/rev], number of revolutions [rev/min], number of passes [n], pressure force [kg], ball diameter [mm]

Sila/ Force [kN]	0,1–0,2–0,3–0,4
Hitrost/ Progress [mm/rev]	0,05–0,1–0,2–0,3
Število vrtljajev/ Number of revolution [vrt/min]	100–200–300–400
Število prehodov/ Number of passes	2–3–4–5

Polirna miza Burnishing bench

Frezalna RK miza Taksan 40T1500 s pokončnim obdelovalnim središčem
Taksan 40T1500 CNC milling bench with a vertical machining center

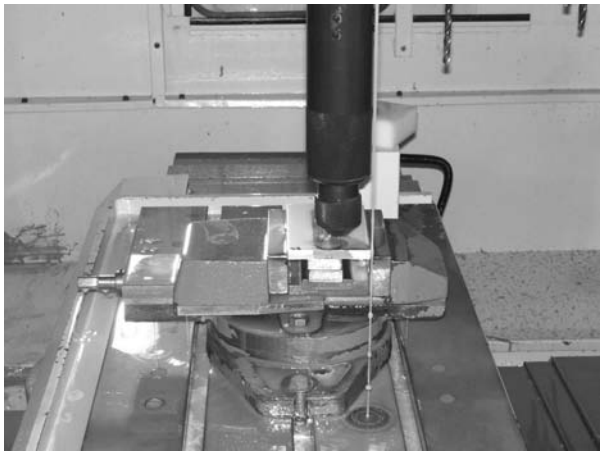

Sl. 2. *Polirni postopek*
Fig. 2. *The burnishing process*

učinke števila prehodov, števila vrtljajev in hitrosti na hrapavost in trdoto površine. Dobljeni rezultati so prikazani v preglednicah 2 do 4. Rezultati so tudi grafično prikazani, in sicer na slikah 3 do 8.

2.1 Učinek delujoče sile in hitrosti poliranja na hrapavost površine

V štirih različnih permutacijah smo uporabili štiri različne sile in štiri različne hitrosti, da bi ugotovili učinke teh parametrov na hrapavost površine. Sto vrtljajev na minuto in dva prehoda

of passes, the number of revolutions, and the feed rate on the surface roughness and hardness were investigated. The results are tabulated in Table 2 to 4. The results were also presented graphically in Figure 3 to 8.

2.1 Effect of the applied force and the feed rate on the surface roughness

Four different applied forces and four different feed rates were used in different permutations to check the effect of these parameters on the surface roughness. One hundred rev/min and

Preglednica 2. *Spreminjanje vrednosti hrapavosti in trdote površine materiala ob različnih hitrostih in delujočih silah ter stalnem številu vrtljajev na minuto (100) ter stalnem številu prehodov naprave (2)*
Table 2. *Variation of the surface-roughness and surface-hardness values for different feed rates and applied forces for a constant number of revolutions per minute (100) and number of passes (2)*

Hitrost Progress [mm/s]	Delujoča sila/Applied force [kN]							
	0,1		0,2		0,3		0,4	
	Hrapavost površine Surface roughness [μmm]	Trdota površine Surface hardness (Brinell)	Hrapavost površine Surface roughness [μmm]	Trdota površine Surface hardness (Brinell)	Hrapavost površine Surface roughness [μmm]	Trdota površine Surface hardness (Brinell)	Hrapavost površine Surface roughness [μmm]	Trdota površine Surface hardness (Brinell)
0,05	0,592	68	0,574	69	0,452	69,7	0,434	71,2
0,1	0,579	67	0,443	67	0,469	69	0,535	70,8
0,2	0,519	66,3	0,413	66,3	0,596	68,2	0,585	69
0,3	0,475	65,4	0,402	66	0,765	66,2	0,690	67,8

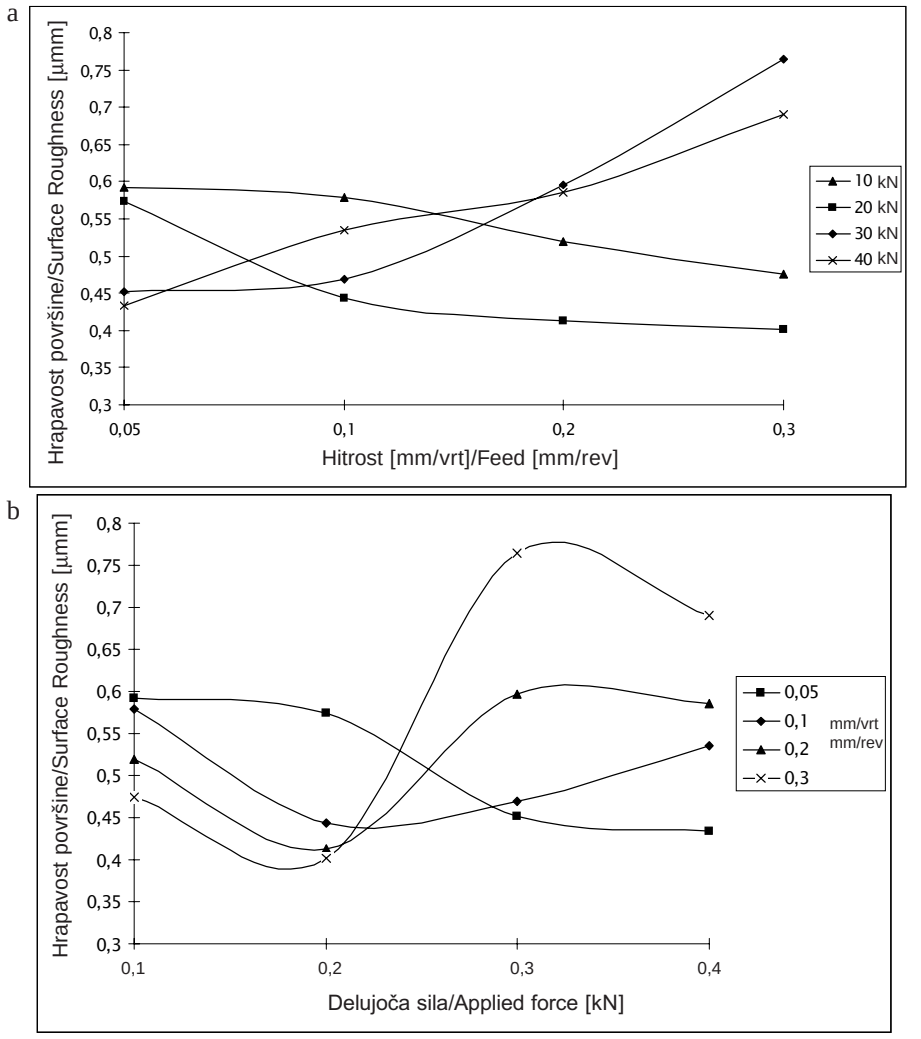

Sl. 3. *Učinek hitrosti poliranja in delujoče sile na hrapavost površine (100 vrt/min in 2 prehoda naprave)*
Fig. 3. *The effect of feed rate and applied force on the surface roughness (100 rev/min and 2 passes)*

polirne naprave sta bili vrednosti preostalih eksperimentalnih parametrov. Dobljene vrednosti hrapavosti in trdote površine so prikazane v preglednici 2 ter slikah 3 in 4.

Če preučimo diagrama slike 3, postane očitno, da povečevanje delujoče sile do določene vrednosti zmanjšuje hrapavost površine. Vrednost, ki presega 0,3 kN pa poveča hrapavost površine. Najbolj gladko površino smo dobili, ko smo delujočo silo in hitrost delovanja določili z vrednostima 0,2 kN in 0,3 mm/vrt. Druga najbolj gladka površina je nastala, ko sta bili vrednosti delujoče sile in hitrosti 0,2 kN in 0,2 mm/vrt. V teku naše raziskave smo najboljše rezultate hrapavosti površine dobili, ko je bila hitrost 0,2 ali 0,3 mm/vrt, delujoča sila pa 0,2 kN.

two passes were used as the other experimental parameters. The resulting surface-roughness and surface-hardness values are given in Table 2 and Figures 3 and 4.

When graphs a and b in Figure 3 are examined, it is clear that increasing the applied force reduces the surface roughness up to a certain value. More than 0.3 kN increases the surface roughness. The smoothest surface was obtained when 0.2 kN and 0.3 mm/rev were used as the applied force and the feed rate. The second smoothest surface was obtained when 0.2 kN and 0.2 mm/rev were used as the applied force and the feed rate. For this study, 0.2 or 0.3 mm/rev as the feed rate and 0.2 kN as the applied force gave the best surface-roughness values.

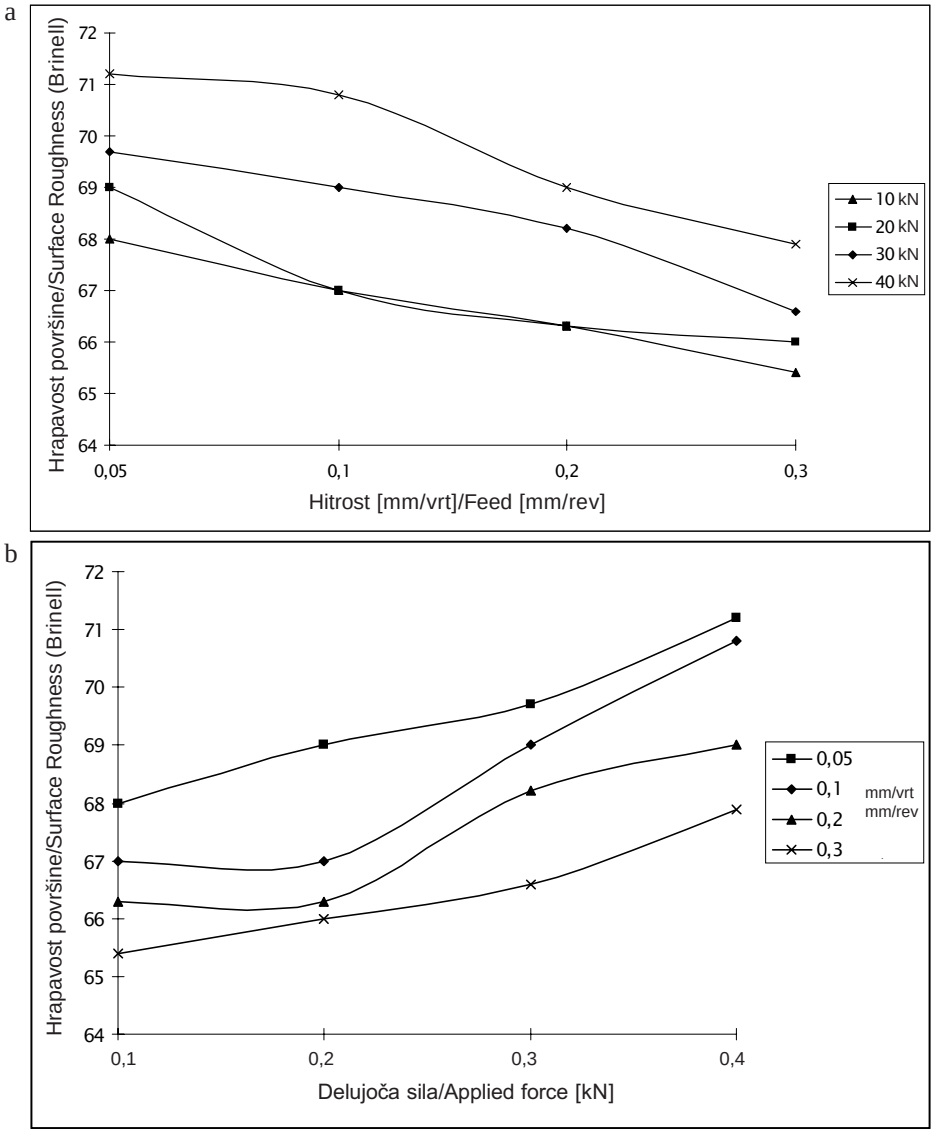

Sl. 4. *Učinek hitrosti poliranja in delujoče sile na trdoto površine (100 vrt/min in 2 prehoda naprave)*
Fig. 4. *The effect of feed rate and applied force on the surface hardness (100 rev/min and 2 passes)*

Ko smo preučili učinke delujoče sile in hitrosti poliranja na trdoto površine (sl. 4), smo ugotovili, da s povečevanjem hitrosti zmanjšujemo trdoto površine, medtem ko s povečevanjem delujoče sile povečujemo trdoto površine. Najboljšo vrednost trdote površine smo dobili pri hitrosti delovanja 0,05 mm/s in maksimalni delujoči sili.

2.2 Učinek števila vrtljajev in delujoče sile na hrapavost in trdoto površine

V štirih različnih permutacijah smo uporabili štiri različna števila vrtljajev in štiri različno delujoče

When the effects of the applied force and the feed rate on the surface hardness were examined (Figure 4), we found that increasing the feed rate reduces the surface hardness, while increasing the applied force increases the surface hardness. The best surface hardness value was obtained with a 0.05 mm/sec feed rate and the maximum applied force.

2.2 The effect of the number of revolutions and the applied force on the surface roughness and hardness

Four different numbers of revolutions and four different applied forces were used in different

sile, da bi ugotovili učinke teh parametrov na hrapavost površine. Hitrost 0,1 mm/vrt in dva prehoda polirne naprave sta bili vrednosti preostalih eksperimentalnih parametrov. Dobljene vrednosti hrapavosti in trdote površine so prikazane v preglednici 3 ter slikah 5 in 6.

Ko preučimo učinke števila vrtljajev in delujoče sile (sl. 5a, b), ugotovimo, da s povečevanjem števila vrtljajev pri delujoči sili 0,1 ali 0,2 kN povečujemo gladkost površine; ko pa silo povečamo nad 0,3 kN, se gladkost površine pri 200 vrt/min spet poslabša. Najbolj gladko površino smo dobili z uporabo sile 0,2 kN pri 400 vrt/min.

permutations to check the effect of these parameters on the surface roughness. A 0.1 mm/rev feed rate and two passes were used as the other experimental parameters. The obtained surface-roughness and surface-hardness values are shown in Table 3 and Figures 5 and 6.

When the number of revolutions and the applied force are examined together (Figure 5 a and b), increasing the number of revolutions with 0.1 and 0.2 kN of applied force increases the smoothness of the surface; however, when more than 0.3 kN is applied, the burnished surface deteriorates after 200 rev/min. The smoothest surface was obtained with 0.2 kN of applied force at 400 rev/min.

Preglednica 3. *Spreminjanje vrednosti trdote in hrapavosti površine materiala zaradi različnih števil vrtljajev in različnih delujočih sil (pri hitrosti 0,1 mm/vrt in dveh prehodih polirne naprave)*
Table 3. *The variation in the surface hardness and roughness with different numbers of revolutions and applied force (feed rate 0.1 mm/rev and number of passes 2)*

Število vrtljajev [vrt/min] Number of revolution [rev/min]	Delujoča sila/Applied force [kN]							
	0,1		0,2		0,3		0,4	
	Hrapavost površine Surface roughness [μmm]	Trdota površine Surface hardness (Brinell)	Hrapavost površine Surface roughness [μmm]	Trdota površine Surface hardness (Brinell)	Hrapavost površine Surface roughness [μmm]	Trdota površine Surface hardness (Brinell)	Hrapavost površine Surface roughness [μmm]	Trdota površine Surface hardness (Brinell)
100	0,579	67	0,443	67,5	0,469	69	0,535	70,3
200	0,540	69	0,410	68,5	0,440	69,3	0,572	71,1
300	0,510	69,2	0,380	68,6	0,470	69,8	0,590	71,2
400	0,519	69,8	0,355	69,7	0,510	70,2	0,670	73

a

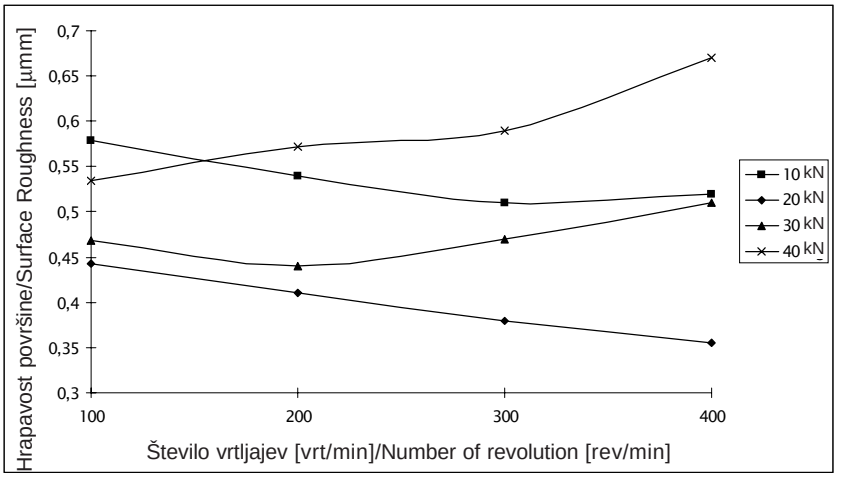

b

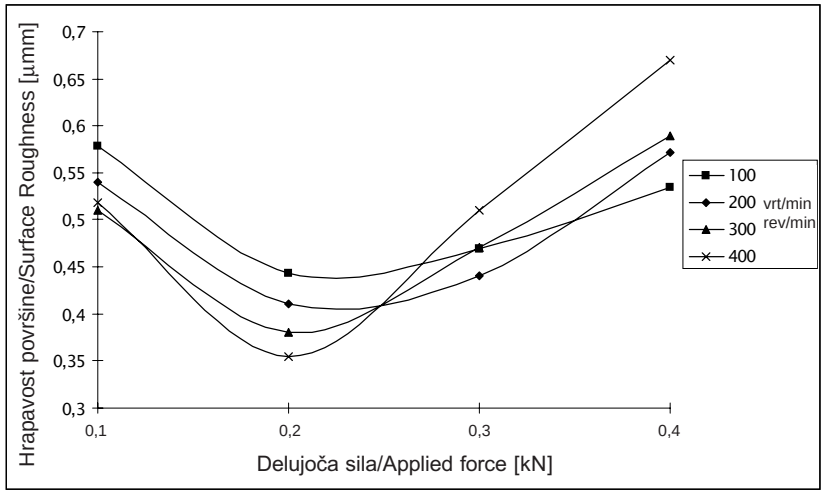

Sl. 5. *Učinek števila vrtljajev in delujoče sile na hrapavost površine*
Fig. 5. *The effect of the number of revolutions and applied force on the surface roughness*

a

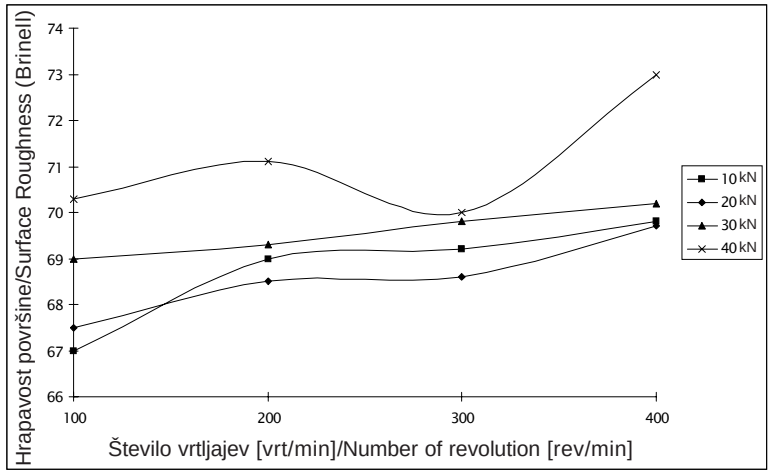

b

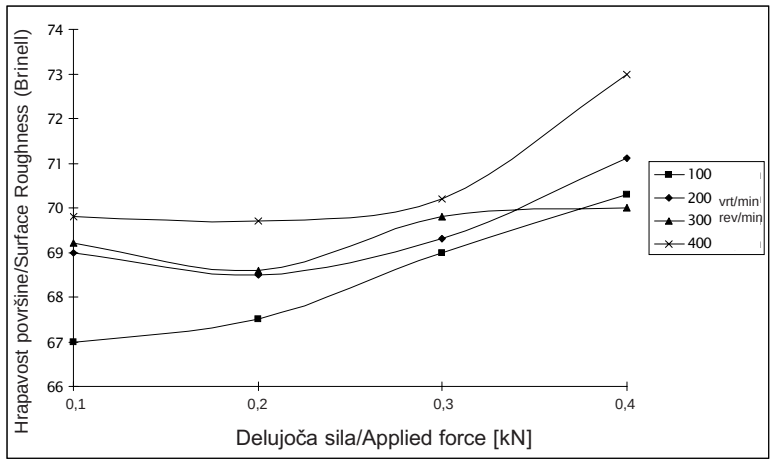

Sl. 6. *Učinek števila vrtljajev in delujoče sile na trdoto površine*
Fig. 6. *The effect of the number of revolutions and the applied force on the surface hardness*

Ko preučimo razmerje med številom vrtljajev in trdoto površine ob upoštevanju različnih delujočih sil, ugotovimo, da se trdota površine povečuje s povečevanjem števila vrtljajev in s povečano delujočo silo. V tem primeru smo najbolj gladko površino dobili pri 400 vrt/min in delujočo silo 0,4 kN.

2.3 Učinek števila prehodov polirne naprave in delujoče sile na hrapavost in trdoto površine

V štirih različnih permutacijah smo uporabili štiri različna števila prehodov polirne naprave in štiri različno delujoče sile, da bi ugotovili učinke teh parametrov na hrapavost in trdoto površine. Hitrost 0,1 mm/s in 300 vrt/min sta bili vrednosti preostalih eksperimentalnih parametrov. Dobljene vrednosti hrapavosti in trdote površine so prikazane v preglednici 4 ter slikah 7 in 8.

S slike 7 lahko razberemo učinke števila prehodov polirne naprave in delujoče sile na hrapavost površine. Povečanje števila prehodov, posebej če gre za več ko 4 prehode, zmanjša gladkost površine. Ugotovili smo, da je tri najbolj primerno število prehodov. Najboljše rezultate dosežemo, če uporabimo silo 0,3 kN.

Diagrama a in b s slike 8 kažeta, da s povečanjem delujoče sile povečamo trdoto površine.

When the relationship between the number of revolutions and the surface hardness is examined by taking into account the different applied forces, the surface hardness increases with an increasing number of revolutions and larger applied forces. At this stage, the smoothest surface was obtained with 400 rev/min and 0.4 kN of applied force.

2.3 Effect of number of passes and applied force on the surface roughness and surface hardness

Four different numbers of passes and four different applied forces were used with different permutations to check the effect of these parameters on the surface roughness and the surface hardness. A 0.1 mm/sec feed rate and 300 rev/min were used as the other experimental parameters. The obtained surface-roughness and surface-hardness values are seen in Table 4 and Figures 7 and 8.

It is possible to see the effect of the number of passes and the applied force on the surface roughness from Figure 7. Increasing the number of passes, especially to more than 4, reduced the surface smoothness. The most suitable number of passes was found to be 3. The force that should be applied for the best result is 0.3 kN.

The graphs a and b in Figure 8 show that increasing the applied force increases the surface

Preglednica 4. *Spreminjanje vrednosti hrapavosti in trdote površine materiala pri različnih delujočih silah in različnem številu prehodov (300 vrt/min in hitrost 0,1 mm/s)*
Table 4. *Variation of the surface-roughness and surface-hardness values for different forces and number of passes (300 rev/min and feed rate 0.1 mm/sec)*

Število prehodov Number of passes [n]	Delujoča sila/Applied force [kN]							
	0,1		0,2		0,3		0,4	
	Hrapavost površine Surface roughness [µmm]	Trdota površine Surface hardness (Brinell)	Hrapavost površine Surface roughness [µmm]	Trdota površine Surface hardness (Brinell)	Hrapavost površine Surface roughness [µmm]	Trdota površine Surface hardness (Brinell)	Hrapavost površine Surface roughness [µmm]	Trdota površine Surface hardness (Brinell)
2	0,51	55	0,38	58	0,47	61	0,53	62
3	0,579	56,3	0,443	62,5	0,415	67	0,47	68
4	0,56	61	0,45	65	0,501	72	0,52	73,2
5	0,57	64	0,47	68	0,53	74	0,61	76,1

a

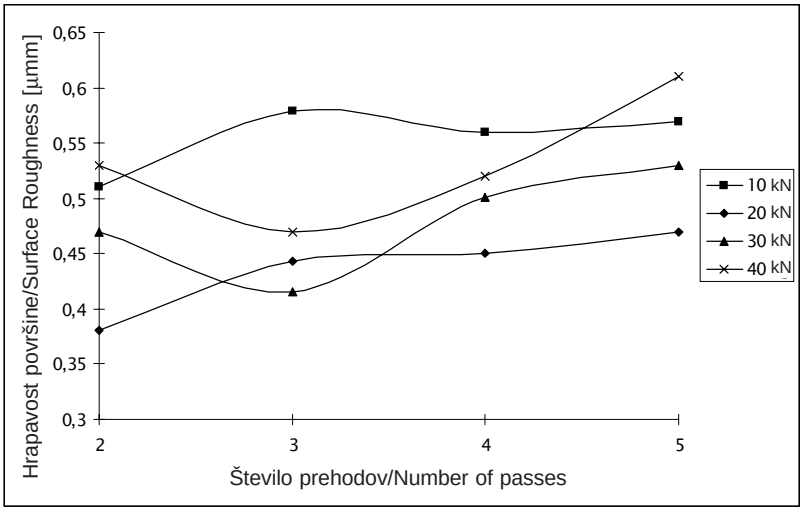

b

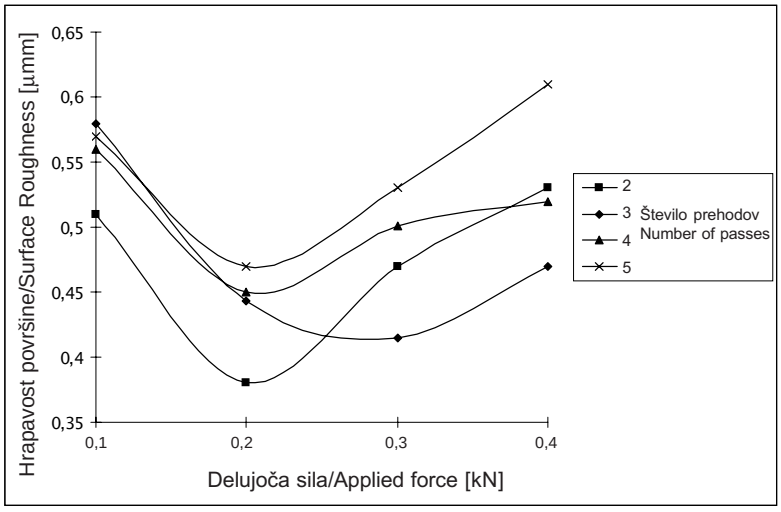

Sl. 7. *Učinek števila prehodov in delujoče sile na hrapavost površine*
Fig. 7. *Effect of the number of passes and the applied force on the surface roughness*

a

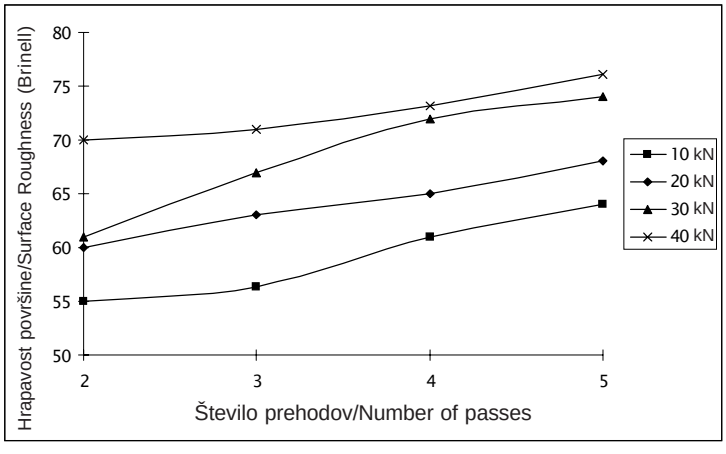

b

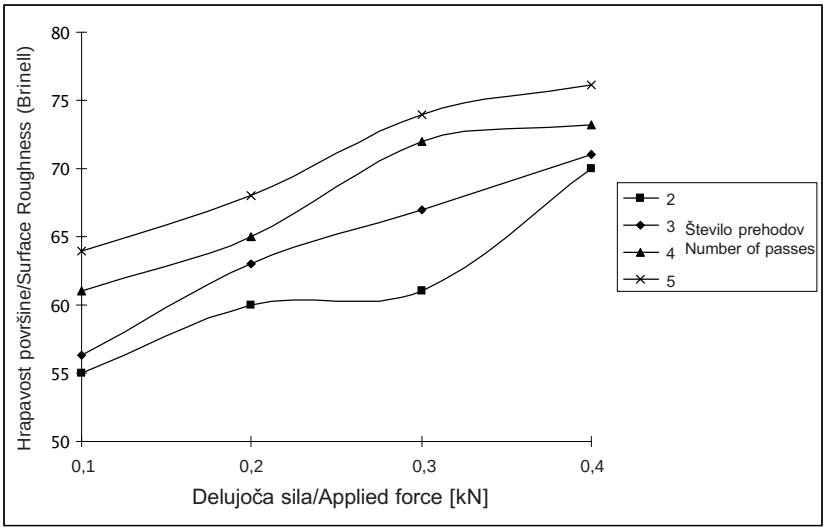

Sl. 8. *Učinek števila prehodov in delujoče sile na trdoto površine*
Fig. 8. *Effect of the number of passes and the applied force on the surface hardness*

Površina je imela največjo trdoto pri petih prehodih in delujoči sili 0,4 kN.

3 SKLEP

Na podlagi raziskave lahko naredimo naslednje sklepe:

- Očitno je, da s povečevanjem delujoče sile do določene vrednosti zmanjšujemo hrapavost površine. Ko pa sila preseže 0,3 kN, se hrapavost poveča. Najbolj gladko površino smo dobili, ko je delujoča sila znašala 0,2 kN, hitrost delovanja naprave pa je bila 0,3 mm/s. Lahko tudi rečemo, da s povečanjem hitrosti zmanjšamo trdoto površine. S povečanjem delujoče sile povečamo trdoto površine.
- S povečanjem števila vrtljajev pri sili 0,1 ali 0,2 kN povečamo gladkost površine; ko pa delujoča sila preseže 0,3 kN in število vrtljajev preseže 200 vrt/min, se kakovost polirane površine zmanjša. Najbolj gladko površino smo pridobili, ko je bila delujoča sila 0,2 kN in število vrtljajev 400 vrt/min. S povečanjem števila vrtljajev in delujoče sile povečamo trdoto površine.
- Ob povečanju števila prehodov polirne naprave, posebej ko imamo več ko štiri prehode, se gladkost površine zmanjša. V naši raziskavi se je izkazalo, da so najbolj primerni trije prehodi, najbolj primerna delujoča sila pa je 0,3 kN. Sila, ki jo moramo uporabiti za doseganje najboljših rezultatov, je 0,3 kN. S povečanjem števila prehodov in delujoče sile povečamo trdoto površine.

hardness. The hardest surface was obtained with 5 passes and an applied force of 0.4 kN.

3 CONCLUSION

The following conclusions can be drawn from this study:

- It is clear that increasing the applied force reduces the surface roughness up to a certain value. More than 0.3 kN increases the surface roughness. The smoothest surface was obtained when 0.2 kN and 0.3 mm/sec were used as the applied force and the feed rate, respectively. It can also be said that increasing the feed rate reduces the surface hardness. Increasing the applied force increases the surface hardness.
- Increasing the number of revolutions with 0.1 and 0.2 kN of force increases the smoothness of the surface; however, when the force applied is more than 0.3 kN, the burnished surface deteriorates above 200 rev/min. The smoothest surface was obtained with 0.2 kN of force and 400 rev/min. Increasing the number of revolutions and the applied force increases the surface hardness.
- Increasing the number of passes, especially to more than 4, reduced the surface smoothness. The most suitable number of passes and applied force were determined to be 3 and 0.3 kN, respectively, for this study. The force that should be applied for the best result is 0.3 kN. Increasing the number of passes and the applied force increases the surface hardness.

4 LITERATURA
4 REFERENCES

[1] Mendi,F. (1996) Takým Tezgâhlarý Teori ve Hesaplarý, ISBN:975-06008-0-3, Ankara, 10-18.

[2] Axir M. H., Khabeery M., H. H. (2003) Influence of orthogonal burnishing parameters on surface characteristics for various materials, *Journal of Materials Processing Technology* 132 (2003) 82–89

[3] Zhang P., Lindemann P. (2005) Effect of roller burnishing on the high cycle fatigue performance of the high-strength wrought magnesium alloy AZ80, *Scripta Materialia*, article in press

[4] N.H. Loh, S.C. Tam, S. Miyazawa (1989) A study of the effects of ball-burnishing parameters on surface roughness using factorial design, J*ournal of Mechanical Working Technology* 18 (1989) 53–61.

[5] S.S.G. Lee, S.C. Tam, N.H. Loh, S. Miyazawa (1992) An investigation into the ball burnishing of an AISI 1045 freeform surface, *Journal of Materials Processing Technology* 29 (1992) 203.

[6] S.S.G. Lee, S.C. Tam, N.H. Loh (1993) Ball burnishing of 316L stainless steel, *Journal of Materials Processing Technology* 37 (1993) 241.

[7] N.H. Loh, S.C. Tam, S. Miyazawa (1989) Statistical analyses of the effects of ball burnishing parameters on surface hardness, *Wear* 129 (1989) 235.

[8] Yashcheritsyn, E.I. Pyatosin, V.V. Votchuga (1987) Hereditary influence of pre-treatment on roller-burnishing surface wear resistance, *Soviet Journal of Friction and Wear* 8 (2) (1987) 87.

[9] M. Fattouh, M.H. El-Axir and S.M. Serage (1988) Investigation into the burnishing of external cylindrical surface of 70/30 Cu-Zn-alloy, *Wear* (1988) 127.

[10] A.N. Niberg (1987) Wear resistance of sideways strengthened by burnishing, *Soviet Engineering Research* 7 (5) (1987) 67.

[11] P.C. Michael, N. Saka, E. Rabinowicz (1989) Burnishing and adhesive wear of an electrically conductive polyestercarbon film, *Wear* 132 (1989) 265.

[12] M. Fattouh, M.M. El-Khabeery (1989) Residual stress distribution in burnishing solution treated and aged 7075 aluminum alloy, *Int. J. Mach. Tools Manufact.* 29 (1) (1989) 153.

[13] F. Klocke, J. Liermann (1998) Roller burnishing of hard turned surface, *Int. J. Mach. Tools Manufact.* 38 (5-6) (1998) 419.

[14] S. Mittal, C.R. Liu (1998) A method of modeling residual stresses in superfinish hard turning, *Wear* 218 (1998) 21.

[15] N.H. Loh, S.C. Tam (1988) Effects of ball burnishing parameters on surface finish—a literature survey and discussion, *Precis. Eng.* 10 (4) (1988) 215–220.

[16] Kaiser Alumimum Co. Malzeme Katalogu (2003)

Avtorjev naslov: dr. Hüdayim Başak
Univerza Gazi
Fakulteta za tehniško
izobraževanje
Oddelek za strojništvo Beşevler
Ankara, Turčija
hbasak@gazi.edu.tr

Author's Address: Dr. Hüdayim Başak
Gazi University
Technical Education Faculty
Mechanical Education
Department Beşevler
Ankara, Turkey
hbasak@gazi.edu.tr

Prejeto: 3.1.2007
Received:

Sprejeto: 25.4.2007
Accepted:

Odprto za diskusijo: 1 leto
Open for discussion: 1 year

Strojniški vestnik - Journal of Mechanical Engineering 53(2007)12, 898-912
UDK - UDC 62-25
Strokovni članek - Speciality paper (1.04)

Izboljšanje dinamičnih značilnosti rotorskega sistema z razvojnim algoritmom

Improving the Dynamic Characteristics of a Rotor System using an Evolutionary Algorithm

Hamit Saruhan
(Duzce University, Turkey)

V tem prispevku je povzeta študija optimalnega oblikovanja, potrebnega za izboljšanje dinamičnih značilnosti gibkega, prevesnega rotorskega sistema. Oblikovanje gibkega rotorskega sistema je zapleten postopek, saj ima veliko število geometričnih parametrov hidrodinamičnih ležajev, ki opravljajo pomembno nalogo pri napovedi dinamičnega obnašanja rotorskega sistema. Pri razporedu rotorskega sistema moramo upoštevati veliko oblikovnih zahtev, s katerimi lahko izboljšamo dinamične značilnosti, povezane z rotorjevim hitrostnim razponom. Za izboljšanje dinamičnih značilnosti rotorskega sistema smo uporabili genetski algoritem, za oblikovanje komponent rotorskega sistema pa smo uporabili metodo končnih elementov. Da bi potrdili učinkovitost in uporabnost predlagane metode, smo uporabili tudi metodo izvedljivih smeri; z njo smo dokazali, da je predlagana metoda oblikovanja rotorskega sistema učinkovita in uporabna za izboljšanje dinamičnih značilnosti rotorskega sistema.

(Ključne besede: rotorski sistemi, optimiranje, genetski algoritmi, metode končnih elementov)

In this paper the optimum design for improving the dynamic characteristics of a flexible, overhung rotor system is studied. The design of a flexible rotor system is a complicated process due to the large number of geometrical parameters of hydrodynamic bearings, which play an important role in the prediction of the dynamic behavior of the rotor system. There are a number of design requirements added to the rotor-system configuration that improve the dynamic characteristics within the rotor's speed range. To improve the dynamic characteristics of the rotor system, a genetic algorithm was employed and the modeling of the components of the rotor system was made with the finite-element method. Also, the method of feasible directions was used in order to validate the efficiency and applicability of the proposed method, and it proved that the proposed method in the rotor-system design is very efficient and useful for improving the dynamic characteristics of the rotor system.

(Keywords: rotor systems, optimization, genetic algorithm, finite element methods)

0 UVOD

Glavni namen tega prispevka je bil razvoj praktičnega postopka, s katerim bi rotorski sistem primerno oblikovali. Zahtevnost in dolgotrajnost oblikovanja rotorskega sistema sta terjali uporabo bolj robustne in učinkovite metode optimiziranja. Zato smo pri oblikovanju rotorskega sistema uporabili genetski algoritem, hkrati pa uporabili tudi metodo mogočih smeri, da bi potrdili učinkovitost in uporabnost predlaganega postopka. Genetski algoritem je vodena tehnika naključnega iskanja najboljše rešitve. Postopki iskanja parametrov

0 INTRODUCTION

The major goal in this paper was to develop a practical procedure by which the rotor system could be designed efficiently. The complexity and time-consuming nature of the design process of the rotor system required the use of a more robust and efficient optimization method. From this point of view, the genetic algorithm was employed in the rotor-system design and the method of feasible directions was also conducted to validate the efficiency and applicability of the proposed method. The genetic algorithm is a guided random search

temeljijo na načelu naravne izbire in genetike [5]. Z genetskim algoritmom lahko ustvarimo pomembno ravnotežje med raziskovanjem in izkoriščanjem iskalnega prostora ([7] in [17]). Razvojni algoritmi so novost na področju analize rotorskih sistemov in v literaturi najdemo le njihove delne študije, kot na primer prispevki avtorjev Saruhan idr. [10], Saruhan idr. [11] ter Qin idr. [19].

1 OPTIMIZACIJA POSTOPKOV

Genetski algoritem je prvi predlagal Holland [12], nadalje pa sta ga razvila De Jong [14] in Goldberg [5]. Genetski algoritem je zelo primeren za reševanje problemov s kompleksnimi, nezveznimi in diskretnimi funkcijami. Genetski algoritem vzdržuje populacijo kodiranih rešitev, ki jih vodi k optimalni rešitvi [5]. Tako v iskalnem prostoru išče dobre osebke in najboljšo mogoče končno rešitev. Namesto da bi se postopek začel z rešitvijo v eni točki v iskalnem prostoru, kakor v primeru numeričnih metod, pa genetski algoritem začne postopek z začetnim naborom naključnih rešitev. Psevdokoda genetskega algoritma je predstavljena na sliki 1. Genetski algoritem se začne z začetnim naborom naključnih rešitev, ki se imenujejo kromosom in so rešitev danega problema. Kromosom je običajno niz z naključnimi kombinacijami stanj 0 in 1, ni pa nujno niz binarnih bitov. Ta niz se razvija prek zaporednih ponovitev, ki se imenujejo generacije. Nizi vsake generacije so ovrednoteni z določenim merilom za njihovo ustreznost. Potem se algoritem nadaljuje in ustvarja novo obliko, dokler niso izpolnjeni zaključni kriteriji. Po ovrednotenju ustreznosti vsakega osebka v populaciji uporabimo genetska opravila

```
Begin /*genetski algoritem*/
 t ← 0;
(začetek)    roditelj(t);
(oceni ustreznost vsakega osebka)    roditelj(t);
WHILE (NOT finished)    DO LOOP
kombiniraj roditelja(t)   da dobiš potomca(t);
oceni potomca(t);
izberi roditelja(t+1)
med roditeljem(t) in potomcem(t);
 t ← t +1;   IF populacija konvergira THEN
end
end
```

Sl. 1. *Psevdokoda genetskega algoritma*

technique. Its parameter search procedures are based on the idea of natural selection and genetics [5]. A remarkable balance between exploration and exploitation of the search space can be made with a genetic algorithm ([7] and [17]). Evolutionary algorithms are new to the field of rotor-system analysis, and in the current literature there are limited studies, such as those of Saruhan et al. [10], Saruhan et al. [11], and Qin et al. [19].

1 OPTIMIZATION PROCEDURES

The genetic algorithm was first proposed by Holland [12] and extended further by De Jong [14] and Goldberg [5]. The genetic algorithm is well suited to the problems with complex, discontinuous, and discrete functions. The genetic algorithm maintains a population of encoded solutions, and guides them towards the optimum solution [5]. Thus, it searches the space of possible individuals and seeks to find the fittest solution. Rather than starting from a single-point solution within the search space, as in numerical methods, the genetic algorithm starts with an initial set of random solutions. The pseudocode of the genetic algorithm is outlined in Fig. 1. The genetic algorithm starts with an initial set of random solutions called a chromosome, representing a solution to the problem at hand. A chromosome is usually a string with random combinations of 0s and 1s, but not necessarily a binary-bit string. The string evolves through successive iterations, called generations. During each generation the strings are evaluated using some measure of fitness. The algorithm then proceeds by generating a new design until the termination criteria have been satisfied. After the evaluation of each individual fitness in the population, the genetic operators, selection,

```
Begin /*the genetic algorithm*/
 t ← 0;
(initialize)    parent(t);
(evaluate fitness of each individual)    parent(t);
WHILE (NOT finished)    DO LOOP
recombine   parent(t)   to yield offspring(t);
evaluate offspring(t);
select parent(t+1)
from parent(t) and offspring(t);
 t ← t +1;   IF population has converged THEN
end
end
```

Fig.1. *The genetic algorithm pseudocode*

– izbiro, križanje in spremembo – da ustvarimo novo generacijo. Po potrebi uporabimo tudi druge genetske posege. Novo ustvarjeni osebki nadomestijo sedanjo generacijo in začne se ponovno vrednotenje ustreznosti novih osebkov. Pri vsaki naslednji generaciji genetski algoritem ustvari nov nabor kromosomov z uporabo najboljših informacij prejšnjih generacij. Zanko ponavljamo, dokler ne najdemo sprejemnljive rešitve.

Metoda izvedljivih smeri je metoda številčnega iskanja, ki se začne z začetno domnevo, se iterativno nadaljuje in na izvedljivem področju išče optimalno rešitev. Metodo izvedljivih smeri je prvi razvil Zoutendijk [6] ter jo kasneje dopolnil Vanderplaats [8]. Metoda izvedljivih smeri temelji na ugotovitvi, da je smer iskanja S_i tista, po kateri že majhen premik ustvari izboljšanje vrednosti namenske funkcije, ne da bi se ob tem porušile dejavne omejitve.

crossover, and mutation, are applied to produce a new generation. Other genetic operators are applied as needed. The newly created individuals replace the existing generation, and re-evaluation is started for the fitness of new individuals. In each succeeding generation, the genetic algorithm creates a new set of chromosomes using the best information from the previous generation. The loop is repeated until an acceptable solution is found.

The method of feasible directions is a numerical search method that starts with an initial guess and proceeds iteratively, searching through the feasible region for an optimal solution. The method of feasible directions was first developed by Zoutendijk [6] and then modified by Vanderplaats [8]. The method of feasible direction is based on the observation that a search direction, S_i, is found such that a small move along it would produce an improvement in the objective function value without violating the active constraints.

$$X_{i+1} = X_i + \alpha\, S_i \tag{1},$$

kjer i pomeni število ponovitve, S je smer gibanja, skalarna količina α določa razdaljo gibanja (iskalna količina) v določeni smeri, X_{i+1} pa je končna točka, ki jo dobimo na koncu iteracije i. Izbira vrednosti S_i je odvisna od lege točke X_i. Algoritem je oblikovan takole:

where i represents the iteration number, S is the direction of movement, the scalar quantity α defines the distance of movement (the search quantity) that must move along the direction, and X_{i+1} is the final point obtained at the end of the i-th iteration. The choice of S_i depends on the position of the point X_i. The algorithm is formulated in the following way:

$$\text{Optimiziraj/Optimize } F(X_i) \tag{2}$$

ob upoštevanju, da je:

Subject to:

$$g_j(X_i) < 0 \quad g_j(X_i) = 0$$
$$j = 1,\ldots, Nom / Ncon \text{ (število omejitev/number of constraints)} \tag{3},$$

kjer sta $F(X_i)$ objektivna in g_j omejitvena funkcija, X_i pa je n-vektor spremenljivk oblikovanja. Zahtevi po uporabnosti in izvedljivosti, vezani na vektor iskanja smeri S, sta matematično izraženi takole:

where $F(X_i)$ and g_j are the objective and constraint functions respectively, X_i and is an n-vector of design variables. Mathematically, the usability and feasibility requirement for the search direction vector, S, can be expressed as follows:

$$\nabla F(X_i)\, S \le 0 \text{ uporabnost/usability} \quad \nabla g_j(X_i)\, S \le 0 \text{ izvedljivost/feasibility} \tag{4}$$

kjer sta $\nabla F(X_i)$ gradient namenske omejitve, $g_j(X_i)$ pa gradient dejavne omejitve j, dobljene na točki X_i. Več informacij o opisani tehniki lahko bralci najdejo v sestavku Vanderplaats [8].

where $\nabla F(X_i)$ is the gradient of the objective and $g_j(X_i)$ is the gradient of the j-th active constraint computed at point X_i. The reader can refer to detailed information about this technique in Vanderplaats [8].

2 PREDSTAVITEV PROBLEMA

Rotorski sistem mora biti oblikovan tako, da ob različnih obratovalnih hitrostih deluje brez

2 THE PROBLEM STATEMENT

The rotor system must be designed to operate without excessive vibration throughout its range of

odvečnega vibriranja. Rotorjeva amplituda je funkcija dinamičnih značilnosti rotorja in ležaja. Ležajevi dinamični parametri imajo pomembno vlogo pri napovedi dinamičnega obnašanja rotorskega sistema ter so pomembni pri določanju odzivnosti in stabilnosti rotorskega sistema [13]. Določitev amplitude odzivnosti je zelo zapleteno zaradi asimetrije koeficientov togosti in dušenja pri križno spojeni tekočinski plasti, ki pa sta odvisna od hitrosti rotorja. Glavi cilj študije je uporaba genetskega algoritma in metode mogočih smeri za potrebe zmanjšanja amplitud odziva na različne hitrosti rotorja pri gibkem vrtilnem sistemu. Začetno fazo razvoja oblikovanja rotorja, ki ga podpirajo ležaji, smo vzpostavili z modeliranjem vrtilnega sistema, predstavljenega na sliki 2 , ki smo ga delno povzeli po viru Roso [2]. Sistem je sestavljen iz velikega diska (vijak) z rotorjem, ki ga podpirata dva pritrjena hidrodinamična trisegmentna ležaja. Rotorski sistem smo simulirali s kombinacijo 31 končnih elementov in 32 leg. Podrobnosti oblike rotorja so razvidne iz preglednice 1. Hitrost rotorja je v razponu med 5.000 min^{-1} in 40.000 min^{-1}, dva ležaja pa sta nameščena na legah 14 in 24. Značilnosti rotorja in uporabljenega maziva so naslednje: obratovalna hitrost tečaja je 28.000 min^{-1}, zunanje breme tečaja je 1401,19 N, tip maziva je mineralno olje, stopnja kakovosti maziva je ISO VG-32, vstopna temperatura maziva je 46,11°C, in vstopni pritisk maziva je 1,757674 bar. Nastavitev izračuna za rotorski sistem temelji na metodi končnih elementov in uporabi metode redukcije matrike. Metoda končnih elementov se je izkazala kot zelo učinkovita za potrebe modeliranja. Njena prednost pred drugimi metodami je v tem, da omogoča večjo natančnost diskretizacije rotorja [16]. Z uporabo metode redukcije matrike, oziroma Guyanove metode redukcije, v algoritmu, ki temelji na končnih elementih, zmanjšamo obseg sistemskih izračunov in njihove stroške, ne da bi s tem bistveno vplivali na točnost rezultatov ([15] in [16]). Z metodo končnih elementov smo določili približek dinamičnega obnašanja rotorskega sistema: rotor smo razdelili na končno število elementov ter nato vsak element označili glede na njegove dinamične značilnosti. Postopno zbiranje posameznih znaličnosti rotorjevih elementov, skupaj s sestavljanjem učinkov ležaja in vijaka, privede do splošne oblike enačb gibanja celotnega sistema takole:

operating speeds. The rotor's amplitude is a function of the dynamic characteristics of both the rotor and the bearing. The bearing's dynamic parameters play an important role in the prediction of the dynamic behavior of the rotor system and they are important in determining the response and the stability of the rotor system [13]. The determination of the response amplitude is much involved due to the asymmetry in the cross-coupled fluid film's stiffness and the damping coefficients, which in turn are dependent on the rotor speeds. The main objective here is the use of the genetic algorithm and the method of feasible directions for the minimization of the response amplitudes within the rotor speed range of the flexible rotor system. The initial phase of developing a design methodology for the rotor supported in the bearings was established with the modeling of the rotor system shown in Fig. 2, partially adapted from Roso [2]. The system consists of a large disc (impeller) with the rotor supported in two hydrodynamic fixed three-lobe bearings. The rotor system is simulated by a combination of 31 finite elements and the 32 stations. Details of the rotor configuration are provided in Table 1. The rotor speed ranged from 5,000 rpm to 40,000 rpm and the two bearings are located at stations 14 and 24 respectively. The rotor and the lubricant properties used are as follows: journal operating speed, 28,000 rpm, journal external load, 1401.19 Newtons, lubricant type (mineral base), lubricant grade (ISO VG-32), lubricant inlet temperature, 46.11°C, and the lubricant inlet pressure, 1.757674 bar. The formulation for the rotor-system calculation is based on the finite-element method using the matrix-reduction method. The finite-element method has proven to be very effective for modeling. The finite-element method has the advantage over other methods in that it provides greater accuracy for the rotor discretization than the other methods [16]. Using a matrix-reduction method, the Guyan Reduction Method, in the finite-element-based algorithm, reduces the size and the computational cost of the system calculations with no significant effect on the accuracy of the results ([15] and [16]). The finite-element method was developed to approximate the dynamic behavior of the rotor system as follows: the rotor is subdivided into a finite number of elements, and each element is characterized by dynamic properties. The successive assembling of the individual rotor-element characterization along with the assembling of the effect due to the bearing and impeller leads to a general form of equations of motion for the complete system as follows:

$$[M]\{\ddot{q}\}+[C]\{\dot{q}\}+[K]\{q\}=\{Q(t)\} \quad (5),$$

kjer je $q=[U_1\ V_1\ \Theta_1\ \Phi_1\ U_2\ V_2\ \Theta_2\ \Phi_2]^T$ vektor premikov (U V) v smeri X in smeri Y ter zavrtitve (Θ Φ) okoli osi X in osi Y. Spodnja indeksa 1 in 2 določata oba konca prikaza končnega elementa; [M], [C], [K] pa predstavljajo matrike mase, dušenja in togosti. {Q(t)} je vektor vzbujevalnih sil in momentov. Amplitudo rotorjevih premikov pri vsakem vozliščnem mestu smo izračunali tako, da smo najprej iz kompleksnih rezultatov izločili realne rešitve. Na posameznem vozliščnem mestu rotorja ima rešitev naslednjo obliko [2]:

where $q=[U_1\ V_1\ \Theta_1\ \Phi_1\ U_2\ V_2\ \Theta_2\ \Phi_2]^T$ is the vector of displacement (U V) in the X-axis and Y-axis and the rotational displacement (Θ Φ) about the X-axis and Y-axis. Subscripts 1 and 2 identify each end of the finite-element representation, and [M], [C], [K] represents the mass, damping, and stiffness matrices respectively. {Q(t)} is the vector of the exciting forces and moments. The amplitude of the rotor displacement at each nodal location is computed by first extracting the real solution from the complex results. The particular solution at a nodal location of the rotor is of the form [2]:

$$U_2=\left(R\left(U_{0,2}\right)+J\left(U_{0,2}\right)\right)e^{J\Omega t} \quad (6)$$

$$V_2=\left(R\left(V_{0,2}\right)+J\left(V_{0,2}\right)\right)e^{J\Omega t} \quad (7)$$

$$R\left(U_2\right)=A_{U_2}\,Cos\,\psi_{U_2}\,Cos\,\Omega t+A_{U_2}\,Sin\,\psi_{U_2}\,Sin\,\Omega t \quad (8)$$

$$R\left(V_2\right)=A_{V_2}\,Cos\,\zeta_{V_2}\,Cos\,\Omega t+A_{V_2}\,Sin\,\zeta_{V_2}\,Sin\,\Omega t \quad (9),$$

kjer so: *R* operator realnega dela, *J* operator imaginarnega dela, *A* lastni vektor, ζ rotacijski premik okoli osi x, ψ vrtilni zasuk okoli osi *y*, *t* čas, Ω pa hitrost vrtenja.

Zaželena je uporaba tehnik optimizacije, da z njimi določimo in izberemo spremenljivke modela, ki jih lahko uporabimo za optimizacijo rotorskega sistema, ki bo izpolnil izbrane kriterije. Obstaja močno razmerje med funkcijami namena, spremenljivk in kriterijev oblikovanja. Vektor spremenljivk oblikovanja vključuje razmerje med osno dolžino segmenta in premerom tečaja (*y*1), razdaljo med segmentom ležaja in obodom (*y*2), prečni razmik ležajev (*y*3), faktor pomika segmenta (*y*4), faktor naprejšnje obremenitve segmenta (*y*5), in usmerjenost ležaja glede na obremenitev (*y*6) ter je izražen takole:

where *R* is real part operator, *J* is an imaginary part operator, *A* is the eigenvector, ζ is the rotational displacement about the x-axis, ψ is the rotational displacement about the y-axis, *t* is the time, and Ω is the rotation speed.

It is desirable to utilize optimization techniques to evaluate and select the design variables that can be used to optimize the rotor system that will satisfy the criteria placed on them. There is a strong relationship among the design-objective, design-variables, and design-criteria functions. The vector of the design variables includes the pad-axial-length to journal-diameter ratio (*y*1), the pad (lobe) to the arc length (*y*2), the bearing radial clearance (*y*3), the pad offset factor (*y*4), the pad preload factor (*y*5), and the bearing orientation with respect to the load (*y*6) expressed as follows:

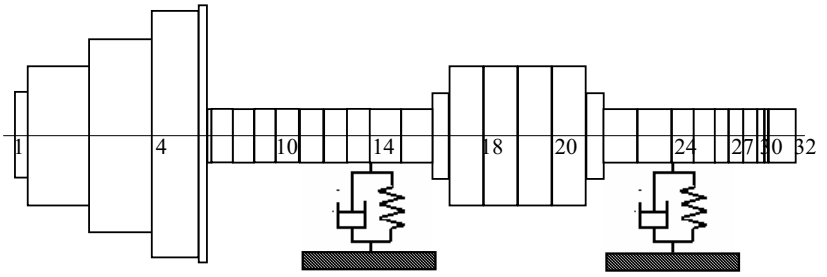

Sl. 2. *Razpored končnih elementov rotorskega sistema*
Fig. 2. *Finite-element configuration of the rotor system*

Preglednica 1. *Rotorjeva razporeditev*
Table 1 *The rotor configuration*

Element rotorja Rotor Element	Lege elementa Element Stations	Dolžina elementa rotorja (mm) Rotor Element Length (mm)	Skupna dolžina el. (mm) Cumulative Element Length (mm)
1	1 2	6,248	6,248
2	2 3	30,142	36,390
3	3 4	30,142	66,532
4	4 5	22,268	88,800
5	5 6	3,810	92,610
6	6 7	2,032	94,642
7	7 8	9,989	104,630
8	8 9	9,989	114,622
9	9 10	9,989	124,612
10	10 11	11,168	135,780
11	11 12	11,168	146,949
12	12 13	11,168	158,117
13	13 14	11,168	169,285
14	14 15	14,744	184,030
15	15 16	14,744	198,775
16	16 17	7,620	206,395
17	17 18	15,875	222,270
18	18 19	15,875	238,145
19	19 20	15,875	254,025
20	20 21	15,875	269,900
21	21 22	8,128	278,028
22	22 23	15,836	293,852
23	23 24	15,836	309,702
24	24 25	10,325	320,014
25	25 26	10,325	330,352
26	26 27	6,350	336,702
27	27 28	6,718	343,408
28	28 29	6,718	350,139
29	29 30	3,048	353,187
30	30 31	15,240	354,711
31	31 32	12,700	367,411

$$X(i) = \begin{bmatrix} (y1), \\ (y2)*(\pi/180), \\ (y3)*(1-y5)/1000), \\ (y4)*2, \\ (y5)*2, \\ (y6)*(\pi/180) \end{bmatrix} \quad (10),$$

kjer je i število oblikovnih spremenljivk. Razmerje med osno dolžino segmenta in premerom tečaja vpliva na nestabilnost, ki jo povzroči tekočinska plast. Ključni parameter, ki ga uporabimo za opis ležajev s pritrjenimi segmenti, je delež konvergentnega segmenta pri celotni dolžini segmenta. To razmerje imenujemo faktor pomika segmenta. Geometrijsko razmerje med segmenti ležaja in tečajem lahko dobimo

where i is the number of design variables. The pad-axial-length to journal-diameter ratio has an affect on the fluid-induced instability. A key parameter used for describing fixed-pad (lobe) bearings is the fraction of the converging pad to full-pad length. This ratio is called the pad-offset factor. A geometric relationship between the bearing pads and the journal can be obtained by constructing the bearing pad

s tem, da ležajne segmente oblikujemo tako, da se njihova središča ne ujemajo s središčem ležaja. S tem na vsakem segmentu ustvarimo konvergentne in divergentne predele tekočinske plasti, zaradi katerih celo v primeru neobremenjenega tečaja v plasti nastane tlak. Ker do pojava pride v odsotnosti tečajeve obremenitve, je le-ta v literature poimenovan kot vnaprejšnja obremenitev ležaja. Ker lahko vnaprejšnja obremenitev vpliva na usrediščenost rotorja, lahko na ta način izboljšamo stabilnost rotorskega sistema. Vse oblikovne spremenljivke sistematično preverimo, da ugotovimo učinek vsake kombinacije in dobimo najmanjšo namensko funkcijo glede na oblikovne kriterije. Tako ugotovimo, da se, na primer: prečni razmik poveča ob povečanju najmanjše debeline tekočinske plasti; da izgubo moči lahko premostimo s krajšanjem dolžine ležajnih segmentov; da povečanje premera tečaja povzroči povečanje izgub; da največji vršni tlak segmenta lahko zmanjšamo do najmanjših vrednosti tako, da povečamo osno dolžino ležajnega segmenta in zmanjšamo parameter vnaprejšnje obremenitve ležaja; ter da se začetna nestabilnost poveča ob povečani vnaprejšnji obremenitvi, ki se zmanjša ob povečanju pomika. Omejitve so pogoji, ki jih moramo izpolniti z optimalnim oblikovanjem in ki pomenijo omejitve funkcij oblikovnih kriterijev, kot na primer temperatura plasti, tlak plasti, pretok maziva, obodni pomik, meje stabilnosti ter geometrijske razlike. Temperatura ležaja je pomemben kriterij, ki ga moramo izpolniti, saj v nasprotnem primeru lahko povzročimo okvaro ležajev tečaja in s tem celotnega rotorskega sistema. Učinek tlaka v tekočinski plasti se kaže v gostoti in viskoznosti maziva. Količina tekočine, ki je potrebna ležaju, je tudi faktor delovanja ležaja. Zaradi omejitev stabilnosti je potrebno poznati najmanjšo vrednost logaritmičnega zmanjšanja za primer nestabilnosti, ta nastane pod vplivom sil tekočinskega vzbujanja. Namenska funkcija se nanaša na ostrino resonance, ki sledi načinu, izkazuje največjo obodno amplitudo. Izraz za namensko funkcijo, ki predstavlja rotorjevo amplitudo odziva, je naslednji:

centers not coinciding with that of the bearing. This would produce converging and diverging film sections along each pad; consequently, fluid film pressures would be generated even with an unloaded journal. Since this condition occurs in the absence of a journal load, it is called, in the literature, a bearing preload. Because the preload can affect the rotor-centerline position, the stability of the rotor system is improved. The design variables are all systematically varied to identify the effects of each combination, finding the minimum objective function along the design criteria, such as the radial clearance increases as the minimum film thickness increases, the power loss decreases by reducing the length of the bearing pads, an increase in the journal diameter would produce an increase in losses, the maximum pad peak pressure is reduced to minimum values by increasing the axial length of the bearing pad and reducing the bearing preload parameter, and the instability threshold increases with larger preloads, which tends to decrease as the offset factor increases. Constraints are conditions that must be met in the optimum design and include restrictions to design criteria functions, such as film temperature, film pressure, lubricant flow, orbital displacement, stability bounds, and geometric inequalities as follows: Bearing temperature is an important criterion that should be met because it can be dangerous enough to give a failure in the journal bearings and thus the whole rotor system. The effect of the pressure in the fluid film is reflected by the density and viscosity of the lubricant. The amount of fluid that needs to be supplied for the bearing is also a factor in the bearing performance. For the stability bounds it is necessary to have a minimum logarithmic decrement value for the mode predicted to become unstable under the process fluid excitation forces. The objective function is referred to as the sharpness of resonance, which aims to track the mode that exhibits the highest orbital amplitude. The statement for the objective function representing the rotor's response amplitude is:

$$F_{\text{objective}} = \sum_{i=1}^{N\text{modes}} \sum_{\text{j}=1}^{N\text{stations}} \left(\omega_i / \left(\omega_{a,i}\ \omega_{b,i} \right) \right)_j \tag{11}$$

$$Fitness\ Function = \sum_{i=1}^{N\text{modes}} \sum_{\text{j}=1}^{N\text{stations}} \left(\omega_i / \left(\omega_{a,i}\ \omega_{b,i} \right) \right)_j + \sum_{\text{j}=1}^{N\text{con}} r_j \left(\max\left[0, g_j \right] \right)^2 \tag{12},$$

kjer je $F_{\text{objective}}$ amplituda odziva, N_{stations} so izbrane lege vzdolž rotorja, na katerih je odziv optimiziran,

where $F_{\text{objective}}$ is the response amplitude, N_{stations} are selected stations along the rotor where the response

$\omega_{a,i}$ in $\omega_{b,i}$ sta frekvenci na obeh straneh resonance imenovani stranska pasova, N_{con} pa je število omejitev.

Funkcija ustreznosti meri in razvršča vektorje kodiranih spremenljivk ter nato izbere povezave, ki vodijo do najboljših rešitev. Problem optimizacije omejitev smo spremenili v problem optimizacije brez omejitev in ga rešili s kaznovanjem vrednosti namenske funkcije s kvadratno kazensko funkcijo, s katero zagotovimo, da namenska funkcija ustreza vsiljenim omejitvam. V primeru kakršnekoli kršitve omejitev je funkcija ustreznosti, ki se nanaša na rešitev, kaznovana in zadržana v izvedljivih področjih oblikovalnega prostora. Za potrebe nadzorovanja in kaznovanja so potrebni kazenski koeficienti, r_j, ki jih uporabimo za različne ravni kršitve posameznih omejitev. Kakor navajajo Homaifar idr. [1], moramo kazenske koeficiente preudarno izbrati, saj so primerne rešitve močno odvisne od vrednosti teh koeficientov.

3 REŠEVANJE PROBLEMA Z GENETSKIM ALGORITMOM

Prvi korak reševanja določenega oblikovalnega problema z genetskim algoritmom je kodiranje oblikovnih spremenljivk kot niz. Ta niz se tipično nanaša na rešitev problema. Namesto da bi začel pri eni sami rešitvi v iskalnem prostoru, kar se zgodi pri numeričnih metodah, se genetski algoritem začne s populacjo rešitev, ki določajo število nizov vsake generacije. Vektorji zveznih oblikovalnih spremenljivk so predstavljeni in diskretizirani natančno do vrednosti ε (za to obravnavo smo določili ε = 0,01). Število števk v binarnem nizu L ocenimo z naslednjim razmerjem [3]:

$$2^L \geq \left[\left(\mathrm{X(i)}_{\text{zgornji/upper}} - X(i)_{\text{spodnji/lower}}\right)/\varepsilon\right]+1 \quad (13),$$

kjer sta $X(i)_{spodnji}$ in $X(i)_{zgornji}$ spodnja in zgornja meja za vektor oblikovnih spremenljivk.

Šest oblikovnih spremenljivk kodiramo v binarnem zapisu {0, 1}, kar prikazuje preglednica 2. Predstavitev vektorja oblikovnih spremenljivk z binarnim nizom $X(i)$ je lahko nastavljena od začetka do konca kot dolgi niz, ki ga imenujemo kromosom. Preglednica 3 prikazuje niz 42 binarnih zapisov, ki označujejo združene vektorje oblikovnih spremenljivk. Z naključno izbranim naborom

is optimized, $\omega_{a,i}$ and $\omega_{b,i}$ are two frequencies on either side of the resonance known as sidebands, and N_{con} is the number of constraints.

The fitness function measures and rates the coded variables' vector in order to select the fittest strings that lead the solution. The constraint optimization problem was transformed into an unconstrained optimization problem and handled by penalizing the objective function value by a quadratic penalty function, which is used to ensure that the objective function meets the imposed constraints. In the case of any violation of a constraint boundary, the fitness function of the corresponding solution is penalized and kept within the feasible regions of the design space. For controlling the penalization process, the penalty coefficients, r_j, are used for a different level of violation of each constraint. The penalty coefficients have to be judiciously selected, Homaifar et al. [1], because the reasonable solutions importantly depend on the values of these coefficients.

3 APPLYING THE GENETIC ALGORITHM TO THE PROBLEM

The first step in applying the genetic algorithm to the assigned design problem is encoding the design variables as a string. This string typically refers to a solution to the problem. Rather than starting from a single point solution within the search space as in numerical methods, the genetic algorithm is initialized with a population of solutions, which specify the number of strings in each generation. The continuous design variables' vectors are represented and discretized to a precision of ε (for this study, ε = 0.01). The number of digits in the binary string,, is estimated from the following relationship [3]:

where $X(i)_{upper}$ in $X(i)_{lower}$ are the lower and upper bounds for the design variables' vector respectively.

The six design variables are coded into binary digits {0, 1}, as shown in Table 2. The binary string representation for the vector of the design variables, $X(i)$, can be placed head-to-tail to form one long string, referred to as a chromosome. Table 3 shows a string of 42 binary digits, denoting the concatenated design variables' vector. A randomly selected set, for this study a 50-string, of potential

Preglednica 2. *Kodiranje vektorja oblikovnih spremenljivk v binarnem zapisu*
Table 2. *Coding of the design variables' vector into binary digits*

Vektor oblikovnih spremenljivk Design variables' vector	Spodnja meja Lower limit	Zgornja meja Upper limit	Dolžina niza String length	Binarni niz Binary string	Razrešena vrednost Decoded value
X(1) (= y1)	0,50	1,00	6	0 1 0 1 0 0	0,658
X(2) (= (y2)*(π/180))	1,50	2,00	6	0 1 0 1 0 0	1,658
X(3) (= (y3)*(1-y5)/1000)	1,40	1,95	7	1 0 1 0 0 1 1	1,759
X(4) (= (y4)*2)	1,00	2,00	7	0 0 1 0 0 0 1	1,133
X(5) (= (y5)*2)	0,00	1,50	8	0 0 1 0 1 0 1 0	0,247
X(6) (= (y6)*(π/180))	0,64	2,37	8	1 0 0 0 1 0 0 1	2,247

Preglednica 3. *Nabor začetne populacije*
Table 3. *A set of the starting population*

	Začetna populacija/Initial population Združeni vektorji spremenljivk od glave do repa/Concatenated variables vectors head-to-tail					
	X(1)	X(2)	X(3)	X(4)	X(5)	X(6)
	010100	**010100**	1010011	**0010001**	00101010	**10001001**
1	0 1 0 1 0 0 **0 1 0 1 0 0** 1 0 1 0 0 1 1 **0 0 1 0 0 0 1** 0 0 1 0 1 0 1 0 **1 0 0 0 1 0 0 1**					
	100111	**100010**	0100101	**1100011**	10101010	**01110110**
2	1 0 0 1 1 1 **1 0 0 0 1 0** 0 1 0 0 1 0 1 **1 1 0 0 0 1 1** 1 0 1 0 1 0 1 0 **0 1 1 1 0 1 1 0**					
.	.	.	.	.	.	.
.	.	.	.	.	.	.
	001101	**0111000**	1001100	**0011100**	00011001	**10001010**
50	0 0 1 1 0 1 **0 1 1 1 0 0 0** 1 0 0 1 1 0 0 **0 0 1 1 1 0 0** 0 0 0 1 1 0 0 1 **1 0 0 0 1 0 1 0**					

izvedljivih rešitev – za potrebe te obravnave smo izbrali 50 nizov – ustvarimo začetno populacijo.

Nadaljnje populacije nastanejo s postopki izbire, križanja in sprememb. Operator izbire določi člane populacije, ki preživijo in sodelujejo v nastanku nove generacije. Vektor oblikovnih spremenljivk z bolj ustreznimi vrednostmi ima večjo možnost, da preživi in je izbran kot roditelj naslednjih generacij. Obstaja več metod izbire. Izbira, ki deluje v algoritemski kodi, temelji na tekmovanju, ki za potrebe združitve naključnih parov uporablja tehniko mešanja. Ta tehnika prerazporedi populacijo v naključno zaporedje. Izbira na osnovi tekmovanja deluje takole: dvojica osebkov iz paritvene skupine je naključno izbrana in dva najbolj ustrezna osebka bosta izbrana kot roditelja. Vsak par roditeljev ustvari dva potomca, kar je predstavljeno z metodo enoličnega križanja

solutions is initialized to form the starting population.

Successive populations are produced by the operations of selection, crossover, and mutation. The selection operator determines those members of the population that survive to participate in the forming of members of the next generation. The design variables' vector with better fitness values is more likely to survive and be chosen as parents for the successive generation. There are many methods to perform the selection. The selection operator used in the algorithm code is a tournament selection, with a shuffling technique for choosing random pairs for mating. The shuffling technique rearranges the population in a random order for selection. The tournament selection approach works as follows: a pair of individuals from the mating pool is randomly picked and the best-fit two

v preglednici 4. Algoritem temelji na strategiji elitistične reprodukcije. Elitizem prisili genetski algoritem, da iz dane generacije obdrži najboljše osebke, ki nespremenjeni preidejo v naslednjo generacijo [18]. S tem se zagotovi, da se genetski algoritem približa ustrezni rešitvi. Povedano z drugimi besedami, elitizem je zaščita pred križanjem in spremembo, ki bi lahko ogrozila trenutno najboljšo rešitev.

V pričujoči obravnavi smo uporabili opravilo enoličnega križanja, pa tudi veliko drugih študij [9] priporoča enolično križanje z verjetnostjo 0,5. Ta poseg je primarni vir novih izvedljivih rešitev in vsebuje iskalni mehanizem, ki učinkovito vodi razvoj skozi iskalni prostor proti optimalni rešitvi. Pri enoličnem križanju ima vsak bit vsakega roditeljskega niza možnost, da se zamenja z ustreznim bitom drugega roditeljskega niza. S tem postopkom naključno pridobimo katerokoli kombinacijo dveh roditeljskih nizov (kromosomov) iz paritvene skupine ter iz roditeljskih nizov nato ustvarimo nove nize potomcev, tako da za vsak bit izvedemo križanje, ki ga izberemo glede na naključno ustvarjeno masko križanja [4]. Kjer je v maski križanja "1", tam je bit potomca kopiran iz prvega roditeljskega niza; kjer pa je v maski "0", tam je bit potomca kopiran iz drugega roditeljskega niza. Drugi niz potomca pa uporablja pravilo, ki je nasprotno pravkar opisanemu pravilu, kar je prikazano v preglednici 4. Za vsak par roditeljskih nizov je naključno ustvarjena nova maska križanja.

Da bi preprečili, da bi se genetski algoritem prezgodaj približal rešitvi, ki ni najboljša, kar se lahko zgodi ob ponavljajoči se rabi izbiro in križanja, uporabljamo opravilo spremembe. Sprememba je v bistvu postopek naključno spremenjenega dela osebka, pri katerem stanje bita spremenimo iz 0 v 1 ali obratno, s čimer nastane nov osebek.

V pričujoči razpravi smo uporabili opravilo sprememb s preskokom. Ta ustvari kromosom, ki je

individuals from this pair will be chosen as a parent. Each pair of parents creates two children, as described in the method for uniform crossover, shown in Table 4. The algorithm is based on an elitist reproduction strategy. Elitism forces the genetic algorithm to retain the best individual in a given generation to proceed unchanged into the following generation [18]. This ensures that the genetic algorithm converges to an appropriate solution. In other words, elitism is a safeguard against the operation of a crossover and a mutation that may jeopardize the current best solution.

A uniform crossover operator is used in this study, and a uniform crossover probability of 0.5 is recommended in many studies [9]. This operator is a primary source of new candidate solutions and provides a search mechanism that efficiently guides the evolution through the solution space towards the optimum. In a uniform crossover, every bit of each parent string has a chance of being exchanged with the corresponding bit of the other parent string. The procedure is to obtain any combination of two parent strings (chromosomes) from the mating pool randomly and generate new child strings from these parent strings by performing a bit-by-bit crossover, chosen according to a randomly generated crossover mask [4]. Where there is a "1" in the crossover mask, the child bit is copied from the first parent string, and where there is a "0" in the mask, the child bit is copied from the second parent string. The second child string uses the opposite rule to the previous one, as shown in Table 4. For each pair of parent strings a new crossover mask is randomly generated.

To prevent the genetic algorithm from prematurely converging to a non-optimal solution, which may diversity away by repeated application of the selection and crossover operators, the mutation operator is used. Mutation is basically a process of randomly altering a part of an individual to produce a new individual by switching the bit position from a 0 to a 1 or vice versa.

The jump mutation operator is used in this study. The jump mutation produces a chromosome

Preglednica 4. *Enolično križanje*
Table 4. *Uniform crossover*

Maska križanja/Crossover mask	1001011100100101110010010111001001011100 10
Roditelj 1/Parent 1	**10100011101010001110101000111010100011101 0**
Roditelj 2/Parent 2	01010100110101010011010101001101010100110 1
Potomec 1/Child 1	**11000011111100001111110000111111000011111 1**
Potomec 2/Child 2	**00110100100011010010001101001000110100100 0**

naključno izbran in vključen v razpon parametra ustreznosti. Obstaja več načinov zaustavitve delovanja genetskega algoritma; po metodi, ki smo jo uporabili v naši razpravi, algoritem ustavimo po določenem številu ustvarjenih generacij. Konvergenca pomeni približevanje enoličnosti. Verjamemo, da se je kromosom približal, ko ima 95% populacije enako vrednost [14]. Osebki populacije so torej vsi, ali večinoma, enaki ali podobni, ko se populacija približa. Nastavitev parametrov genetskega algoritma za potrebe te razprave je naslednja: dolžina kromosoma = 42, velikost populacije = 50, število generacij = 77, verjetnost križanja = 0,5 in verjetnost spremembe = 0,001.

4 REZULTATI

Raziskali smo dinamične značilnosti rotorskega sistema in dobili rezultate, ki omogočajo primerjavo obeh metod optimizacije. Razmerje med faznimi koti amplitud odziva rotorskega sistema v smereh X in Y in hitrostjo rotorja v razponu od 5000 min^{-1} do 40000 min^{-1} na posameznih lokacijah je prikazano na slikah 3 do 6. V smereh X in Y, ki sta prileţni obema legama ležajev, smo dobili odziv rotorja, da bi določili amplitudo premika. Največji premik smo ugotovili na mestu 1, ki se ujema z lego konice vijaka. V primeru uporabe genetskega algoritma znaša največji premik približno 0,000146 mm v smeri X pri hitrosti 16000 min^{-1} in 0,000143 mm v smeri Y pri hitrosti 37000 min^{-1}, medtem ko v primeru uporabe metode izvedljivih smeri največji premik znaša 0,000320 mm v smeri X pri hitrosti 19000 min^{-1} in 0,000323 mm v smeri Y pri hitrosti 19000 min^{-1}. Najmanjši premik pri uporabi genetskega algoritma znaša približno 0,000065 mm v smeri X pri hitrosti 10000 min^{-1} in 0,000067 mm v smeri Y pri hitrosti 5600 min^{-1} (na legi 24), medtem pa pri uporabi metode izvedljivih smeri najmanjši premik znaša 0,000020 mm v smeri X pri hitrosti 6400 min^{-1} in 0,000016 mm v smeri Y pri hitrosti 5600 min^{-1} (na legi 20). Rezultati so pokazali, da se rotorjevi hitrosti, pri katerih se pojavita največja in najmanjša amplituda, spreminjata. V celoti so mesta koničnih odzivov dobro usklajena, četudi se zdi, da so ob uporabi genetskega algoritma manjša kakor ob uporabi metode izvedljivih smeri. Ti pomembni izsledki ustrezajo določeni specifikaciji vsiljenih omejitev in rotorskemu sistemu omogočijo, da ohrani svojo stabilnost.

that is randomly picked to be in the range of the appropriate parameter. There are many different ways to stop running the genetic algorithm, one method is to stop after a particular number of generations, which is the method used in this study. Convergence is the progression toward uniformity. A chromosome is said to have converged when 95% of the population share the same value [14]. Thus, most or all individuals in the population are identical or similar when the population has converged. The setting parameters of the genetic algorithm for this study are as follows: chromosome length = 42, population size = 50, number of generation = 77, crossover probability = 0.5, mutation probability = 0.001.

4 RESULTS

The dynamic characteristics of the rotor system were studied and the results are given for comparing both optimization methods. The rotor-system response amplitudes' corresponding phase angles in the X and Y directions versus the rotor speed range from 5000 rpm to 40000 rpm for stations are represented in Fig.3, Fig.4, Fig.5, and Fig.6. The rotor response was obtained in the X and Y directions adjacent to both bearing locations to determine the displacement amplitude. The highest displacement is found at station 1, corresponding to the station at the impeller's nose. The peak displacement is approximately 0.000146 mm in the X direction at 16000 rpm and 0.000143 mm in the Y direction at 37000 rpm using the genetic algorithm, while it is 0.000320 mm in the X direction at 19000 rpm and 0.000323 mm in the y direction at 19000 rpm using the method of feasible directions. The lowest displacement is approximately 0.000065 mm in the X direction at 10000 rpm and 0.000067 mm in the Y direction at 5600 rpm (at station 24) using the genetic algorithm, while it is 0.000020 mm in the X direction at 6400 rpm and 0.000016 mm in the y direction at 5600 rpm (at station 20) using the method of feasible directions. The results showed that the rotor speed at which the highest and the lowest amplitudes occurred varies. Overall, the locations of the peak responses are in good agreement, although they appear to be lower with the genetic algorithm than those using the method of feasible directions. These significant outcomes satisfy the imposed constraint specification and allow the rotor system to maintain its stability.

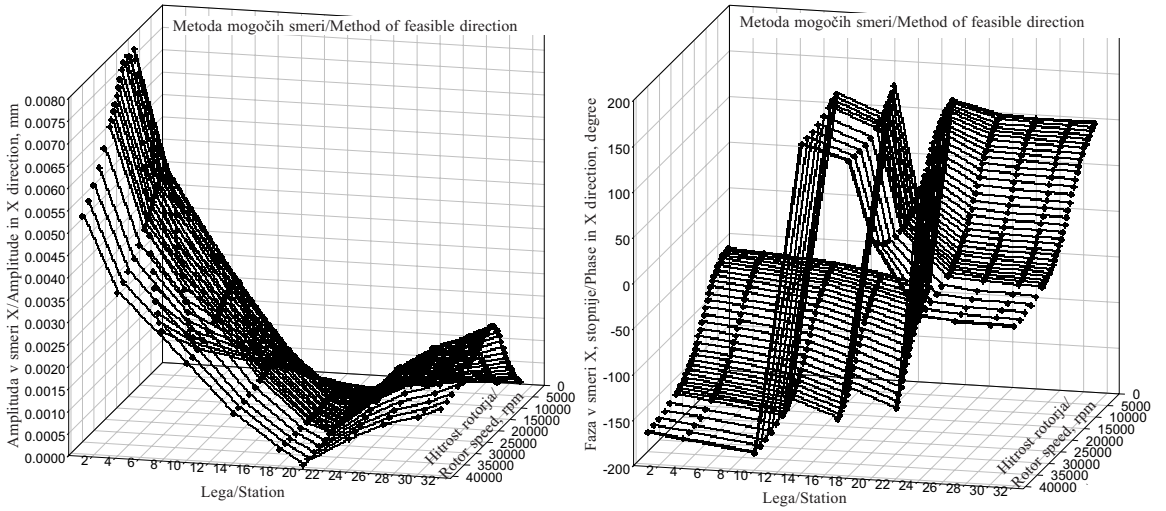

Sl. 3. *Rotorjeva amplituda odziva in fazni kot v smeri X (metoda mogočih smeri)*
Fig. 3. *The rotor's response amplitude and the phase angle in the X direction (the method of feasible directions)*

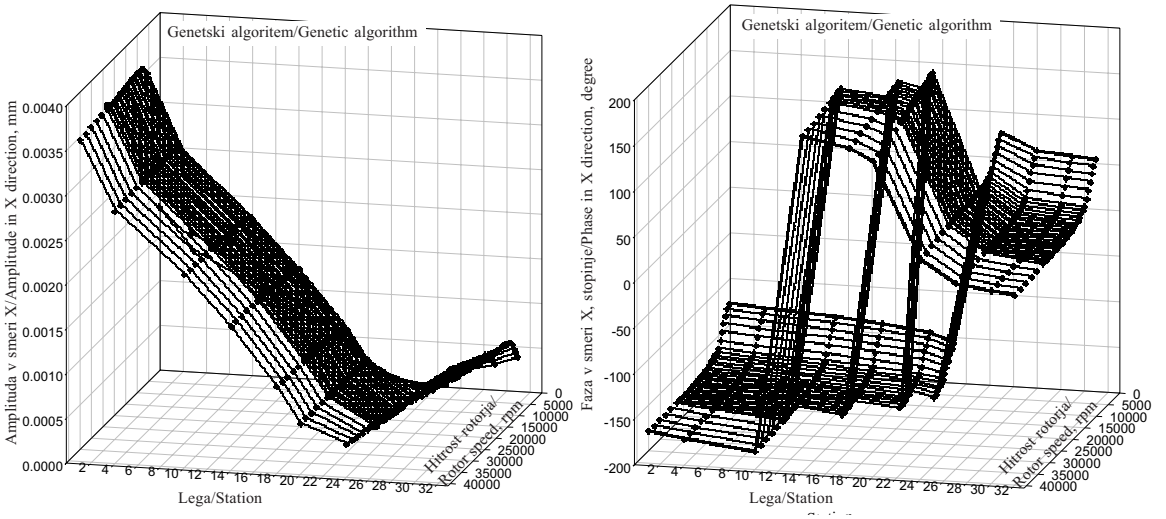

Sl. 4. *Rotorjeva amplituda odziva in fazni kot v smeri X (genetski algoritem)*
Fig. 4. *The rotor's response amplitude and the phase angle in the X direction (the genetic algorithm)*

5 SKLEPI

Poglavitni cilj oblikovanja rotorskega sistema je minimalizacija amplitude odziva na različne rotorjeve obratovalne hitrosti. Dinamične značilnosti rotorskega sistema morajo biti oblikovane tako, da pri nobeni obratovalni hitrosti ne pride do čezmerne amplitude odziva. Da bi izračunali odziv gibkega rotorja, ki ga podpirata dva prečna drsna ležaja s pritrjenimi segmenti, smo uporabili genetski algoritem. Da bi dobili čim bolj natančne podatke o amplitudi gibanja rotorskega

5 CONCLUSIONS

The minimization of the response amplitude within the operating speed range of the rotor system is primary among the design objectives. The dynamic characteristics of the rotor system must be designed to operate without an excessive response amplitude throughout its operating-speed range. A genetic algorithm was employed to compute the response of the flexible rotor supported in two fixed-lobe journal bearings. The finite-element-method-based computer code was coupled

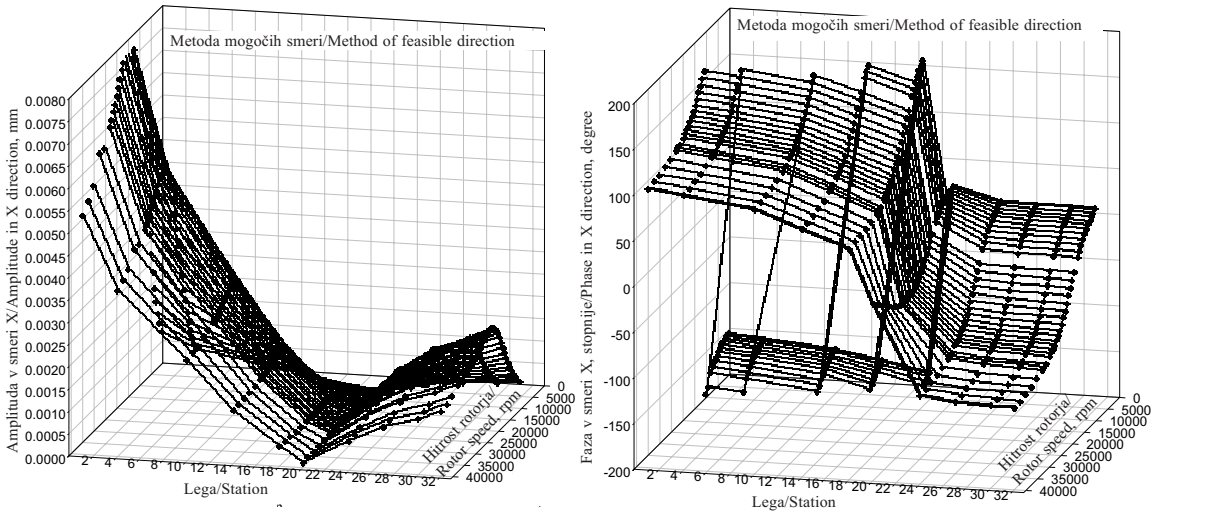

Sl. 5. *Rotorjeva amplituda odziva in fazni kot v smeri Y (metoda mogočih smeri)*
Fig. 5. *The rotor's response amplitude and the phase angle in the Y direction (the method of feasible directions)*

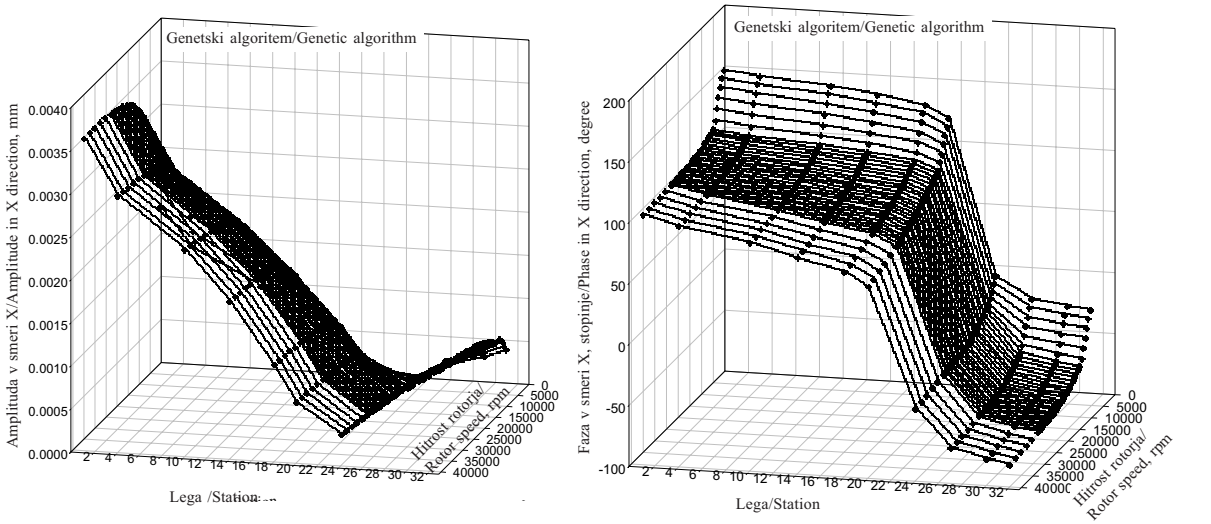

Sl. 6. *Rotorjeva amplituda odziva in fazni kot v smeri Y (genetski algoritem)*
Fig. 6. *The rotor's response amplitude and the phase angle in the Y direction (the genetic algorithm)*

sistema, smo optimizacijske algoritme združili z računalniško kodo, ki temelji na metodi končnih elementov. Uporaba metode končnih elementov skupaj z genetskim algoritmom pri oblikovanju značilnega prevesnega rotorskega sistema z veliko hitrostjo terja veliko zmogljivost pomnilnika in s tem veliko računalniškega napora. Vendar pa to težavo lahko premostimo z izrabo sodobnih računalniških zmogljivosti. Rezultati, ki jih predstavljamo v tem prispevku, potrjujejo primernost izbrane metode, s katero smo vplivali na amplitudo rotorjevega odziva. Metodo

to these optimization algorithms to extract more accurately the required information about the amplitude of the motion of the rotor system. Using the finite-element method with a genetic algorithm in a typical high-speed overhung rotor-system design requires a significant amount of memory storage, and this requires more computational effort. However, this disadvantage is not significant with the current computing capability. The results presented in this paper demonstrate an approach which possesses considerable suitability for the rotor-amplitude response. The method of feasible

izvedljivih smeri smo uporabili z namenom, da potrdimo učinkovitost in uporabnost predlagane metode ter tako pokažemo, da je predlagana metoda zelo primerna za oblikovanje rotorskega sistema. Za obe metodi smo grafično prikazali spremembe amplitude odziva rotorskega sistema v vodoravni in navpični legi. Iz celotnih rezultatov namenske funkcije smo z genetskim algoritmom dobili boljše rezultate od tistih, ki smo jih dosegli z metodo mogočih smeri. Genetski algoritem omogoča raziskovati številne različne konfiguracije oblikovnih spremenljivk in tako tudi prispeva k boljšemu razumevanju splošnega rotorskega in ležajnega obnašanja.

directions is conducted to validate the efficiency and applicability of the proposed method and, it proved that the proposed method in the rotor-system design is very efficient and useful. Plots of the variation of the rotor system's response amplitudes in the horizontal and vertical directions for both methods are presented. From the overall results of the objective function, the genetic algorithm was able to obtain better results than those obtained using the method of feasible directions. The genetic algorithm allows the exploration of many different configurations of design variables and therefore also contributes to a better understanding of the rotor and the bearing behavior in general.

6 LITERATURA
6 REFERENCES

[1] A. Homaifar, C.X. Qi, and S.H. Lai (1994) Constrained optimization via genetic algorithms, *Simulation*, 62, (1994), 242-254.

[2] C.A. Roso (1997) Design optimization of rotor-bearing systems for industrial turbomachinery applications, Ph.D. Dissertation, *University of Kentucky*.

[3] C.Y. Lin and P. Hajela (1992) Genetic algorithms in optimization problems with discrete and integer design variables, *Engineering Optimization*, 19 (1992), 309-327.

[4] D. Beasley, D.R. Bull, and R.R. Martin (1993) An overview of genetic algorithms: Part 2. Research topics. *University Computing* , 15 (1993), 170-181.

[5] D.E. Goldberg (1989) Genetic algorithms in search, optimization, and machine learning reading, *Addison-Wesley*, MA.

[6] G.G. Zoutendijk (1969) Method of feasible directions. *Elsevier*, Amsterdam.

[7] G. Mitsuo and C. Runwei (1997) Genetic algorithms and engineering design, *John Wiley, Pub.*, New York.

[8] G.N.Vanderplaats (1984) Numerical optimization techniques for engineering designs, *McGraw-Hill*.

[9] G. Syswerda (1989) Uniform crossover in genetic algorithms, *Proceedings of the 3rd International Conference on Genetic Algorithms*.

[10] H. Saruhan, K.E. Rouch, and C.A. Roso (2001) Design optimization of fixed pad journal bearing for rotor system using a genetic algorithm approach, *International Symposium on Stability Control of Rotating Machinery, ISCORMA-1*, Lake Tahoe, Nevada.

[11] H. Saruhan, K.E. Rouch, and C.A. Roso (2004) Design optimization of tilting-pad journal bearing using a genetic algorithm approach, *International Journal of Rotating Machinery*, 10(4), (2004) 301-307.

[12] J.H. Holland (1975) Adaptation in natural and artificial systems, *University of Michigan Press*.

[13] J.T.Sawicki, R.J. Capaldi, and M.L. Adams (1997) Experimental and thoretical rotordynamic characteristics of a hybrid journal bearing, *Transaction of the ASME*, 119 (1997) 132-141.

[14] K.De Jong (1975) The analysis and behavior of class of genetic adaptive systems, Ph.D. Dissertation, *University of Michigan*.

[15] K.E. Rouch (1977) Finite element analysis of rotor bearing systems with matrix reduction, Ph.D. Dissertation, *Marquette University*.

[16] K.E. Rouch and J.S. Kao (1980) Dynamic reduction in rotor dynamics by the finite element method, *Transactions of the ASME*, 102 (1980), 360-368.

[17] L. Davis (1991) Handbook of genetic algorithms, *Van Nostrand Reinhold*, New York.

[18] M. Mitchell (1997) An introduction to genetic algorithms, *The MIT Press*, Massachusetts.
[19] P. Qin, Y. Shen, J. Zhu, and H. Xu (2005) Dynamic analysis of hydrodynamic bearing – Rotor system based on neural network, *International Journal of Engineering Science*, 43 (2005) 520-531.

Avtorjev naslov: Hamit Saruhan
Univerza Duzce
Oddelek za oblikovanje strojev
81620-Duzce, Turčija
hamitsaruhan@hotmail.com

Author's Address: Hamit Saruhan
Duzce University
Mechanical Design Division
81620-Duzce, Turkey
hamitsaruhan@hotmail.com

Prejeto: 26.10.2006
Received:
Sprejeto: 25.4.2007
Accepted:
Odprto za diskusijo: 1 leto
Open for discussion: 1 year

Osebne vesti - Personal Events

Zoisovo priznanje za pomembne dosežke na področju proizvodnih tehnologij in sistemov prof. dr. Jožetu Baliču

Doktor Jože Balič, profesor na Fakulteti za strojništvo Univerze v Mariboru, je pomembno prispeval k razvoju na področju avtomatizacije obdelovalnih postopkov in sistemov ter računalniško podprtih inteligentnih sistemov. Njegovo raziskovalno delo je usmerjeno v snovanje in modeliranje procesov ter razvoj delujočih sistemov. Prav zato ga lahko uvrščamo med pionirje raziskav in razvoja proizvodne kibernetike v srednji Evropi.

Raziskoval je prilagodljive izdelovalne sisteme v realnem okolju. Pri tem je preučeval predvsem modele, strukturo in izdelovalna orodja. Z uporabo nevronskih mrež je raziskoval sedanje strukture izdelovalnih sistemov ter njihove realne omejitve in specifične možnosti. Pri avtomatizaciji obdelovalnih postopkov je treba uporabiti različne modele za optimiranje. Profesor Balič je pri tem uporabil nevronske mreže za simulacijo in z opredelitvijo vodilnih parametrov določil optimalne pogoje za uporabo obdelovalnih postopkov. Obravnaval je različne zasnove skupinske tehnologije in predvsem opredelil primernost posameznih tehnoloških postopkov pri prilagodljivem izdelovalnem sistemu. V zadnjem obdobju ja raziskoval modele umetne inteligence za opredelitev izdelovalnih pogojev in sistemov.

Pomembna je tudi njegova publicistična dejavnost. V obdobju 2000 do 2006 je raziskovalne dosežke objavil sam ali v soavtorstvu v štirih knjigah pri tujih založbah. Je avtor ali soavtor 15 univerzitetnih učbenikov in štirih patentov.

Diplome - Diploma Degrees

DIPLOMIRALI SO

Na Fakulteti za strojništvo Univerze v Ljubljani so pridobili naziv univerzitetni diplomirani inženir strojništva:

dne *30. novembra 2007*: Klemen KOŠIR, Andrej KOVIČ, Sašo PANTAR, Martina PRIMOŽIČ, Dragomir STAKOVIĆ.

*

Na Fakulteti za strojništvo Univerze v Ljubljani so pridobili naziv diplomirani inženir strojništva:

dne *15. novembra 2007*: Lar HERNOG, Marko KOVAČIČ, Matjaž LUZAR, Marjan ŽAGAR;

dne *19. novembra 2007*: Mojca KOSEM, Andrej MASTNAK, Jernej PRIMON, Aleš ŠKOFIC, Gregor ZIBELNIK.

Vsebina 2007 - Contents 2007

Seznam recenzentov 2007 - List of Reviewers in 2007

prof. dr. Ivo Alfirević, University of Zagreb
prof. dr. Ivan Anžel, Univerza v Mariboru, FS
prof. dr. Ivan Bajsić, Univerza v Ljubljani, FS
prof. dr. Jože Balič, Univerza v Mariboru, FS
prof. dr. Adrian Bejan, Duke University
prof. dr. Miha Boltežar, Univerza v Ljubljani, FS
prof. dr. Borut Buchmeister, Univerza v Mariboru, FS
prof. dr. Peter Butala, Univerza v Ljubljani, FS
prof. dr. Alexander Czinki, University of Applied Science
prof. dr. Mirko Čudina, Univerza v Ljubljani, FS
prof. dr. Franci Čuš, Univerza v Mariboru, FS
prof. dr. Božin Donevski, University St. Kliment Ohridski
prof. dr. Jože Duhovnik, Univerza v Ljubljani, FS
prof. dr. Matija Fajdiga, Univerza v Ljubljani, FS
prof. dr. Iztok Golobič, Univerza v Ljubljani, FS
prof. dr. Karl Gotlih, Univerza v Mariboru, FS
prof. dr. Imre Horvath, Delft TU
prof. dr. Aleš Hribernik, Univerza v Mariboru, FS
prof. dr. Matjaž Hriberšek, Univerza v Mariboru, FS
prof. dr. Karel Jezernik, Univerza v Mariboru, FS
prof. dr. Mihael Junkar, Univerza v Ljubljani, FS
prof. dr. Mitjan Kalin, Univerza v Ljubljani, FS
prof. dr. Zlatko Kampuš, Univerza v Ljubljani, FS
prof. dr. Breda Kegl, Univerza v Mariboru, FS
prof. dr. Edi Kiker, Univerza v Mariboru, FS
doc. dr. Pino Koc, Univerza v Ljubljani, FMF
prof. dr. Janez Kopač, Univerza v Ljubljani, FS
prof. dr. Franc Kosel, Univerza v Ljubljani, FS
doc. dr. Janez Kušar, Univerza v Ljubljani, FS
prof. dr. Milan Marčič, Univerza v Mariboru, FS
prof. dr. Dorian Marjanović, University of Zagreb
prof. dr. Vladimir Medica, University of Rijeka
prof. dr. Bagirathy Nadarajah, University of Manchester
prof. dr. Marko Nagode, Univerza v Ljubljani, FS
prof. dr. Maks Oblak, Univerza v Mariboru, FS
prof. dr. Ivan Petrović, University of Zagreb
prof. dr. Alojz Poredoš, Univerza v Ljubljani, FS
prof. dr. Ivan Prebil, Univerza v Ljubljani, FS
prof. dr. Rudolf Pušenjak, Univerza v Mariboru, FS
prof. dr. Zoran Ren, Univerza v Mariboru, FS
prof. dr. Bernd Sauer, University of Kaiserlautern
prof. dr. Aloj Sluga, Univerza v Ljubljani, FS
prof. dr. Marko Starbek, Univerza v Ljubljani, FS
prof. dr. Brane Širok, Univerza v Ljubljani, FS
prof. dr. Milan Stehlik, Johannes Kepler University
prof. dr. Antun Stoić, J.J. Strsossmayer University of Osijek
prof. dr. Mladen Šercer, University of Zagreb
prof. dr. Boris Štok, Univerza v Ljubljani, FS
prof. dr. Ferdinand Trenc, Univerza v Ljubljani, FS
prof. dr. Matija Tuma, Univerza v Ljubljani, FS
prof. dr. Toma Udiljak, University of Zagreb
prof. dr. Jouke C. Verlinden, Delft TU
prof. dr. Hinko Wolf, University of Zagreb
prof. dr. dr. Janez Žerovnik, Univerza v Mariboru, FS

Navodila avtorjem* - Instructions for Authors*

Članki morajo vsebovati:
- naslov, povzetek, besedilo članka in podnaslove slik v slovenskem in angleškem jeziku,
- dvojezične preglednice in slike (diagrami, risbe ali fotografije),
- seznam literature in
- podatke o avtorjih.

Strojniški vestnik izhaja od leta 1992 v dveh jezikih, tj. v slovenščini in angleščini, zato je obvezen prevod v angleščino. Obe besedili morata biti strokovno in jezikovno med seboj usklajeni. Članki naj bodo kratki in naj obsegajo približno 8 strani. Izjemoma so strokovni članki, na željo avtorja, lahko tudi samo v slovenščini, vsebovati pa morajo angleški povzetek.

Za članke iz tujine (v primeru, da so vsi avtorji tujci) morajo prevod v slovenščino priskrbeti avtorji. Prevajanje lahko proti plačilu organizira uredništvo. Če je članek ocenjen kot znanstveni, je lahko objavljen tudi samo v angleščini s slovenskim povzetkom, ki ga pripravi uredništvo.

VSEBINA ČLANKA

Članek naj bo napisan v naslednji obliki:
- Naslov, ki primerno opisuje vsebino članka.
- Povzetek, ki naj bo skrajšana oblika članka in naj ne presega 250 besed. Povzetek mora vsebovati osnove, jedro in cilje raziskave, uporabljeno metodologijo dela,povzetek rezulatov in osnovne sklepe.
- Uvod, v katerem naj bo pregled novejšega stanja in zadostne informacije za razumevanje ter pregled rezultatov dela, predstavljenih v članku.
- Teorija.
- Eksperimentalni del, ki naj vsebuje podatke o postavitvi preskusa in metode, uporabljene pri pridobitvi rezultatov.
- Rezultati, ki naj bodo jasno prikazani, po potrebi v obliki slik in preglednic.
- Razprava, v kateri naj bodo prikazane povezave in posplošitve, uporabljene za pridobitev rezultatov. Prikazana naj bo tudi pomembnost rezultatov in primerjava s poprej objavljenimi deli. (Zaradi narave posameznih raziskav so lahko rezultati in razprava, za jasnost in preprostejše bralčevo razumevanje, združeni v eno poglavje.)
- Sklepi, v katerih naj bo prikazan en ali več sklepov, ki izhajajo iz rezultatov in razprave.
- Literatura, ki mora biti v besedilu oštevilčena zaporedno in označena z oglatimi oklepaji [1] ter na koncu članka zbrana v seznamu literature. Vse opombe naj bodo označene z uporabo dvignjene številke[1].

OBLIKA ČLANKA

Besedilo članka naj bo pripravljeno v urejevalnilku Microsoft Word. Članek nam dostavite v elektronski obliki.

Ne uporabljajte urejevalnika LaTeX, saj program, s katerim pripravljamo Strojniški vestnik, ne uporablja njegovega formata.

Enačbe naj bodo v besedilu postavljene v ločene vrstice in na desnem robu označene s tekočo številko v okroglih oklepajih

* So v postopku spreminjanja.

Papers submitted for publication should comprise:
- Title, Abstract, Main Body of Text and Figure Captions in Slovene and English,
- Bilingual Tables and Figures (graphs, drawings or photographs),
- List of references and
- Information about the authors.

Since 1992, the Journal of Mechanical Engineering has been published bilingually, in Slovenian and English. The two texts must be compatible both in terms of technical content and language. Papers should be as short as possible and should on average comprise 8 pages. In exceptional cases, at the request of the authors, speciality papers may be written only in Slovene, but must include an English abstract.

For papers from abroad (in case that none of authors is Slovene) authors should provide Slovenian translation. Translation could be organised by editorial, but the authors have to pay for it. If the paper is reviewed as scientific, it can be published only in English language with Slovenian abstract, that is prepared by the editorial board.

THE FORMAT OF THE PAPER

The paper should be written in the following format:
- A Title, which adequately describes the content of the paper.
- An Abstract, which should be viewed as a mini version of the paper and should not exceed 250 words. The Abstract should state the principal objectives and the scope of the investigation, the methodology employed, summarize the results and state the principal conclusions.
- An Introduction, which should provide a review of recent literature and sufficient background information to allow the results of the paper to be understood and evaluated.
- A Theory
- An Experimental section, which should provide details of the experimental set-up and the methods used for obtaining the results.
- A Results section, which should clearly and concisely present the data using figures and tables where appropriate.
- A Discussion section, which should describe the relationships and generalisations shown by the results and discuss the significance of the results making comparisons with previously published work. (Because of the nature of some studies it may be appropriate to combine the Results and Discussion sections into a single section to improve the clarity and make it easier for the reader.)
- Conclusions, which should present one or more conclusions that have been drawn from the results and subsequent discussion.
- References, which must be numbered consecutively in the text using square brackets [1] and collected together in a reference list at the end of the paper. Any footnotes should be indicated by the use of a superscript[1].

THE LAYOUT OF THE TEXT

Texts should be written in Microsoft Word format. Paper must be submitted in electronic version.

Do not use a LaTeX text editor, since this is not compatible with the publishing procedure of the Journal of Mechanical Engineering.

Equations should be on a separate line in the main body of the text and marked on the right-hand side of the page with numbers in round brackets.

* Subject to changes.

Enote in okrajšave

V besedilu, preglednicah in slikah uporabljajte le standardne označbe in okrajšave SI. Simbole fizikalnih veličin v besedilu pišite poševno (kurzivno), (npr. *v, T, n* itn.). Simbole enot, ki sestojijo iz črk, pa pokončno (npr. ms^{-1}, K, min, mm itn.).

Vse okrajšave naj bodo, ko se prvič pojavijo, napisane v celoti v slovenskem jeziku, npr. časovno spremenljiva geometrija (ČSG).

Slike

Slike morajo biti zaporedno oštevilčene in označene, v besedilu in podnaslovu, kot sl. 1, sl. 2 itn. Posnete naj bodo v ločljivosti, primerni za tisk, v kateremkoli od razširjenih formatov, npr. BMP, JPG, GIF. Diagrami in risbe morajo biti pripravljeni v vektorskem formatu, npr. CDR, AI.

Pri označevanju osi v diagramih, kadar je le mogoče, uporabite označbe veličin (npr. *t, v, m* itn.), da ni potrebno dvojezično označevanje. V diagramih z več krivuljami, mora biti vsaka krivulja označena. Pomen oznake mora biti pojasnjen v podnapisu slike.

Vse označbe na slikah morajo biti dvojezične.

Preglednice

Preglednice morajo biti zaporedno oštevilčene in označene, v besedilu in podnaslovu, kot preglednica 1, preglednica 2 itn. V preglednicah ne uporabljajte izpisanih imen veličin, ampak samo ustrezne simbole, da se izognemo dvojezični podvojitvi imen. K fizikalnim veličinam, npr. *t* (pisano poševno), pripišite enote (pisano pokončno) v novo vrsto brez oklepajev.

Vsi podnaslovi preglednic morajo biti dvojezični.

Seznam literature

Vsa literatura mora biti navedena v seznamu na koncu članka v prikazani obliki po vrsti za revije, zbornike in knjige:

[1] A. Wagner, I. Bajsić, M. Fajdiga (2004) Measurement of the surface-temperature field in a fog lamp using resistance-based temperature detectors, *Stroj. vestn.* 2(2004), pp. 72-79.
[2] Vesenjak, M., Ren Z. (2003) Dinamična simulacija deformiranja cestne varnostne ograje pri naletu vozila. *Kuhljevi dnevi '03*, Zreče, 25.-26. september 2003.
[3] Muhs, D. et al. (2003) Roloff/Matek Maschinenelemente – Tabellen, 16. Auflage. *Vieweg Verlag*, Wiesbaden.

SPREJEM ČLANKOV IN AVTORSKE PRAVICE

Uredništvo Strojniškega vestnika si pridržuje pravico do odločanja o sprejemu članka za objavo, strokovno oceno recenzentov in morebitnem predlogu za krajšanje ali izpopolnitev ter terminološke in jezikovne korekture.

Avtor mora predložiti pisno izjavo, da je besedilo njegovo izvirno delo in ni bilo v dani obliki še nikjer objavljeno. Z objavo preidejo avtorske pravice na Strojniški vestnik. Pri morebitnih kasnejših objavah mora biti SV naveden kot vir.

PLAČILO OBJAVE

Avtorji vseh prispevkov morajo za objavo plačati prispevek v višini 20,00 EUR na stiskano stran prispevka. Prispevek se zaračuna po sprejemu članka za objavo na seji Uredniškega odbora.

Units and abbreviations

Only standard SI symbols and abbreviations should be used in the text, tables and figures. Symbols for physical quantities in the text should be written in italics (e.g. *v, T, n,* etc.). Symbols for units that consist of letters should be in plain text (e.g. ms^{-1}, K, min, mm, etc.).

All abbreviations should be spelt out in full on first appearance, e.g., variable time geometry (VTG).

Figures

Figures must be cited in consecutive numerical order in the text and referred to in both the text and the caption as Fig. 1, Fig. 2, etc. Pictures may be saved in resolution good enough for printing in any common format, e.g. BMP, GIF, JPG. However, graphs and line drawings sholud be prepared as vector images, e.g. CDR, AI.

When labelling axes, physical quantities, e.g. *t, v, m,* etc. should be used whenever possible to minimise the need to label the axes in two languages. Multi-curve graphs should have individual curves marked with a symbol, the meaning of the symbol should be explained in the figure caption.

All figure captions must be bilingual.

Tables

Tables must be cited in consecutive numerical order in the text and referred to in both the text and the caption as Table 1, Table 2, etc. The use of names for quantities in tables should be avoided if possible: corresponding symbols are preferred to minimise the need to use both Slovenian and English names. In addition to the physical quantity, e.g. *t* (in italics), units (normal text), should be added in new line without brackets.

All table captions must be bilingual.

The list of references

References should be collected at the end of the paper in the following styles for journals, proceedings and books, respectively:

[1] A. Wagner, I. Bajsić, M. Fajdiga (2004) Measurement of the surface-temperature field in a fog lamp using resistance-based temperature detectors, *Stroj. vestn.* 2(2004), pp. 72-79.
[2] Vesenjak, M., Ren Z. (2003) Dinamična simulacija deformiranja cestne varnostne ograje pri naletu vozila. *Kuhljevi dnevi '03*, Zreče, 25.-26. september 2003.
[3] Muhs, D. et al. (2003) Roloff/Matek Maschinenelemente – Tabellen, 16. Auflage. *Vieweg Verlag*, Wiesbaden.

ACCEPTANCE OF PAPERS AND COPYRIGHT

The Editorial Committee of the Journal of Mechanical Engineering reserves the right to decide whether a paper is acceptable for publication, obtain professional reviews for submitted papers, and if necessary, require changes to the content, length or language.

Authors must also enclose a written statement that the paper is original unpublished work, and not under consideration for publication elsewhere. On publication, copyright for the paper shall pass to the Journal of Mechanical Engineering. The JME must be stated as a source in all later publications.

PUBLICATION FEE

For all papers authors will be asked to pay a publication fee prior to the paper appearing in the journal. However, this fee only needs to be paid after the paper is accepted by the Editorial Board. The fee is €20.00 per printed paper page.